

# **Preparative Recovery of Bioactive Molecules from Conditioned Medium of CHO-K1 Cell Culture**

**Vom Promotionsausschuss der Technischen  
Universität Hamburg**

**zur Erlangung des akademischen Grades**

**Doktor-Ingenieur (Dr.-Ing.)**

**genehmigte Dissertation**

**von**

**Alan Eduardo Castillo Salvador**

**aus**

**Ciudad de México, Mexiko**

**2019**

---

Gutachter:

1. **Prof. Dr. rer. nat. A.P. Zeng**
2. **Prof. Dr.-Ing M. Schlüter**

Tag der mündlichen Prüfung: 26. März 2019

## Summary

Mammalian cells produce a vast variety of proteins and peptides with diverse physicochemical properties that are released from the cell either through active secretion or as a result of cell lysis following cellular death. The entirety of these molecules is known as the “secretome” and it includes autocrine factors, which regulate cellular processes like cell growth and death, proteolytic enzymes and host cell proteins (HCPs). During the time course of a cultivation and as the cell density increases, the proteins and peptides of the secretome accumulate and produce the so-called conditioned medium. This work examines the biological activity of conditioned medium and its influence in the growth, death and metabolic kinetics of CHO-K1 cell culture. Conditioned medium was generally associated with a 24 hours delayed reduction in the specific death rate and an increase in the viability of exponentially growing cells, regardless if it was harvested in the late or early exponential phase of growth. Conditioned medium harvested in the early exponential phase of growth was associated with a moderate increase in the specific growth rate after 24 hours of cultivation. A membrane adsorption chromatography method was developed for the preparative capture, recovery and fractionation of the bioactive molecules responsible for some of the determined effects. This resulted in the isolation of two fractions with biological activity when supplemented to exponentially growing cells. The first fraction, which represented 25.7% of the total protein content in conditioned medium, was associated with an increase of  $6\% \pm 3.0\%$  in viability, apoptosis reduction, increase of  $12\% \pm 3.3\%$  in the maximal specific growth rate, increased lactate consumption after glutamine depletion and sudden cellular death following the complete depletion of glucose. The second fraction, which corresponded to 1.2% of the total protein content in conditioned medium, was associated with a  $28\% \pm 9.4\%$  reduction in the specific growth rate after 24 hours of cultivation. This work offers a fast, flexible and robust method to study the highly complex secretome of CHO-K1 cells and its role in cell culture technology. Furthermore, the acquired results suggest the interplay of two opposing signaling molecules during the batch cultivation of CHO-K1 cell culture and the possible production and accumulation of autoinhibitors previously described in the literature for hybridoma cells.

**Keywords:** Cell Culture Technology, Secretome, Conditioned Medium, Cellular Metabolism, Autoinhibitor, Membrane Adsorption Chromatography, Hydrophobic Interaction Chromatography, Cation Exchange Chromatography

---

---

# Contents

<b>Summary .....</b>	<b>I</b>
<b>Contents .....</b>	<b>II</b>
<b>List of Figures .....</b>	<b>IV</b>
<b>List of Tables .....</b>	<b>X</b>
<b>1 Motivation and Objectives.....</b>	<b>1</b>
<b>2 Introduction .....</b>	<b>2</b>
2.1 Cell Culture Technology in the Biopharmaceutical Industry .....	2
2.2 Cell Metabolism .....	2
2.3 Medium Design .....	7
2.4 Conditioned Medium and the Secretome of CHO-K1 .....	9
2.5 Ion Exchange Chromatography .....	12
2.6 Hydrophobic Interaction Chromatography .....	17
2.7 Membrane Adsorption Chromatography.....	22
<b>3 Materials and Methods .....</b>	<b>23</b>
3.1 Conditioned Medium and the Kinetics of CHO-K1 Cell Culture .....	23
3.1.1 Cell culture .....	23
3.1.2 Analytical Methods .....	24
3.1.3 Determination of Kinetic Parameters .....	24
3.1.4 Statistical Analysis .....	27
3.1.5 Kinetics of Conditioned Medium.....	28
3.1.6 Separation of Conditioned Medium by Molecular Weight (cutoff 10 kDa) .....	28
3.1.7 Effect of the Conditioned to Fresh Medium Ratio .....	30
3.1.8 Effects of the Age of the Parent Culture .....	31
3.2 Cation Exchange Chromatography Purification Step.....	33
3.2.1 Membrane Adsorbers .....	33
3.2.2 Buffers for Fractionation.....	33
3.2.3 Electrophoresis .....	34

## CONTENTS

---

3.2.4	Determination of Protein Concentrations.....	35
3.2.5	Generation of Conditioned Medium .....	35
3.2.6	Capture and Fractionation of the Conditioned Medium Components .....	36
3.2.7	Fraction Evaluation .....	42
3.3	Hydrophobic Interaction Chromatography Purification Step.....	48
3.3.1	Production of Elution E2 Fraction .....	48
3.3.2	Screening for Optimal Conditions .....	49
3.3.3	Testing of HIC Elution in Cell Culture .....	52
<b>4</b>	<b>Results.....</b>	<b>57</b>
4.1	Conditioned Medium and the Kinetics of CHO-K1 Cell Culture .....	57
4.1.1	Kinetics of Conditioned Medium.....	57
4.1.2	Separation of Conditioned Medium by Molecular Weight (cutoff 10 kDa).....	61
4.1.3	Effect of the Conditioned to Fresh Medium Ratio .....	69
4.1.4	Effects of the Age of the Parent Culture .....	74
4.1.5	Concluding Remarks.....	82
4.2	Cation Exchange Chromatography and Evaluation of Fractions .....	83
4.2.1	Capture and Fractionation of the Conditioned Medium Components .....	83
4.2.2	Fraction Evaluation .....	86
4.2.3	Concluding Remarks.....	104
4.3	Hydrophobic Interaction Chromatography and Evaluation of Fractions .....	106
4.3.1	Screening for Optimal Conditions .....	106
4.3.2	Testing of HIC Elution in cell Culture.....	107
4.3.3	Concluding Remarks.....	122
<b>5</b>	<b>Discussion .....</b>	<b>123</b>
<b>6</b>	<b>Summary and Outlook.....</b>	<b>130</b>
<b>7</b>	<b>References .....</b>	<b>132</b>
<b>8</b>	<b>Lebenslauf .....</b>	<b>142</b>

---

## List of Figures

**Figure 1** Fate of the glucose transported into CHO cells during the exponential phase of growth. Between 75% - 90% is transformed into lactate through the glycolytic pathway, while 4% - 8% is fully oxidized into CO<sub>2</sub> in the tricarboxylic acid (TCA) cycle inside of the mitochondrion. Less than 10% is diverted into pentose phosphate pathway (PPP) for the synthesis of nucleotides..... 3

**Figure 2** Simplified depiction of the main pathways by which the two main substrates, glucose and glutamine are metabolized inside of the cell. Glucose is transported across the plasma membrane through the glucose transporter 1 (GLUT1). Glucose is then transformed into glucose-6-phosphate (G6P) by the enzyme Hexokinase (HK). G6P can then either be diverted into the pentose phosphate pathway (PPP) or into the glycolytic pathway generating phosphoenolpyruvate (PEP). PEP is transformed into pyruvate by the enzyme pyruvate kinase (PK). Pyruvate can be then transformed into alanine or into lactate by the enzyme lactate dehydrogenase (LDH). Pyruvate can also be transported into the mitochondrion, where it enters the tricarboxylic acid (TCA) cycle after being transformed into acetyl-CoA by the enzyme pyruvate dehydrogenase (PDH). Glutamine is transformed to glutamate and ammonium by the phosphate activated glutaminase (PAG) enzyme at the mitochondrial membrane. Glutamate then enters the TCA cycle inside of the mitochondrion and can be transformed into malate, then pyruvate and end with the production of lactate in a process called glutaminolysis. .... 4

**Figure 3** Representation of the titration curves of an acidic protein (blue curve), a neutral protein (orange curve) and a basic protein (grey curve)..... 13

**Figure 4** Representation of a bind and elute process. The first step is the equilibration of the chromatography medium with buffer at the corresponding conditions that allow most of the components to be separated to bind to the ligands. The load material adjusted to binding conditions and containing the components to be separated is then introduced into the chromatography medium. A wash step is then performed to remove loosely bound impurities. Elution and the separation of the bound components is performed using a linear or stepwise gradient. Finally tightly bound impurities are removed from the chromatography medium using a cleaning solution..... 14

**Figure 5** Representation of an isocratic flow through process. The chromatography medium and the load material are adjusted to the corresponding conditions that allow the molecule to be purified not to bind while the impurities are retained. .... 15

**Figure 6** Depiction of the binding of positively charged molecules into a cation exchanger and their elution from the chromatographic medium by either increasing the conductivity (salt gradient elution) or the pH (pH gradient elution) of the mobile phase..... 17

**Figure 7** Representation of the thermodynamically driven spontaneous aggregation of two non-polar molecules in aqueous solution which results in a decrease in entropy. .... 19

**Figure 8** Hoffmeister series listing different ions in order of their influence on the hydrophobic interaction of proteins. The ions to the left have the property of increasing the surface tension of water, thus increasing the hydrophobic interaction (salting-out) (Queiroz et al. 2001). .... 20

## LIST OF FIGURES

---

<b>Figure 9</b> Mechanism by which a protein binds into and elutes from the ligands of a hydrophobic interaction chromatography medium. The medium is first equilibrated with a high salt buffer to enhance the hydrophobic effect. The proteins then bind into the ligands at their hydrophobic patches. The proteins are finally eluted using a low salt buffer. ....	21
<b>Figure 10</b> Graph depicting the growth kinetics described by <i>Model II</i> . $N_v$ , $N_{ap}$ , and $N_d$ represent respectively the viable, apoptotic and non-viable cell densities, while $\mu$ , $k_{ap}$ and $k_d$ represent the specific growth, apoptosis induction and specific death rates respectively. ....	26
<b>Figure 11</b> Two-step elution at pH 5. The first elution (E1) was collected by increasing the pH of the mobile phase to 10. The second elution E2 was collected by increasing the salt concentration of the mobile phase to 1 M NaCl. ....	38
<b>Figure 12</b> Total cell density ( $N_t$ ) (A) and viability (B) of the cultures inoculated in CHOMACS CD growth medium containing 0 vol% and 25 vol% conditioned medium (CM). The values given in the graphs were calculated as the average of the triplicate cultures and the error bars represent the standard deviation...	57
<b>Figure 13</b> Specific growth ( $\mu$ ) (A) and death ( $k_d$ ) (B) rates calculated differentially between the time points of each sample of the cultures inoculated in CHOMACS CD growth medium containing 0 vol% and 25 vol% conditioned medium (CM). The values given in the graphs were calculated as the average of the triplicate cultures and the error bars represent the standard deviation. ....	58
<b>Figure 14</b> Glucose concentration ( $c_{Glc}$ ) (A) of the cultures throughout the cultivation and the glucose consumption rate ( $q_{s,Glc}$ ) (B) plotted against the average glucose concentration between the corresponding time-points of the cultures inoculated in CHOMACS CD growth medium containing 0 vol% and 25 vol% conditioned medium (CM). The values given in the graphs were calculated as the average of the triplicate cultures and the error bars represent the standard deviation. ....	59
<b>Figure 15</b> Glutamine concentration ( $c_{Gln}$ ) (A) of the cultures throughout the cultivation and the glutamine consumption rates ( $q_{s,Gln}$ ) (B) plotted against the average glutamine concentration between each time-point. The values given in the graphs were calculated as the average of the triplicate cultures and the error bars represent the standard deviation. ....	60
<b>Figure 16</b> Lactate concentration ( $c_{Lac}$ ) profiles (A) of the cultures and the lactate production rates ( $q_{p,Lac}$ ) (B) plotted against the average lactate concentration between each time-point of the cultures inoculated in CHOMACS CD growth medium containing 0 vol% and 25 vol% conditioned medium (CM). The values given in the graphs were calculated as the average of the triplicate cultures and the error bars represent the standard deviation. ....	61
<b>Figure 17</b> Total cell density ( $N_t$ ) of the cultures supplemented with the < 10 kDa and > 10 kDa fractions (A) and cultivated in either conditioned medium (CM) or fresh medium (FM) (B). Furthermore, the respective specific growth rates ( $\mu$ ) calculated differentially between the time-points of each sample are also shown (C, D). The values represent the average calculated for the corresponding triplicate cultures and the error bars display the standard deviation. ....	62
<b>Figure 18</b> Significance analysis performed to determine the degree of similarity between the progressions of the specific growth rate of each culture. ....	63

<b>Figure 19</b> Viability of the cultures supplemented with the < 10 kDa and > 10 kDa fractions (A) and the cultures cultivated with either conditioned (CM) or fresh medium (FM) (B), and the respective specific death rates ( $k_d$ ) calculated differentially between the time-points of each sample (C, D). The values represent the average calculated for the corresponding triplicate cultures and the error bars display the standard deviation. ....	66
<b>Figure 20</b> Significance analysis performed to determine the degree of similarity between the progressions of the specific death rate of each culture.....	67
<b>Figure 21</b> Total cell density ( $N_t$ ) (A) and viability (B) measured at 0, 23 and 49 hours of cultivation for the cultures inoculated at a low cell density in growth medium containing 17 vol%, 58.6 vol% and 100 vol% conditioned medium (CM) .....	69
<b>Figure 22</b> Specific growth rates ( $\mu$ ) calculated differentially between the time-points of each sample for the cultures inoculated at a low cell density in growth medium containing 17 vol%, 58.6 vol% and 100 vol% conditioned medium (CM) .....	70
<b>Figure 23</b> Specific death rates ( $k_d$ ) calculated differentially between the time-points of each sample for the cultures inoculated at a low cell density in growth medium containing 17 vol%, 58.6 vol% and 100 vol% conditioned medium (CM) .....	71
<b>Figure 24</b> Specific growth rates ( $\mu$ ) of the cultures inoculated at a low cell density in growth medium containing 17 vol%, 58.6 vol% and 100 vol% conditioned medium (CM) compared to the specific growth rate of the parent culture. ....	72
<b>Figure 25</b> Specific death rates ( $k_d$ ) of the cultures inoculated at a low cell density in growth medium containing 17 vol%, 58.6 vol% and 100 vol% conditioned medium (CM) compared to the specific death rate of the parent culture. ....	73
<b>Figure 26</b> Total cell densities ( $N_t$ ) (A) and the specific growth rates ( $\mu$ ) (B) calculated differentially between the time-points of each sample for the young (YPC) and the medium aged (MPC) parent culture. Cultivation of the parent cultures was not performed in triplicates and the $N_t$ and viability were determined once from a single sample, for this reason no error bars are available .....	75
<b>Figure 27</b> Total cell density ( $N_t$ ) (A) and viability (B) of the cultures inoculated in 100% fresh CHOMACS CD. LCD1 and MCD1 were inoculated from the young parent culture (YPC). LCD2 and MCD2 were inoculated from the medium aged parent culture (MPC). The columns correspond to the average calculated for the corresponding triplicate cultures and the error bars display the standard deviation. ....	76
<b>Figure 28</b> Specific growth rates ( $\mu$ ) of the inoculated cultures compared to the specific growth rate of their respective parent culture. The values of the inoculated cultures represent the average calculated for the corresponding biological triplicate and the error bars display the standard deviation. The columns representing the parent cultures do not show any error bars, since no triplicate cultures were performed and the $N_t$ and viability were determined once from a single sample.....	77
<b>Figure 29</b> Specific death rates ( $k_d$ ) of the inoculated cultures compared to the specific death rate of their respective parent culture. The values of the inoculated cultures represent the average calculated for the corresponding biological triplicate and the error bars display the standard deviation. The columns	



## LIST OF FIGURES

---

representing the parent cultures do not show any error bars, since no triplicate cultures were performed and the $N_t$ and viability were determined once from a single sample.....	78
<b>Figure 30</b> Viability of the cultures plotted against their corresponding total cell density ( $N_t$ ) (A) and the specific death rate ( $k_d$ ) plotted against the $N_t$ averaged between the time-point of each sample (B) .....	80
<b>Figure 31</b> Total cell density normalized death rates of the inoculated cultures .....	80
<b>Figure 32</b> pH ( $\circ$ ) and conductivity ( $\blacksquare$ ) values plotted against the volumetric ratio of Buffer B for the pre-mixed elution buffers (A) and the collected fractions (B). .....	83
<b>Figure 33</b> Protein recovered in each fraction of the pH-gradient elution experiment. The error bars display the standard deviation from the three measures samples. ....	84
<b>Figure 34</b> SDS-Page showing the precipitated fractions (lanes 3-8), conditioned medium (lane 1) and adjusted load material (lane 2). The conditioned medium was harvested in the late exponential phase of growth. Capture was performed at pH 3. Elution from the membrane was achieved through the stepwise pH increase of the mobile phase: Lane 3: pH 4.36; Lane 4: pH 5.73; Lane 5: pH 6.42; Lane 6: 7.03; Lane 7: pH 8.58; Lane 8: pH 9.98.....	85
<b>Figure 35</b> Protein recovered in each fraction of the TE1 experiment. The error bars display the standard deviation from the three measures samples. ....	86
<b>Figure 36</b> Protein recovered in each fraction of the TE2 experiment. The error bars display the standard deviation from the three measures samples. ....	87
<b>Figure 37</b> Total cell density ( $N_t$ ) (A), percentage of apoptotic cells (apop%) (B) and viability (C) measured for the culture supplemented with the pooled fractions (E1) and the negative control (NC). The values of the graph represent the average calculated for the triplicate cultures and the error bars display the standard deviation. ....	88
<b>Figure 38</b> Specific growth ( $\mu$ ) (A), apoptosis ( $k_{ap}$ ) (B) and death ( $k_d$ ) (C) rates calculated differentially between the time-points of each sample. The graphs show the average of the triplicate cultures and the error bars depict the standard deviation. ....	90
<b>Figure 39</b> Glucose concentration ( $c_{Glc}$ ) (A) and the glucose consumption rate ( $q_{s,Glc}$ ) calculated differentially between the time-points of each sample, plotted against the average glucose concentration between each time-point (B). The error bars display the standard deviation of the triplicate cultures. ...	91
<b>Figure 40</b> Glutamine concentration ( $c_{Gln}$ ) (A) and the glutamine consumption rate ( $q_{s,Gln}$ ) calculated differentially between the time-points of each sample, plotted against the average glutamine concentration between each time-point (B). The error bars display the standard deviation of the triplicate cultures. ...	92
<b>Figure 41</b> Lactate concentration ( $c_{Lac}$ ) (A) and lactate production rate ( $q_{Lac}$ ) plotted against the average lactate concentration used to determine each rate (B) of the E1 and NC calculated as the average of each triplicate culture with the error bars displaying the standard deviation. ....	94
<b>Figure 42</b> Protein recovered in each fraction of the TE3 experiment. The error bars display the standard deviation from the three measures samples. ....	95

---

---

<b>Figure 43</b> Specific growth ( $\mu$ ) (A) and death ( $k_d$ ) (B) rates calculated for the culture supplemented with the elution E2 fraction (E2) and the negative control (NC). The values given in the graphs show the average calculated for each triplicate culture and the error bars display the standard deviation. ....	96
<b>Figure 44</b> Viable cell density ( $N_v$ ) to glucose yield ( $Y_{x/s, Glc}$ ) (A) and the lactate to glucose yield ( $Y_{p/s}$ ) (B) calculated after the 25 hours of cultivation. The values given in the graphs show the average calculated for each triplicate culture and the error bars display the standard deviation. ....	96
<b>Figure 45</b> Accumulated protein recovered in the fractions of elution E1 and E2 of the first optimization experiment E2.EXP1. The error bars display the standard deviation of the three samples measured. ....	97
<b>Figure 46</b> Protein recovered in each fraction of the stepwise salt gradient of the elution E2 from the E2.EXP1 experiment. The error bars display the standard deviation of the three samples measured. ....	98
<b>Figure 47</b> Accumulated protein recovered in the fractions of elution E1 and E2 of the second optimization experiment E2.EXP2. The error bars display the standard deviation of the three samples measured. ....	99
<b>Figure 48</b> Protein recovered in each fraction of the stepwise salt gradient of the elution E2 from the second optimization experiment E2.EXP2. The error bars display the standard deviation of the three samples measured. ....	100
<b>Figure 49</b> Specific growth rate ( $\mu$ ) of the cultures supplemented with the fractions X0 X5 from the first optimization experiment E2.EXP1. No error bars are displayed, since the screening was performed without biological replicates. ....	101
<b>Figure 50</b> Specific growth rate ( $\mu$ ) of the cultures supplemented with the fractions X1.C – X1.4 from the second optimization experiment E2.EXP2. The values were calculated as the average of the triplicate cultures and the error bars display the standard deviation. ....	102
<b>Figure 51</b> Specific death rate ( $k_d$ ) of the cultures supplemented with the fractions X1.C – X1.4 from the second optimization experiment E2.EXP2. The values were calculated as the average of the triplicate cultures and the error bars display the standard deviation. ....	103
<b>Figure 52</b> Protein recovered in each fraction of the two-step elution CE9. Fraction X3 was used for the screening of optimal binding conditions for the Phenyl membrane. The error bars display the standard deviation of the three samples measured. ....	106
<b>Figure 53</b> Protein recovered in each fraction of the two-step elution CE10. Fraction X4 was used for binding into the Phenyl membrane under optimized conditions. The error bars display the standard deviation of the three samples measured. ....	108
<b>Figure 54</b> Specific growth rates ( $\mu$ ) calculated after 23 hours of cultivation for the experiment performed to examine the effect of the elution E2 fraction X4. The values were calculated as the average of the triplicate cultures and the error bars display the standard deviation. ....	110
<b>Figure 55</b> Percentile decrease in $\mu$ between LCD and LCD N30, and MCD CM and NC30. ....	111

## LIST OF FIGURES

---

<b>Figure 56</b> Specific death rates ( $k_d$ ) calculated after 23 hours of cultivation for the experiment performed to examine the effect of the elution E2 fraction X4. The values were calculated as the average of the triplicate cultures and the error bars display the standard deviation. ....	112
<b>Figure 57</b> Specific growth rate ( $\mu$ ) of the cultures supplemented with either the HIC elution (HE) or phosphate buffer (Phos NC) and cultivated in either conditioned (NC CM) or fresh (NC FM) medium. The values correspond to the average of the triplicate cultures and the error bars display the standard deviation. ....	113
<b>Figure 58</b> Percentile reduction determined after supplementation of the fraction X4 from elution E2 (left column) and the HIC elution HE (right column). ....	115
<b>Figure 59</b> Specific death rate ( $k_d$ ) of the cultures supplemented with either the HIC elution (HE) or phosphate buffer (Phos NC) and cultivated in either conditioned (NC CM) or fresh (NC FM) medium. The values correspond to the average of the triplicate cultures and the error bars display the standard deviation. ....	116
<b>Figure 60</b> Viable cell density ( $N_v$ ) to glucose yield ( $Y_{x/s, Glc}$ ) of the cultures supplemented with either the HIC elution (HE) or phosphate buffer (Phos NC) and cultivated in either conditioned (NC CM) or fresh (NC FM) medium. The values correspond to the average of the triplicate cultures and the error bars display the standard deviation. ....	117
<b>Figure 61</b> Percentile change in $Y_{x/s, Glc}$ of the cultures between 0 - 21 and 0 - 46 cultivation hours. ....	118
<b>Figure 62</b> Viable cell density ( $N_v$ ) to glutamine yield ( $Y_{x/s, Gln}$ ) of the cultures supplemented with either the HIC elution (HE) or phosphate buffer (Phos NC) and cultivated in either conditioned (NC CM) or fresh (NC FM) medium. The values correspond to the average of the triplicate cultures and the error bars display the standard deviation. ....	119
<b>Figure 63</b> Percentile change in $Y_{x/s, Gln}$ of the cultures between 0 - 21 and 0 - 46 cultivation hours. ....	120
<b>Figure 64</b> Lactate to glucose yield ( $Y_{p/s}$ ) of the cultures supplemented with either the HIC elution (HE) or phosphate buffer (Phos NC) and cultivated in either conditioned (NC CM) or fresh (NC FM) medium. The values correspond to the average of the triplicate cultures and the error bars display the standard deviation. ....	121

---

## List of Tables

<b>Table 1</b> Pipetting scheme for the inoculation of the experiment “Separation of the Components in Conditioned Medium by Molecular Weight (cutoff 10 kDa)”.....	30
<b>Table 2</b> Pipetting scheme for the inoculation of the experiment “Effects of the Conditioned to Fresh Medium Ratio” .....	31
<b>Table 3</b> Cultures inoculated in 100% fresh CHOMACS CD medium for the experiment "Effect of the Age of the Parent Culture". The parent culture used, and the starting cell density and viability are shown....	32
<b>Table 4</b> List of buffers used with Sartobind S .....	34
<b>Table 5</b> List of batch cultivations performed for the generation of conditioned medium.....	36
<b>Table 6</b> pH and conductivity of the pre-mixed buffers used for the recovery of each fraction and the corresponding elution volumes. ....	38
<b>Table 7</b> Fractions collected from all three two-step elution experiments with their respective elution volumes and the manner they were recovered from the membrane.....	39
<b>Table 8</b> NaCl concentration profile used for E2.EXP1 together with the corresponding elution volumes. A total of 6 fractions were collected covering a concentration range between 0 and 1 M. ....	41
<b>Table 9</b> NaCl concentration profile used for the second optimization experiment E2.EXP2 and the corresponding elution volume of each one of the seven collected fraction. ....	41
<b>Table 10</b> List of two-step elution experiments performed in this chapter and their corresponding binding pH and conductivities, the conditioned medium used, the total protein loaded, the percentage of the membrane dynamic binding capacity used and the size of the membrane adsorber. ....	42
<b>Table 11</b> Volume of pre-culture, fraction and BoC2 buffer used for the supplementation of each culture and negative control, together with the NaCl concentration ranges calculated for the cultures supplemented with fraction and the final salt concentration of the negative controls. ....	45
<b>Table 12</b> Volume of pre-culture, fraction and BoC2 buffer used for the supplementation of each culture and negative control, together with the NaCl concentration ranges calculated for the cultures supplemented with fraction and the final salt concentration of the negative controls. ....	47
<b>Table 13</b> Batch cultivations performed for the generation of the conditioned medium used for the development of the HIC purification step.....	48
<b>Table 14</b> , binding pH and conductivity, conditioned medium used, amount of loaded protein, percentage of membrane binding capacity used and size of the membrane of both two-step elution experiments performed to generate the fractions of elution E2 used for the development of the HIC purification step. ....	49

## LIST OF TABLES

---

<b>Table 15</b> Fractions collected in both two-step elution experiments, the method of elution and their respective elution volumes.....	49
<b>Table 16</b> List of the experiments performed with different salt species at different concentrations for the screening of optimal binding conditions.....	50
<b>Table 17</b> Composition of the different buffers used with the phenyl membrane adsorber.....	50
<b>Table 18</b> Amount of salt, buffer HB and Elution E2 from CE9 given to each reaction tube, followed by the load volume, the final salt concentration including the NaCl concentration of E2, and final pH after adjustment.....	51
<b>Table 19</b> Cultures inoculated for the examination of the effect of fraction X4 from the elution E2 from the CE10 two-step elution experiment.....	53
<b>Table 20</b> Pipetting scheme used for the inoculation of the cultures used to examine the effect of fraction X4 from the elution E2 from the CE10 two-step elution experiment.....	54
<b>Table 21</b> Amount of NaCl and volume of buffer HB added for the adjustment of elution E2 fraction X4 to binding conditions. The protein material recovered from this experiment was tested on growing cells.....	55
<b>Table 22</b> Pipetting scheme used for the inoculation of the cultures used to examine the effect of the HIC elution (HE) from the 3 M NaCl experiment.....	56
<b>Table 23</b> Coincidence % of the specific growth rate between the cultures compared and determined by calculating the ratio of the number of time intervals without significant differences ( $p > 0.05$ ) to the total amount compared, in this case 7 per culture.....	64
<b>Table 24</b> Matrix displaying the percentile differences calculated for each time interval that showed significant differences ( $p < 0.05$ ). A negative value means that $\mu$ of either the $< 10$ kDa or the CM was lower than the compared culture. A positive value means the opposite.....	65
<b>Table 25</b> Coincidence % of the specific death rates between the cultures compared and determined by calculating the ratio of the number of time intervals without significant differences ( $p > 0.05$ ) to the total amount compared, in this case 7 per culture.....	68
<b>Table 26</b> , significance values calculated from the student's t-test after comparing the $\mu$ of each inoculated culture against each other.....	77
<b>Table 27</b> Significance values calculated from the student's t-test after comparing the $k_d$ of each inoculated culture against each other.....	79
<b>Table 28</b> , p-values calculated from the significance analysis, in which the total cell density normalized death rates were compared against each other.....	80
<b>Table 29</b> Total protein loaded, percentage of membrane binding capacity used and total recovery yield for each experiment of the screening for optimal binding conditions.....	107

---

**Table 30** Total protein loaded, percentage of dynamic membrane capacity used and total protein collected in the different fraction of the 3 M NaCl experiment. Fractions HE1, HE2 and HE3 were pooled together and tested on growing cells. .... 109

**Table 31** Compilation of the accumulated recovery yields of elutions E1 and E2, total recovery yield, the volume of the membrane and whether protein quantification was performed prior to freezing and storing for every cation exchanger experiment performed. .... 126

# 1 Motivation and Objectives

The rapid growth of the biopharmaceutical industry in the recent years and the growing demand to increase volumetric productivity make the optimization of mammalian cell culture processes crucial. The most common strategies include cell line development, medium design, process control (e.g. complex feeding strategies) and mathematical modeling. Yet, little attention has been given to extracellular signaling molecules and intercellular communication.

Mammalian cells react to external stimuli through a series of chemical reactions known as biochemical and signaling pathways. This mechanism helps the cells to adapt to changing environments and is highly regulated. Physical, chemical and biological stimuli to which the cells continuously react include changes in temperature, substrate concentration, metabolic waste products, pH, osmolarity, and growth and autocrine factors. The latter are usually peptides and proteins that interact with highly specialized receptors at the cell surface. They are responsible for the regulation of many cellular processes like proliferation, colony formation, cell survival, adhesion, differentiation and growth inhibition. While growth factors are routinely supplemented to serum-free growth medium in a recombinant form, autocrine factors are produced by the cells themselves and accumulate, creating the so called conditioned medium. The identification of autocrine factors and the thorough understanding of the mechanisms by which they interact with the cells, the cultivation parameters responsible for their production and which biochemical cascades are regulated, could potentially lead to the development of better cultivation strategies and a more specialized growth medium design.

The objectives of this work were the examination of the effect of conditioned medium on the growth and metabolic kinetics of CHO-K1 cell culture and the development of a method for the capture, recovery and fractionation of the bioactive molecules responsible for the effects. This was accomplished through membrane adsorption chromatography and the assessment of the recovered fractions was performed on exponentially growing cells.

## 2 Introduction

### 2.1 Cell Culture Technology in the Biopharmaceutical Industry

Since the clinical approval of human plasminogen activator (tPA Activase) in 1986, Chinese Hamster Ovary (CHO) cells have become the most important cell line for the industrial production of recombinant therapeutic proteins. More than 50% of the over 100 approved protein pharmaceuticals are produced in CHO cells with growing global annual revenue of over US\$100 billion. These cells are highly adaptable, can grow to high cell densities in suspension and serum-free medium, production can be scaled up to working volumes of 20,000 l, and perform posttranslational modifications on the recombinant protein (Bandaranayake, Almo 2014; Zhu 2012; Wurm 2004; Wurm, Hacker 2011). Process optimization, media and feed development, and cell line development and engineering has led to productivities of up to 15 g/l (Gronemeyer et al. 2014). Furthermore, a perfusion process in a wave reactor utilizing tangential flow filtration has reached a final cell density of  $2.14 \times 10^8$  cells/ml (Clincke et al. 2013).

The first CHO cells were isolated 1956 from a spontaneously immortalized population of fibroblast cells from the cultures ovarian cells of partially inbred Chinese hamster. Several cell lines with different characteristics, nevertheless with a common proline synthesis deficiency, belong to the CHO designation. These include CHO-K1, isolated in 1957, its descendant DXB11, isolated in 1980, and CHO-DG44 (Wurm, Hacker 2011).

### 2.2 Cell Metabolism

The metabolism of mammalian production cell lines is compartmentalized and takes place either in the cytosol or in the mitochondria. Glucose and glutamine are the main substrates used for the production of the ATP and NADH necessary to sustain the anabolic functions of the cells. The main metabolic pathways are glycolysis, pentose phosphate pathway (PPP), the tricarboxylic acid (TCA) cycle, glutaminolysis and oxidative phosphorylation. Consumption of the substrates is deregulated and depends strongly on their concentration in the growth medium (Ozturk, Hu 2005; Gupta et al. 2017). The metabolism of production cell lines resembles that of cancer cells and is characterized by a high glucose uptake and its conversion to lactate under fully aerobic conditions, coupled with a constrained incorporation of pyruvate into the TCA cycle (WARBURG 1956). Between 75% and 90% of the consumed glucose is transformed into lactate after glycolysis by the enzyme lactate dehydrogenase



(LDH), while 4% - 8% is used for the generation of nucleotide precursors through the PPP, and < 10% is oxidized to CO<sub>2</sub> in the TCA cycle (Figure 1) (Mulukutla et al. 2010; Young 2013; Ozturk, Hu 2005).

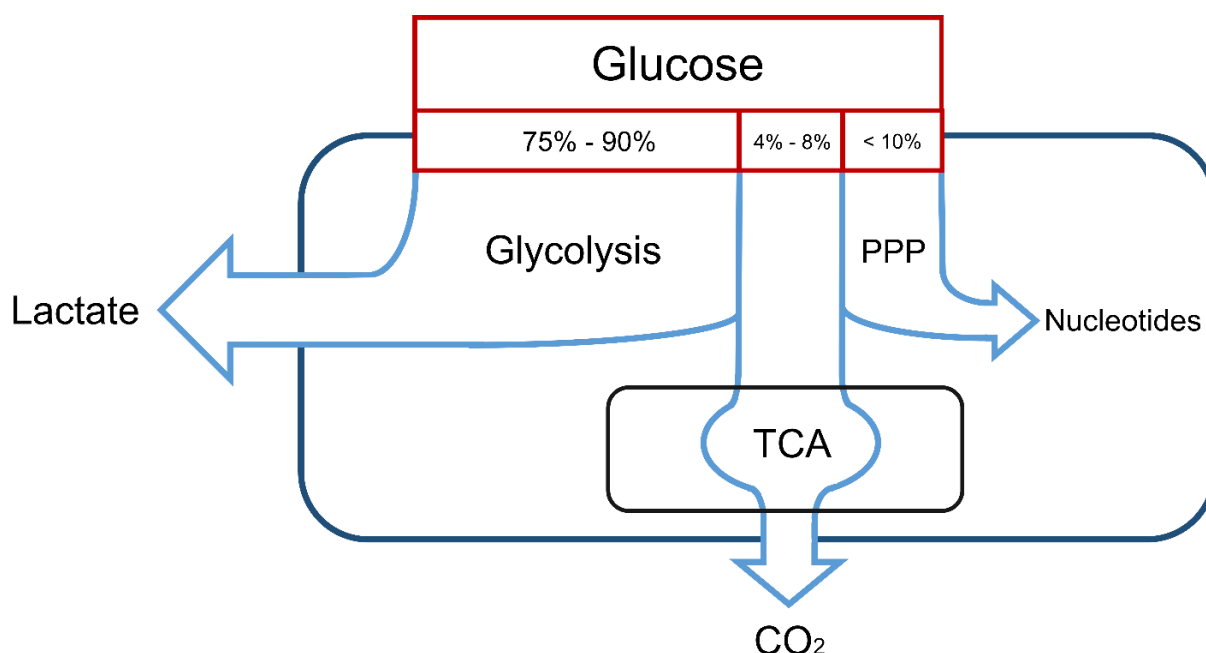


**Figure 1** Fate of the glucose transported into CHO cells during the exponential phase of growth. Between 75% - 90% is transformed into lactate through the glycolytic pathway, while 4% - 8% is fully oxidized into CO<sub>2</sub> in the tricarboxylic acid (TCA) cycle inside of the mitochondrion. Less than 10% is diverted into pentose phosphate pathway (PPP) for the synthesis of nucleotides.

This energetic inefficient behavior has been linked to the overexpression of several glycolytic enzymes, especially GLUT1, a high-affinity glucose transporter, and hexokinase 2 (HK2), the initial glycolytic enzyme, and the downregulation of enzymes responsible for the mitochondrial translocation and oxidation of glucose derived pyruvate. This peculiarities have been correlated with the deregulation of the transcription factors cMyc and hypoxia-inducible factor 1 (HIF1), and the insulin pathway's downstream effector Akt (Mulukutla et al. 2010; Young 2013). The high energy demand of exponentially growing cells, in combination with the poor pyruvate translocation from the cytosol into the mitochondrion and the depletion of citrate due the lipid generation, requires anaplerotic reactions for the replenishment of intermediates to keep the TCA cycle operating. This is accomplished by the transformation of glutamine to glutamate and ammonium by the phosphate activated glutaminase (PAG) enzyme at the mitochondrial membrane.

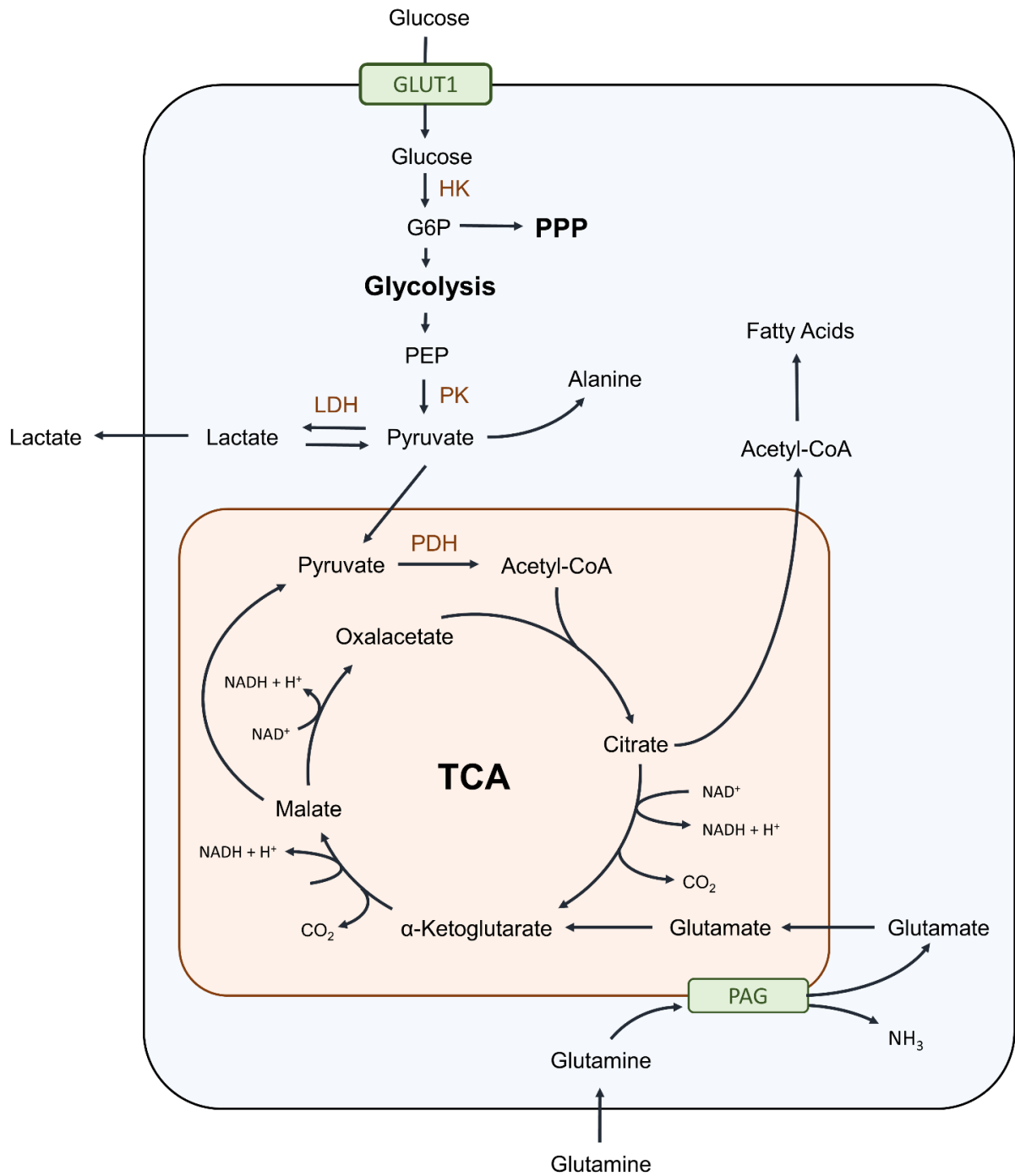


**Figure 2** Simplified depiction of the main pathways by which the two main substrates, glucose and glutamine are metabolized inside of the cell. Glucose is transported across the plasma membrane through the glucose transporter 1 (GLUT1). Glucose is then transformed into glucose-6-phosphate (G6P) by the enzyme Hexokinase (HK). G6P can then either be diverted into the pentose phosphate pathway (PPP) or into the glycolytic pathway generating phosphoenolpyruvate (PEP). PEP is transformed into pyruvate by the enzyme pyruvate kinase (PK). Pyruvate can be then transformed into alanine or into lactate by the enzyme lactate dehydrogenase (LDH). Pyruvate can also be transported into the mitochondrion, where it enters the tricarboxylic acid (TCA) cycle after being transformed into acetyl-CoA by the enzyme pyruvate dehydrogenase (PDH). Glutamine is transformed to glutamate and ammonium by the phosphate activated glutaminase (PAG) enzyme at the mitochondrial membrane. Glutamate then enters the TCA cycle inside of the mitochondrion and can be transformed into malate, then pyruvate and end with the production of lactate in a process called glutaminolysis.

The glutamate is then transported into the mitochondrion where it is deamidated to  $\alpha$ -ketoglutarate and enters the TCA cycle. Deamidation can occur either through glutamate dehydrogenase (GDH), releasing a second ammonium, or through the action of transaminases, producing alanine when combined with pyruvate, or aspartate when combined with oxaloacetate. Once in the TCA cycle, the glutamate can be used for the synthesis of lipids and other precursors like pyridine, purine, amino-sugars, NAD, and asparagine. Furthermore, it can be transformed into lactate through malate or undergo complete oxidation to CO<sub>2</sub> in a process called glutaminolysis (Ozturk, Hu 2005; Moreadith, and Lehninger 1984; Mulukutla et al. 2010; Young 2013). The rapid and inefficient consumption of glucose and glutamine leads to the accumulation of lactate and ammonium which can be detrimental to the cell growth. Lactate is associated with the acidification of the growth medium, increase in osmolarity and cell growth inhibition at concentrations higher than 20 mM. Ammonium has been associated with growth inhibition at concentrations higher than 2 – 4 mM (Ozturk, Hu 2005).

The metabolism of the cell can adapt to changing conditions and is influenced by the available substrates and the cultivation environment previously experienced. This has an ultimate effect on the specific growth and death rates of the cells and determines how substrates, the recombinant product and byproducts are consumed or produced (Ozturk, Hu 2005). Understanding the parameters that affect consumption and production rates is crucial for the development of cultivation strategies in which a maximal productivity is achieved and the accumulation of inhibitory byproducts is minimized. The characterization of a batch cultivation through the specific growth rate of the cells results in the identification of three main growth phases with distinct metabolic states. During the exponential growth phase the cells proliferate rapidly and consume glutamine and glucose at high rates, accumulating lactate, alanine, and ammonium, among other byproducts. The stationary phase follows, where the growth stagnates, the substrates become limiting and the production of lactate decreases or is even consumed. The last stage is the decline phase, characterized by the decrease of the cell density, loss of viability, depletion of substrates and consumption of byproducts. Metabolic flux analysis (MFA) performed by Templeton et al. (2013) showed that antibody production by CHO cells was at its highest in the stationary phase, when the oxidative state of the cells was at its maximum, most of the energy was produced in the TCA cycle and lactate was being consumed instead of produced. Furthermore, glucose was being diverted to the PPP in the late exponential and stationary phases. Wahrheit et al. (2014) identified through MFA three different metabolic states that corresponded to the phases of growth: Overflow metabolism, balanced metabolism and maintenance metabolism. The inefficient overflow-metabolism happened at the beginning of the cultivation at abundant substrate concentrations, and was characterized by a high uptake of glucose and glutamine, and high glycolytic

## 2. INTRODUCTION

---

and glutaminolytic activities, coupled with high anabolic activity and energy spilling in form of the productions of byproducts. The change to the balanced metabolism, characterized by comparable catabolic and anabolic activities, happened after glutamine was depleted, which resulted in a decrease in the specific growth rate. A net consumption of lactate occurred and glycolytic activity decreased. Additionally, the activity of glycolytic enzymes was examined using selective permeabilization techniques to distinguish between cytosolic and mitochondrial activities. Wahrheit et al. (2014) argued that in the overflow state, glycolytic enzymes associate with each other, thus channeling the substrate more efficiently and ending in the overproduction and accumulation of lactate in the cytosol. Moreover, it was suggested that Hexokinase (HK), which is the rate limiting non-reversible reaction of the glycolytic pathway, associates with the mitochondrion, thus allowing better supply of ATP and stimulating glycolytic flux. Dissociation of glycolytic enzymes at lower glucose concentrations or due to acidification of the cytosol pH, and better availability of pyruvate and its replenishment through the consumption of lactate, allows a better connectivity between glycolysis and the TCA cycle, resulting in a more balanced metabolic state.

A metabolic shift in which the cells change from lactate production to consumption has been widely studied and its mechanism is not well understood. Experiments using different substrates and feeding strategies have shed some light on the regulation of lactate production and the modulation of the metabolic shift. Experiments using a mixture of different ratios of glucose and galactose, which is metabolized at a lower rate, showed that high glucose concentrations result in a high production of lactate. Once glucose is depleted consumption of galactose and lactate is triggered (Wilkens et al. 2011). Furthermore Li et al. (2012) showed that feeding sodium pyruvate at the time of the metabolic shift can be used to extend the lactate production phase and prolong its depletion. These experiments showed that lactate metabolism might be closely related to the production of ammonium and to the alanine metabolism. Alanine, also produced from pyruvate, accumulated throughout the cultivation. Once lactate was depleted, consumption of alanine was triggered, presumably via alanine dehydrogenase or alanine transaminase, producing and accumulating ammonium. In other words, feeding pyruvate during the cultivation caused a short boost of lactate production, prevented alanine consumption and lowered ammonium concentration. Nevertheless, lactate consumption was never completely hindered. A further experiment in which sodium lactate was fed at the time of metabolic shift, also showed the same decrease in production of ammonium. Luo et al. (2012) studied the effect of copper, an essential cofactor for mitochondrial function, while analyzing relevant metabolites. The results showed that lactate consumption was favored in conditions of high copper. Low copper conditions was related to lactate production and the accumulation of many intracellular metabolites,

especially alanine. Luo et al. (2012) argued that impaired mitochondrial function caused these metabolites to accumulate in the cell, and that with an adequate respiratory capacity, the cells would not need to generate energy via glycolysis. Zagari et al. (2013) examined the role of glutamine on lactate metabolism. Experiments at different glucose concentrations showed little influence, while supplementing glutamine before its depletion induced an almost stoichiometric increase in lactate production. Zagari et al. (2013) argued that lactate was produced through glutaminolysis. This contrasts with the data from Wilkens et al. (2011), in which the glucose concentration had a clear influence in the production of lactate. Proteomic analysis of cells going through metabolic shift and glucose limitation has shown a strong decrease in the expression of  $\alpha$ -enolase (Pascoe et al. 2007; Wingens et al. 2015). Pascoe et al. (2007) associated this down-regulation with the steady decrease in glucose uptake rate linked to glucose depletion during the time course of a cultivation. It is important to consider that each cell line and subclone is different and will show different lactate profiles to different substrates and feeding strategies. (Wilkens et al. 2011; Luo et al. 2012; Li et al. 2012; Zagari et al. 2013)

### 2.3 Medium Design

The growth medium of production cell lines must contain the necessary components to support the high glucose and glutamine demands of exponentially growing cells and the production of the recombinant product, while ensuring cell survival and the consistent quality of the product. In the past *in vitro* cultivation of mammalian cells was performed in biological fluids like serum and blood extracts. The reduction of the media components to the minimum required to support cell growth led to the development of chemically defined basal media like Eagle's basal media (EBM) and *Dubelcco's* modified Eagle medium (DMEM). The composition of basal media varies depending on the cell line and consists typically of extra purified water, salt, glucose and other carbon sources, essential and non-essential amino acids, trace elements and vitamins. These media are usually supplemented with serum from animal of human origin to supply the cells with growth factors, protective elements, carrier proteins and micronutrients (Ozturk, Hu 2005).

Supplementation with serum or other components from animal origin is widely avoided in the industrial manufacturing of therapeutic bioproducts due batch to batch variations, limited availability, high cost and high protein content, which makes downstream processing more challenging. In addition, waste products and proteases contained in serum can be detrimental to cell growth and the quality of the product. There is also the potential risk of transferring contaminants like viruses, mycoplasma and

prions into the final product (Liu, Morrow 2016; Ozturk, Hu 2005; Zhu 2012). Examples for the replacement of components from animal origin include bovine serum albumin, which can be substituted with recombinant albumin or cyclodextrin as carriers for lipids. Transferrin, which binds iron and transports it into the cell through specific cell surface receptors can be replaced by selenite or other ferrous salts in combination with sodium citrate. Selenite has also shown to be effective in transporting iron and other trace metals into the cells, additionally to its antioxidant and detoxifying effects (Zhang et al. 2006; Bai et al. 2011).

The development of complex serum-free growth media for a specific cell line is often empirical, time consuming and labor intensive. Nevertheless it has often led to an increase in productivity, efficiency and cost effectiveness of the process. There are several approaches for medium development, and one of them is the supplementation of basal medium with components from defined sources like hormones, growth factors, carrier molecules and a variety of small molecules that include aromatic carboxylic acids, hydroxamic acids and acetamides. Their effect on the cell culture can be assessed one at a time. Statistical methods like design of experiments (DoE) and Plackett-Burman design allow the testing of simultaneous components and their interaction with each other, thus reducing the optimization time and increasing efficiency (Zhang et al. 2013a; Liu, Morrow 2016; Allen et al. 2008; Gronemeyer et al. 2014).

Plant and yeast hydrolysates have been used as undefined substitutes for serum. They have been associated with an overall improvement of cell culture performance, as they serve as a source of vitamins, lipids, minerals, and di- and tri-peptides (Heidemann et al. 2000; Spearman et al. 2014; Mosser et al. 2013). Furthermore, it has been shown that their effect is not solely nutritional, but some peptides, especially tripeptides composed of glycine, alanine, serine, threonine, lysine and histidine, act as growth factors promoting cell growth and enhancing the viability of the culture and the production of the recombinant protein (Franek et al. 2000; Franěk, Katinger 2002; BURTEAU et al. 2003)

Proliferation, mitogenesis, survival, attachment and differentiation of mammalian cells are controlled by polypeptide growth factors, which include fibroblast growth factors (FGF), insulin-like growth factors (IGF), epithelial growth factor (EGF), nerve growth factor (NGF), platelet derived growth factor (PDGF) and transforming growth factor (TGF). They are usually active at a concentration range of 1 – 10 ng/ml and must be supplemented to serum-free basal medium (Ozturk, Hu 2005). Production cells lines usually have lower growth factors requirements. Nevertheless, the exponential growth phase during a batch cultivation is short. This is not exclusively the effect of nutrient depletion and the

accumulation of by-products, but rather the rapid consumption mitogenic growth factors responsible for the stimulation of cellular growth. These growth limiting factors have been identified as Insulin and IGF-I (Ljunggren, Häggström 1995; Mamounas et al. 1989).

Insulin and IGF-I belong to the insulin family of hormones and are known to regulate carbohydrate, lipid, protein metabolism, glucose and amino acid transport, DNA synthesis and cell division through the generation of transmembrane signals. Moreover, IGF-I has been shown to promote cell survival by preventing apoptosis and cell death in the absence of serum (Mamounas et al. 1989; Sell et al. 1995; Sunstrom et al. 2000). Recombinant versions of IGF-I can be supplemented to serum-free chemically defined growth media. LongR<sup>3</sup> (LR3), which is a recombinant fusion protein analogue of IGF-I has shown an increase in viability, protein productivity and protein N-glycosilytion (Qian et al. 2017).

### 2.4 Conditioned Medium and the Secretome of CHO-K1

Mammalian cells produce a vast variety of proteins and peptides with diverse physicochemical properties that are released from the cell either through active secretion or as a result of cell lysis following cellular death. The entirety of these molecules is known as the “secretome” and it includes autocrine factors, which regulate cellular processes like cell growth and death, proteolytic enzymes and host cell proteins (HCPs) (Chaudhuri et al. 2015).

During the time course of a cultivation and as the cell density increases, the proteins and peptides of the secretome accumulate and produce the so-called conditioned medium. Its biological activity is well known and has been used for therapeutic applications or made cell-based therapies even possible (Sugino et al. 2016; Johnson et al. 2014; Park et al. 2010; Chen et al. 2014). Its study on a variety of different cell lines has resulted in the isolation and identification of the molecules responsible for the regulation of many cellular processes like proliferation, colony formation, cell survival, adhesion, differentiation and growth inhibition (Zsebo et al. 1990; Burgess et al. 1977; Zeng et al. 1998; Rønning et al. 1991; Lee et al. 1995; Lauffenburger, Cozens 1989).

The regulatory effect of these so called autocrine factors is the result of their interaction with highly specific cell surface receptors and is influenced by the production rate and diffusion coefficient of the factors, binding to and dissociation from the receptors, receptor density, intracellular trafficking and the geometry of the system (Lauffenburger, Cozens 1989). Furthermore, their link to cell density has been studied and it is argued that the higher the cell density, the higher the availability of the factors and the more likely they are to bind to the corresponding cell receptors.

## 2. INTRODUCTION

---

The initial growth rate of some cell lines is deeply affected by the availability of specific growth factors. This gives rise to phenomena like the inoculum density effect, in which a minimal inoculum size is required to stimulate cell proliferation. Through the proteomic analysis of the conditioned medium of CHO cell culture, Lim et al. (2013) was able to identify eight different proteins whose recombinant versions were able to stimulate cellular growth at very low cell densities when supplemented to serum-free growth medium. Spens, et.al (2005) separated the conditioned medium of NS0 myeloma cell cultures through gel filtration and was able to identify fractions with a molecular weight of 20 – 25 kDa that were able to decrease the initial lag phase and increase peak cell density. Dutton et al. (1999) examined the impact of the inoculum size and initial concentration of conditioned medium on the specific growth rate and the maximal cell density of hybridoma cell culture. A correlation between an initial concentration of 30% - 40% conditioned medium with the elimination of initial lag phase and an increase in the viable cell density was observed. Moreover, an increase in conditioned medium was linked to the onset of the decline phase.

Loss of viability and decrease in the specific growth rate at the later stages of a cultivation is usually attributed to the depletion of substrates and amino acids, and to the accumulation of toxic metabolites like ammonia and lactate. Nevertheless, experiments on hybridoma cell culture have suggested the buildup of an unknown inhibitory factor produced by the cells themselves. Dodge et al. (1987) examined the transition into the decline phase of hybridoma cultures at different glucose and conditioned medium concentrations. The dilution with PBS of the conditioned medium in which the cells were growing resulted in the delay of cellular death. Lee et al. (1995) produced chemostate data at different cell densities, glutamine concentrations and oxygen partial pressure. The results showed a linear increase of the specific death rate to an increasing cell density, linking the loss of viability to the production of a non-growth linked autoinhibitor, which seemed to have a greater effect at higher oxygen concentrations. Further examination of conditioned medium harvested at different stages of cultivation from two separate cell lines showed that the autoinhibitor was not cell line specific. Zeng et al. (1998) proposed a kinetic model in which the specific growth rate of the culture can be determined through the concentration of the substrates, inhibitory metabolites and the accumulation of the unknown autoinhibitor up to a critical concentration, after which the growth rate decreases.

Ultrafiltration of conditioned medium and testing of the fraction on growing cells have identified the size of the unknown autoinhibitor at 2000 Da (Dodge et al. 1987) and 3000 Da (Lee et al. 1995). This has led to the development of continuous perfusion processes, in which toxic metabolites and inhibitors are removed from the growth medium, resulting in optimal substrate utilization (Büntemeyer et al. 1992). Nevertheless, the identity of the autoinhibitor remains unknown. In other studies, an autocrine



inhibitor identified as murine  $\beta$ -galactoside binding protein (mGBP) has been isolated from the conditioned medium of embryonic fibroblasts and has shown to be a negative regulator of the cell cycle and inhibit cell proliferation (Wells, Mallucci 1991, 1992).

The composition of the secretome of CHO cell culture, and therefore of its conditioned medium, is affected by a number of factors that include process related parameters and the physiology of the cell. Jin et al. (2010) examined different cultivation process parameters and their influence on the protein profiles of culture supernatants. Temperature shifts, different media components, effect of feeding strategy and bioreactor agitation speed showed a relatively small effect. Generally there were only minor changes in the relative abundance of some proteins, especially in the acidic region, while no different protein species were detected between the tested cultures. The experiments showed that the protein profiles remained relatively stable, as long as the cultures were kept in a healthy state. Furthermore osmolality, dissolved oxygen concentration or ammonium has been reported to have an effect on intracellular processing, and thus cause differences in the glycosylation of recombinant and native proteins (Yuk, 2015). The differences in HCP composition were examined by Woolley et al. (2009) to monitor cellular stress due to nutrient depletion and by-product accumulation. For this purpose protein markers associated to cell death and apoptosis were identified and quantified used SELDI-TOF mass spectroscopy.

The most important parameters influencing the composition of the conditioned medium is the cultivation duration, and the viability and shear stress sensibility of the cells at the time of harvest (Tait et al. 2012; Jin et al. 2010; Valente et al. 2014). Protein concentration in the growth medium of non-recombinant cells remains low throughout cultivation until the cell viability decreases. Jin et al. (2010) studied the effect of the viability and cultivation duration on the HCP profile and found that low molecular weight species were more abundant at day 15 compared to day 9 of cultivation, suggesting protein degradation. Furthermore his 2D-DIGE analysis showed a greater abundance of acidic proteins in younger cultures (Day 9 compared to Day 15). Tait et al. (2012) studied the effect that harvesting time and energy dissipation have on the HCP profile. They described a correlation between the transition from the early decline phase to the steady decrease in viability, with a larger number of spot changes in 2D-gels. Supernatant proteins that showed statistical change with increased harvesting time were shown to be proteins involved in cellular metabolism and protein folding, which are usually considered intracellular. They argued that the cells are more susceptible to shear stress when the viability is higher, and that the harvesting method has a profound effect on the breakage of cells and the release of intracellular proteins.

The secretome has a profound effect on the quality of biopharmaceutical products and the overall performance of bioprocesses. For example, proteolytic enzymes are a cause of product degradation, peptides and proteins may contribute to accumulation of waste products and pH fluctuations during fermentation, and impurities in the end product may cause adverse immunological reactions on patients (Chaudhuri et al. 2015; Singh 2011).

### 2.5 Ion Exchange Chromatography

Ion exchange chromatography (IEX) is widely used for the separation and purification of biological molecules like proteins, peptides and nucleic acids. Its relatively low cost, versatility, scalability, good dynamic binding capacity, simple buffers, high working flow rates and large choice of ligands make it a reliable option for process development (Ng et al. 2009; Ahamed et al. 2008; Shukla, Yigzaw 2007). This method is based on the electrostatic attraction between the active sites in the stationary phase with the molecules in the mobile phase. At specific conditions cation exchangers are negatively charged, while anion exchangers are positively charged. This allows them to bind molecules with the respective opposite charge. The amphoteric residues at the surface of complex biological molecules exhibit different electrostatic charges in aqueous solution according to the  $pK_a$  of each residue. The net surface charge of a molecule is determined as the sum of all its surface charges and it is dependent on the pH of the surrounding matrix. The net surface charge can be predicted with the previous knowledge of the isoelectric point ( $pI$ ), which describes the pH at which the net surface charge of a molecule is equal to zero. This results in a positive and a negative charge at pH values lower and higher than the  $pI$  respectively. Figure 3 shows a representation of the titration curves of an acidic protein (blue curve), a neutral protein (orange curve) and a basic protein (grey curve). Depending on the pH of the solution, the net surface charge of the proteins is either positive or negative, making them able to bind either a cation or an anion exchanger respectively (Ozturk, Hu 2005; Shukla et al. 2006; Fekete et al. 2015).

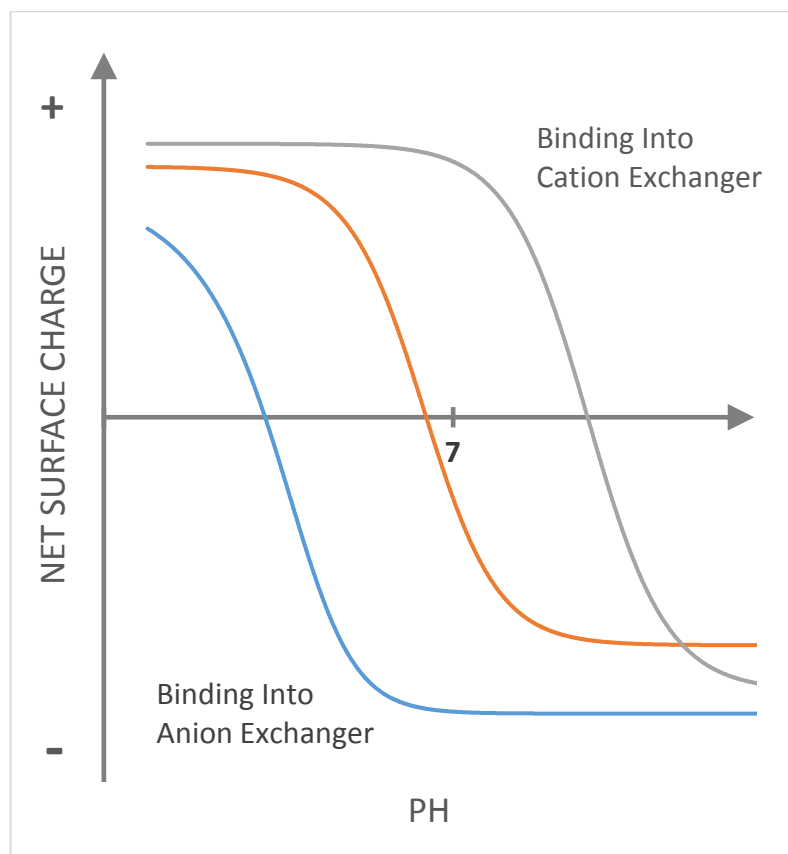


**Figure 3** Representation of the titration curves of an acidic protein (blue curve), a neutral protein (orange curve) and a basic protein (grey curve).

The functional groups in the stationary phase can be classified in strong or weak ion exchangers. This does not describe the strength of the adsorption, but rather how the ionization state of the ligands changes at different pH values. The functional groups of weak ion exchangers are able to lose and take protons due to their intrinsic buffer capacity, resulting in the ion exchanger capacity to be determined by the pH. On the other hand, strong ion exchangers have functional groups with very low or very high pK values that remain fully ionized over wide pH ranges and do not lose ion exchanger capacity (Kröner, Hubbuch 2013; Shukla et al. 2006; Kopaciewicz, Regnier 1983).

There are two main approaches in which an IEX separations can be operated. They are generally known as bind-and-elute and flow-through modes. In the first one, the solution containing the mixture of molecules to be separated is adjusted to the specific conditions that allow their binding into the ion exchanger. These conditions are typically of low conductivity and low pH for cation exchanger and high pH for anion exchangers. Elution of bound molecules is then achieved by either increasing the ionic strength, thus increasing the conductivity, or changing the pH of the mobile phase. The separation of the mixture occurs when the changes in conductivity or pH are performed following a linear or a stepwise gradient. The slope of the linear gradient and the number and size of the steps will have an

ultimate impact in the quality of the separation, the concentration of the collected fractions and the length of the process. The resolution of molecules with similar retention times is favored using a linear gradient. However, pre-mixing of the gradient using sophisticated equipment is required and linearity can be influenced by bed inhomogeneities and extra-column mixing. Stepwise elution is the method of choice for process-scale applications because it is technically simpler to achieve and its buffer consumption is lower. Bind-and-elute chromatography is useful for assessing the optimal binding conditions of a molecule of interest, for the separation of mixtures with unknown properties and for the concentration of diluted starting materials. Nevertheless it is limited by the binding capacity of the ion exchanger. (Liu et al. 2010; Shukla et al. 2006; Lee, Micky Fu Xiang et al. 2014; Yamada et al. 2017; Ahamed et al. 2008; Ozturk, Hu 2005).

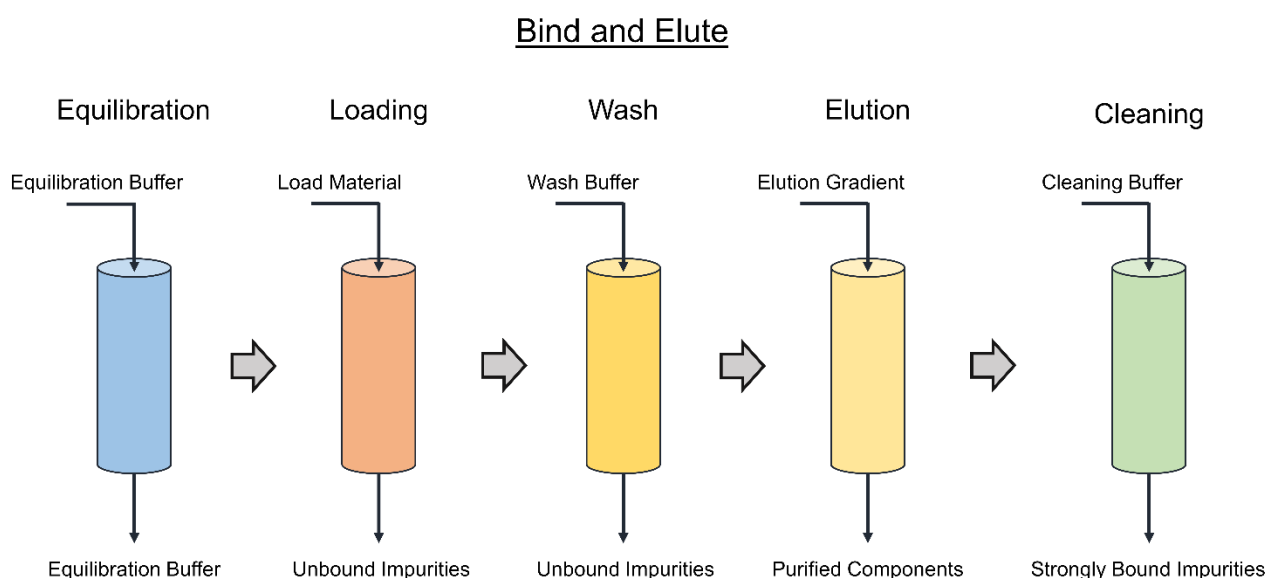


**Figure 4** Representation of a bind and elute process. The first step is the equilibration of the chromatography medium with buffer at the corresponding conditions that allow most of the components to be separated to bind to the ligands. The load material adjusted to binding conditions and containing the components to be separated is then introduced into the chromatography medium. A wash step is then performed to remove loosely bound impurities. Elution and the separation of the bound components is performed using a linear or stepwise gradient. Finally tightly bound impurities are removed from the chromatography medium using a cleaning solution.

Flow-through mode is usually implemented for the isocratic removal of impurities from a mixture containing a molecule of interest with known properties. The pH and conductivity of the load material are adjusted in such a way that the molecule of interest does not bind while the impurities are retained in the stationary phase. This mode of chromatography is widely used as a polishing step for the removal of small amounts of impurities like DNA, host cell proteins (HCP), virus, endotoxins and aggregates.

(Knudsen et al. 2001; Riordan et al. 2009; Liu et al. 2010; Yamada et al. 2017; Lee, Micky Fu Xiang et al. 2014; Ozturk, Hu 2005).

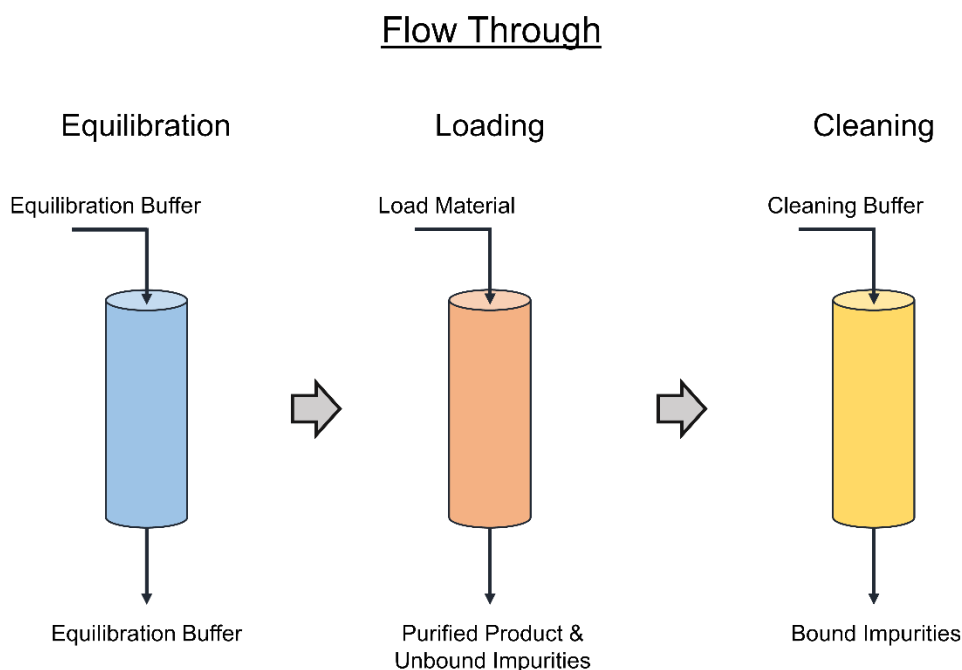


**Figure 5** Representation of an isocratic flow through process. The chromatography medium and the load material are adjusted to the corresponding conditions that allow the molecule to be purified not to bind while the impurities are retained.

Elution from ion exchangers results from the disruption of the complex electrostatic interaction between the functional groups in the stationary phase and the charged molecules. Increasing the ionic strength of the mobile phase is the most commonly used elution method with sodium chloride as the salt of choice. Nonetheless different salts will have different effects on the selectivity of the separation (Shukla et al. 2006; Kopaciewicz, Regnier 1983; Fekete et al. 2015).

Elution through changes in the pH of the mobile phase is essentially achieved through the modification of the surface net charge of the bound molecules until they are no longer able to interact with the ion exchanger. This technique has proven to be very effective for the resolution of molecules with very similar physicochemical characteristics. It has been used for the separation of protein isoforms with very similar *pI* values and the fractionation of the crude protein mixture of *E.coli* (Ahamed et al. 2007), for the separation of basic and acidic isoforms of monoclonal antibodies (Talebi et al. 2013) or for the resolution of tryptic peptides (Kang, Frey 2004). It can be performed in two different forms. One is referred to as “chromatofocusing” and is based on the creation of an internal pH gradient along a chromatography column packed with a weak anion-exchanger that has been titrated with an amphoteric

buffer. Separation occurs when the loaded molecules interact with the pH gradient and migrate differently along the column depending on their  $pI$  values (Ng et al. 2009; Mhatre et al. 1995; Fekete et al. 2015; Bates et al. 2000).

The second method is known as “pH-gradient IEX” and is performed in the bind-and-elute mode with an externally mixed pH gradient. Elution is achieved analogously to the salt gradient elution described above, but instead of increasing the conductivity, the net surface charge of the bound molecules is modified by changing the pH of the mobile phase. Molecules are released from the ion exchanger when pH of the mobile phase equals their isoelectric point. Separation is then the result of the difference in  $pI$  of the molecules in the mixture. This technique requires a strong ion exchanger that remains charged in a wide pH range and does not have any buffer interaction with the changing pH of the mobile phase. (Ahamed et al. 2007; Ahamed et al. 2008; Zhang et al. 2013b; Rea et al. 2011; Kröner, Hubbuch 2013; Ng et al. 2009).

Selecting the adequate buffer system for an IEX separation is crucial for its success. The buffer species should be non-toxic, assure the stability of the product and must provide adequate buffer capacity within the range in which the ion exchanger is operated without interacting with the functional groups (Shukla et al. 2006; Ozturk, Hu 2005). Typical buffers used in applications in which differences in ionic strength are the basis for the separation consist of a single buffer species titrated at a specific pH and adjusted to the required conductivity. Salt linear or stepwise gradients for the elution are generated through the mixing of a low and a high ionic strength buffer with the same pH, resulting in highly predictable and reproducible conductivity profiles. On the other hand, externally mixed pH gradients require complex buffer systems that are able to provide buffer capacity in a wide pH range. Predictable pH gradients profiles can be achieved by mixing buffer species with  $pK_a$  values evenly distributed within the pH range of the application. This results in an even buffer capacity and a linear titration curve that allows for the generation of a linear pH gradient through the mixing of a low and a high pH buffer (Ahamed et al. 2008; Ahamed et al. 2007; Zhang et al. 2013b; Rea et al. 2011; Mhatre et al. 1995; Kröner, Hubbuch 2013).

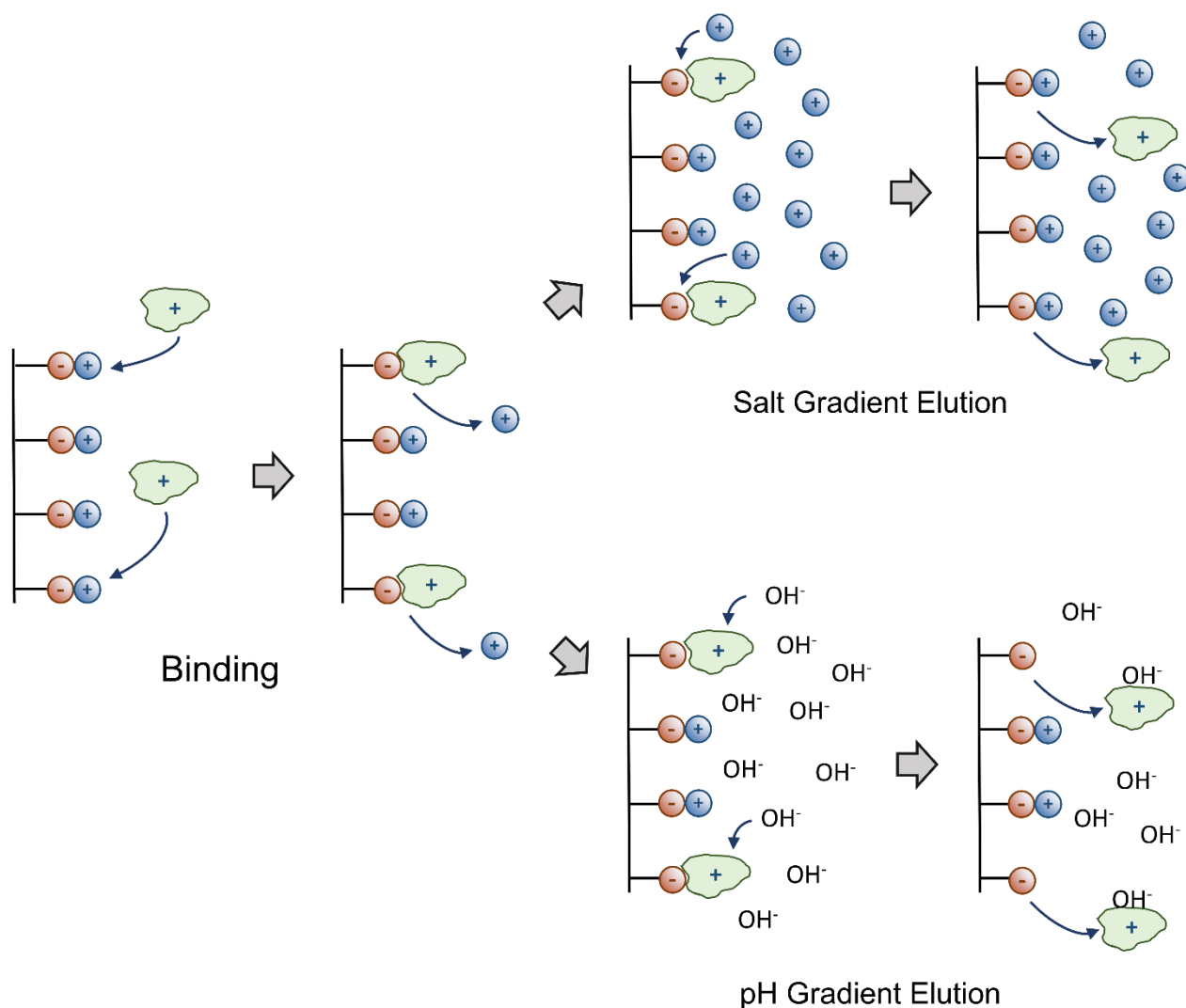


**Figure 6** Depiction of the binding of positively charged molecules into a cation exchanger and their elution from the chromatographic medium by either increasing the conductivity (salt gradient elution) or the pH (pH gradient elution) of the mobile phase.

## 2.6 Hydrophobic Interaction Chromatography

This method is usually implemented for the separation of biopolymers like proteins, peptides and nucleic acids. It is mainly used as a polishing step for the removal of aggregates and dimers, and is mostly complementary to other chromatography purification steps. Furthermore, the chromatography medium is available in both, as resin and as membrane adsorber. The principles of the separation can be understood through the interplay of two different mechanisms. The first being the weak hydrophobic interaction between the molecules in the mobile phase and the hydrophobic ligands in the stationary phase. The second mechanism is the modulation of the hydrophobic interaction with

kosmotropic salts. Structural damage and loss of biological activity is less in hydrophobic interaction chromatography (HIC) implementations compared with ion-exchange or affinity chromatography, where the interactions are much stronger (Queiroz et al. 2001; Shukla et al. 2006; Baca et al. 2016; Kuczewski et al. 2010).

Hydrophobic interaction is the result of complex thermodynamic solvation processes of non-polar solutes in polar environments. It is an important mechanism responsible for many biological processes like protein folding, antibody-antigen interactions, enzyme-substrate reactions and the maintenance of lipid bilayer structures (Queiroz et al. 2001).

The introduction of a non-polar molecule in an aqueous mobile phase results in the thermodynamically unfavorable formation of a cavity, at which border an overall increase in the order of water molecules is experienced. This process is not spontaneous and results in a decrease of entropy ( $\Delta S < 0$ ) and an overall positive change in free energy ( $\Delta G > 0$ ), which is proportional to the surface tension of the mobile phase. Hydrophobic interaction is the spontaneous association of two or more non-polar compounds in an effort to reduce the energy required to keep them in aqueous solution. This causes the movement of ordered water molecules from the border of the cavity into the more unstructured bulk water, resulting in an increase in entropy ( $\Delta S > 0$ ) (Queiroz et al. 2001; Shukla et al. 2006; Chandler 2005).



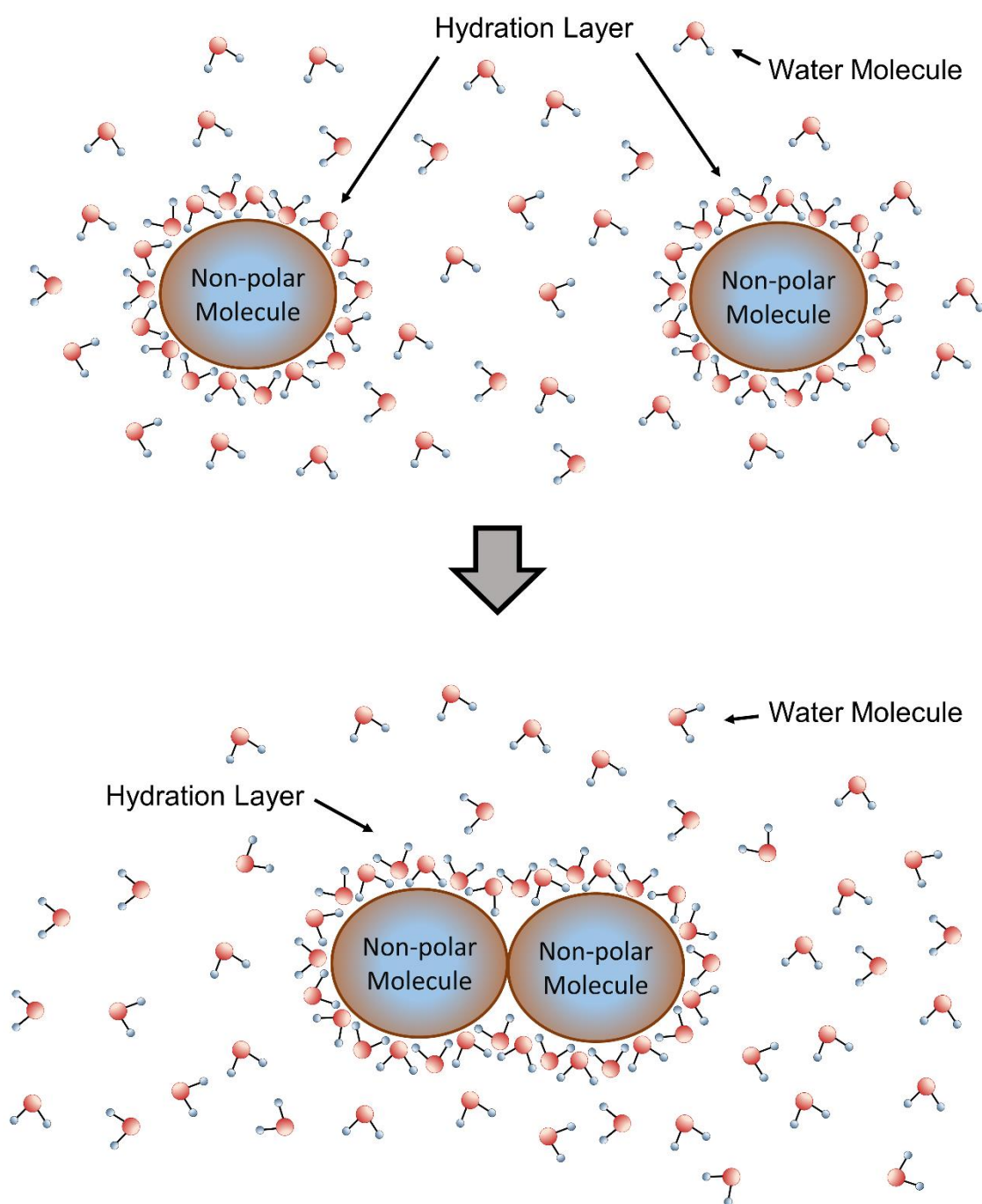


**Figure 7** Representation of the thermodynamically driven spontaneous aggregation of two non-polar molecules in aqueous solution which results in a decrease in entropy.

The ligands in the HIC stationary phase are usually short alkyl chains with 8 carbons or less, or phenyl groups. Hydrophobic interaction between them and the hydrophobic regions of biomolecules is induced by increasing the ionic strength of the mobile phase with kosmotropic salts. These are presented at the beginning of the Hoffmeister Series (Figure 8) and are known for their salting-out effects (protein precipitation). They increase the surface tension of the mobile phase, and because of

## 2. INTRODUCTION

---

their high polarity, they form a strong hydration layer around themselves. Higher concentrations of kosmotropic salts displace more water molecules from the hydrophobic pockets, leaving them more exposed and increasing the strength of the hydrophobic interaction. Chaotropic salts on the other hands, which are presented at the end of the Hoffmeister series (Figure 8) and are known for their salting-in effect (increase of protein solubility), disrupt hydrogen bonds between water molecules and reduce the surface tension of the aqueous phase. This results in the disruption of hydrophobic interactions and the denaturation of proteins at higher ionic strengths (Queiroz et al. 2001; Shukla et al. 2006; Baca et al. 2016; Kuczewski et al. 2010; Ozturk, Hu 2005).

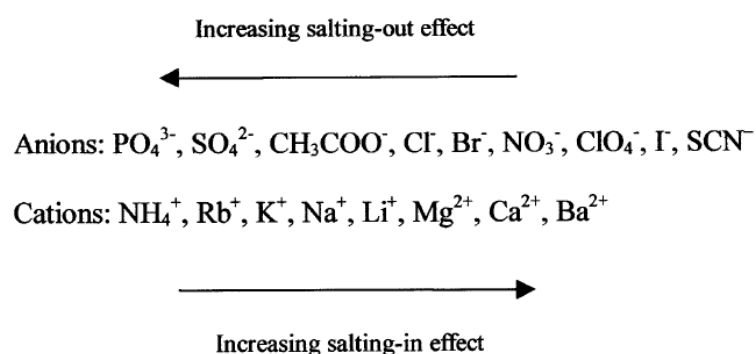


**Figure 8** Hoffmeister series listing different ions in order of their influence on the hydrophobic interaction of proteins. The ions to the left have the property of increasing the surface tension of water, thus increasing the hydrophobic interaction (salting-out) (Queiroz et al. 2001).

The design of an HIC process for the separation of proteins requires the thorough screening of ligands using different salts at different concentrations in a pH range that assures the stability of the product. The type of salt, its concentration, the temperature and the pH of the mobile phase will all have different effects on the retention and selectivity of the process and the binding capacity of the stationary phase. Maximal binding capacity is usually achieved at salt concentrations just below the point at which the proteins precipitate. The effect of the pH is usually unpredictable, as changes in pH may cause charged groups near hydrophobic patches to be titrated or vice versa, thus changing the strength of the hydrophobic interaction. Furthermore, conditions that result in changes of the 3D conformation of the proteins can affect the selectivity of the separation. Temperature increases the strength of hydrophobic interactions (Shukla et al. 2006; Senczuk et al. 2009; Kramarczyk et al. 2008; Queiroz et al. 2001; Chandler 2005).

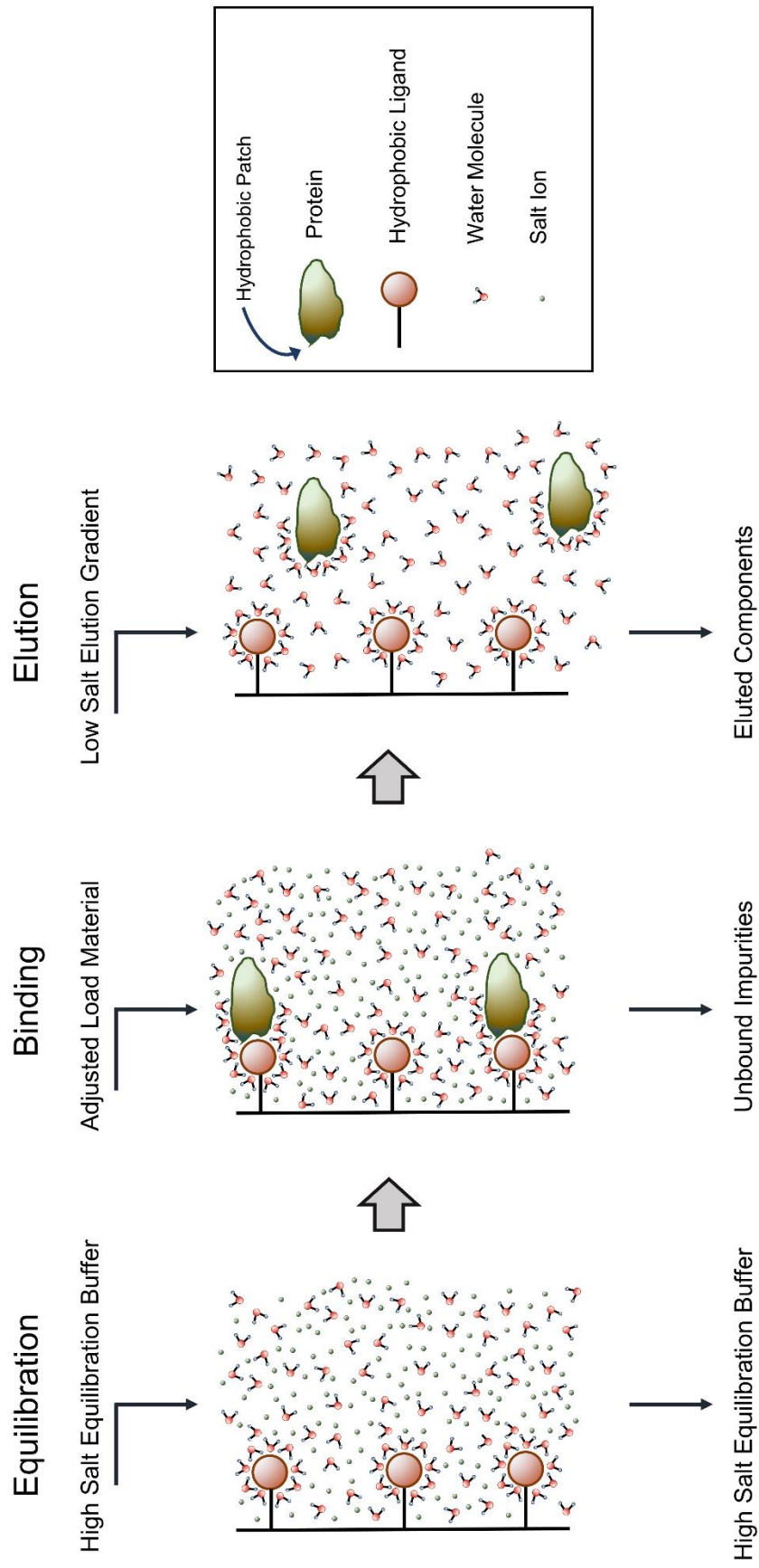


**Figure 9** Mechanism by which a protein binds into and elutes from the ligands of a hydrophobic interaction chromatography medium. The medium is first equilibrated with a high salt buffer to enhance the hydrophobic effect. The proteins then bind into the ligands at their hydrophobic patches. The proteins are finally eluted using a low salt buffer.

HIC can be implemented in the bind-and-elute mode and protein recovery is achieved by decreasing the ionic strength of the mobile phase following a linear or stepwise gradient. Nevertheless, the binding capacity of the stationary phase is limited compared to ion exchangers. Increasing the number of hydrophobic ligands leads to an increase in binding capacity with the risk of the stationary phase becoming too hydrophobic, and thus causing irreversible binding. Furthermore, binding capacity is negatively affected by increasing molecular sizes. For this reasons HIC is mostly used isocratically in the flow-through mode to remove small amount of impurities that are more hydrophobic than the product itself, for example protein aggregates (Shukla et al. 2006; Queiroz et al. 2001; Ozturk, Hu 2005).

### 2.7 Membrane Adsorption Chromatography

Membrane adsorbers (MA's) are microporous polymeric membranes, which have been chemically coupled with functional ligands that allow for the chromatographic separation of biomolecules. They are well established in the biopharmaceutical industry as a polishing step for the removal of small amounts of impurities and are operated almost exclusively in a flow-through mode. Ligand chemistries include reversed phase (RP), hydrophobic interaction (HI), affinity, and ion exchange (IEX). The main advantage of membrane adsorbers over traditional packed bed columns is the elimination of mass transfer limitations. The active ligands, located in the pores of the membrane, can be reached through convection, rather than diffusion. Furthermore the low transmembrane pressure drop allows for higher flow rates to be used (Ghosh 2002; Weaver et al. 2013a; Shukla et al. 2006; Kuczewski et al. 2010; Knudsen et al. 2001). Even though MA's have proven to be more suitable for the removal of large molecules and virus particles at low concentrations (Weaver et al. 2013b), they have been successfully implemented in a two-step process for the fractionation of bioactive peptides from a complex mixture (400 – 10,000 Da) of hydrolyzed milk proteins (Leeb et al. 2014). In addition, Recio et al. developed an ion exchange chromatography method using an MA to bind a protein of interest. Then hydrolysis in situ was performed, followed by a wash step to remove hydrolyzed peptide impurities. Finally a highly pure concentrate of an antimicrobial active peptides was eluted from the membrane (Recio, Visser 1999).

## 3 Materials and Methods

The isolation of bioactive components from the conditioned medium of CHO-K1 was achieved in three main stages. The first one consisted in the establishment of the biological activity of conditioned medium and the assessment of its effect on the growth, death and metabolic kinetics of exponentially growing cells. The second step consisted in the development of a cation exchanger membrane adsorption process for the preparative capture and recovery of the bioactive components in conditioned medium. The final stage was the development a hydrophobic interaction membrane adsorption step for the orthogonal purification of the bioactive components recovered from the cation exchanger.

### 3.1 Conditioned Medium and the Kinetics of CHO-K1 Cell Culture

The kinetic study of conditioned medium involved four experiments. The first experiment consisted in the cultivation of exponentially growing cells in serum and protein-free growth medium supplemented with conditioned medium generated by the cells themselves and harvested in the late exponential phase of growth. The accumulation of growth inhibitory components was expected and the results were compared to a negative control cultivated simultaneously only in fresh growth medium. The size of the bioactive molecules was roughly estimated in the second experiment by separating the components of conditioned medium harvested in the late exponential phase into two fraction using an ultrafiltration membrane with a cutoff of 10 kDa. The fractions were then tested on exponentially growing cells. The third and fourth experiments examined respectively the influence of conditioned medium originated from the exponential phase of growth and the age of the parent culture on the initial growth and death rates of the cells. These two experiments were performed for the identification of the parameters that might have an influence in the initial lagging phase after inoculation and the delayed onset of maximal specific growth rate.

#### 3.1.1 Cell culture

A non-recombinant CHO-K1 cell line adapted to suspension and serum-free medium was used throughout this work. The cell line was generously donated by Prof. Dr. Thomas Noll (Cell Culture Technology Group, University Bielefeld, Germany). Cells for all the experiments were harvested from a semi-continuous culture kept in the exponential growth phase by diluting it every 3 to 4 days to  $3 \times 10^5$  cells/ml. Chemically defined CHOMACS CD (Mytenyl Biotech GmbH, Bergisch Gladbach, Germany) medium supplemented with L-glutamine to a final concentration of 4 mM was used for all

experiments. The growth medium was free of serum, proteins, animal derived components and growth factors. Cultivation took place on an orbital shaker at 250 RPM in a humidified incubator with an atmosphere controlled at 36.5° C and 5% CO<sub>2</sub> in either 125 ml, 250 ml or 500 ml disposable shaking flasks (Corning Inc., Germany) with a working volume of 40, 80 ml and 160 ml respectively, or in 50 ml Tubespin Bioreactor 50 (TPP Techno Plastic Products AG, Trasadingen, Switzerland) cultivation tubes with a working volume between 8 – 12 ml.

#### 3.1.2 Analytical Methods

Total cell density ( $N_T$ ) was determined using the Z2 Coulter Counter Analyzer (Beckman Coulter Inc., Brea, California, USA) after a 1:100 dilution in PBS + 2mM EDTA. The percentage of apoptotic cells ( $apop\%$ ) and the viability ( $Viab$ ) were determined simultaneously using a Cytoflex flow cytometer (Beckman Coulter Inc., Brea, California, USA) after staining approx.  $10^5$  cells for 15 minutes with 5  $\mu$ l AnnexinV (Sigma Aldrich, Munich, Germany) solution and propidium iodide to a final concentration of 0.25  $\mu$ g/ml. Glucose, lactate and glutamine concentrations were analyzed enzymatically using the YSI 2900 Biochemistry Analyzer (Yellow Spring Instruments, Yellow Springs, Ohio, USA).

#### 3.1.3 Determination of Kinetic Parameters

Kinetic parameters were estimated differentially between two time points using two different models. The first model (*Model I*) was used when only the percent viability ( $Viab$ ) was measured using propidium iodide (PI). The second model (*Model II*) was used when the percent viability ( $Viab$ ) and the percentage of apoptotic cells ( $apop\%$ ) were measured simultaneously using Annexin V and PI.

##### Model I

*Specific Growth and Death Rates:*

$$\frac{dN_v}{dt} = (\mu - k_d) \cdot N_v \quad (1)$$

$$\frac{dN_d}{dt} = k_d \cdot N_v \quad (2)$$

$$N_t = N_v + N_d \quad (3)$$

$$Viab = \frac{N_v}{N_t} \quad (4)$$

Where  $N_t$  refers to the total cell density,  $Viab$  the percent viability,  $N_v$  the viable cell density and  $N_d$  the non-viable cell density.  $\mu$  represents the specific growth rate and  $k_d$  the specific death rate.

*Nutrient Uptake and Product Excretion Rates:*

$$\frac{dc_{Glc}}{dt} = -q_{s,Glc} \cdot N_v \quad (5)$$

$$\frac{dc_{Gln}}{dt} = -q_{s,Gln} \cdot N_v \quad (6)$$

$$\frac{dc_{Lac}}{dt} = q_{p,Lac} \cdot N_v \quad (7)$$

Where  $c_{Glc}$ ,  $c_{Gln}$ ,  $c_{Lac}$ , represent the glucose, glutamine and lactate concentration respectively and  $q_{s,Glc}$ ,  $q_{s,Gln}$ ,  $q_{s,Lac}$ , the specific glucose uptake rate, glutamine uptake rate and lactate production rate respectively.

*Yield Coefficients*

$$Y_{x/s,Glc} = -\frac{dN_v}{dc_{s,Glc}} \quad (8)$$

$$Y_{p/s} = \frac{dc_{s,Lac}}{dc_{Glc}} \quad (9)$$

Where  $Y_{x/s,Glc}$  and  $Y_{p/s}$ , represent the viable cell density to glucose and lactate to glucose yields respectively.

#### Model II

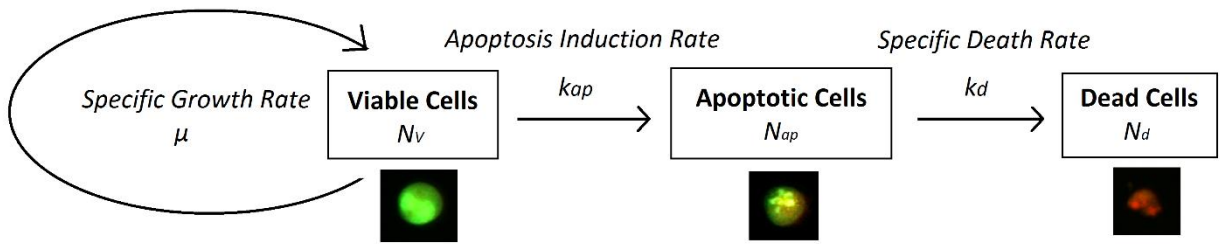


**Figure 10** Graph depicting the growth kinetics described by *Model II*.  $N_v$ ,  $N_{ap}$ , and  $N_d$  represent respectively the viable, apoptotic and non-viable cell densities, while  $\mu$ ,  $k_{ap}$  and  $k_d$  represent the specific growth, apoptosis induction and specific death rates respectively.

*Specific Growth and Death Rates:*

$$\frac{dN_v}{dt} = (\mu - k_{ap}) \cdot N_v \quad (10)$$

$$\frac{dN_{Apop}}{dt} = (k_{Ap} - k_d) \cdot N_v \quad (11)$$

$$\frac{dN_d}{dt} = k_d \cdot N_{ap} \quad (12)$$

$$N_t = N_v + N_{ap} + N_d \quad (13)$$



$$Viab = \frac{N_v}{N_t} \quad (14)$$

$$apop\% = \frac{N_{Ap}}{N_t} \quad (15)$$

Where  $N_t$  refers to the total cell density,  $Viab$  to the percent viability,  $apop\%$  to the percentage of apoptotic cells,  $N_v$  to the viable cell density,  $N_{Ap}$  to the apoptotic cell density and  $N_D$  to the non-viable cell density.  $\mu$  represents the specific growth rate,  $k_{ap}$  the apoptosis induction rate and  $k_d$  the specific death rate.

*Nutrient Uptake and Product Excretion Rates:*

$$\frac{dc_{Glc}}{dt} = -q_{s,Glc} \cdot (N_v + N_{ap}) \quad (16)$$

$$\frac{dc_{Gln}}{dt} = -q_{s,Gln} \cdot (N_v + N_{ap}) \quad (17)$$

$$\frac{dc_{Lac}}{dt} = q_{p,Lac} \cdot (N_v + N_{ap}) \quad (18)$$

Where  $c_{Glc}$ ,  $c_{Gln}$ ,  $c_{Lac}$ , represent the glucose, glutamine and lactate concentration respectively and  $q_{s,Glc}$ ,  $q_{s,Gln}$ ,  $q_{s,Lac}$ , the specific glucose uptake rate, glutamine uptake rate and lactate production rate respectively.

#### 3.1.4 Statistical Analysis

The statistical significance of the results was assessed by applying the Student's t-test. Differences between groups were considered significant at  $p < 0.05$  and of low significance at  $p < 0.1$ .

#### 3.1.5 Kinetics of Conditioned Medium

The effects of conditioned medium harvested in the late exponential phase of growth were examined by inoculating a CHO-K1 cell culture in a mixture of 1:4 conditioned medium (CM) to fresh CHOMACS CD (FM) supplemented with 4 mM L-glutamine and comparing it to a negative control inoculated in 100% CHOMACS CD supplemented with 4mM L-glutamine. Cultivation was carried out in triplicates in 125 ml disposable shaking flasks with a working volume of 40 ml at an average starting cell density and viability of  $2.52 \pm 0.190 \times 10^5$  cells /ml and  $96.5\% \pm 1.02\%$ .

Conditioning of the growth medium was performed by cultivating CHO-K1 cells for 65 hours in a 125 ml disposable shaking flask with a working volume of 40 ml to a final cell density of  $6.5 \times 10^6$  cells/ml. For the harvest of the conditioned medium, the culture was centrifuged at  $6800 \times g$  and room temperature for 15 minutes prior to the experiment and the supernatant was transferred to a sterile vessel. A total of 30 ml (10 ml for each replicate) of fresh conditioned medium were mixed with 90 ml CHOMACS CD.

The cells used for the inoculation of the experiment originated from the same culture used for the conditioning of the growth medium. Two times 5 ml of the culture were centrifuged down at  $1967 \times g$  for 3 minutes at room temperature, the supernatants were removed, and the pellets was resuspended in either the 120 ml CM – CHOMACS CD mixture (25%CM culture) or in 120 ml fresh CHOMACS CD (NC culture).

The experiment started once the 120 cell suspension was evenly distributed in three shaking flasks, each one representing a replicate culture. The cultures were cultivated for 142 hours and samples for the determination of total cell density, viability, apoptosis percent and glucose, lactate, and glutamine concentrations were taken every 24 hours. The kinetic parameters were calculated using *Model I* (see *Determination of Kinetic Parameters*).

#### 3.1.6 Separation of Conditioned Medium by Molecular Weight (cutoff 10 kDa)

The kinetic effects of conditioned medium and two of its fractions were examined simultaneously on exponentially growing cells. The conditioned medium was harvested from the late exponential phase of growth and its proteins were separated by molecular weight using an ultrafiltration membrane with a 10 kDa cutoff. The cells used for both, the conditioning of the growth medium and the inoculation of the experiments, were produced at the same time. A parent culture was inoculated in a 125 ml

disposable shaking flask with a working volume of 40 ml in CHOMACS CD growth medium. The cells were harvested from the continuous culture, inoculated at  $5.8 \times 10^5$  cells/ml, and cultivated for 19 hours to a cell density of  $1.2 \times 10^5$  cells/ml ( $\mu = 0.042$  1/h). This parent culture was then diluted 1:1 with fresh CHOMACS CD and the doubled volume distributed equally in two 125 ml disposable flasks. One culture was further replenished with 10 ml fresh growth medium and was used for the conditioning of the medium. The other culture was kept in the exponential phase of growth through dilution with fresh medium and was used to generate the cells necessary for the experiments.

#### Production of Conditioned Medium and Molecular Weight Fractions

The culture used for the conditioning of the growth medium had a working volume of 50 ml and a starting cell density and viability of  $6.5 \times 10^5$  cells/ml and 97.21%. It was cultivated for 71 hours and reached a final cell density and viability of  $11.2 \times 10^6$  cells/ml and 93.67% ( $\mu = 0.041$  1/h). Prior to the experiment the culture was centrifuged at  $6800 \times g$  and room temperature for 15 minutes, and the supernatant transferred into a sterile vessel. Ultrafiltration of 20 ml of the harvested conditioned medium was performed using the Amicon UF centrifugation unit (Millipore, Burlington, Massachusetts, USA) at  $5000 \times g$  until most of the liquid had passed through the membrane and into the collection vessel. At the end of the process, the permeate and retentate had a final volume of 19.3 and 0.6 ml respectively, resulting in a 33 times concentration of the proteins with a molecular weight higher than 10 kDa. The permeate was sterile filtered through a PES syringe filter and stored cold until further use ( $< 10$  kDa fraction). The retentate was mixed with 20 ml fresh CHOMACS CD medium, sterile filtered through a PES syringe filter and stored cold until further use ( $> 10$  kDa fraction).

#### Testing on CHO-K1 Cell Culture

Testing was carried out directly after harvesting and fractionation. Exponentially growing CHO-K1 cells were inoculated in triplicates (3 x 40 ml) at a starting cell density of  $3 \times 10^5$  cells/ml in fresh CHOMACS CD growth medium mixed with either, conditioned medium, the  $< 10$  kDa fraction or the  $> 10$  kDa fraction, and supplemented with L-glutamine to a final concentration of 4 mM according to Table 1. The lactate concentration of the conditioned medium was measured at 1.99 g/l, resulting in a final concentration of 0.33 g/l in culture. A sodium lactate stock solution measured at 14.87 g/l was used to correct the lactate concentration of the cultures to match the concentration increase caused by the conditioned medium. A negative control (NC), in which the volume of conditioned medium was substituted with fresh CHOMACS CD, was cultivated in triplicates simultaneously. The lactate concentration of the NC was also corrected according to Table 1.

### 3. MATERIALS AND METHODS

The cells necessary for the experiment were produced in the split parent culture described above. It had a starting a cell density and viability of  $6.07 \times 10^5$  and 97.17% at the beginning of the first dilution step, and reached  $7.99 \times 10^6$  cell/ml and 92.18% viability after 55 hours of cultivation ( $\mu = 0.046$  1/h). Subsequently, half of its volume was taken and substituted with fresh CHOMACS CD, resulting in a cell density and viability of  $3.17 \times 10^5$  and 92.68%. The diluted culture was then cultivated for 21 hours to a final cell density and viability of  $7.43 \times 10^5$  and 94.58% ( $\mu = 0.043$  1/h).

The experiment started after the necessary inoculation volume was added to the corresponding mixture, which was then evenly distributed among three 125 ml disposable shaking flasks, each one corresponding to one replicate with a working volume of 40 ml each. The growth medium of the inoculation volume was not exchanged, resulting in a conditioned medium carryover of 4.03 vol% for each culture. The cultures were cultivated for 167 hours and the kinetic parameters were calculated using *Model II* (see *Determination of Kinetic Parameters*).

**Table 1** Pipetting scheme for the inoculation of the experiment “Separation of the Components in Conditioned Medium by Molecular Weight (cutoff 10 kDa)”

	Fraction Volume	Fresh CHOMACS CD	200 mM Gln Stock Solution	Sodium Lactate Stock Solution	Inoculation Volume	Total Volume	CM vol%
	[ ml ]	[ ml ]	[ ml ]	[ ml ]	[ ml ]	[ ml ]	[ vol% ]
< 10 kDa	19.3	93.4	2.4	0.1	4.8	120	4.03
> 10 kDa	20.6	89.6	2.4	2.6	4.8	120	4.03
Conditioned Medium	20.0	92.8	2.4	0	4.8	120	20.69
Negative Control	0	110.1	2.4	2.7	4.8	120	4.03

#### 3.1.7 Effect of the Conditioned to Fresh Medium Ratio

The influence of different amounts of conditioned medium (CM) on the specific growth and death rates of CHO cells was examined in this experiment. Cells from a parent culture were inoculated in CHOMACS CD growth medium supplemented with 4 mM L-glutamine containing 17.1 vol%, 58.6 vol% and 100 vol% of conditioned medium. Cultivation was performed in triplicates in 50 ml reaction tubes with a working volume of 11 ml at an average starting cell density and viability of  $3.52 \pm 0.130 \times 10^5$  cells/ml and  $95.4\% \pm 1.34\%$ .

### 3. MATERIALS AND METHODS

The parent culture originated from the continuous culture and was inoculated at  $4.70 \pm 0.433 \times 10^5$  cells/ml and cultivated for 27 hours to a total cell density of  $1.20 \pm 0.002 \times 10^6$  cells/ml ( $\mu = 0.035 \pm 0.0036$  1/h). The culture was then diluted approximately 1:1 to a total cell density and viability of  $6.18 \pm 0.036 \times 10^5$  cells/ml and  $94.6\% \pm 0.62\%$  and cultivated for additional 22 hours to a final total cell density and viability of  $1.72 \pm 0.018 \times 10^6$  cells/ml and  $93.1\% \pm 1.71\%$  ( $\mu = 0.050 \pm 0.0007$  1/h;  $k_d = 0.004 \pm 0.0005$  1/h).

Prior to the experiment 45 ml of CM were harvested from the parent culture by centrifuging the cells down at  $6800 \times g$  and room temperature for 15 minutes and transferring the supernatant to a sterile vessel. Table 2 gives the inoculation volume, conditioned medium and CHOMACS CD medium supplemented with 4 mM L-glutamine used for each culture calculated to a final volume of 35 ml.

The experiment started once the 35 ml cell suspension was evenly distributed in three reaction tubes, each one representing a replicate culture. The cultures were cultivated for 49 hours and samples for the determination of total cell density, viability, apoptosis percent and glucose, lactate, and glutamine concentrations were taken every 24 hours. The kinetic parameters were calculated using *Model I* (see *Determination of Kinetic Parameters*).

**Table 2** Pipetting scheme for the inoculation of the experiment “Effects of the Conditioned to Fresh Medium Ratio”

Culture	Parent Culture	Conditioned Medium	CHOMACS CD
	[ ml ]	[ ml ]	[ ml ]
17.1% CM	6	0	29
58.6% CM	6	14.5	14.5
100% CM	6	29	0

#### 3.1.8 Effects of the Age of the Parent Culture

The effects of the starting cell density and the cell density of the parent culture at the moment of inoculation on the growth and death kinetics of the cells were examined. Two parent cultures were cultivated to different cell densities and were used to inoculate two cultures each, one at a low (LCD) and the other one at a medium cell density (MCD), both in 100% fresh CHOMACS CD growth

### 3. MATERIALS AND METHODS

medium supplemented with 4 mM L-glutamine. Each cultivation was performed in triplicates in 50 ml reaction tubes with a working volume of 11 ml.

Both parent cultures originated from the same continuous culture, which had a total cell density of  $12.2 \times 10^6$  cells/ml, and were inoculated at the same time. The young parent culture (YPC) was inoculated at a total cell density and viability of  $9.29 \times 10^5$  cells/ml and 93.2% and was cultivated for 22 hours to  $1.83 \times 10^6$  cells/ml and 88.1% viability ( $\mu = 0.034$  1/h;  $k_d = 0.006$  1/h). Then it was diluted with fresh CHOMACS CD medium to a total cell density and viability of  $3.87 \times 10^5$  cells/ml and 95.4% and was cultivated for further 23 hours to a final cell density of  $1.09 \times 10^6$  cells/ml and 95.0% viability ( $\mu = 0.047$  1/h;  $k_d = 0.002$  1/h). The medium aged parent culture (MPC) was inoculated at a total cell density and viability of  $6.37 \times 10^5$  cells/ml and 95.2% and cultivated for 22 hours to  $1.18 \times 10^6$  cells/ml and 92.2% viability ( $\mu = 0.030$  1/h;  $k_d = 0.003$  1/h). Then it was diluted with fresh CHOMACS CD medium to a total cell density and viability of  $2.78 \times 10^5$  cells/ml and 95.7% and cultivated for further 67 hours to a final cell density of  $5.27 \times 10^6$  cells/ml and 93.2% viability ( $\mu = 0.047$  1/h;  $k_d = 0.004$  1/h).

Prior to the experiment, the corresponding inoculation volume for a total of 33 ml was centrifuged down at  $1967 \times g$  for 3 minutes at room temperature and the supernatant was removed to avoid effects of carry-over conditioned medium. The pellet was then re-suspended in 33 ml fresh and pre-heated CHOMACS CD medium. Table 3 shows the parent cultures used for the inoculation of each culture, together with the starting cell density and viability.

**Table 3** Cultures inoculated in 100% fresh CHOMACS CD medium for the experiment "Effect of the Age of the Parent Culture". The parent culture used, and the starting cell density and viability are shown.

Inoculated Culture	Parent Culture	Starting Cell Density	Viability
		[ cells / ml ]	[ % ]
LCD1	YPC	$3.51 \pm 0.005 \times 10^5$	$95.5 \pm 1.80$
MCD1		$1.05 \pm 0.021 \times 10^6$	$94.9 \pm 1.65$
LCD2	MPC	$5.11 \pm 0.125 \times 10^5$	$95.2 \pm 3.21$
MCD2		$1.03 \pm 0.014 \times 10^6$	$95.0 \pm 1.90$

The experiment started once the 33 ml cell suspension was evenly distributed in three reaction tubes, each one representing a replicate culture. Because of the different cultivation times of both parent

cultures, all the cultures of the experiment could not be inoculated simultaneously. The cultures corresponding to the YPC were examined first. Cultivation time was 24 hours and samples for the determination of total cell density, viability, apoptosis percent and glucose, lactate, and glutamine concentrations were taken. The kinetic parameters were calculated using *Model I* (see *Determination of Kinetic Parameters*).

## 3.2 Cation Exchange Chromatography Purification Step

This section presents the development of a cation exchanger membrane adsorption process for the capture, recovery and concentration of the secretome and possible bioactive components from the conditioned medium of CHO cell culture. The end process was the result of a series of optimization steps that focused mainly in the prevention of protein degradation and the maximization of the recovery yield. A total of six bind-and-elute experiments were performed, four of which produced fractions that were supplemented to exponentially growing cells to assess their effect on the growth and death kinetics.

### 3.2.1 Membrane Adsorbers

Sartobind S membrane adsorber from Sartorius Stedim Biotech (Goettingen, Germany) was used in this work for the capture and fractionation of the proteins in the conditioned medium (CM) of CHO-K1 cells. Sartobind S is a strong cation exchanger with sulfonic acid serving as ligand. At low pH values proteins are generally positively charged, thus allowing binding. Low conductivity values increase binding capacity. Elution from the membrane was achieved by increasing the pH and/or the salt concentration of the mobile phase. Pico, MA 75, and MA 100 capsule modules with a membrane volume of 0.08, 2.1 and 2.8 ml and a dynamic binding capacity of 2, 52.5, and 70 mg protein per unit respectively were used for the experiments.

### 3.2.2 Buffers for Fractionation

All the chemicals used for the buffers had been tested by manufacturer and were suitable for cell culture. Citric acid, sodium phosphate ( $\geq 99.0\%$ ), N,N-bis(2-hydroxyethyl)glycine (BICINE) (PharmaGrade), 2-(cyclohexylamino)ethanesulfonic acid (CHES) (Pharma Grade), ammonium sulphate ( $\geq 99.0\%$ ), sodium chloride ( $\geq 99.0\%$ ), and potassium chloride ( $\geq 99.0\%$ ) were obtained from

### 3. MATERIALS AND METHODS

Sigma Aldrich (Munich, Germany). The buffers were stored at 4° C for no longer than two weeks and were filtered through a PVDF filter to remove solid particles.

The mobile phase for the pH gradient elution (pH 3 – 10) experiments was composed of 20 mM citrate , 20 mM phosphate, 20 mM CHES, 20 mM BICINE (Ahamed et al. 2008). The low pH binding buffer (Buffer A) was adjusted to pH 3 using 2 M HCl while the high pH elution buffer (Buffer B) was adjusted to pH 10 using 1 M NaOH.

Table 4 lists the buffers used in the bind and elute experiments together with their respective composition and pH. The binding buffer (Buffer A2) used for the generation of the fractions that were later tested on growing cells was composed of 20 mM citrate adjusted to pH 5. The buffer for the first elution (E1) was composed of 20 mM phosphate, 20 mM CHES, 20 mM BICINE adjusted to pH 10 (Buffer BoC1). The buffer for the second elution (E2) was composed of 20 mM phosphate, 20 mM CHES, 20 mM BICINE, 1 M NaCl adjusted to pH 10 (Buffer BoC2). A wash step between loading and elution was performed using a buffer composed of 20 mM phosphate, 20 mM CHES, 20 mM BICINE adjusted to pH 5 (Buffer AoC). It was crucial to avoid carry-over of citrate into the cell culture because of the significant effect it has on CHO-K1 cells (Bai et al. 2011; Zhang et al. 2006).

**Table 4** List of buffers used with Sartobind S

Buffer A	20 mM citrate , 20 mM phosphate, 20 mM CHES, 20 mM BICINE	pH 3
Buffer B	20 mM citrate , 20 mM phosphate, 20 mM CHES, 20 mM BICINE	pH 10
Buffer A2	20 mM citrate	pH 3 or 5
Buffer AoC	20 mM phosphate, 20 mM CHES, 20 mM BICINE	pH 5
Buffer BoC1	20 mM phosphate, 20 mM CHES, 20 mM BICINE	pH 10
Buffer BoC2	20 mM phosphate, 20 mM CHES, 20 mM BICINE, 1 M NaCl	pH 10

#### 3.2.3 Electrophoresis

SDS PAGE was used to visualize the proteins in the conditioned medium and the fractions generated in the pH – stepwise increase experiment. Prior to electrophoresis, proteins in the samples were precipitated using a TCA-NLS protocol used for the concentration and analysis of low-abundance



secreted proteins from conditioned medium (Chevallet et al. 2007). The samples were cooled in ice and mixed with sodium lauroyl sarcosinate (NLS) and trichloroacetic acid (TCA) to a final concentration of 1% and 7.5% respectively. The proteins were precipitated on ice for 2 hours and subsequently centrifuged at 10000 x g 10 min at 4° C. The supernatants were removed and the pellets were washed twice with 2 ml of precooled tetrahydrofuran. The samples were centrifuged one more time and the supernatants removed. The almost invisible pellets were dissolved in 40 µl Laemmli buffer, incubated for 10 min at 95° C, and loaded into a 10% polyacrylamide gel. Proteins were separated at 200 V and the gel was stained using Roti-Blue.

The precipitation protocol showed very low protein yield in the fractions eluted at higher pH values. For this reason and for the purpose of comparability, all the fraction samples were adjusted to an approximate pH of 6.4 prior to precipitation. This pH corresponded to a volumetric ratio of elution buffer B to binding buffer A of 50%. The necessary volume of either buffer A or buffer B that needed to be added to each sample was calculated according to the measured pH of each fraction using the linear regression.

#### 3.2.4 Determination of Protein Concentrations

Protein concentration was determined after Bradford using Protein Assay Dye Reagent Concentrate (Bio Rad, Hercules, California, USA). The reaction was performed simultaneously on three samples taken from the protein solution to be quantified. The protein concentration corresponded then to the average of the three samples.

#### 3.2.5 Generation of Conditioned Medium

Conditioning of the growth medium used for the experiments was carried out in a 2 L bioreactor VSF 2000 (Bioengineering AG, Wald, Switzerland) with a working volume of 1200 ml in chemically defined, protein-free CHOMACS CD medium. Cells were inoculated at a starting cell density of  $5 \times 10^5$  cells/ml and cultivated at a constant temperature of 37° C and dissolved oxygen saturation of 30% for 70 – 90 hours until the late exponential phase. The  $6 \times 10^8$  cells needed for the inoculation of the bioreactor were produced in a parent culture through the stepwise expansion of cells harvested from the continuous suspension culture (see *Cell Culture* from the Chapter *Conditioned Medium and the Kinetics of CHO-K1 Cell Culture*). The first step was inoculated at  $3 \times 10^5$  cells/ml with a working volume of 40 ml and specific growth rate of approx. 0.045 1/h. The inoculation culture was diluted 1:1 with fresh growth medium over the course of the next 4 days until a working volume of 160 ml was

### 3. MATERIALS AND METHODS

achieved. The cells were kept growing in the exponential phase of growth by avoiding the cells to exceed a cell density of  $4 \times 10^6$  cells/ml before any dilution step. At the time of harvest the culture the culture was removed from the bioreactor and the cell suspension was centrifuged at  $17700 \times g$  and  $4^\circ \text{C}$  for 30 mins. The supernatant was then used for the bind and elute experiments. Because of the low protein concentration of conditioned medium (approx. 0.08 mg/ml), it was necessary to produce large amounts of harvest to be able to purify enough protein material that could cause an effect when given to growing cells.

Table 5 summarizes the bioreactor cultivations performed for the production of conditioned medium. The time of harvest and the total cell density and protein concentration achieved at the end of each batch cultivation is also presented.

**Table 5** List of batch cultivations performed for the generation of conditioned medium

Batch Name	Time of Harvest	Total Cell Density	Protein Concentration	Remarks
	[ h ]	[ cells / ml ]	[ mg / ml ]	
CM1	88	$14.2 \times 10^6$	$0.09 \pm 0.016$	Stored at $-20^\circ \text{C}$
CM2	91	$7.52 \times 10^6$	$0.06 \pm 0.007$	Stored at $-20^\circ \text{C}$
CM3	71	$5.25 \times 10^6$	$0.08 \pm 0.005$	Used fresh
CM4	68	$9.27 \times 10^6$	$0.04 \pm 0.011$	Used fresh
CM11	71	$6.79 \times 10^6$	$0.08 \pm 0.013$	Used fresh
CM12	72	$8.01 \times 10^6$	$0.08 \pm 0.005$	Used fresh

#### 3.2.6 Capture and Fractionation of the Conditioned Medium Components

After clarification, the harvest was diluted with loading buffer and the pH and conductivity were lowered to the desired values using 2 M HCl and MiliQ water respectively. Precipitated matter, which manifested more at lower pH values, was removed using  $0.22 \mu\text{m}$  PES membrane filters (Millipore, Billerica, Massachusetts, USA). The adjusted load material was kept on ice to avoid degradation of the proteins during the long loading step. Loading of the conditioned medium into the Sartobind S membrane adsorber was performed using a peristaltic pump at the recommended flow rates. The

temperature of the adjusted load material was increased to 25° C using a double walled heat exchanger. A 0.22 µm PES Millex-GP filter unit (Millipore, Billerica, Massachusetts, USA) was connected before the membrane adsorber to remove any newly formed precipitates.

A wash step after loading, and protein elution were performed using a syringe pump Aladdin-1000 (World Precision Instruments, Sarasota, Florida, USA). Disposable syringes were filled up with either the wash or the corresponding elution buffers and injected into the membrane with the pump.

The bound proteins were recovered from the membrane by injecting the desired elution volume of the corresponding elution buffer into the membrane, while collecting the flow-through in centrifugation tubes. After taking a small 200 µl sample, the collected fractions were mixed approx. 1:1 with fresh CHOMACS medium and stored at -20° C in order to increase the stability of the eluted proteins.

#### Fractionation with a stepwise increase of pH

Optimal binding conditions were examined through a bind-and-elute experiment at pH 3, in which bound proteins were recovered from the membrane through the stepwise linear increase of the pH of the mobile phase. This was carried out after diluting the conditioned medium from the batch fermentation CM1 with binding buffer A (20 mM citrate, 20 mM phosphate, 20 mM bicine, 20 mM CHES, pH 3). The pH was then adjusted to 3.01 with 2 M HCl resulting in a final conductivity of 11.64 mS/cm (24.9° C).

Buffers for the elution were prepared beforehand by mixing low pH binding buffer A (20 mM citrate, 20 mM phosphate, 20 mM bicine, 20 mM CHES, pH 3) with high-pH elution buffer B (20 mM citrate, 20 mM phosphate, 20 mM bicine, 20 mM CHES, pH 10) at increasing ratios. The linear relationship between the increasing ratio of buffer B to buffer A was examined beforehand.

The elution volume was 5.7 ml which corresponded to 2.7 membrane volumes and was performed by injecting the elution mixtures into the membrane at 1 ml/min using a syringe pump, while collecting the flow-through. The first elution step consisted of 20% elution buffer B (pH 4.36, 6.49 mS/cm, 20.5° C) and the last one of 100% buffer B (pH 9.98, 16.98 mS/cm, 20.7° C).

Table 6 presents the pH and conductivity of the pre-mixed buffers used for the recovery of each fraction and the corresponding elution volumes.

### 3. MATERIALS AND METHODS

**Table 6** pH and conductivity of the pre-mixed buffers used for the recovery of each fraction and the corresponding elution volumes.

	Fraction		X1	X2	X3	X4	X5	X6
pH – stepwise gradient	pH	[ M ]	4.36	5.73	6.42	7.03	8.58	9.98
	Conductivity	[ mS / cm ]	6.49	9.34	10.11	11.79	14.04	16.98
	Elution Volume	[ ml ]	5.8	5.6	5.7	5.8	5.6	5.7

#### Two-step elution for increased protein recovery

In order to increase protein recovery and minimize loss due to precipitation at low pH, capture of the secretome was tested at pH 5. To achieve this, the conditioned medium was diluted in binding buffer A2 (0.2 mM citrate, pH 5) and the pH was adjusted to 5 using a 2 M HCl solution. The weaker binding of the proteins to the cation exchanger ligands caused by the higher binding pH was compensated by adjusting the conductivity of the load material down to 7 mS/cm with deionized water. Bound proteins were recovered from the membrane in a two-step elution (Figure 11). The first elution (E1) was achieved by increasing the pH of the mobile phase from 5 to 10 (E1) through the injection of elution buffer without citrate BoC1 (20 mM phosphate, 20 mM bicine, 20 mM CHES, pH 10) into the membrane. The remaining bound proteins were recovered in the second elution (E2), which was performed by injecting the high salt elution buffer without citrate BoC2 (20 mM phosphate, 20 mM bicine, 20 mM CHES, 1 M NaCl, pH 10) into the membrane, in order to increase the NaCl concentration of the mobile phase from 0 to 1 M (E2).

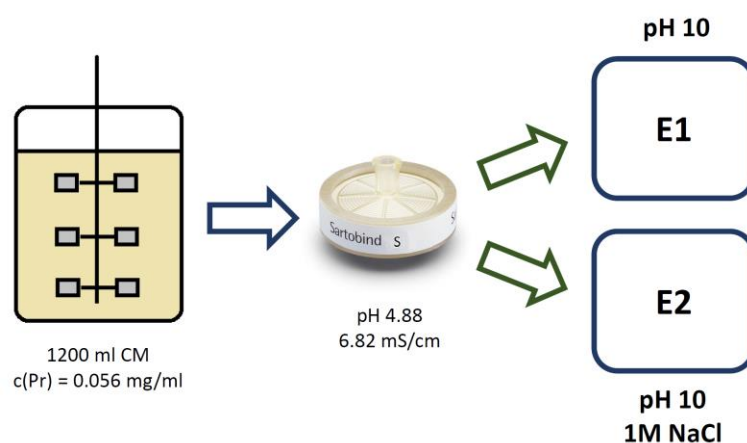


**Figure 11** Two-step elution at pH 5. The first elution (E1) was collected by increasing the pH of the mobile phase to 10. The second elution E2 was collected by increasing the salt concentration of the mobile phase to 1 M NaCl.

### 3. MATERIALS AND METHODS

A total of three two-step elution experiments were performed: TE1, TE2, and TE3. TE1 was a small scale experiment performed in order to test the new binding conditions and using conditioned medium that had been stored at -20° C. Both experiments TE2 and TE3 produced fractions that were later supplemented to growing cells with the purpose of assessing their effect on the growth, death and metabolic kinetics. The conditioned medium used for TE2 and TE3 was used immediately after harvesting and had not been frozen. Table 7 presents the fractions collected from all three two-step elution experiments with their respective elution volumes and the manner they were recovered from the membrane.

**Table 7** Fractions collected from all three two-step elution experiments with their respective elution volumes and the manner they were recovered from the membrane.

	Elution		E1 pH 10			E2 pH 10 / 1 M NaCl	
TE1	Fractions Collected		E1			E2	
	Elution Volume	[ ml ]	3.7			1.2	
TE2	Fractions Collected		X1	X2		X3	X4
	Elution Volume	[ ml ]	7.6	3.4		50.9	3.7
TE3	Fractions Collected		X1	X2	X3	X4	X5
	Elution Volume	[ ml ]	1.3	3.6	1.8	3.5	1.9

#### Optimization of Elution Parameters for E2

Recovery of elution E2 was optimized in two Bind & Elute experiments, in which two stepwise gradients with increasing NaCl concentration were tested. The first experiment (E2.EXP1) resulted in the separation of E2 into five different fractions covering a NaCl concentration range between 0 and 1 M. The recovered fractions were tested on growing cells in order to identify the concentration at which the bioactive molecules responsible for the effects of E2 elute from the cation exchanger. Further optimization was performed in the second experiment (E2.EXP2) in a concentration range between 0 and 0.2 M NaCl, which corresponded to the concentration of the fraction from E2.EXP1 that showed a positive effect.

Sartobind S MA 75 with a membrane volume of 2.1 ml was used in E2.EXP1 for the capture of the conditioned medium components, while Sartobind S MA 100 with a membrane volume of 2.8 ml was used for E2.EXP2. Adjustment of the conditioned medium to binding conditions and loading into the cation exchanger was performed following the same procedure as in the two-step-elution experiments. Immediately after clarification: the conditioned medium was diluted with binding buffer A2 (see *Buffers for Fractionation*) and adjusted with 2 M HCl to pH 5. The conductivity was then lowered to approx. 7 mS/cm with MilliQ water and precipitated matter was removed using 22 µm PES membrane filters. The adjusted protein solution was kept on ice to avoid protein degradation. Conditioned medium from the CM11 and CM12 batch cultivations (see *Generation of Conditioned Medium*) were used for E2.EXP1 and E2.EXP2 respectively.

Loading into the membrane adsorber was performed using a peristaltic pump at 20 and 30 ml/min for E2.EXP1 and E2.EXP2 respectively after increasing the temperature of the protein solution to 25° C in a double walled heat exchanger. A 0.22 µm PES Millex-GP filter unit was connected before the membrane adsorber to remove any newly formed precipitates. The flow-through was collected during the loading step, and its volume was used to calculate the total protein loaded. A total of 71.1 and 75.1 mg protein were loaded into the membrane for E2.EXP1 and E2. EXP2 respectively, which corresponded to 135% and 107% of the membrane dynamic binding capacity. Following the loading step, the membrane was washed with 25 ml AoC buffer (see *Buffers for Fractionation*) at 10 ml/min.

Following the wash step, elution E1 was recovered from the membrane by injecting BoC1 buffer (see *Cation Exchanger Buffers*) into the membrane adsorber with a syringe pump while collecting the flow-through. The elution volumes of elution E1 for E2.EXP1 and E2.EXP2 were 7.2 and 11.9 ml respectively.

Pre-mixed elution buffers, which had been prepared beforehand by mixing BoC1 buffer with BoC2 buffer (see *Buffers for Fractionation*) at different ratios, were then used for the stepwise elution of the remaining bound molecules from the membrane adsorber. They were filtered prior to use through a PVDF syringe filter into a disposable syringe to remove solid particles and the corresponding elution volumes were injected into the membrane using a syringe pump at a flow rate of 1 ml/min.

The stepwise salt gradient was performed by injecting first the buffer with the lowest NaCl concentration into the membrane and collecting the flow-through, which contained the molecules that eluted at those specific conditions. This step was repeated using the rest of the elution buffers in order of increasing salt concentration. A 200 µl sample was taken from each flow through for the Bradford

### 3. MATERIALS AND METHODS

assay. At the end of the experiment, the collected fractions were mixed approximately 1:1 with fresh CHOMACS CD medium supplemented with 4 mM L-glutamine and were stored at -20°C until further use.

Table 8 presents the NaCl concentration profile used for E2.EXP1 together with the corresponding elution volumes. A total of 6 fractions were collected covering a concentration range of 0-1 M.

**Table 8** NaCl concentration profile used for E2.EXP1 together with the corresponding elution volumes. A total of 6 fractions were collected covering a concentration range between 0 and 1 M.

	Fraction		X0	X1	X2	X3	X4	X5
E2.EXP1 Profile 1	NaCl concentration	[ M ]	0.2	0.2	0.4	0.6	0.8	1
	Elution Volume	[ ml ]	1.4	6.0	4.3	4.6	4.4	4.5

The fractions collected using the elution buffer mixed to a final concentration of 0.2 M NaCl showed positive results during the first optimization experiment. The next step was the further separation of this fraction using elution buffers within the range of 0 to 0.2 M NaCl. Table 9 presents the NaCl concentration profile used for the second optimization experiment E2.EXP2 and the corresponding elution volume of each one of the seven collected fraction. Fractions X1.0 – X1.4 fell within the range of interest, while fractions X2 and X3 were collected in order to be able to calculate the total recovery yield, thus allowing comparison between both separations.

**Table 9** NaCl concentration profile used for the second optimization experiment E2.EXP2 and the corresponding elution volume of each one of the seven collected fraction.

	Fraction		X1.0	X1.1	X1.2	X1.3	X1.4	X2	X3
E2.EXP2 Profile 2	NaCl concentration	[ M ]	0.05	0.05	0.1	0.15	0.2	0.4	0.1
	Elution Volume	[ ml ]	0.9	6.1	6.1	6.0	6.1	6.5	7.4

Table 10 summarizes the parameters of the six bind-and-elute experiments that were performed and presents their corresponding binding pH and conductivities, the conditioned medium used, the total

### 3. MATERIALS AND METHODS

protein loaded, the percentage of the membrane dynamic binding capacity used and the size of the membrane adsorber.

**Table 10** List of two-step elution experiments performed in this chapter and their corresponding binding pH and conductivities, the conditioned medium used, the total protein loaded, the percentage of the membrane dynamic binding capacity used and the size of the membrane adsorber.

Fractionation Experiment	Binding pH	Conductivity	Conditioned Medium	Loaded Protein	% of Dynamic Binding Capacity	Membrane Size
	[ - ]	[ mS / cm ]		[ mg ]	[ % ]	[ ml ]
pH – stepwise increase	3.01	11.64 (24.9° C)	CM1	25.69	48.93	2.1
TE1	4.88	6.82 (24.6° C)	CM2	1.84	92.00	0.08
TE2	5.00	6.87 (20.9° C)	CM3	87.22	124.60	2.8
TE3	5.00	6.41 (22.3° C)	CM4	20.19	38.46	2.1
E2.EXP1	4.94	6.86 (24.3° C)	CM11	71.1	135	2.1
E2.EXP2	5.01	6.63 (22.5° C)	CM12	75.1	107	2.8

#### 3.2.7 Fraction Evaluation

The conditioned medium fractions recovered from the TE2 and TE3 experiments were sterile filtered using a 0.20 µm PES Rotilabor syringe filter (Carl Roth, Karlsruhe, Germany) and either supplemented to fresh CHOMACS CD growth medium or directly given to growing cells.

##### Testing of First Elution E1

The conditioned medium components for this experiment were recovered from the second two-step elution experiment TE2 and corresponded to the pooled X1 and X2 fraction of elution E1. Testing was carried out in triplicates in 125 ml disposable shaking flasks with a working volume of 40 ml each. Exponentially growing CHO-K1 cells were inoculated at a starting cell density of  $3 \times 10^5$  cells/ml in CHOMACS CD growth medium supplemented with 4 mM L-glutamine and the E1 elution fraction to a final protein concentration of 0.1 mg/ml. A negative control (NC) was cultivated simultaneously in triplicates under the same starting conditions, except that instead of the fraction, the same volume of



elution buffer BoC1 without protein was supplemented to the growth medium. The final concentration of the BoC1 buffer in both, the negative and positive controls, was 4.9 vol% (0.98 mM phosphate, 0.98 mM CHES, 0.98 mM BICINE).

The cells for the experiment were harvested from a parent culture that originated from the continuous culture. It was inoculated at a total cell density ( $N_t$ ) and viability of  $1.53 \pm 0.04 \times 10^6$  cells/ml and  $89.6\% \pm 2.82\%$  and was cultivated for 18 hours reaching an  $N_t$  and viability of  $2.94 \pm 0.081 \times 10^6$  cells/ml and  $90.1\% \pm 2.94\%$  ( $\mu = 0.039 \pm 0.0009$  1/h;  $k_d = 0.004 \pm 0.0035$  1/h). The culture was then diluted with fresh CHOMACS CD growth medium to an  $N_t$  and viability of  $7.25 \pm 0.152 \times 10^5$  cells/ml  $88.4\% \pm 1.90\%$  and was cultivated for further 32 hours until it reached  $2.96 \pm 0.081$  cells/ml with a viability of  $93.4\% \pm 1.64\%$  ( $\mu = 0.048 \pm 0.0029$  1/h;  $k_d = 0.002 \pm 0.0012$  1/h) prior to inoculation of the experiment.

The inoculation volume was centrifuged down, the supernatant removed and the pellet resuspended in the growth medium containing either the fraction or the BoC1 buffer. Medium exchange of the inoculation volume was performed through centrifugation to avoid overlapping effects caused by bioactive molecules found in the carry-over conditioned medium. The experiment started once the cell suspension was evenly distributed among three shaking flasks, each one corresponding to one replicate with a working volume of 40 ml. The cultures were cultivated for 112 hours and samples were taken every 24 hours. The kinetic parameters were calculated using *Model II* (see *Determination of Kinetic Parameters*).

#### Testing of Second Elution E2 from the Two-Step Elution Experiment

The protein material for this experiment was recovered from the third two-step elution experiment TE3 and corresponded to the fraction X4 from elution E2. Testing was carried out in triplicates (3 x 10 ml working volume) by adding the fraction to cells growing at an  $N_t$  of  $1.08 \times 10^6$  cells/ml, specific growth rate of  $\mu = 0.045$  h<sup>-1</sup> and 93.97% viability to a final protein concentration of 0.029 mg/ml. A negative control was cultivated simultaneously in triplicates under the same starting conditions and was given the same volume of elution buffer BoC2 (20 mM phosphate, 20 mM bicine, 20 mM CHES, 1 M NaCl, pH 10) without protein. Final elution buffer and NaCl concentration in both the negative (NC) and positive (E2) controls were 5.3% (1.96 mM phosphate, 1.06 mM CHES, 1.06 mM BICINE) and 52 mM respectively.

The cells for the experiment were harvested from the continuous culture and inoculated 21 hours prior to the experiment at  $N_t$  of  $4.5 \times 10^5$  cells/ml. No medium exchange nor resuspension in fresh medium was performed before fraction X4 or buffer BoC2 were given to the cultures. The experiment started after adding fraction X4 or the buffer to the cell suspension, which was then distributed among three cultivation tubes, each one corresponding to one replicate with a working volume of 10 ml each. The cultures were cultivated for 25 hours and the kinetic parameters were calculated using *Model I* (see *Determination of Kinetic Parameters*).

#### Testing of the Optimized Elution E2 Fractions

Screening of the six collected fractions X0 – X5 from the E2.EXP1 experiment was performed by supplementing an exponentially growing culture with a working volume of 10 ml and an average  $N_t$  of  $8.43 \pm 0.472 \times 10^5$  cells/ml. In order to be able to test all the fractions simultaneously, testing was carried out without any replicate cultures. Furthermore, the increasing NaCl concentration of the fraction limited the total volume that could be given to the culture without negatively affecting the growth due to the increasing osmolarity. For this reason a final NaCl concentration of 30 mM was chosen as the upper limit for the cultures to which fractions X2 – X5 were given, and the supplementation volume was calculated accordingly. This resulted in significantly less fraction volume being given to the latter cultures, and thus lower final protein concentrations. Nonetheless, the volumes of fractions X0 and X1 were calculated to a final protein concentration of 0.02 mg/ml protein. Because of the void volume of 1.3 ml of the Sartobind S MA 75 and back-mixing effects inside of the capsule, the salt concentration of the collected fractions did not match the salt concentration of the pre-mixed buffer used for the recovery and was calculated as a range between a maximum and a minimum. Three negative controls, X0 NC, X1 NC and NC30, were supplemented with elution buffer BoC2 to match the maximal NaCl concentration of the cultures X0, X1 and X2 – X5 respectively. They were cultivated simultaneously to the supplemented cultures and an undisturbed culture (NC) without supplementation of either buffer or NaCl. Total cultivation time was 17 hours.

The cells for the experiment were produced in a pre-culture harvested from the continuous culture. It was inoculated at an  $N_t$  and viability of  $4.77 \times 10^5$  cells/ml and 96.7% and was cultivated for 21 hours to an  $N_t$  and viability of  $1.09 \times 10^6$  cells/ml and 93.4%. At the time of the experiment the pre-culture was in the exponential phase of growth, showing a specific growth rate of 0.041 1/h. The pre-culture was supplemented without any medium exchange or dilution with fresh medium.

### 3. MATERIALS AND METHODS

Table 11 presents volume of pre-culture, E2.EXP1 fraction and BoC2 buffer used for the supplementation of each culture and negative control, together with the NaCl concentration ranges calculated for the cultures supplemented with fraction and the final salt concentration of the negative controls. The fractions were thawed the same day of the experiment at room temperature and were sterile filtered using a 0.22  $\mu$ m PES sterile syringe membrane.

**Table 11** Volume of pre-culture, fraction and BoC2 buffer used for the supplementation of each culture and negative control, together with the NaCl concentration ranges calculated for the cultures supplemented with fraction and the final salt concentration of the negative controls.

Supplemented Cultures (E2.EXP1)	Fraction	Pre-culture	NaCl Concentration	Protein Concentration
	[ ml ]	[ ml ]	[ mM ]	[ mg / ml ]
X0	0.3	10	0.3 – 3.3	0.02
X1	1.7	10	12.9 – 14.5	0.02
X2	1.7	10	21.8 – 25.7	0.01
X3	1.1	10	24.6 – 27.1	0.004
X4	0.8	10	25.7 – 27.7	0.001
X5	0.6	10	26.5 – 28.2	0
Negative Controls	BoC2 Buffer	Pre-culture	NaCl Concentration	Protein Concentration
	[ $\mu$ l ]	[ ml ]	[ mM ]	[ mg / ml ]
NC X0	34	10	3.4	0
NC X1	170	10	16.7	0
NC30	300	10	29.1	0
NC	0	10	0	0

Fractions X1.0 – X1.4 recovered from the E2.EXP2 experiment, which covered a NaCl concentration range between 0 and 0.2 M, were tested in triplicates on cells growing exponentially at an average  $N_t$  of  $9.05 \pm 0.360 \times 10^5$  cells/ml and a working volume of 9 ml. Fractions X1.0 and X1.1 were pooled together and were tested as one fraction (X1.C).

The screening was planned by targeting a specific supplementation volume instead of a specific protein concentration because of the different amounts of protein recovered in each fraction. The low NaCl

### 3. MATERIALS AND METHODS

---

concentration used for elution allowed for larger supplementation volumes to be used, which resulted in a maximal salt concentration of 34.2 mM for the culture corresponding to fraction X1.4. A negative control (NC30) culture was prepared to match this maximal NaCl concentration by giving the buffers BoC1 and BoC2 in the right amounts. Furthermore, the salt concentration of the rest of the supplemented cultures was also corrected to 34.2 mM using a 1 M NaCl stock solution mixed in fresh CHOMACS CD medium supplemented with 4 mM L-glutamine, thus allowing their comparison to NC30.

The cells for the experiment were produced in a pre-culture that was harvested from the continuous culture. It was inoculated at an  $N_t$  and viability of  $7.99 \times 10^5$  cells/ml and 97.1% and was cultivated for 25 hours to an  $N_t$  and viability of  $2.58 \times 10^6$  cells/ml and 93.2%. At the time of the experiment the pre-culture was in the exponential phase of growth, showing a  $\mu$  of 0.049 1/h. The pre-culture was mixed with fresh CHOMACS CD medium at the moment of supplementation to lower the cell density. A second negative control (NC), which was diluted with the same amount of fresh medium, was cultivated simultaneously without the supplementation of buffer or salt.

Table 12 presents the preparation of every supplemented culture and negative control. The volumes were calculated taking into consideration the triplicate cultivation, for this reason the total volume used was 27 ml. Every single culture was inoculated, according to the calculations, in 17.11% of the fractionation buffer (3.4 mM phosphate, 3.4 mM bicine, 3.4 mM CHES) and 26% of the conditioned medium from the pre-culture. The final NaCl concentration range of the cultures supplemented with fraction was calculated analogously to the previous experiment taking into consideration the 4.3 ml void volume of the Sartobind S MA100 membrane adsorber. The fractions were thawed at the same day of the experiment at room temperature and were sterile filtered using a 0.22  $\mu$ m PES sterile syringe membrane. The experiment started once all the components were mixed together and the culture was evenly distributed among three cultivation tubes, each one representing one replicate culture. Total cultivation time was 22 hours.

### 3. MATERIALS AND METHODS

**Table 12** Volume of pre-culture, fraction and BoC2 buffer used for the supplementation of each culture and negative control, together with the NaCl concentration ranges calculated for the cultures supplemented with fraction and the final salt concentration of the negative controls.

Supplemented Cultures (E2.EXP2)	Fraction	Pre-culture	CHOMACS CD	1 M NaCl	NaCl Concentration	Protein Concentration
	[ ml ]	[ ml ]	[ ml ]	[ $\mu$ l ]	[ mM ]	[ mg / ml ]
X1.C	10	7	9.3	691	29.4 – 34.2	0.08
X1.2	10	7	9.6	461	28.3 – 34.2	0.05
X1.3	10	7	9.8	236	28.3 – 34.2	0.04
X1.4	10	7	10	0	28.3 – 34.2	0.03
Negative Controls	BoC1	Pre-culture	CHOMACS CD	BoC2	NaCl Concentration	Protein Concentration
	[ ml ]	[ ml ]	[ ml ]	[ $\mu$ l ]	[ mM ]	[ mg / ml ]
NC30	3.7	7	15.4	924	34.2	0
NC	0	7	20	0	0	0

The volumes were calculated taking into consideration the triplicate cultivation, for this reason the total volume used was 27 ml. Every single culture was inoculated, according to the calculations, in 17.11% of the fractionation buffer (3.4 mM phosphate, 3.4 mM bicine, 3.4 mM CHES) and 26% of the conditioned medium from the pre-culture. The final NaCl concentration range of the cultures supplemented with fraction was calculated analogously to the previous experiment taking into consideration the 4.3 ml void volume of the Sartobind S MA100 membrane adsorber. The fractions were thawed at the same day of the experiment at room temperature and were sterile filtered using a 0.22  $\mu$ m PES sterile syringe membrane. The experiment started once all the components were mixed together and the culture was evenly distributed among three cultivation tubes, each one representing one replicate culture. Total cultivation time was 22 hours.

### 3.3 Hydrophobic Interaction Chromatography Purification Step

A hydrophobic interaction membrane adsorption purification step was developed for the orthogonal fractionation of the second elution E2. Different salts at different concentrations were examined to find the binding conditions with the highest recovery yield. Once found, a one-step elution experiment was performed and the recovered proteins were tested on exponentially growing cells.

#### 3.3.1 Production of Elution E2 Fraction

Two two-step elution experiments were performed using the Sartobind S cation exchanger for the production of the fractions of elution E2 that were used for the development and testing of the HIC-MA step. Conditioning of the growth medium, harvest, capture and fraction recovery were performed following the same procedure described in the Chapter *Cation Exchange Chromatography Purification Step* for the two-step-elution cation exchanger experiments.

Table 13 summarizes the bioreactor cultivations performed for the conditioning of the growth medium. The time of harvest and the total cell density and protein concentration achieved prior to capture into the cation exchanger are presented.

**Table 13** Batch cultivations performed for the generation of the conditioned medium used for the development of the HIC purification step

Batch Name	Time of Harvest	Total Cell Density	Protein Concentration	Remarks
	[ h ]	[ cells / ml ]	[ mg / ml ]	
CM9	69	$6.86 \times 10^6$	$0.07 \pm 0.007$	Used fresh
CM10	70	$8.19 \times 10^6$	$0.07 \pm 0.003$	Used fresh

Table 14 presents the binding conditions at which the components of the conditioned medium were captured into the Sartobind S cation exchanger. The table presents the binding pH and conductivity, the conditioned medium used for each experiment, the amount of protein loaded and the percentage of the membrane binding capacity used, and finally the size of the membrane adsorber.

### 3. MATERIALS AND METHODS

**Table 14**, binding pH and conductivity, conditioned medium used, amount of loaded protein, percentage of membrane binding capacity used and size of the membrane of both two-step elution experiments performed to generate the fractions of elution E2 used for the development of the HIC purification step.

Fractionation Experiment	Binding pH	Conductivity	Conditioned Medium	Loaded Protein	% of Dynamic Binding Capacity	Membrane Size
	[ - ]	[ mS / cm ]		[ mg ]	[ % ]	[ ml ]
CE9	4.98	6.81 (23.2° C)	CM9	65.5	127.8	2.1
CE10	4.99	6.99 (23.6° C)	CM10	37.3	71.0	2.1

Table 15 depicts the fractions collected in both two-step elution experiments, the method of elution and their respective elution volumes. Several fractions of each elution were collected to maximize protein concentration and minimize elution volume.

**Table 15** Fractions collected in both two-step elution experiments, the method of elution and their respective elution volumes.

	Elution		E1 pH 10		E2 pH 10 / 1 M NaCl	
			X1	X2	X3	X4
CE9	Fractions Collected					
	Elution Volume	[ ml ]	8.4	2.1	7.2	2.2
CE10	Fractions Collected		X1	X2	X3	X4
	Elution Volume	[ ml ]	1.0	6.3	2.1	8.0

#### 3.3.2 Screening for Optimal Conditions

Ammonium sulfate, sodium chloride and potassium chloride were tested in a concentration range of 1 – 3 mM in 10 mM phosphate buffer at pH 7. Table 16 shows the experiments performed with their corresponding salts and concentrations. The protein material for this examination was the fraction X3 from the second elution E2 recovered from the CE9 experiment, which had a protein concentration of  $0.45 \pm 0.088$  mg/ml and a NaCl concentration between 0.41 – 0.58 M after recovery and after being

### 3. MATERIALS AND METHODS

mixed approximately 1:1 with fresh CHOMACS medium. It had been stored at -20° C after recovery and was thawed and aliquoted before the first set of experiments. One aliquot was used directly after thawing, while the rest were stored again at -20° C until used. The experiments corresponding to the same salt concentration were performed on the same day. The protein concentration of the E2 fraction X3 had decreased prior to the screening experiments, possibly due to the freezing and thawing process, and was in average  $0.12 \pm 0.027$  mg/ml prior to binding into the phenyl membrane.

**Table 16** List of the experiments performed with different salt species at different concentrations for the screening of optimal binding conditions

Added Salt Concentration	Ammonium Sulfate	Sodium Chloride	Potassium Chloride
1 M	Exp 1.1	Exp 2.1	Exp 3.1
2 M	Exp 1.2	Exp 2.2	Exp 3.2
3 M	-	Exp 2.3	-

#### Buffers

Table 17 shows the composition of the different buffers used with the phenyl membrane adsorber. The buffers were stored at 4° C for no longer than two weeks and were filtered through a PVDF syringe filter and transferred into a disposable syringe before loading into the membrane.

**Table 17** Composition of the different buffers used with the phenyl membrane adsorber.

Experiment		Buffer	Composition	pH
Equilibration Buffer	Exp 1.1	HA 1.1	10 mM phosphate, 1M natrium sulfate	pH 7
	Exp 1.2	HA 1.2	10 mM phosphate, 2M natrium sulfate	pH 7
	Exp 2.1	HA 2.1	10 mM phosphate, 1M sodium chloride	pH 7
	Exp 2.2	HA 2.2	10 mM phosphate, 2M sodium chloride	pH 7
	Exp 2.3	HA 2.3	10 mM phosphate, 3M sodium chloride	pH 7
	Exp 3.1	HA 3.1	10 mM phosphate, 1M potassium chloride	pH 7
	Exp 3.2	HA 3.2	10 mM phosphate, 2M potassium chloride	pH 7
Elution Buffer		HB	10 mM phosphate	pH 7



### 3. MATERIALS AND METHODS

All the chemicals used for the buffers had been tested by manufacturer and were suitable for cell culture. Sodium phosphate ( $\geq 99.0\%$ ), ammonium sulfate ( $\geq 99.0\%$ ), sodium chloride ( $\geq 99.0\%$ ), and potassium chloride ( $\geq 99.0\%$ ).

#### Adjustment of Load Material to Binding Conditions

Adjustment of the protein solution to the different binding conditions was performed in 50 ml disposable reaction tubes according to Table 18. The amount of salt needed for a specific loading volume was calculated, weighed in a microscale, given into the tube and mixed with low salt elution buffer HB (10 mM phosphate, pH 7) until fully dissolved at room temperature. Then the fraction was given, its volume filled up with buffer HB to the desired loading volume and the pH measured and adjusted with 1 M NaOH. The equilibrated load solution was then filtered through a PES syringe filter to remove precipitates and subsequently transferred into a disposable syringe. The final salt concentration presented on Table 18 was calculated from the salt weighed plus the molar NaCl concentration of the elution E2 fraction used.

**Table 18** Amount of salt, buffer HB and Elution E2 from CE9 given to each reaction tube, followed by the load volume, the final salt concentration including the NaCl concentration of E2, and final pH after adjustment.

	Experiment	Salt	Buffer HB	Elution E2 fraction	Load Volume	Final Salt Concentration	Final pH
		[ g ]	[ ml ]	[ ml ]	[ ml ]	[ M ]	[ - ]
Ammonium Sulfate	Exp 1.1	1.33	8.07	1.25	10	1.06 – 1.08	7.00
	Exp 1.2	2.69	7.47	1.28	10	2.09 – 2.11	7.00
Sodium Chloride	Exp 2.1	0.58	8.15	1.25	10	1.04 – 1.07	7.00
	Exp 2.2	1.16	9.07	1.3	10	2.04 – 2.06	7.02
	Exp 2.3	2.63	10.02	3.74	15	3.10 – 3.15	6.96
Potassium Chloride	Exp 3.1	0.75	8.15	1.29	10	1.06 – 1.08	6.98
	Exp 3.2	1.55	8.15	1.12	10	2.12 – 2.14	7.03

#### Capture and One-Step Elution

Sartobind Phenyl pico membrane adsorbers from Sartorius Stedim Biotech (Goettingen, Germany) with a membrane volume of 0.08 ml, a dynamic binding capacity of 0.6 mg protein per unit and 0.4 ml void volume were used in the experiments. Equilibration, loading, wash and elution were performed in that order using a syringe pump and disposable syringes. The membrane was equilibrated at 1 ml/min with 4 ml of the corresponded equilibration buffer according to Table 18. During loading, the flow-through was collected and weighed to determine the exact protein loaded. After loading and before elution, a wash step was performed with 4 ml of the corresponding equilibration buffer to remove protein solution still held in the membrane capsule and to avoid carryover into the collected fractions. Elution of the proteins was achieved by reducing the salt concentration of the mobile phase to 0 M in one single step. This was carried out by injecting elution buffer HB (10 mM phosphate, pH 7) at 1 ml/min into the phenyl membrane, while collecting the flow-through. Two fractions were collected in the experiments corresponding to 1 M salt, the first was 2.5 ml and the second 1 ml. In the experiments corresponding to 2 M salt three fractions were collected, the first was 0.5 ml, the second 1 ml and the third 1 ml. In the experiment corresponding to 3 M, two fractions were collected, both of 1 ml.

#### 3.3.3 Testing of HIC Elution in Cell Culture

Sodium chloride at a concentration of 3 M was selected for the capture of the proteins in elution E2 into the Sartobind Phenyl membrane adsorber. The protein material was the fraction X4 of elution E2 recovered from the CE10 experiment. The fraction had been mixed approximately 1:1 with fresh CHOMACS CD medium and had a NaCl concentration between 0.44 – 0.59 M. It had a measured protein concentration of  $0.17 \pm 0.009$  mg/ml after recovery and  $0.13 \pm 0.008$  mg/ml at the time of the phenyl experiment. It was stored at -20° C after recovery and was thawed before each experiment.

#### Examination of the Source Material

The effect of the E2 fraction X4 was tested before capture into the Sartobind Phenyl membrane adsorber. Furthermore, the influence of the total cell density ( $N_t$ ) and conditioned medium harvested in the exponential phase of growth on the intensity of the effect was explored. The E2 fraction was tested in biological triplicates (3 x 9 ml working volume) to a calculated final protein concentration of  $0.009 \pm 0.0005$  mg/ml and 3.1 vol% of elution buffer BoC2 (0.62 mM phosphate, 0.62 mM CHES, 0.62 mM Bicine, 30.7 M NaCl) to exponentially growing cells at a low cell density (LCD) growing in

### 3. MATERIALS AND METHODS

conditioned medium, and at a medium cell density (MCD) growing in conditioned (CM) and in fresh medium (FM) (Table 19).

**Table 19** Cultures inoculated for the examination of the effect of fraction X4 from the elution E2 from the CE10 two-step elution experiment.

	Culture	Description	Salt Concentration [ mM ]
Low Cell Density (LCD)	LCD	Low cell density + E2 in conditioned medium	22.6 – 30.7
	LCD NC30	Low cell density + BoC2 in conditioned medium	30.7
Medium Cell Density (MCD)	MCD CM	Medium cell density + E2 in conditioned medium	22.6 – 30.7
	MCD FM	Medium cell density + E2 in fresh medium	22.6 – 30.7
	NC30	Medium cell density + BoC2 in conditioned medium	30.7
	NC	Undisturbed negative control	0

Two negative controls were cultivated simultaneously in conditioned medium at a low (LCD NC30) and at a medium (NC30) cell density, both without protein and supplemented with elution buffer BoC2 at the same concentration of the positive controls. Undisturbed cells were cultivated as a third negative control (NC) at a medium cell density without supplementation of BoC2 to examine the effect of the added salt and buffer. Cells for the experiment were produced in a parent culture simultaneously used for the conditioning of the medium. It was harvested from the continuous culture (see *Cell Culture* from the *Materials and Methods* Section from the Chapter *Conditioned Medium and the Kinetics of CHO-K1 Cell Culture*), inoculated at  $3.92 \pm 0.055 \times 10^5$  cells/ml and a viability of  $95.6\% \pm 0.59\%$  in 80 ml and cultivated for 24 hours to  $1.22 \pm 0.036 \times 10^6$  cell/ml and 94.1% viability ( $\mu = 0.049 \pm 0.0006$  1/h). The culture was then diluted with fresh CHOMACS CD to  $4.89 \pm 0.268 \times 10^5$  cells/ml with a viability of  $95.7\% \pm 0.51\%$ , and was cultivated for 16 hours reaching  $9.97 \pm 0.253 \times 10^5$  cells/ml with a viability of  $95.3\% \pm 1.39\%$  ( $\mu = 0.045 \pm 0.0033$  1/h). The experiment started once the parent culture was combined with elution E2 fraction or BoC2 elution buffer and fresh CHOMACS CD according to Table 20, and the resulting volume evenly distributed in three 50 ml cultivation tubes. The cell density of the LCD cultures was reduced by combining 7.7 ml of the parent culture with 17.9 ml conditioned medium harvested at 2500 x g for 15 min at room temperature. The cultures were cultivated for 23 hours and samples were taken at 0 and 23 cultivation hours. The kinetic parameters were calculated

### 3. MATERIALS AND METHODS

using Model I (see *Determination of Kinetic Parameters* from the *Materials and Methods* Section from the Chapter *Conditioned Medium and the Kinetics of CHO-K1 Cell Culture*).

**Table 20** Pipetting scheme used for the inoculation of the cultures used to examine the effect of fraction X4 from the elution E2 from the CE10 two-step elution experiment.

Culture	Fraction	Parent Culture	CHOMACS CD	BoC2 Buffer	Starting N <sub>t</sub>
	[ ml ]	[ ml ]	[ ml ]	[ µl ]	[ 10 <sup>5</sup> cells/ ml ]
LCD	1.4	25.6*			0.28 ± 0.005
LCD NC		25.6*	0.57	829	0.32 ± 0.009
MCD CM	1.4	25.6			1.08 ± 0.048
MCD FM	1.4	25.6			1.09 ± 0.039
NC30		25.6	0.57	829	1.11 ± 0.045
NC		27			1.16 ± 0.035
*The cell density of the LCD cultures was reduced by combining 7.7 ml of the parent culture with 17.9 ml conditioned medium harvested at 2500 x g for 15 min at room temperature.					

#### Capture into Phenyl Membrane and Testing in Cell Culture

The remaining Elution E2 fraction X4 was thawed and adjusted to the binding conditions following the method described in section *Adjustment of Load Material to Binding Conditions* according to Table 21. A total of  $0.85 \pm 0.053$  mg protein were loaded into the membrane, which corresponded to 142.04% if the dynamic binding capacity. Equilibration, loading, wash and elution were performed in that order using a syringe pump and disposable syringes. Equilibration and the wash step after loading were performed with 4 ml at 1 ml/min with buffer HA2.3 (10 mM phosphate, 3 M NaCl, pH7). During loading, the flow-through was collected and weighed to determine the exact loaded protein. Elution of the components was performed at 0.1 ml/ml and achieved by reducing the salt concentration of the mobile phase to 0 M in one step by injecting elution buffer HB (10 mM phosphate, pH 7) through the membrane. A total of 7 fractions were collected to determine the adequate elution volume: PE (0.4 ml), HE1 (0.5 ml), HE2 (0.5 ml), HE3 (0.5 ml), S1 (0.5 ml), S2 (0.5 ml), S3 (0.5 ml).

### 3. MATERIALS AND METHODS

**Table 21** Amount of NaCl and volume of buffer HB added for the adjustment of elution E2 fraction X4 to binding conditions. The protein material recovered from this experiment was tested on growing cells.

	NaCl	Buffer HB	Elution E2 fraction	Load Volume	Final Salt Concentration	Final pH
	[ g ]	[ ml ]	[ ml ]	[ ml ]	[ M ]	[ - ]
3 M NaCl Experiment	3.51	11.34	7.59	20	3.23 – 3.27	6.99

The effect of the recovered proteins was examined in triplicates (3 x 7 ml working volume) on cells growing exponentially in their own conditioned medium at a starting cell density of  $3.62 \pm 0.159 \times 10^5$  cells/ml and a calculated final protein concentration of  $0.007 \pm 0.0038$  mg/ml.

The cells for the experiment were harvested from the continuous culture, inoculated at  $4.12 \times 10^5$  cells/ml and 96.2% viability in 40 ml and cultivated for 21 hours to  $7.07 \pm 0.016$  cells/ml and  $95.0\% \pm 1.19\%$  viability ( $\mu = 0.027$  1/h). The culture was then diluted to a final volume of 100 ml with fresh CHOMACS CD, resulting in a total cell density ( $N_t$ ) of  $2.85 \pm 0.048 \times 10^5$  cell/ml and  $94.1\% \pm 1.36\%$  viability, and was cultivated for 47 hours reaching an  $N_t$  and viability of  $2.73 \pm 0.057 \times 10^6$  cell/ml and 92.0%. During the last 24 hours of cultivation the culture showed a specific growth rate ( $\mu$ ) of  $0.058 \pm 0.0011$  1/h. Prior to the experiment, 60 ml of the parent culture were centrifuged down at  $6800 \times g$  for 15 min at room temperature to harvest the conditioned medium. Testing was carried out after mixing the pooled fractions with the inoculation volume and the harvested conditioned medium according to Table 22. Three negative controls were cultivated simultaneously in triplicates (3 x 7 ml working volume). In the first one (Phos NC) the volume of the pooled fractions was substituted with elution buffer HB recovered from an unused membrane capsule, simulating the recovery of the pooled fractions: the capsule was filled with high salt buffer HA2.3, then 0.4 ml of elution buffer HB were injected into the membrane and the flow through discarded. Finally, further 1.5 ml of buffer HB were injected through the membrane, collected, sterile filtered through a PES membrane and given to the negative control. The second (NC CM) and the third (NC FM) negative controls consisted of only the inoculation volume and the harvested conditioned medium or fresh CHOMACS CD respectively. The experiment started once the mixtures had been evenly distributed in three 50 ml reaction tubes, each corresponding to one replicate. Samples of the cell suspension were taken at 0, 21 and 46 cultivation hours from each culture to determine the  $N_t$ , viability and glucose ( $c_{Glc}$ ), lactate ( $c_{Lac}$ ) and glutamine ( $c_{Gln}$ ) concentrations. The kinetic parameters were calculated using Model I (see *Determination of*

### 3. MATERIALS AND METHODS

---

*Kinetic Parameters from the Materials and Methods Section from the Chapter Conditioned Medium and the Kinetics of CHO-K1 Cell Culture).*

**Table 22** Pipetting scheme used for the inoculation of the cultures used to examine the effect of the HIC elution (HE) from the 3 M NaCl experiment

	Elution / Buffer	Conditioned Medium	Fresh Medium	Inoculation Volume	Total Volume	Conditioned Medium
	[ ml ]	[ ml]	[ ml ]	[ ml ]	[ ml ]	[ vol% ]
HE	1.5	17.24	0	2.26	21	92.86
Phos NC	1.5	17.24	0	2.26	21	92.86
NC CM	0	18.74	0	2.26	21	100
NC FM	0	0	18.74	2.26	21	10.76

## 4 Results

### 4.1 Conditioned Medium and the Kinetics of CHO-K1 Cell Culture

#### 4.1.1 Kinetics of Conditioned Medium

Figure 12 depicts the total cell density (A) and viability (B) of the cultures inoculated in CHOMACS CD growth medium containing 0 vol% and 25 vol% conditioned medium (CM) respectively. The reported values were calculated as the average of triplicate cultures and the error bars represent the standard deviation. The culture growing without conditioned medium reached a maximum cell density of  $9.79 \pm 0.778 \times 10^6$  cells/ml at 118 cultivation hours, which was  $15\% \pm 9.4\%$  higher ( $p < 0.05$ ) than that of the culture growing with conditioned medium, which reached a maximum total cell density of  $8.11 \pm 0.033 \times 10^6$  cells/ml at the same cultivation time. The viability of both cultures showed a very similar progression, steadily decreasing until 72 cultivation hours, followed by a steady increase, and finally plummeting on the last day. The culture growing without conditioned medium showed a consistently lower viability and was an average of  $10\% \pm 7.5\%$  lower ( $p < 0.05$ ) between 72 and 94 hours, reaching a minimum of  $79.0\% \pm 3.45\%$  at 72 hours. Except for the last day, the viability of the culture cultivated in conditioned medium did not drop below 85% and reached  $89.0\% \pm 0.78\%$  at 72 hours.

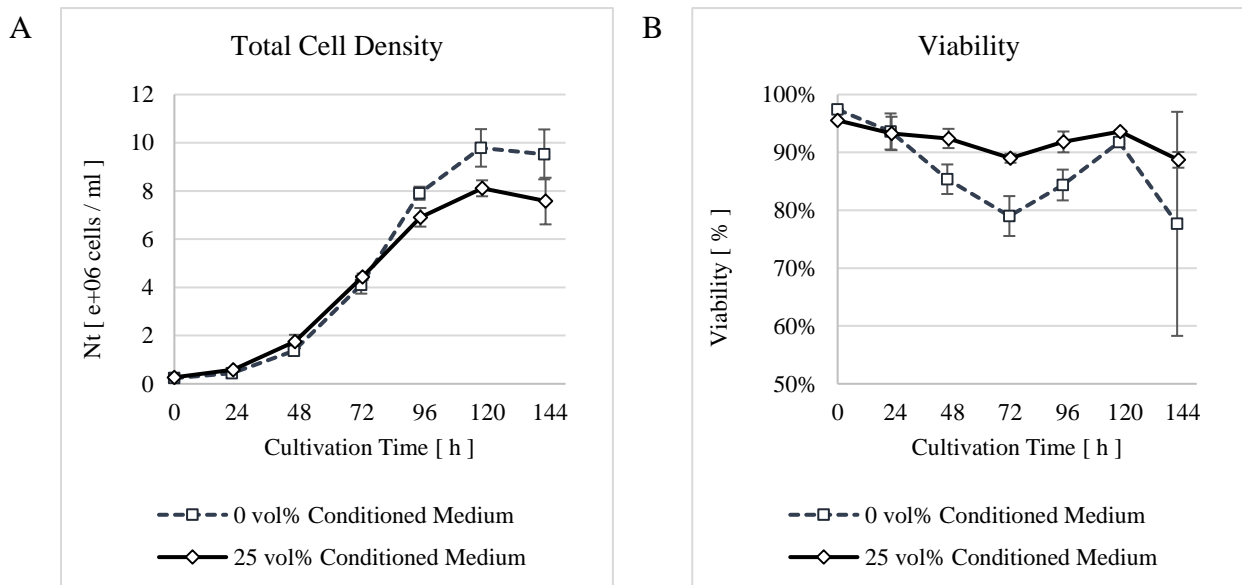


**Figure 12** Total cell density ( $N_t$ ) (A) and viability (B) of the cultures inoculated in CHOMACS CD growth medium containing 0 vol% and 25 vol% conditioned medium (CM). The values given in the graphs were calculated as the average of the triplicate cultures and the error bars represent the standard deviation.

## 4. RESULTS

Figure 13 presents the specific growth (A) and death (B) rates calculated differentially between the time points of each sample. The values given in the graphs were calculated as the average of the triplicate cultures and the error bars represent the standard deviation.

The specific growth rates ( $\mu$ ) of both cultures followed a very similar progression and did not significantly differ from each other during the first 48 hours of cultivation and between the last 94 to 142 hours. They were calculated respectively for the 0 vol% and 25 vol% CM cultures at  $0.029 \pm 0.0070$  and  $0.036 \pm 0.0050$  1/h during the first 24 hours and reached their maximum at  $0.053 \pm 0.0048$  and  $0.049 \pm 0.0045$  1/h between 24 and 48 hours of cultivation. The maximal growth rate ( $\mu_{\max}$ ) was followed by a steady decrease until the end of the cultivation for the 25 vol% CM culture, while the 0 vol% CM only decreased slightly during the next 24 hours, followed by the same steady decrease as its counterpart. Between 48 and 96 hours  $\mu$  of the 25 vol% CM culture was consistently lower an average of  $31\% \pm 17.1\%$  ( $p < 0.05$ ).

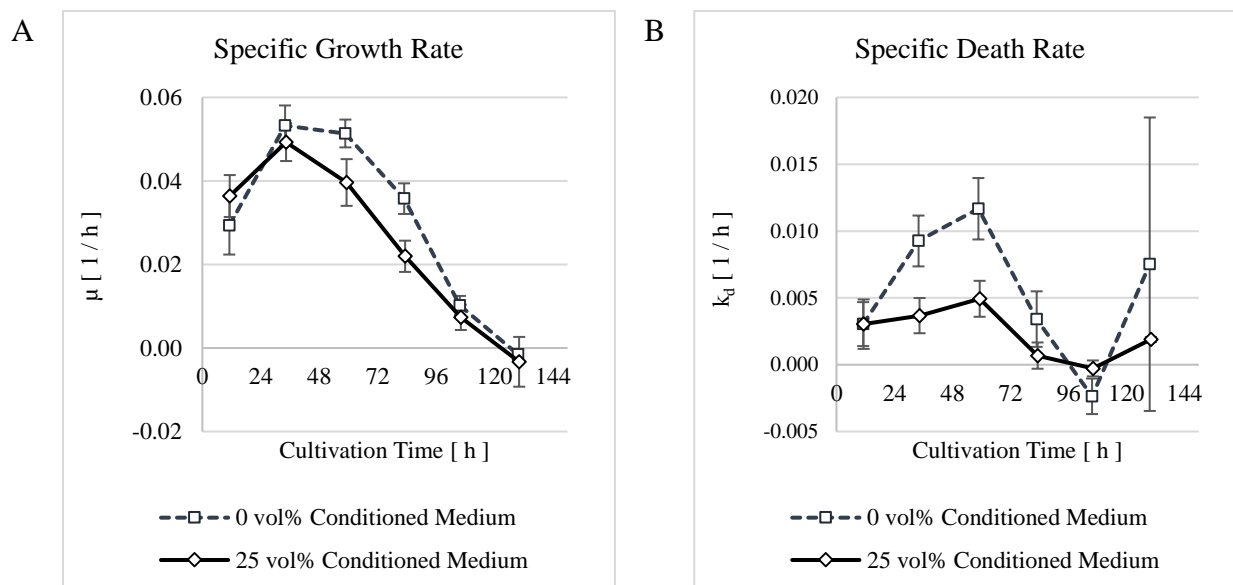


**Figure 13** Specific growth ( $\mu$ ) (A) and death ( $k_d$ ) (B) rates calculated differentially between the time points of each sample of the cultures inoculated in CHOMACS CD growth medium containing 0 vol% and 25 vol% conditioned medium (CM). The values given in the graphs were calculated as the average of the triplicate cultures and the error bars represent the standard deviation.

The specific death rates ( $k_d$ ) of both cultures also followed a very similar progression that mirrored the progression of the viability described above: a steady increase, followed by a steady decrease and finishing with a sudden increase at the end of the cultivation. The maximal specific death rate was reached for both cultures between 48 and 72 hours of cultivation and was calculated at  $0.012 \pm 0.0023$  and  $0.005 \pm 0.0013$  1/h respectively for the 0 vol% CM and 25 vol% cultures. The  $k_d$  of the culture



## 4. RESULTS

cultivated in conditioned medium was consistently lower than its counterpart between 24 and 96 hours of cultivation, and was an average of  $59\% \pm 21.7\%$  ( $p < 0.05$ ) lower between 24 and 72 cultivation hours.

Figure 14 shows the glucose concentration (A) of the cultures throughout the cultivation and the glucose consumption rate (B) plotted against the average glucose concentration between the corresponding time-points. The values given in the graphs were calculated as the average of the triplicate cultures and the error bars represent the standard deviation.

The glucose concentration ( $c_{\text{Glc}}$ ) of both cultures decreased steadily as the cultivation progressed, with the culture cultivated in conditioned medium showing consistently lower values than its counterpart. The latter was a result of the glucose depletion of the CM prior to the inoculation. The graphs show a decrease in glucose consumption rate ( $q_{\text{s,Glc}}$ ) with decreasing glucose concentration in the growth medium that follows a rather parabolic progression. Both glucose consumptions curves are very similar for both cultures, and at concentrations lower than 30 mM the glucose consumption rates of both cultures remained constant below  $0.05 \mu\text{mol}$  glucose per  $10^6$  cells per ml.

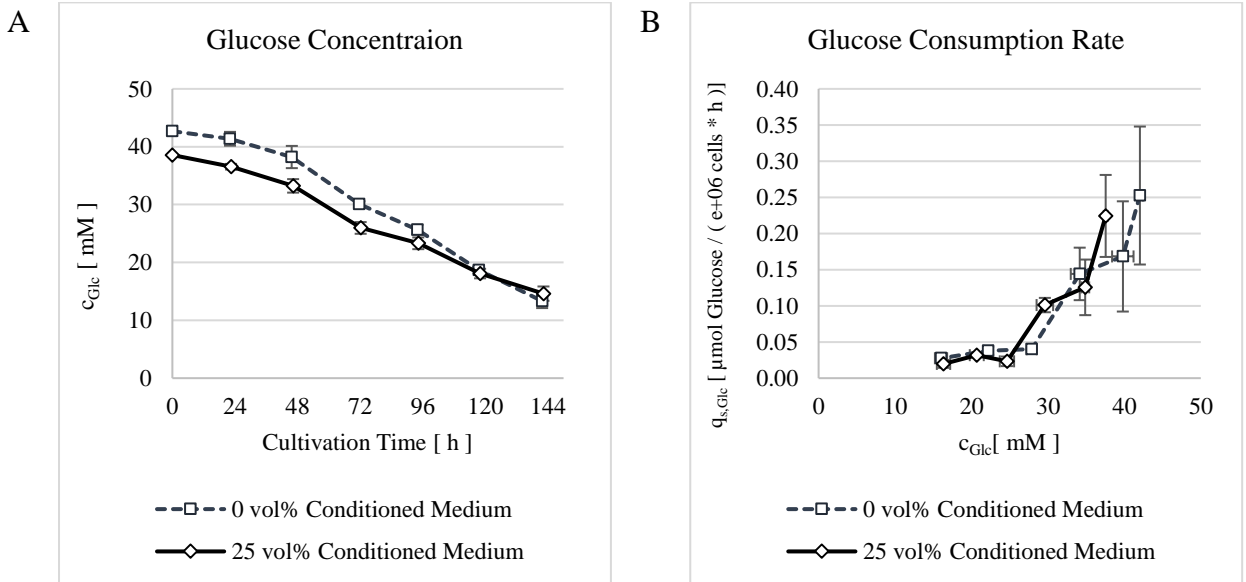
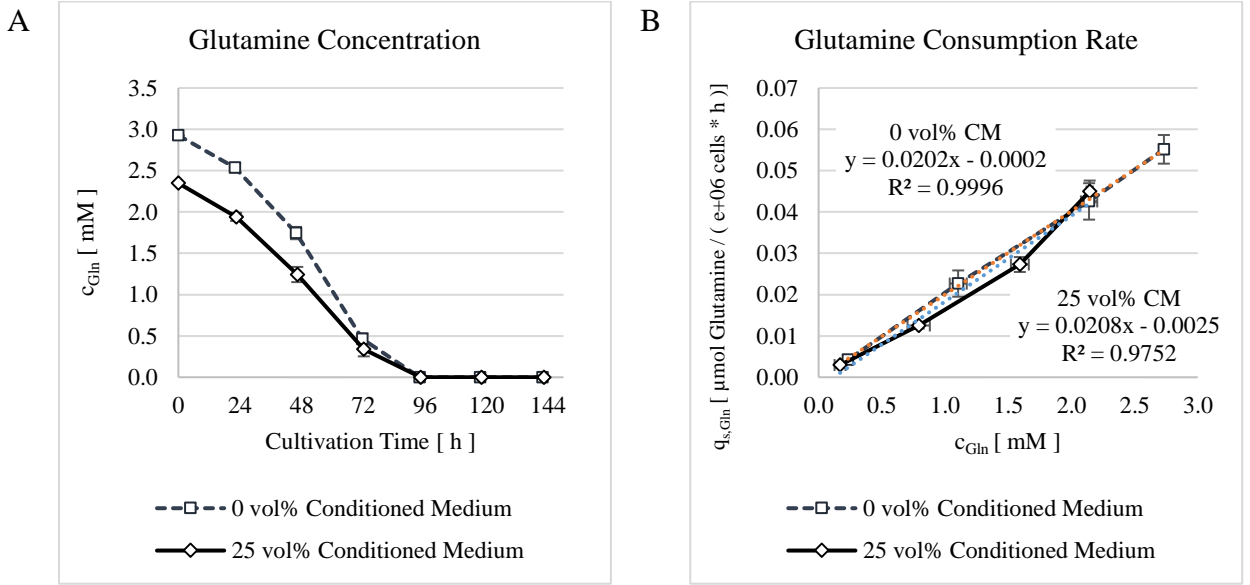


**Figure 14** Glucose concentration ( $c_{\text{Glc}}$ ) (A) of the cultures throughout the cultivation and the glucose consumption rate ( $q_{\text{s,Glc}}$ ) (B) plotted against the average glucose concentration between the corresponding time-points of the cultures inoculated in CHOMACS CD growth medium containing 0 vol% and 25 vol% conditioned medium (CM). The values given in the graphs were calculated as the average of the triplicate cultures and the error bars represent the standard deviation.

## 4. RESULTS

Figure 15 shows the glutamine concentration (A) of the cultures throughout the cultivation and the glutamine consumption rates (B) plotted against the average glutamine concentration between each time-point. The values given in the graphs were calculated as the average of the triplicate cultures and the error bars represent the standard deviation.

The glutamine concentration ( $c_{\text{Gln}}$ ) of both cultures followed a steady decrease as the cultivation advanced until being completely depleted between 72 and 96 cultivation hours. The lower  $c_{\text{Gln}}$  of the culture cultivated with CM is a result of the glutamine depletion in the conditioned medium prior to inoculation. The results show a linear correlation between the glutamine consumption rate ( $q_{\text{s,Gln}}$ ) and increasing  $c_{\text{Gln}}$  in the growth medium for both cultures. Linear regression shows a much better fit for the cultivation carried out without CM ( $R^2 = 0.9996$ ) than its counterpart ( $R^2 = 0.9752$ ).



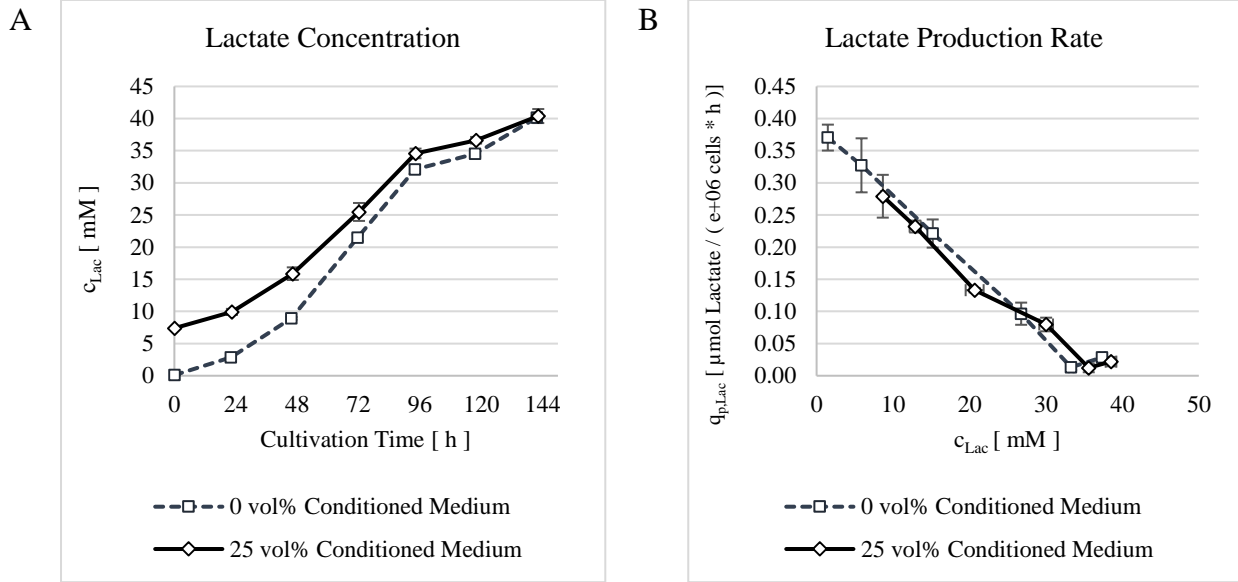
**Figure 15** Glutamine concentration ( $c_{\text{Gln}}$ ) (A) of the cultures throughout the cultivation and the glutamine consumption rates ( $q_{\text{s,Gln}}$ ) (B) plotted against the average glutamine concentration between each time-point. The values given in the graphs were calculated as the average of the triplicate cultures and the error bars represent the standard deviation.

Figure 16 shows the lactate concentration profiles (A) of the cultures and the lactate production rates (B) plotted against the average lactate concentration between each time-point. The values given in the graphs were calculated as the average of the triplicate cultures and the error bars represent the standard deviation.

The lactate concentration ( $c_{\text{Lac}}$ ) of both cultures followed a similar progression, steadily increasing until 96 cultivation hours, when the production seemed to reach a plateau, nevertheless still accumulating. The beginning of the plateau coincides with the time at which glutamine is completely

## 4. RESULTS

depleted. The higher  $c_{\text{Lac}}$  of the 25% CM culture is a result of the lactate already present in the conditioned medium. The lactate productions rates ( $q_{\text{p,Lac}}$ ) followed an identical linear progression, decreasing with the accumulation of lactate in the growth medium until it reached almost zero.



**Figure 16** Lactate concentration ( $c_{\text{Lac}}$ ) profiles (A) of the cultures and the lactate production rates ( $q_{\text{p,Lac}}$ ) (B) plotted against the average lactate concentration between each time-point of the cultures inoculated in CHOMACS CD growth medium containing 0 vol% and 25 vol% conditioned medium (CM). The values given in the graphs were calculated as the average of the triplicate cultures and the error bars represent the standard deviation.

These results show clear indications of an influence of conditioned medium on the growth and death of CHO cells, with no influence on the glucose and glutamine uptake and lactate production rates. Cultivation with conditioned medium was associated with a delayed decrease in the specific growth rate coupled with a simultaneous increase in the viability, which resulted in the reduction of the specific death rate. Both cultures reached their maximum specific growth rate after 24 hours once the total cell density had increased.

### 4.1.2 Separation of Conditioned Medium by Molecular Weight (cutoff 10 kDa)

Figure 17 shows the total cell density of the cultures supplemented with the  $< 10$  kDa and  $> 10$  kDa fractions (A) and cultivated in either conditioned medium (CM) or fresh medium (FM) (B). Furthermore, the respective specific growth rates ( $\mu$ ) calculated differentially between the time-points of each sample are also shown (C, D). The values represent the average calculated for the corresponding triplicate cultures and the error bars display the standard deviation.

## 4. RESULTS

The graphs show that the CM and < 10 kDa cultures followed a very similar progression when compared with each other. The same was the case for the > 10 kDa and FM cultures. The highest cell densities were achieved by the > 10 kDa and FM cultures at 144 cultivation hours, reaching  $15.97 \pm 0.490 \times 10^6$  and  $16.02 \pm 0.019 \times 10^6$  cell/ml respectively, followed by a slight decrease during the last 24 hours. The < 10 kDa and CM cultures reached a maximum cell density of  $12.41 \pm 1.444 \times 10^6$  and  $12.21 \pm 0.234 \times 10^6$  cell/ml respectively at the end of the cultivation.

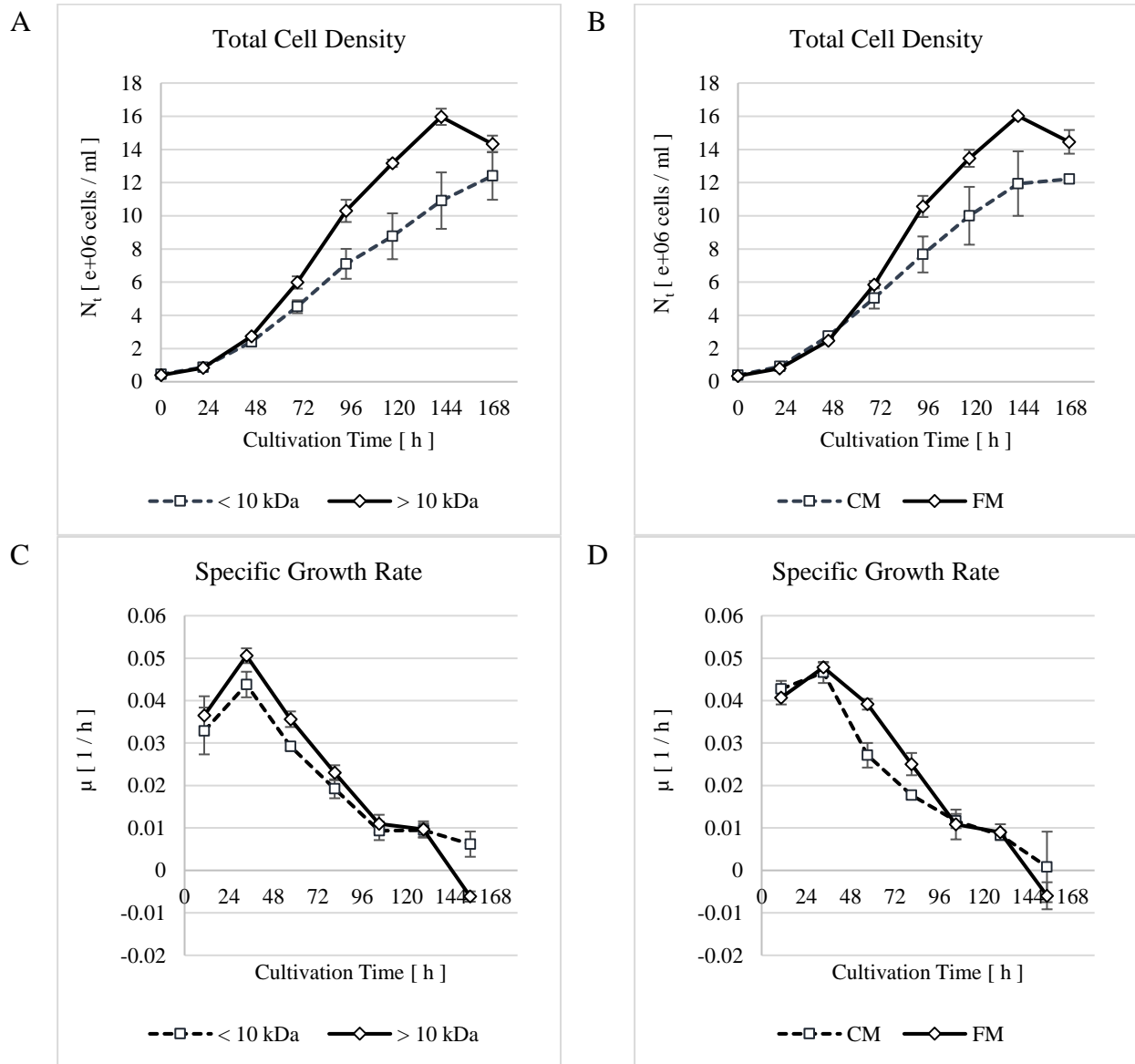


**Figure 17** Total cell density ( $N_t$ ) of the cultures supplemented with the < 10 kDa and > 10 kDa fractions (A) and cultivated in either conditioned medium (CM) or fresh medium (FM) (B). Furthermore, the respective specific growth rates ( $\mu$ ) calculated differentially between the time-points of each sample are also shown (C, D). The values represent the average calculated for the corresponding triplicate cultures and the error bars display the standard deviation.

## 4. RESULTS

The four cultures reached their  $\mu_{\max}$  between 24 and 48 hours of cultivation ( $< 10$  kDa:  $\mu_{\max} = 0.44 \pm 0.0030$  1/h,  $> 10$  kDa:  $\mu_{\max} = 0.051 \pm 0.0017$  1/h; CM:  $\mu_{\max} = 0.047 \pm 0.0025$  1/h; FM:  $\mu_{\max} = 0.048 \pm 0.0011$  1/h), followed by a steady decrease until the end. The decrease was mostly linear for the fraction supplemented cultures, while parabolic for the CM and FM cultures. Both the  $> 10$  kDa and FM cultures showed a negative  $\mu$  of  $-0.006 \pm 0.0012$  and  $-0.006 \pm 0.0032$  1/h respectively by the end of the cultivation, while the CM culture showed a  $\mu$  of  $0.001 \pm 0.0083$  1/h. The specific growth rate of the  $< 10$  kDa culture remained at  $0.006 \pm 0.0030$  1/h at the end of the cultivation.

Figure 18 shows the significance analysis performed to determine the degree of similarity between the progressions of the specific growth rate of each culture. It shows on the left a matrix containing the p-values calculated after comparing the each specific growth at every time interval. The red colored cells represent the compared time intervals with  $p < 0.05$ . The right side shows a graph in which the p-values of the compared cultures are plotted against the cultivation time. A total of 11 significantly different time intervals were determined, mostly between 24 and 96 cultivation hours.

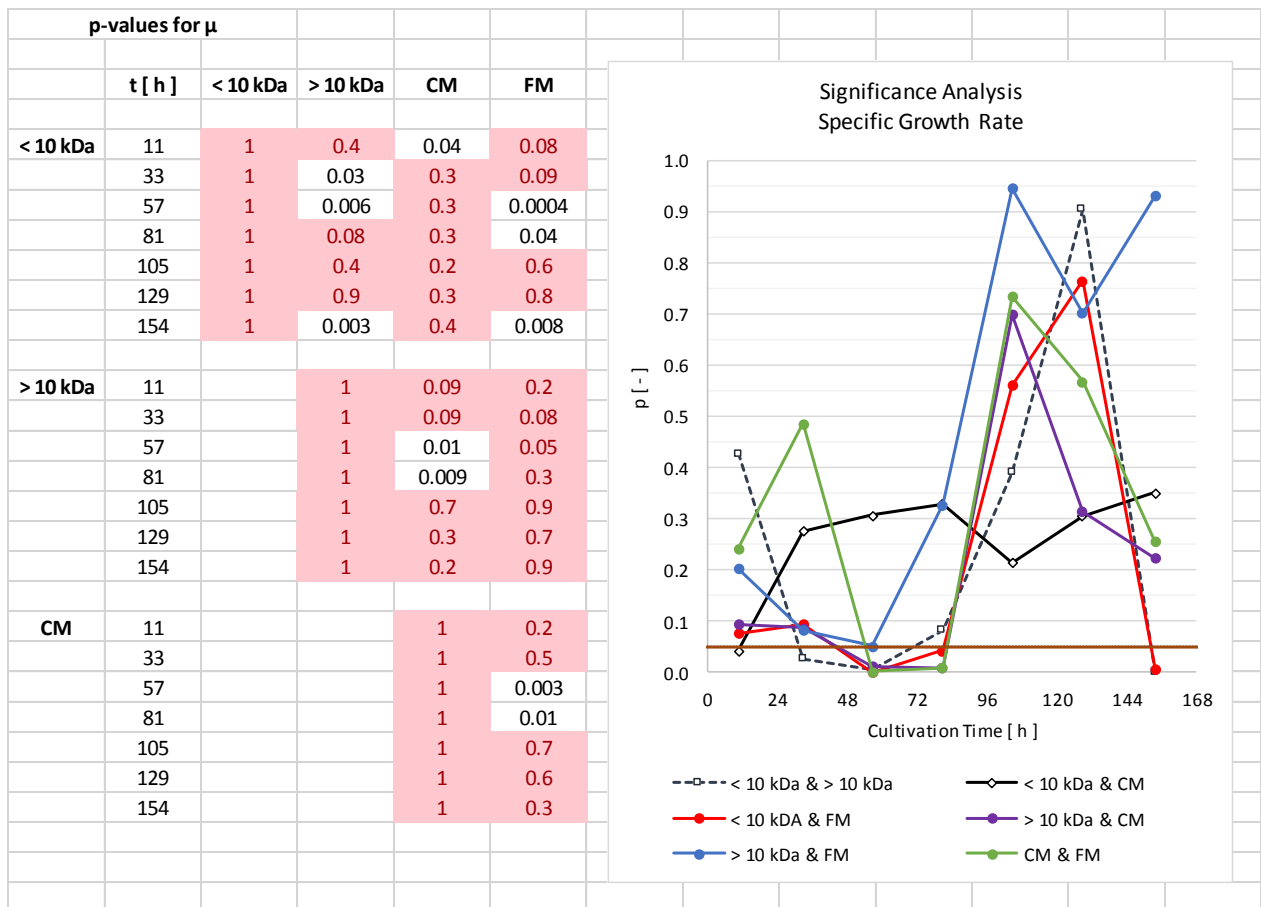


**Figure 18** Significance analysis performed to determine the degree of similarity between the progressions of the specific growth rate of each culture.

## 4. RESULTS

Table 23 presents the degree of similarity among the cultures. The coincidence % was determined by calculating the ratio of the number of time intervals without significant differences ( $p > 0.05$ ) to the total amount compared, in this case 7 per culture. The results show that there was a 100% coincidence between the  $> 10$  kDa and FM cultures. Furthermore, the  $< 10$  kDa and CM cultures showed a high coincidence of 86%, differing from each other only during the first 24 cultivation hours. At this time interval the specific growth rate of the  $< 10$  kDa culture was  $23\% \pm 4.0\%$  lower than the CM culture.

The least coincidence % resulted from the comparison between the  $< 10$  kDa with the  $> 10$  kDa and the FM cultures, showing only 57% similarity for both, with their significantly different values found between 24 and 72 cultivation hours and during the last time interval. The coincidence % between the CM and FM and the  $> 10$  kDa and CM cultures was 71%, and their significantly different values were found between 48 and 96 cultivation hours.

**Table 23** Coincidence % of the specific growth rate between the cultures compared and determined by calculating the ratio of the number of time intervals without significant differences ( $p > 0.05$ ) to the total amount compared, in this case 7 per culture.

$\mu$ -Coincidence %	$< 10$ kDa	$> 10$ kDa	CM	FM
$< 10$ kDa	100%	57%	86%	57%
$> 10$ kDa	-	100%	71%	100%
CM	-	-	100%	71%
FM	-	-	-	100%

Table 24 displays the percentile differences calculated for each time interval that showed significant differences ( $p < 0.05$ ). The  $< 10$  kDa culture was compared against the  $> 10$  kDa, CM and DM cultures, while the CM culture was compared to the  $> 10$  kDa and FM cultures. A negative value means that  $\mu$  of either the  $< 10$  kDa or the CM was lower than the compared culture. A positive value means the opposite.

The growth rate of the CM culture was an average of  $23\% \pm 11.3\%$  and  $30\% \pm 11.1\%$  lower than the  $> 10$  kDa and FM cultures respectively between 48 and 96 cultivation hours. During the same time interval the specific growth rate of the  $< 10$  kDa culture was an average of  $24\% \pm 6.8\%$  lower than the FM culture. The maximal specific growth rate of the  $< 10$  kDa calculated between 24 and 48 cultivation

## 4. RESULTS

hours was reduced by  $13\% \pm 1.0\%$  compared to the  $> 10$  kDa culture and remained  $18\% \pm 1.1\%$  lower during the next 24 hours.

**Table 24** Matrix displaying the percentile differences calculated for each time interval that showed significant differences ( $p < 0.05$ ). A negative value means that  $\mu$  of either the  $< 10$  kDa or the CM was lower than the compared culture. A positive value means the opposite.

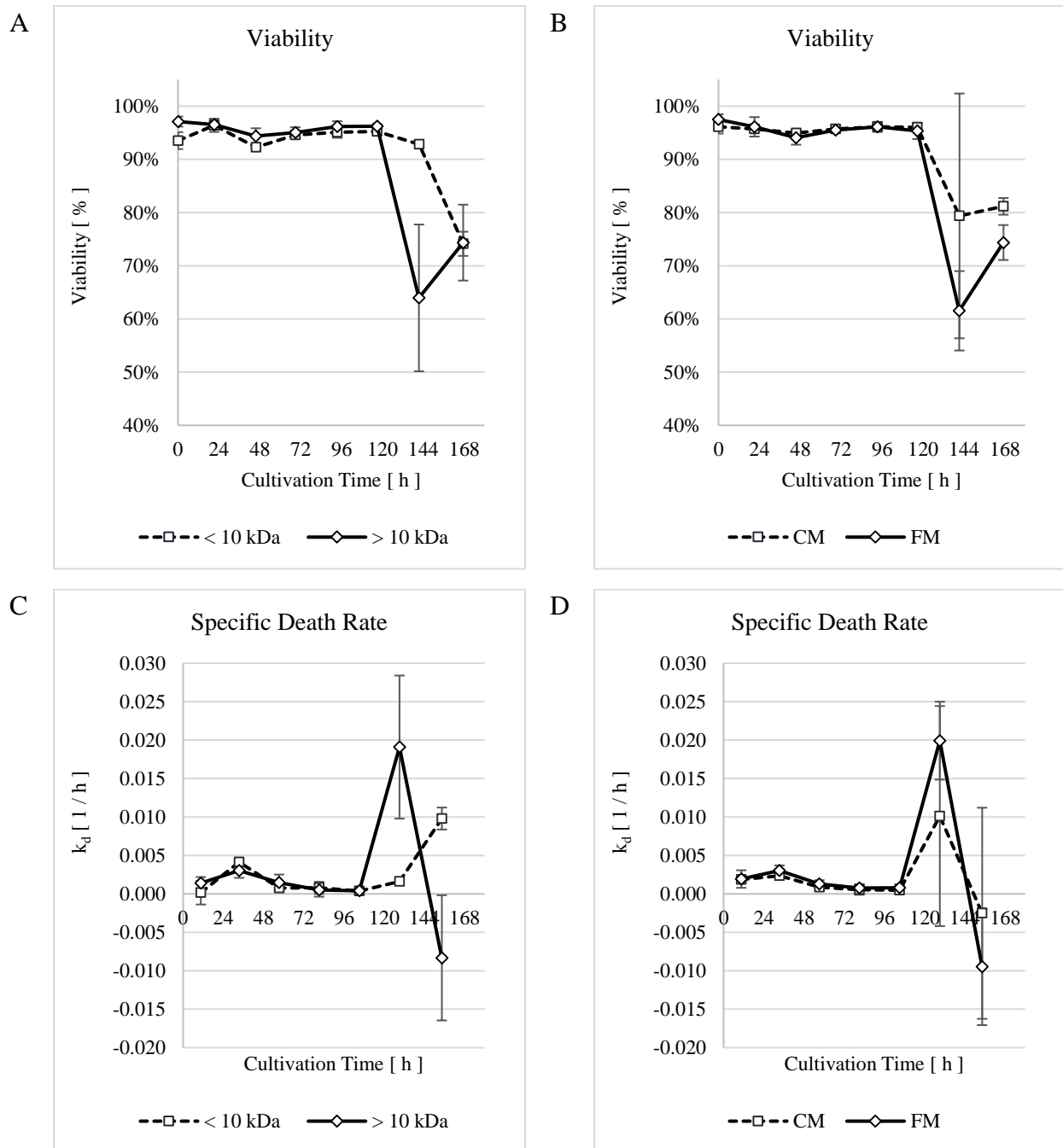
	t [ h ]	$> 10$ kDa	CM	FM
< 10 kDa	11		$-23\% \pm 4.0\%$	
	33	$-13\% \pm 1.0\%$		
	57	$-18\% \pm 1.1\%$		$-25\% \pm 1.2\%$
	81			$-23\% \pm 3.6\%$
	105			
	129			
	154	$201\% \pm 2.8\%$		$204\% \pm 146.1\%$
CM	11			
	33			
	57	$-24\% \pm 2.8\%$		$-31\% \pm 3.4\%$
	81	$-23\% \pm 2.0\%$		$-29\% \pm 3.3\%$
	105			
	129			
	154			

Figure 19 shows the viability of the cultures supplemented with the  $< 10$  kDa and  $> 10$  kDa fractions (A) and the cultures cultivated with either conditioned (CM) or fresh medium (FM) (B). Furthermore, the respective specific death rates ( $k_d$ ) calculated differentially between the time-points of each sample are also shown (C, D). The values represent the average calculated for the corresponding triplicate cultures and the error bars display the standard deviation.

The viability of all four cultures had almost identical progressions during the first 120 hours of the cultivation. They all started with an average viability of  $96.1\% \pm 2.46\%$  that slightly decreased until 48 hours, never falling below 90%, followed by a slight increase until 120 cultivation hours. The viability of the  $> 10$  kDa, CM and FM cultures then plummeted respectively to  $64.0\% \pm 12.79\%$ ,  $79.4\% \pm 23.00\%$  and  $61.5\% \pm 7.46\%$  at 144 hours, followed by a slight increase during the next 72 hours and ending with a viability of  $74.3\% \pm 7.13\%$ ,  $81.2\% \pm 1.57\%$  and  $74.4\% \pm 3.29\%$  respectively. The viability of the  $< 10$  kDa culture remained above 90% one day longer than the rest of the cultures and

## 4. RESULTS

ended at  $74.1\% \pm 2.27\%$ . The large standard deviation of the CM culture was the result of the viability of one of the triplicate cultures being at 52.8% while the other two were above 90%.



**Figure 19** Viability of the cultures supplemented with the < 10 kDa and > 10 kDa fractions (A) and the cultures cultivated with either conditioned (CM) or fresh medium (FM) (B), and the respective specific death rates ( $k_d$ ) calculated differentially between the time-points of each sample (C, D). The values represent the average calculated for the corresponding triplicate cultures and the error bars display the standard deviation.

The  $k_d$  of all four cultures followed an almost identical progression, increasing at the beginning and reaching a local maximum with an average of  $0.003 \pm 0.0012$  1/h between 24 and 48 cultivation hours.



#### 4. RESULTS

All four cultures underwent a slight decrease until 120 cultivation hours, followed by a sudden spike between 120 and 144 hours, and ending in negative values, except for the < 10 kDa culture, whose  $k_d$  remained low and ended at  $0.010 \pm 0.0014$  1/h, higher than the rest.

Figure 20 shows the significance analysis performed to compare the  $k_d$  of the four cultures with each other in order to identify the time intervals that showed significant differences. The left side shows a matrix containing the calculated p-values, with the red colored cells corresponding to  $p > 0.05$ . The right side presents a graph in which the p-values were plotted against the cultivation time. Five time intervals with significant differences were identified, all corresponding to the < 10 kDa culture. The first one resulted from the comparison with the CM culture and was found between 24 and 48 hours. The rest were found between 144 and 168 cultivation hours.

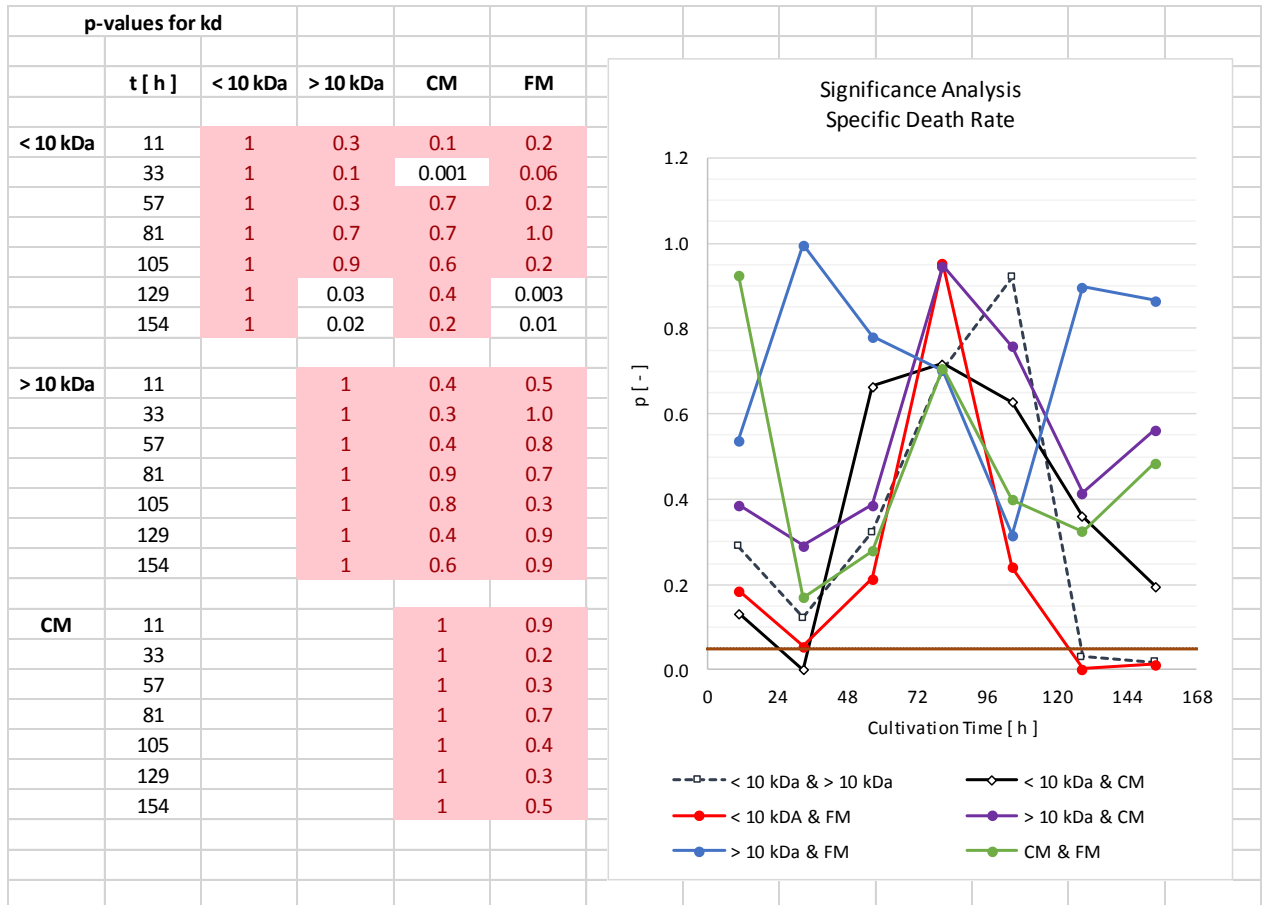


**Figure 20** Significance analysis performed to determine the degree of similarity between the progressions of the specific death rate of each culture.

Table 25 present the coincidence % of the specific death rates calculated analogously to the specific growth rates. It shows a high coincidence % among the  $k_d$  values of the four cultures, with 100% for the comparison between the > 10 kDa, and the CM and FM cultures, and between the CM and FM

## 4. RESULTS

cultures. The least coincidence % was identified at 71% between the < 10 kDa, and the > 10 kDa and FM cultures. Comparison between the < 10 kDa and CM cultures showed a high coincidence of 86%.

The results showed that the  $k_d$  of the < 10 kDa culture was  $77\% \pm 9.9\%$  higher than the CM culture at the local maximum. The next significantly different time intervals were between 120 and 144 hours, where the death rate of the < 10 kDa culture was an average of  $92\% \pm 48.0\%$  lower than the > 10 kDa and FM cultures. The last significantly different time intervals were identified at the end of the cultivation, when the death rates of the > 10 kDa and FM cultures were negative, while the < 10 kDa culture remained positive.

**Table 25** Coincidence % of the specific death rates between the cultures compared and determined by calculating the ratio of the number of time intervals without significant differences ( $p > 0.05$ ) to the total amount compared, in this case 7 per culture.

$k_d$ -Coincidence %	< 10 kDa	> 10 kDa	CM	FM
< 10 kDa	100%	71%	86%	71%
> 10 kDa	-	100%	100%	100%
CM	-	-	100%	100%
FM	-	-	-	100%

The coincidence analysis showed that the effects on  $\mu$  associated with the supplementation of the cells with conditioned medium are most likely to be replicated by supplementing the cells with the conditioned medium components smaller than 10 kDa. Additionally, supplementation with the > 10 kDa fraction did not produce significantly different results compared to cultivating the cells in mostly fresh CHOMACS CD (there was a minimum of 4.03 vol% conditioned medium carry-over in each culture from the inoculation volume). Moreover, the < 10 kDa fraction seemed to have a positive effect on the specific growth rate of the cells towards the end of the cultivation, delaying the decrease of the total cell density, compared to the > 10 kDa and FM cultures that showed negative specific growth rates.

The slight increase in viability between 144 and 168 hours of the > 10 kDa and FM cultures correlated with the drop in total cell density described above and is an indication of loss of death cells, possibly due to lysis. A drop in the total cell density was not observed in the < 10 kDa and CM cultures and

## 4. RESULTS

their viabilities remained high for a longer time. This indicates the possible delay of cellular death by the conditioned medium and its < 10 kDa components.

### 4.1.3 Effect of the Conditioned to Fresh Medium Ratio

Figure 21 shows the total cell density (A) and viability (B) measured at 0, 23 and 49 hours of cultivation for the cultures inoculated at a low cell density in growth medium containing different ratios of conditioned medium (CM). Each time-point shows a set of three columns, each one corresponding from left to right to 17%, 58.6% and 100% CM. The values of each column were determined as the average of the triplicate cultures and the error bars display the standard deviation.

The 100% CM culture reached the highest total cell density ( $N_t$ ) at the end of the cultivation ( $3.15 \pm 0.14 \times 10^6$  cells/ml) compared to the 17% CM ( $2.64 \pm 0.13 \times 10^6$  cells/ml) and 58.6% CM ( $2.59 \pm 0.02 \times 10^6$  cells/ml). The viability of the 17% CM dropped to  $90.0\% \pm 1.49\%$  at the end of the cultivation, while the viability of the 58.6% CM ( $94.7\% \pm 0.68\%$ ) and 100% CM ( $94.4\% \pm 0.67\%$ ) cultures remained higher and fairly similar.

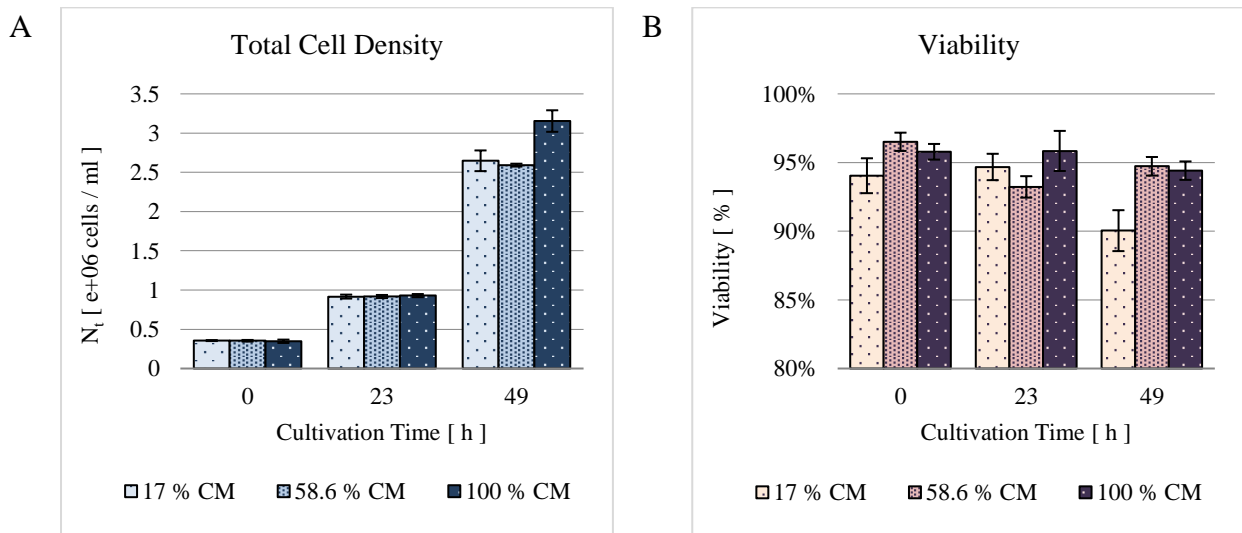


**Figure 21** Total cell density ( $N_t$ ) (A) and viability (B) measured at 0, 23 and 49 hours of cultivation for the cultures inoculated at a low cell density in growth medium containing 17 vol%, 58.6 vol% and 100 vol% conditioned medium (CM)

Figure 22 shows the specific growth rates ( $\mu$ ) of the cultures throughout the cultivation. The graph presents two sets of three columns, which correspond each one from left to right to the 17% CM, 58.6% CM and 100% CM cultures. The values of each column were determined as the average  $\mu$  of the triplicate cultures and the error bars display the standard deviation. During the first 24 cultivation hours

## 4. RESULTS

all three cultures showed very similar  $\mu$  without any significant differences when compared to each other (17% CM:  $0.043 \pm 0.0016$  1/h; 58.6% CM:  $0.043 \pm 0.0006$  1/h; 100% CM:  $0.044 \pm 0.0031$  1/h). The specific growth rates remained without any significant changes during the next 25 cultivation hours (17% CM:  $0.045 \pm 0.0021$  1/h; 58.6% CM:  $0.043 \pm 0.0005$  1/h; 100% CM:  $0.045 \pm 0.0005$  1/h).

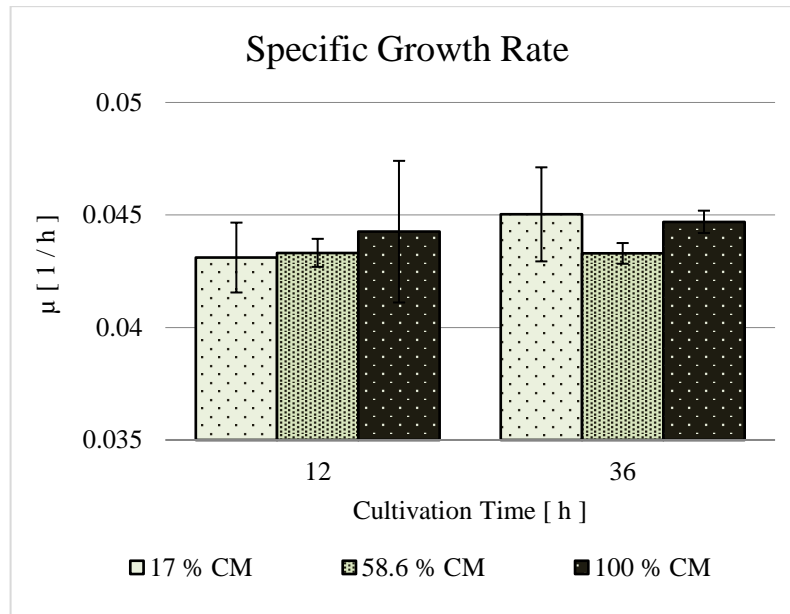


**Figure 22** Specific growth rates ( $\mu$ ) calculated differentially between the time-points of each sample for the cultures inoculated at a low cell density in growth medium containing 17 vol%, 58.6 vol% and 100 vol% conditioned medium (CM)

Figure 23 shows the specific death rates ( $k_d$ ) of the cultures presented analogously to the specific growth rates. The columns of each set correspond from left to right to the 17% CM, 58.6% CM and 100% CM cultures, the values were determined as the average  $k_d$  of the triplicate cultures and the error bars display the standard deviation. During the first 23 cultivation hours, the  $k_d$  of the 17% CM, 58.6% CM and 100% CM cultures were calculated at  $0.002 \pm 0.0005$  1/h,  $0.004 \pm 0.0005$  1/h and  $0.002 \pm 0.0011$  1/h respectively. The death rates of the 17% CM and 100% CM cultures were not significantly different from each other, while the death rate of the 58.6% CM culture was almost two-fold higher than the other two cultures (17% CM:  $p < 0.05$ ; 58.6% CM:  $p < 0.1$ ). Between 23 and 49 cultivation hours, the death rates of the 17% CM, 58.6% CM and 100% CM cultures were calculated at  $0.005 \pm 0.0013$  1/h,  $0.002 \pm 0.0005$  1/h and  $0.002 \pm 0.0001$  1/h respectively. During this time interval, the  $k_d$  of the 58.6% CM and 100% CM cultures did not significantly differ from each other, while the 17% CM culture was almost two-fold and three-fold higher than the 58.6% CM ( $p < 0.05$ ) and 100% CM ( $p < 0.05$ ) cultures respectively. A lower percentage of conditioned medium seemed to increase the  $k_d$

## 4. RESULTS

of the cells after 24 hours, which is also evident in the drop in viability of the 17% CM in the last day of cultivation (Figure 21 (B)).

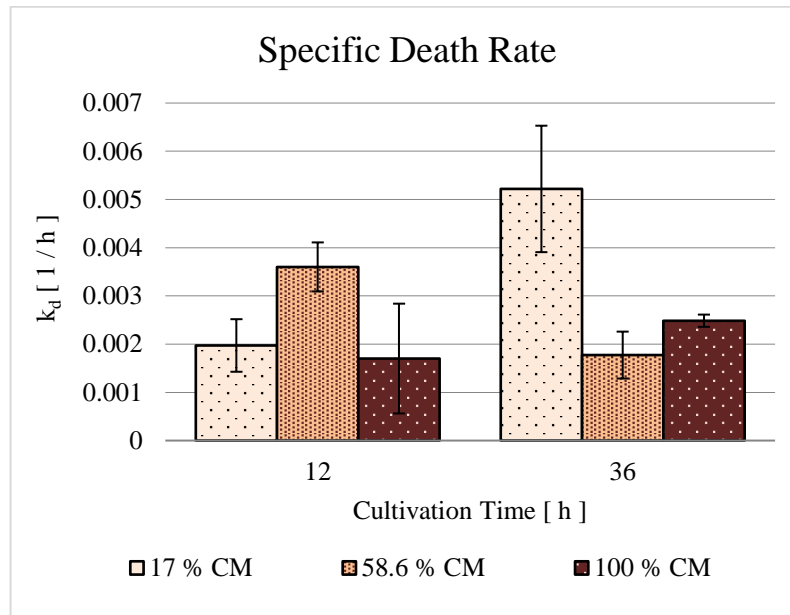


**Figure 23** Specific death rates ( $k_d$ ) calculated differentially between the time-points of each sample for the cultures inoculated at a low cell density in growth medium containing 17 vol%, 58.6 vol% and 100 vol% conditioned medium (CM)

Figure 24 compares the specific growth rates of the inoculated cultures and the parent culture and shows three pairs of columns. The left columns of each set correspond respectively from left to right to the specific growth rates of the 17% CM, 58.6% CM and 100% CM cultures calculated during the first 23 cultivation hours. The error bars display the standard deviation calculated from the specific growth rates of the triplicate cultures. The right columns of each set all correspond to the  $\mu$  of the parent culture calculated for the last 22 cultivation hours. Because a single parent culture was performed, three samples were taken simultaneously for the determination of the total cell density and viability. The growth rate and the standard deviation, displayed in the error bars of the columns, were calculated from the average of the three samples. The  $\mu$  of the inoculated cultures was in average  $12\% \pm 7.6\%$  lower ( $p < 0.001$ ) than the parent culture. This demonstrates a significant decrease in the specific growth rate of the cells that did not seem to be affected by the conditioned medium present at the moment of inoculation, but rather by the change in cell density from  $1.72 \pm 0.018 \times 10^6$  to  $3.52 \pm 0.130 \times 10^5$  cells/ml.

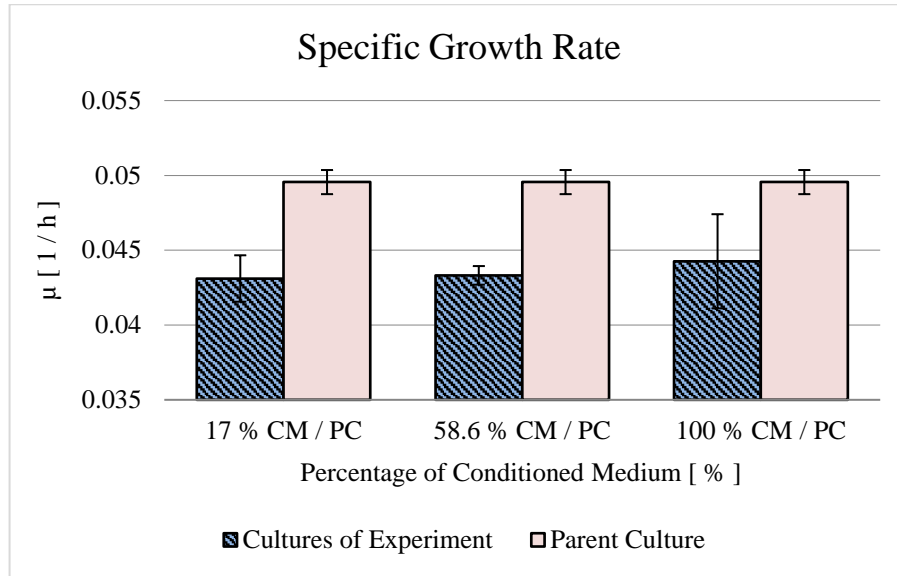


**Figure 24** Specific growth rates ( $\mu$ ) of the cultures inoculated at a low cell density in growth medium containing 17 vol%, 58.6 vol% and 100 vol% conditioned medium (CM) compared to the specific growth rate of the parent culture.

Figure 25 compares the specific death rates ( $k_d$ ) of the cultures calculated during the first 23 cultivation hours with the  $k_d$  of the parent culture calculated during the last 22 cultivation hours. The right column of each one of the three pairs represents the  $k_d$  of the parent culture determined from the three samples taken, with their standard deviation displayed in the error bars. The left columns correspond from left to right to the  $k_d$  of the 17% CM, 58.6% CM and 100% CM cultures. The error bars display the standard deviation of the triplicate cultures.

The  $k_d$  of the 17% CM and 100% CM cultures were in average  $49\% \pm 45.3\%$  lower than the death rate of the parent culture with very low significance values of  $p = 0.14$  and  $p = 0.15$  respectively. The specific death rate of the 58.6% CM culture remained unchanged. This results show indications of minor effects in the specific death rate cause by the decrease in total cell density.

## 4. RESULTS

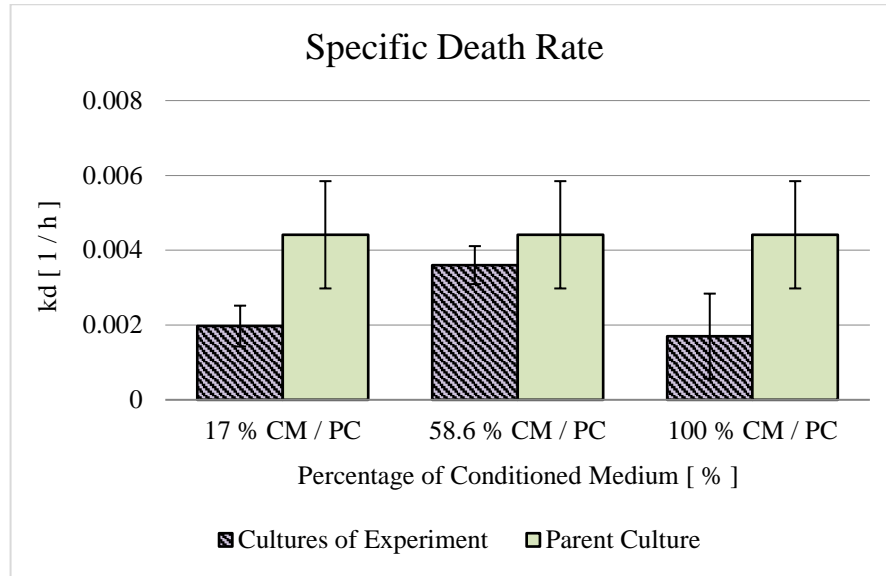


**Figure 25** Specific death rates ( $k_d$ ) of the cultures inoculated at a low cell density in growth medium containing 17 vol%, 58.6 vol% and 100 vol% conditioned medium (CM) compared to the specific death rate of the parent culture.

This experiment was performed to determine if components in conditioned medium have an influence in the initial growth phase of the cells. The conditioned medium was expected to contain growth stimulating elements, since the parent culture used for conditioning of the medium and generation of the cells for the experiment was growing most probably at its  $\mu_{\max}$  ( $0.050 \pm 0.0008$  1/h) at a moderate  $N_t$  ( $1.72 \pm 0.017 \times 10^6$  cells/ml) with a high viability ( $93.1\% \pm 1.71\%$ ). This contrasts with the previous experiments in which the conditioned medium was harvested from the late exponential phase of growth and was expected to contain growth inhibitory elements.

The results of this experiment indicated no influence of different amount of conditioned medium at the moment of inoculation on the specific growth rate of the cultures inoculated at low cell densities during the first 24 hours of cultivation. Nevertheless, there were indications of a moderate increase in the specific growth rate of the culture inoculated in 100% conditioned medium between 24 and 48 cultivation hours, resulting in a higher total cell density at the end of the experiment, compared to the other two cultures.

During the first 24 hours of cultivation all three cultures showed a significantly lower  $\mu$  compared to the parent culture used for inoculation, which was presumably growing at its maximum rate ( $\mu = 0.050 \pm 0.0008$  1/h) and had a moderate total cell density of  $1.72 \pm 0.017 \times 10^6$  cells/ml. This initial decreased  $\mu$  after inoculation, or “lagging”, did not seem to be affected by any amounts of conditioned medium present at the beginning of the cultivation.

Except for the 58.6% CM culture, the different amounts of conditioned medium did not seem to have a significant effect on the specific death rate of the cells during the first 24 cultivation hours. The increased  $k_d$  of the 58.6% CM culture could have been the result of an unknown number of factors. The effects of conditioned medium was more evident between 24 and 48 cultivation, at which time the  $k_d$  of the culture cultivated with 17% conditioned medium increased substantially compared to the rest of the cultures and its viability dropped to around 90%. The viability of the other two cultures remained at around 95% at the end of the cultivation.

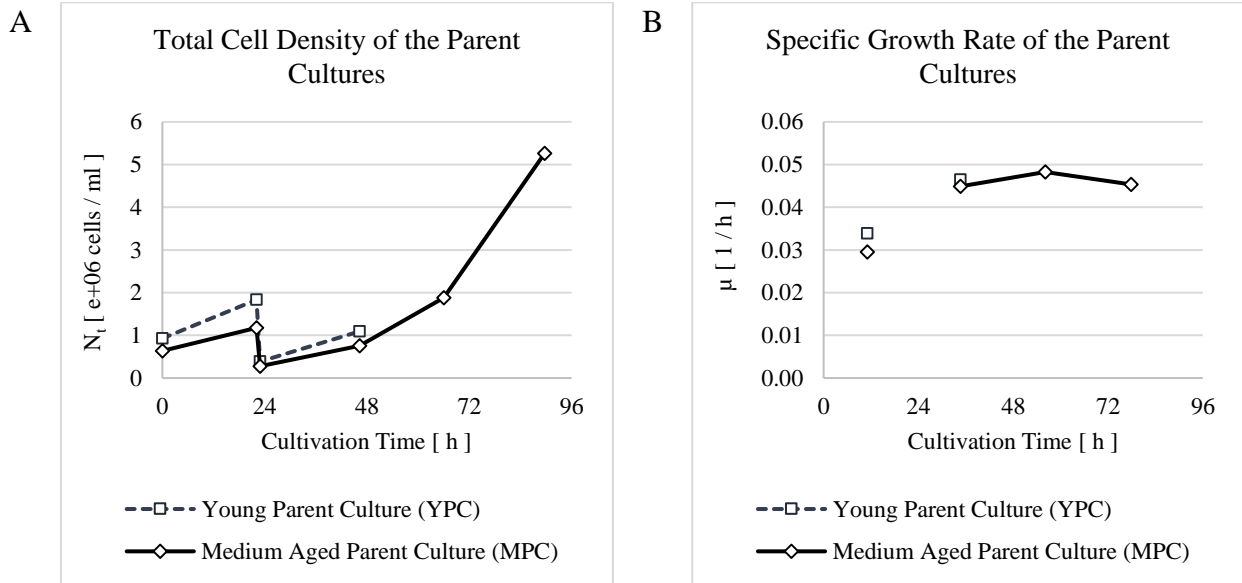
### 4.1.4 Effects of the Age of the Parent Culture

Figure 26 shows the total cell densities (A) and the specific growth rates (B) calculated differentially between the time-points of each sample for the young (YPC) and the medium aged (MPC) parent culture. Cultivation of the parent cultures was not performed in triplicates and the total cell density ( $N_t$ ) and viability were determined once from a single sample, for this reason no error bars are available in the graphs of Figure 26.

The cultures LCD1 and MCD1 cultures were inoculated from the cells produced in the YPC parent culture that was growing at a total cell density of  $1.18 \times 10^6$  cells/ml and showed at a specific growth ( $\mu$ ) and death rate ( $k_d$ ) of 0.046 and 0.002 1/h respectively during the last 23 hours of cultivation. The cultures LCD2 and MCD2 were inoculated from the MPC parent culture, which was growing at an  $N_t$  of  $5.28 \times 10^6$  cells/ml and showed a  $\mu$  and  $k_d$  of 0.047 and 0.004 1/h respectively during the last 24 hours of cultivation. This parent culture had reached its maximum specific growth rate ( $\mu_{max}$ ) already between 24 and 48 cultivation hours, and was in a process of “deceleration” at the moment of inoculation. Given the fact that both parent cultures showed an almost identical  $\mu$  progression, it can be assumed that the YPC had not yet reached its  $\mu_{max}$  and was in a process of “acceleration” at the moment of inoculation. During the first 24 hours of cultivation and prior to the first medium replenishment the growth rate of the YPC and MPC were calculated at 0.034 and 0.030 1/h respectively. Both cultures showed a moderately low specific growth rate, despite the fact that they were growing in fresh medium and the inoculation total cell density was not extremely high:  $9.29$  and  $6.37 \times 10^5$  cells/ml for YPC and MPC respectively. This is most probably a consequence of the state of the continuous culture that was used to inoculate both parent cultures, which had a total cell density of  $12.20 \times 10^6$  and had been growing without medium replenishment for several days.



## 4. RESULTS



**Figure 26** Total cell densities ( $N_t$ ) (A) and the specific growth rates ( $\mu$ ) (B) calculated differentially between the time-points of each sample for the young (YPC) and the medium aged (MPC) parent culture. Cultivation of the parent cultures was not performed in triplicates and the  $N_t$  and viability were determined once from a single sample, for this reason no error bars are available

Figure 27 shows the total cell density (A) and viability (B) of the cultures inoculated in 100% fresh CHOMACS CD medium from the young (YPC) and the medium aged (MPC) parent cultures. The graphs show two sets of four columns. The first two columns of each correspond respectively from left to right to the cultures inoculated at a low (LCD1) and medium cell density (MCD1) from the YPC. The next two columns of each set were inoculated from the MPC and correspond respectively from left to right to the low (LCD2) and medium cell density (MCD2) cultures inoculated from the MPC. The columns correspond to the average calculated for the corresponding triplicate cultures and the error bars display the standard deviation. The viability of the cultures did not significantly differ from each other at the moment of inoculation and was measured at around 95%. It then decreased during the next 23 cultivation hours, except in the case of the LCD1 culture, which remained unchanged. The viability decreased was more pronounced for the MCD1 and MCD2 cultures.

## 4. RESULTS

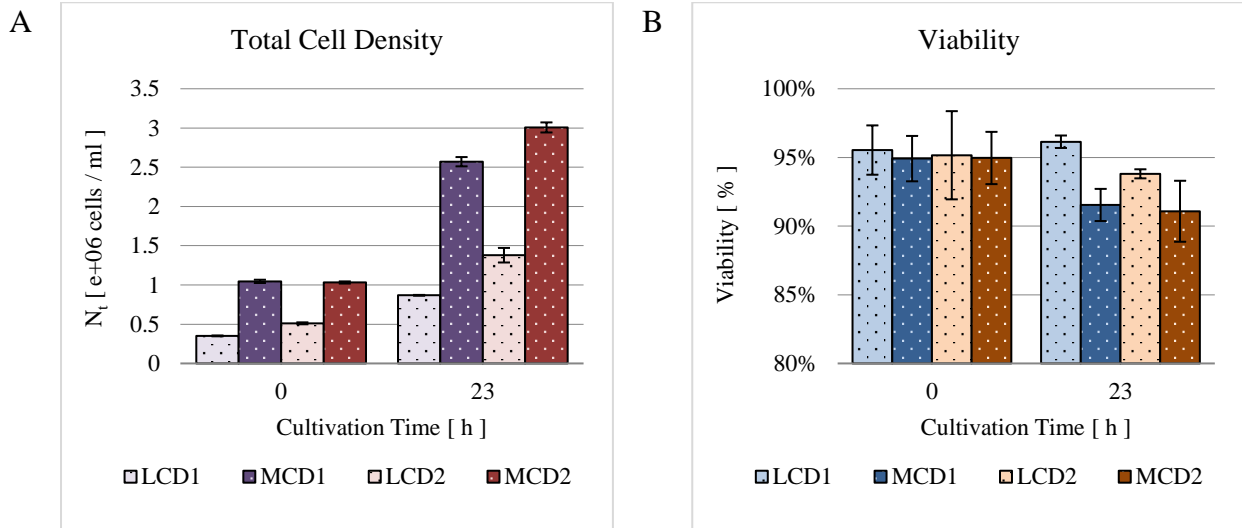


**Figure 27** Total cell density ( $N_t$ ) (A) and viability (B) of the cultures inoculated in 100% fresh CHOMACS CD. LCD1 and MCD1 were inoculated from the young parent culture (YPC). LCD2 and MCD2 were inoculated from the medium aged parent culture (MPC). The columns correspond to the average calculated for the corresponding triplicate cultures and the error bars display the standard deviation.

Figure 28 compares the specific growth rates ( $\mu$ ) of the inoculated cultures to the  $\mu$  of their respective parent culture. The graph shows four pairs of columns. The left columns of each pair correspond from left to right to the  $\mu$  of the LCD1, MCD1, LCD2 and MCD2 cultures respectively calculated after 23 cultivation hours. The values of the columns were determined as the average specific growth rate of the triplicate cultures, and the error bars display the standard deviation. The right columns of each pair correspond to the  $\mu$  of the parent cultures, either the YPC or the MPC, calculated for the last 24 hours of cultivation. The parent cultures do not display error bars since no replicate cultures were performed and the  $N_t$  and viability were determined from one single sample. The lack of standard deviation and replicate measurements only permits comparison without significance analysis between the inoculated cultures and their respective parent cultures.

The  $\mu$  of the LCD1 and MCD1 cultures were calculated respectively at  $0.041 \pm 0.004$  and  $0.042 \pm 0.0019$  1/h and were lower than the  $\mu$  of the corresponding parent culture YPC, which was calculated at 0.047 1/h. The cultures LCD2 and MCD2 showed a  $\mu$  calculated at  $0.043 \pm 0.0034$  and  $0.047 \pm 0.0015$  1/h respectively, being the latter higher than the  $\mu$  of the corresponding parent culture MPC, which was measured at 0.045 1/h.

## 4. RESULTS

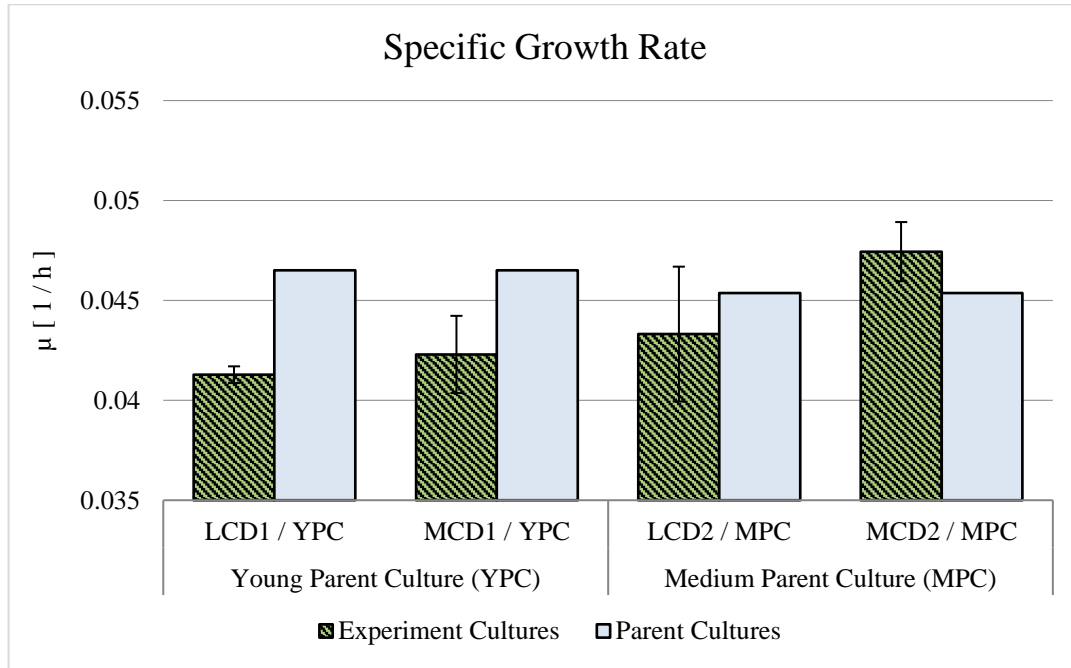


**Figure 28** Specific growth rates ( $\mu$ ) of the inoculated cultures compared to the specific growth rate of their respective parent culture. The values of the inoculated cultures represent the average calculated for the corresponding biological triplicate and the error bars display the standard deviation. The columns representing the parent cultures do not show any error bars, since no triplicate cultures were performed and the  $N_t$  and viability were determined once from a single sample.

Table 26 presents a matrix containing the significance p-values calculated after comparing the  $\mu$  of the inoculated cultures against each other. It shows that the  $\mu$  of both cultures inoculated from the YPC were significantly different ( $p < 0.05$ ) from the MCD2 inoculated from the MPC. Both LCD1 and MCD1 were lower than MCD2 by of  $18\% \pm 2.9\%$  and  $11\% \pm 4.9$  respectively. LCD2 was also  $9\% \pm 7.7\%$  lower than MCD2, nonetheless with a very low significance value of  $p = 0.12$ .

**Table 26**, significance values calculated from the student's t-test after comparing the  $\mu$  of each inoculated culture against each other.

$\mu$ p-values	LCD1	MCD1	LCD2	MCD2
LCD1	1.0	0.4	0.4	0.002
MCD1	-	1.0	0.7	0.02
LCD2	-	-	1.0	0.12
MCD2	-	-	-	1.0

## 4. RESULTS

Figure 29 compares the specific death rates ( $k_d$ ) of the inoculated cultures with their respective parent cultures. The results are presented in the same fashion as the specific growth rates. Each one of the four pairs of columns compares one of the inoculated cultures to their corresponding parent cultures. The  $k_d$  of the inoculated cultures are represented by the column on the right side of each pair, and correspond in order from left to right to the LCD1, MCD1, LCD2 and MCD2 cultures. Their values were calculated as the average of each triplicate culture and the error bars display the standard deviation. The columns on the left side of each pair represent the  $k_d$  of the two parent cultures. The first two correspond to the  $k_d$  of the young parent culture (YOC) and the next two to the medium aged culture (MPC). The columns do not display error bars, since the specific death rates were determined from one single culture and one single sample.

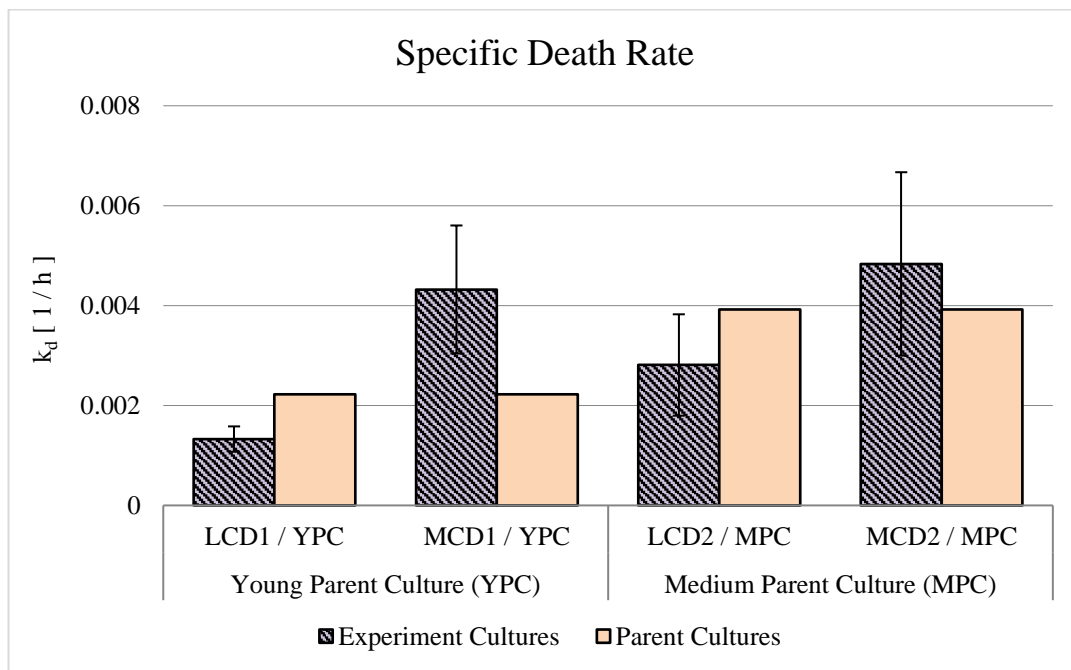


**Figure 29** Specific death rates ( $k_d$ ) of the inoculated cultures compared to the specific death rate of their respective parent culture. The values of the inoculated cultures represent the average calculated for the corresponding biological triplicate and the error bars display the standard deviation. The columns representing the parent cultures do not show any error bars, since no triplicate cultures were performed and the  $N_t$  and viability were determined once from a single sample.

The  $k_d$  of the LCD1 and MCD1 cultures were calculated at  $0.001 \pm 0.0003$  and  $0.004 \pm 0.0013$  1/h respectively, while their parent culture (YPC) was calculated at 0.002 1/h. The cultures LCD2, MCD2 and their parent culture (MPC) showed a  $k_d$  of  $0.003 \pm 0.0010$ ,  $0.005 \pm 0.0018$  and 0.004 1/h respectively. The low cell density cultures, LCD1 and LCD2, both showed a lower specific death rate than their respective parent culture. The opposite was the case for the medium cell density cultures,

#### 4. RESULTS

MCD1 and MCD2, both showing higher  $k_d$  than their respective parent cultures. Statistical analysis between the parent and inoculated cultures cannot be performed due to the single determination of the viability and  $N_t$  of the parent cultures.

Table 27 displays the p-values calculated after comparing the  $k_d$  of the inoculated cultures with each other. Comparison between LCD1 and the medium cell density cultures both resulted in significant difference with  $p < 0.05$ . The  $k_d$  of the LCD1 culture was  $69\% \pm 10.8\%$  and  $73\% \pm 11.7\%$  lower than MCD1 and MCD2 respectively. Comparison between both low cell density cultures also showed differences with low significance ( $p < 0.1$ ). The  $k_d$  of the LCD1 culture was  $53\% \pm 19.3\%$  lower than the death rate of LCD2. The latter was lower than both medium cell density cultures, nonetheless it showed a very low significance value of  $p = 0.17$  and  $p = 0.18$  for MCD1 and MCD2 respectively. Comparison between the  $k_d$  of both medium cell density cultures did not result in any significant differences.

**Table 27** Significance values calculated from the student's t-test after comparing the  $k_d$  of each inoculated culture against each other.

$k_d$ p-values	LCD1	MCD1	LCD2	MCD2
LCD1	1.0	0.02	0.07	0.03
MCD1	-	1.0	0.18	0.7
LCD2	-	-	1.0	0.17
MCD2	-	-	-	1.0

These results also show that a higher  $N_t$  can be associated with a higher  $k_d$  and with a decrease in viability after inoculation in medium containing no conditioned medium. Figure 30 shows the viability of the cultures plotted against their corresponding  $N_t$  (A) and the  $k_d$  plotted against the  $N_t$  averaged between the time-point of each sample (B). The graphs show a linear tendency of the viability to decrease ( $R^2 = 0.918$ ) and the  $k_d$  to increase ( $R^2 = 0.965$ ) with increasing  $N_t$ .

## 4. RESULTS

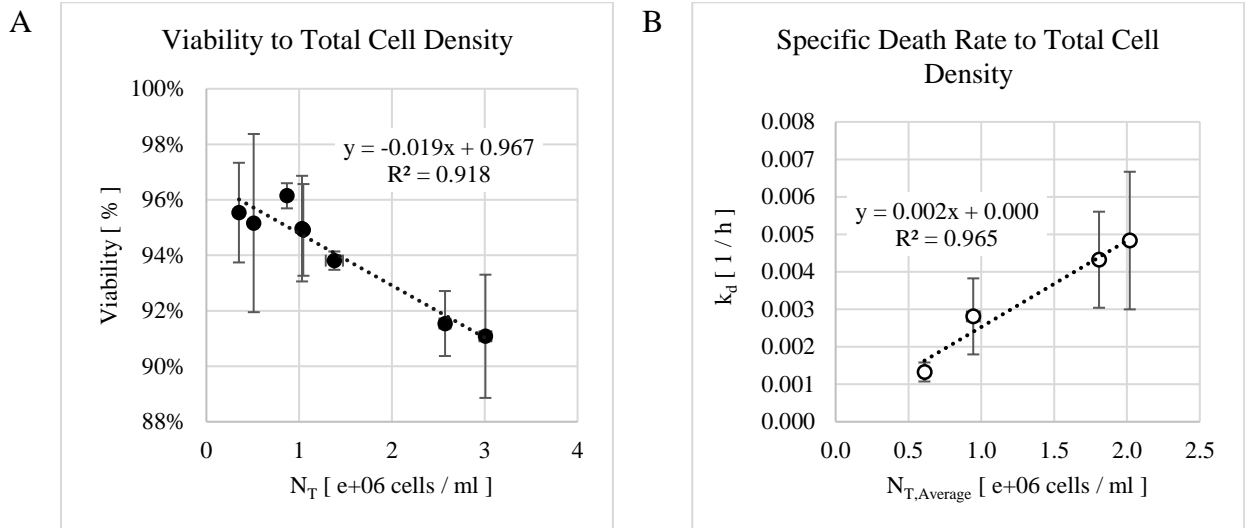


**Figure 30** Viability of the cultures plotted against their corresponding total cell density ( $N_t$ ) (A) and the specific death rate ( $k_d$ ) plotted against the  $N_t$  averaged between the time-point of each sample (B)

Figure 31 displays the  $k_d$  divided by the  $N_t$  averaged between the time-point of each sample. Furthermore, Table 28 present the p-values calculated from the significance analysis, in which the total cell density normalized death rates were compared against each other. The columns of the graph show very similar values, and the values of the table demonstrate that there are no significant differences among the normalized death rates of the cultures. The average normalized death rate of all four cultures is  $0.002 \pm 0.0017$  ml/(h  $\times 10^6$  cells), which corresponds to the slope calculated for the linear regression of the  $k_d$  to  $N_t$  plot. This value represent the magnitude in which  $k_d$  decreased with increasing  $N_t$  during this experiment.

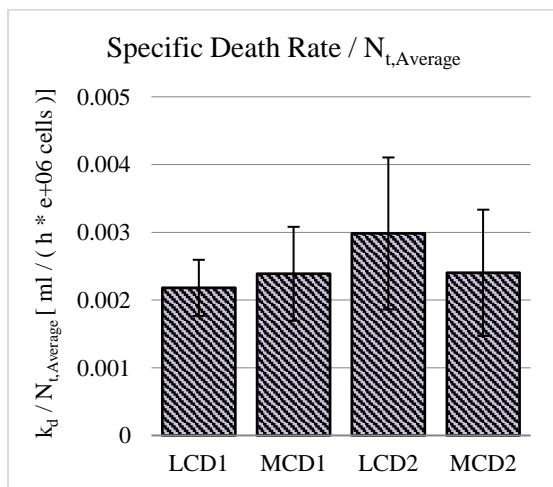


**Figure 31** Total cell density normalized death rates of the inoculated cultures

**Table 28**, p-values calculated from the significance analysis, in which the total cell density normalized death rates were compared against each other

$k_d/TCD$ p-values	LCD1	MCD1	LCD2	MCD2
LCD1	1.0	0.7	0.3	0.7
MCD1	-	1.0	0.5	1.0
LCD2	-	-	1.0	0.5
MCD2	-	-	-	1.0

## 4. RESULTS

---

This experiment was performed to examine the influence of the age of the parent culture in the initial  $\mu$  after inoculation since conditioned medium from exponentially growing cells showed no effects.

These results showed that the age of the parent culture did not have any significant effects on the  $\mu$  of the cultures inoculated in growth medium without conditioned medium at a low  $N_t$  during the first 24 hours of cultivation. An increased  $\mu$  was only achieved through the inoculation at an  $N_t$  of around  $1 \times 10^6$  cells/ml using the parent culture experiencing a  $\mu$  that was close to its maximum, but had already passed it. Comparison between both medium cell density cultures, showed that inoculation from the YPC, which showed very similar  $\mu$  to MPC, nevertheless was at an early phase of growth and still in the “acceleration” stage, resulted in a lower  $\mu$  that was not significantly different from the low cell density cultures.

The experiment also showed a decrease in the viability of the cultures and an increase in their  $k_d$  with increasing  $N_t$ . This effect seemed to be moderately affected by the age of the parent culture only at a low cell density, resulting in the  $k_d$  of the LCD2 culture to be higher and its viability lower than LCD1. Both MCD cultures showed the same  $k_d$  and drop in viability, regardless of the age of their respective parent culture.

### 4.1.5 Concluding Remarks

The experiments in this chapter revealed the biological activity of conditioned medium and the influence of the age of the inoculation culture and the starting cell density on the specific growth and death rates of the cells. The study of conditioned medium carries a lot of difficulties due its complex nature and the large number of factors that may alter its composition. Its effects could be attributed, among others, to the presence of inhibitory metabolites like lactate and ammonia, the depletion of glucose and glutamine, suboptimal cultivation conditions caused by changes in pH and osmolarity and bioactive molecules secreted by the cells.

Conditioned medium was generally associated with a delayed improvement in the survival of the cells, resulting in an increase in viability and a decrease in the specific death rate regardless if the conditioned medium originated from the early or the late exponential phase of growth. The conditioned medium harvested in the late exponential phase, which was expected to contain growth inhibitory factors, was associated with a delayed decrease in the specific growth rate, resulting in a lower total cell density, without altering the glucose glutamine and lactate uptake and consumption rates. This effect could be traced back to the components in conditioned medium with a molecular weight smaller than 10 kDa. The examination of conditioned medium originated from cells growing in the exponential phase of growth showed a delayed minor increase in specific growth rate and total cell density.

It was also established that inoculation at a low total cell density of around  $3 \times 10^5$  cells/ml causes a reduction in the specific growth rate of the cells within the first 24 hours of cultivation. This cell density phenomenon is well known in mammalian cells. It is referred to in the literature as initial lagging and is often attributed to the low availability of growth stimulating factors in the growth medium produced by the cells themselves. The nature of the initial lagging was examined in two experiments and it was shown that a combination of the age of the parent culture and the starting cell density have an influence on the specific growth rate, rather than the presence of conditioned medium harvested from the exponential phase of growth. The initial lagging was reduced by inoculating at a medium total cell density of around  $10^6$  cells/ml using a parent culture that had already experienced its maximal specific growth rate and was in a process of deceleration. The same experiments also showed a linear increase in the specific death rate of the cells with increasing total cell density in the absence of conditioned medium.



## 4.2 Cation Exchange Chromatography and Evaluation of Fractions

### 4.2.1 Capture and Fractionation of the Conditioned Medium Components

#### Fractionation with a stepwise increase of pH

Mixing of the conditioned medium with the buffer A at pH 3 resulted in the instantaneous and considerable formation of cloudiness. This made subsequent filtering difficult and made it necessary to replace the PES membrane several times throughout the procedure.

Figure 32 shows the measured pH and conductivity of the pre-mixed elution buffers plotted against the percentage of buffer B used for their preparation (A). The graph shows a strong linear correlation between the pH ( $R^2=0.9994$ ) and the conductivity ( $R^2=0.9972$ ) to increasing ratios of buffer B. The latter exhibited a higher conductivity than its counterpart buffer A, which was the result of the adjustment to pH 10 using a 1 M NaOH solution. The pH and conductivity of the collected fractions are also shown (B). After the buffers went through the membrane and the proteins were collected, the linearity decreased slightly, resulting in  $R^2=0.9942$  for the pH and  $R^2=0.9776$  for the conductivity. There was also a general shift of both curves into lower values caused by back-mixing at each step with the previous elution buffer still held inside of the membrane capsule, which has a void volume of 1.3 ml.

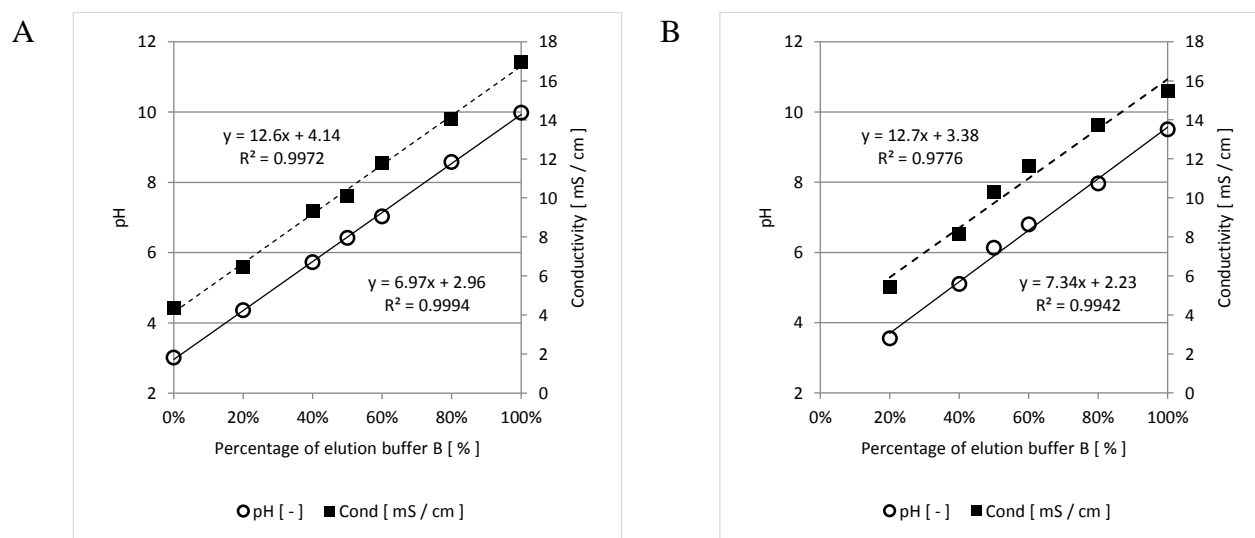
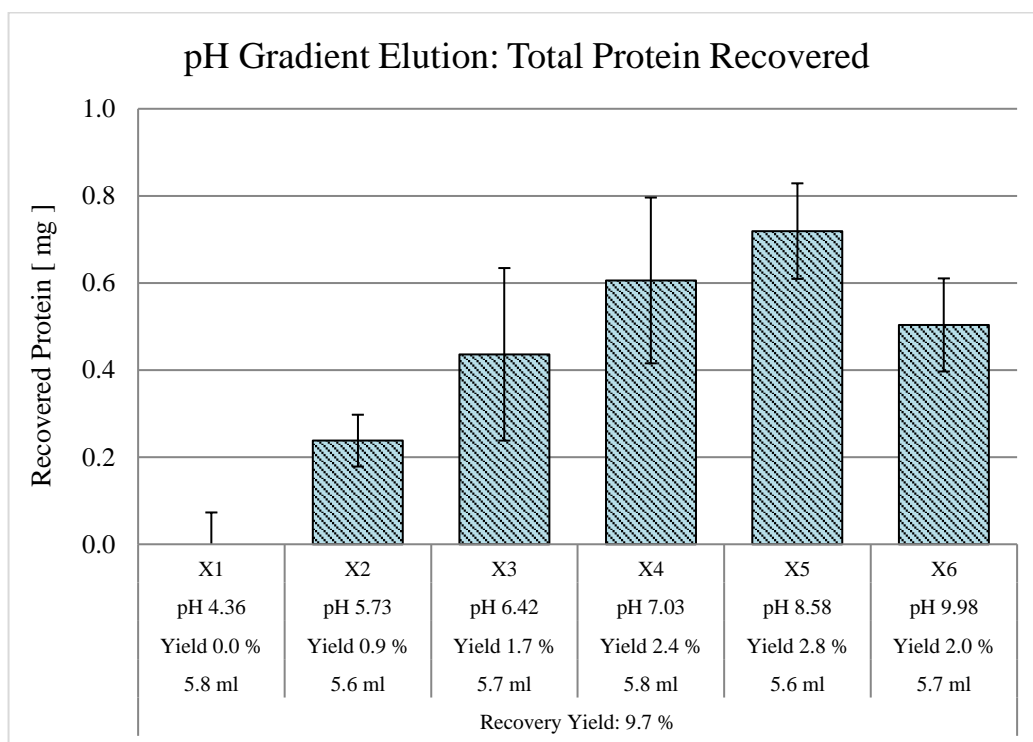


**Figure 32** pH (○) and conductivity (■) values plotted against the volumetric ratio of Buffer B for the pre-mixed elution buffers (A) and the collected fractions (B).

## 4. RESULTS

Figure 33 shows the results of the Bradford analysis performed on the collected fractions. Each column represents the total protein and the error bars display standard deviation of the three measured samples. The pH of each elution buffer used, the recovery yield and the elution volume are shown under each column.

No protein was measured in fraction X1 at the pH 4.36 step and elution started at values higher than pH 5.73, whose corresponding fraction X2 contained  $0.2 \pm 0.06$  mg protein. Elution increased with increasing pH and the fraction containing the most protein was recovered at pH 8.58 with  $0.7 \pm 0.11$  mg (X5). Fractions X3, X4 and X6 contained a total of  $0.4 \pm 0.20$ ,  $0.6 \pm 0.19$  and  $0.5 \pm 0.11$  mg protein respectively. A total of  $2.5 \pm 0.05$  mg protein was recovered, which represented  $9.7\% \pm 1.76\%$  of the total protein loaded into the membrane.



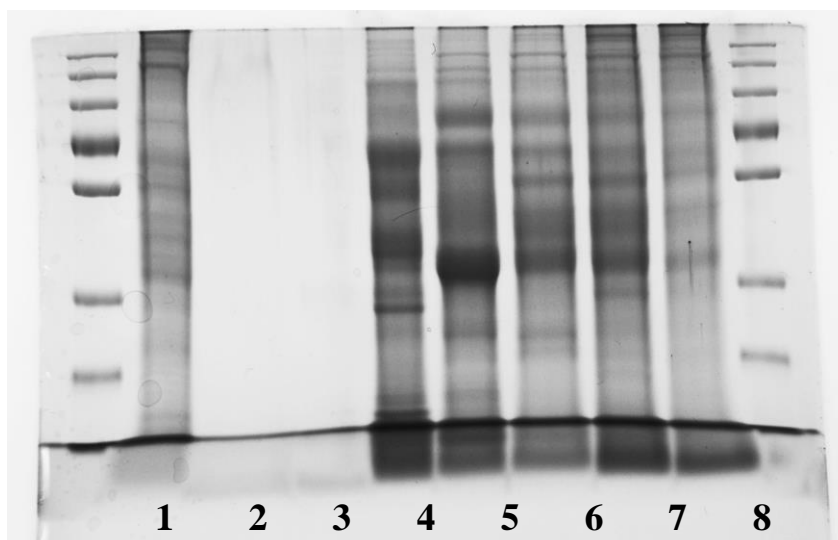
**Figure 33** Protein recovered in each fraction of the pH-gradient elution experiment. The error bars display the standard deviation from the three measures samples.

Figure 34 shows the SDS gel performed on the fractions (lanes 3-8), conditioned medium (lane 1) and adjusted load material (lane 2) after precipitation following the NLS-TCA protocol (see *Electrophoresis*). No proteins were seen in the lanes containing the adjusted load material and the first elution step at pH 4.36, while many protein bands that smeared along the gel could be noticed in the lanes corresponding to the conditioned medium and the elution steps with pH higher than 5.73 (lanes 4-8). All of this was consistent with the Bradford analysis presented in Figure 33. Many protein bands

## 4. RESULTS

---

were distributed across the lanes of several elution steps and their molecular weight could be vaguely traced back to bands found in the conditioned medium lane.



**Figure 34** SDS-Page showing the precipitated fractions (lanes 3-8), conditioned medium (lane 1) and adjusted load material (lane 2). The conditioned medium was harvested in the late exponential phase of growth. Capture was performed at pH 3. Elution from the membrane was achieved through the stepwise pH increase of the mobile phase: Lane 3: pH 4.36; Lane 4: pH 5.73; Lane 5: pH 6.42; Lane 6: 7.03; Lane 7: pH 8.58; Lane 8: pH 9.98.

Total recovery yield after adjusting the conditioned medium down to pH 3 was rather low, which could be the result of protein loss due to the substantial precipitation observed after dilution with the binding buffer A. Since elution from the cation exchanger requires the net charge of the protein to reach zero, these results indicate that the *pI* distribution of the collected proteins was shifted into the more basic values.

### Two step elution for increased protein recovery

Mixing of the conditioned medium with the binding buffer A2 at pH 5 did not result in the considerable formation of cloudiness observed at pH 3, making filtering faster and fouling of the PES membrane less frequent.

Figure 35 presents the results of the small scale TE1 experiment. The columns in the graph represent the protein recovered in each fraction and the error bars display the standard deviation calculated from the three measured samples. The yield of each fraction, their corresponding elution volumes and the conditions at which they were recovered are shown under each column. Furthermore, the total recovery yield is shown at the bottom of the graph.

## 4. RESULTS

Protein recovery for the fractions E1 and E2 was determined at  $0.8 \pm 0.11$  and  $0.1 \pm 0.01$  mg respectively, accounting for a yield of  $40.7\% \pm 7.76\%$  and  $6.0\% \pm 0.90\%$ . A total of  $0.9 \pm 0.11$  mg protein was recovered from the membrane, representing  $46.7\% \pm 8.2\%$  of the total protein loaded. Most of the protein was recovered in the E1 fraction recovered at pH 10, which compared to the pH gradient elution experiment, represents a substantial increase of more than three-fold in the total recovery yield.

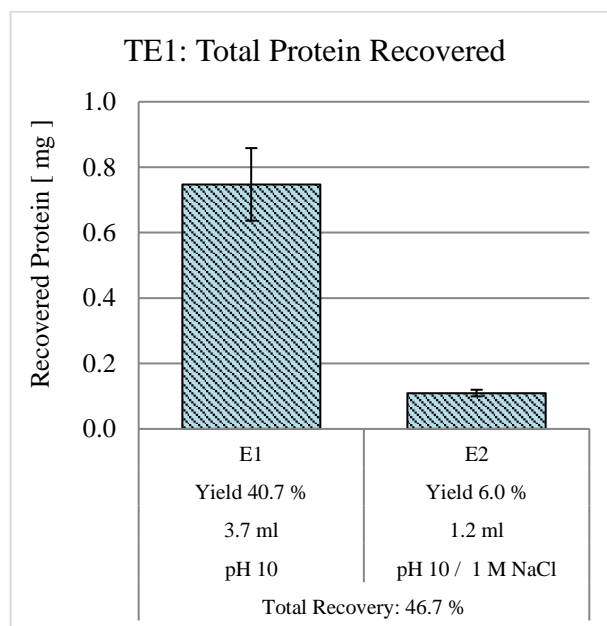


**Figure 35** Protein recovered in each fraction of the TE1 experiment. The error bars display the standard deviation from the three measures samples.

### 4.2.2 Fraction Evaluation

#### Testing of Fractions from Elution E1

Figure 36 shows the results of the TE2 experiment performed to produce the fractions of elution E1 that were tested on growing cells. The columns of the graph show the protein recovered in each fraction with the error bars displaying the standard deviation of the three measured samples. The amount of protein determined for fractions X1, X2, X3 and X4 was  $16.2 \pm 2.34$ ,  $6.2 \pm 0.10$ ,  $12.9 \pm 0.51$  and  $0.2 \pm 0.1$  mg respectively, which accounted to  $18.6\% \pm 2.90\%$ ,  $7.1\% \pm 0.43\%$ ,  $14.8\% \pm 0.68\%$  and  $0.2\% \pm 0.01\%$  of the protein loaded. A total of  $35.5 \pm 2.40$  mg protein was recovered from the membrane, representing a total recovery yield of  $40.7\% \pm 3.64\%$ . The pooled fractions X1 and X2, which corresponded to  $25.7\% \pm 3.08\%$  of the proteins in the conditioned medium, were supplemented to

## 4. RESULTS

growing cells following the procedure described in the *Materials and Methods* section of this chapter (see *Testing of Fractions from Elution E1*).

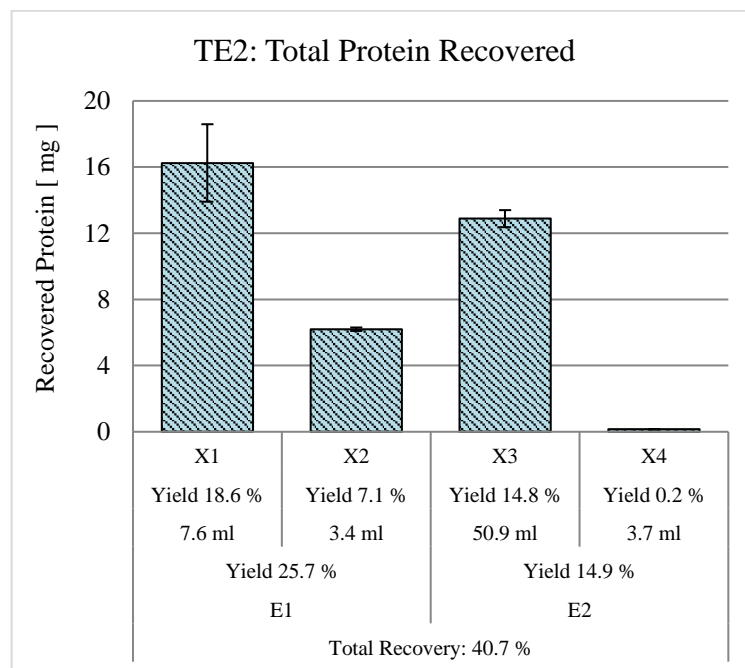


**Figure 36** Protein recovered in each fraction of the TE2 experiment. The error bars display the standard deviation from the three measures samples.

Several effects were associated with the supplementation of the fractions X1 and X2 from elution E1. Figure 37 depicts the total cell density (A), percentage of apoptotic cells (B) and viability (C) measured for the culture supplemented with the pooled fractions (E1) and the negative control (NC). The values of the graph represent the average calculated for the triplicate cultures and the error bars display the standard deviation. The E1 culture was cultivated for 168 due to its fast and sudden decline towards the end of the cultivation, while the NC culture was cultivated for 192 hours.

The culture supplemented with the E1 fractions showed a higher total cell density ( $N_t$ ), higher viability and lower percentage of apoptotic cells (apop%) throughout most of the cultivation. Both cultures were inoculated at an average of  $3.24 \pm 0.17 \times 10^5$  cells/ml and reached a maximum  $N_t$  of  $14.27 \pm 0.407$  and  $16.14 \pm 0.209 \times 10^6$  cells/ml for the NC and E1 cultures respectively at 149 and 136 cultivation hours. The  $N_t$  of the E1 culture was significantly ( $p < 0.05$ ) higher by  $18\% \pm 7.0\%$  than the NC for almost the entire cultivation, except for the last day, when it suddenly plummeted down to  $10.32 \pm 0.383 \times 10^6$  cells/ml after reaching its maximum. The progression of the NC culture was slower at the end of the cultivation and the  $N_t$  decline was much less abrupt.

## 4. RESULTS

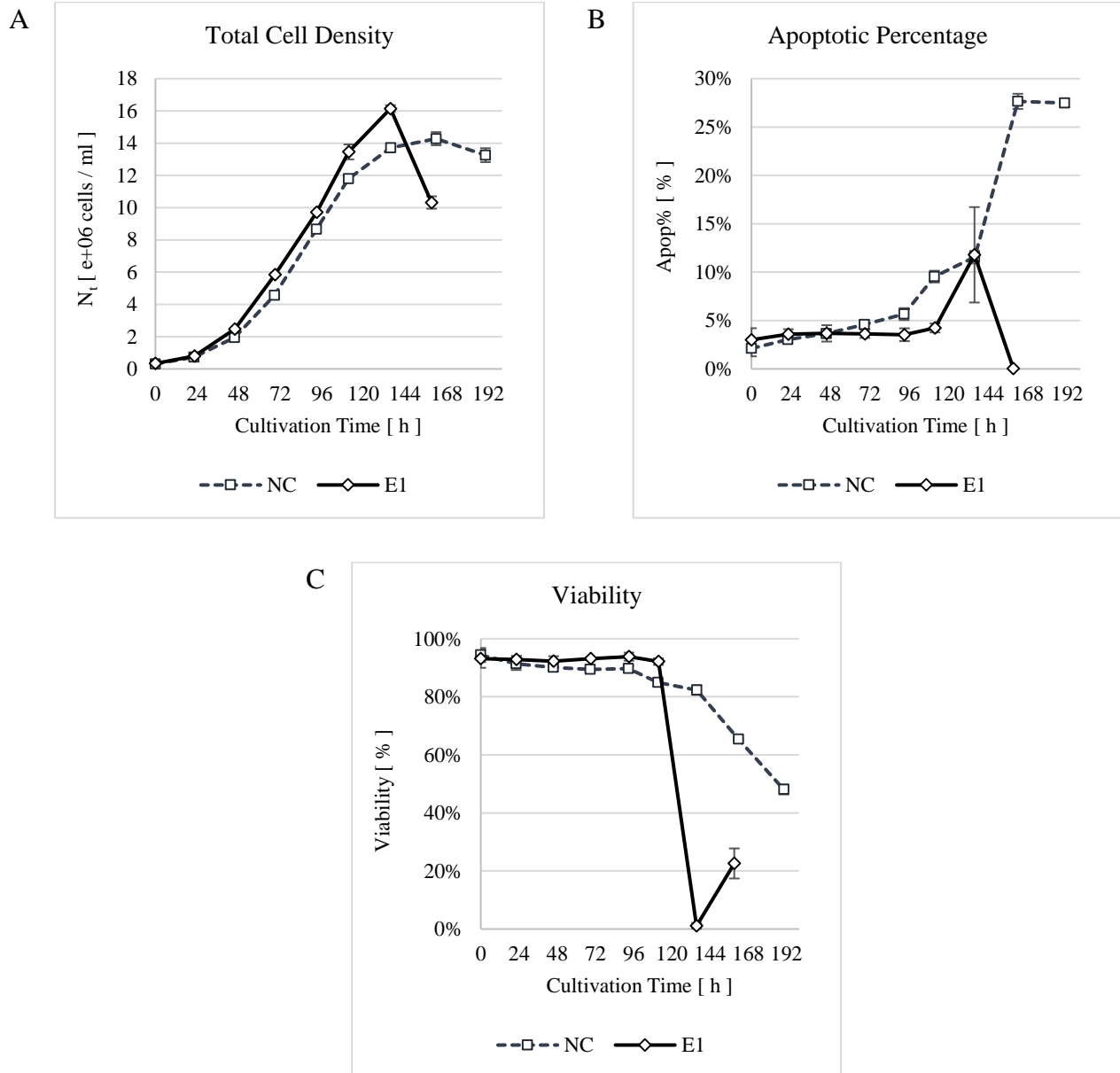


**Figure 37** Total cell density ( $N_t$ ) (A), percentage of apoptotic cells (apop%) (B) and viability (C) measured for the culture supplemented with the pooled fractions (E1) and the negative control (NC). The values of the graph represent the average calculated for the triplicate cultures and the error bars display the standard deviation.

The apop% of the E1 culture remained below 5% during the first 120 hours, followed by an abrupt increase to  $11.8\% \pm 4.93\%$  at 144 hours and plummeted down to 0% at the end of the cultivation. The progression of the NC culture showed a consistent increase in apop% during the first 144 hours, followed by a substantial increase during the last 48 hours cultivation, ending at  $27.5\% \pm 0.44\%$ . During the first 72 cultivation hours there was no significant difference in apop% between both cultures. Between 96 and 120 hours, the E1 culture was significantly ( $p < 0.05$ ) lower than the NC culture by  $47\% \pm 14.6\%$ .

## 4. RESULTS

---

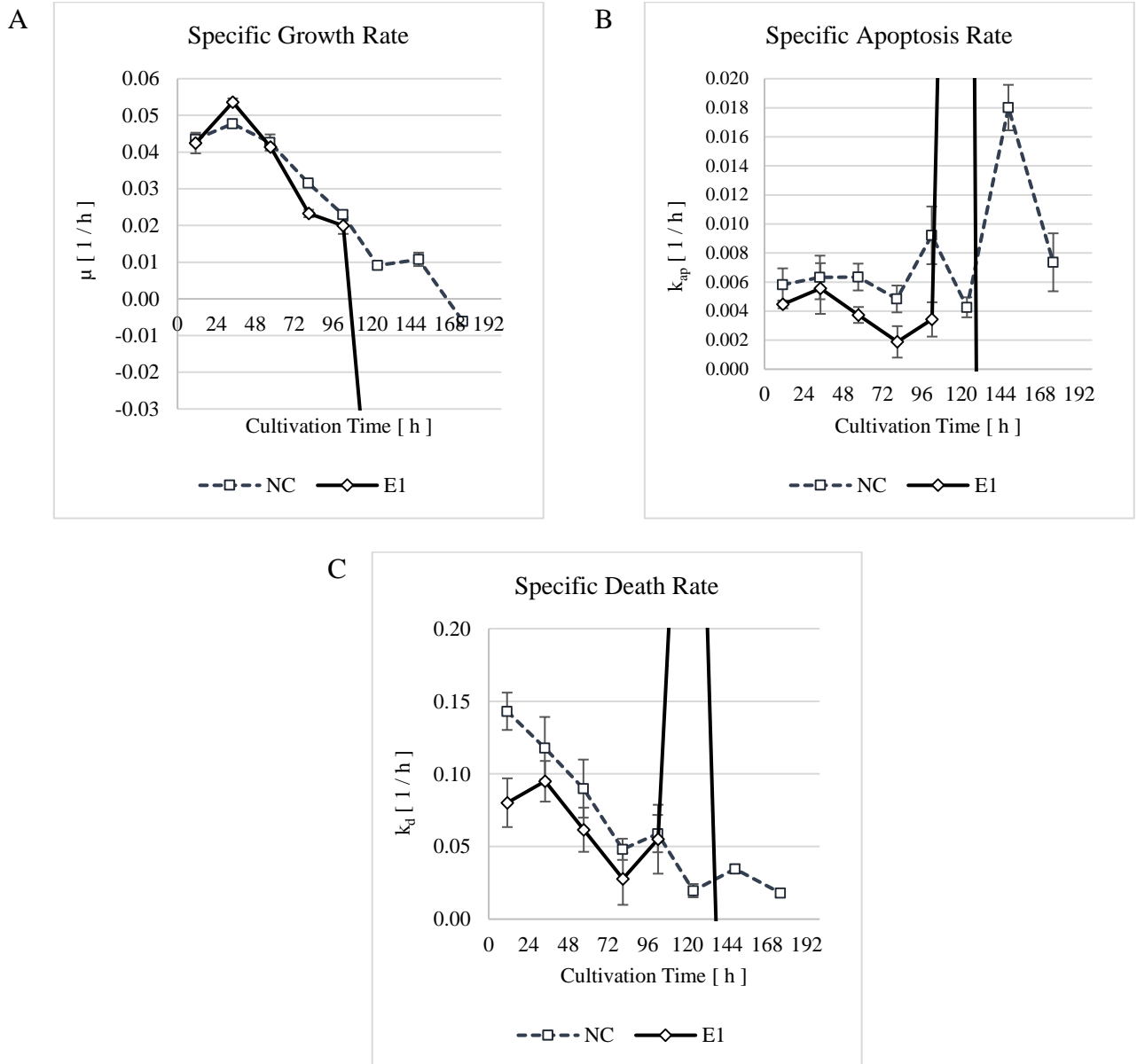
The viability of the E1 culture was significantly ( $p < 0.05$ ) higher than the NC by  $6\% \pm 3.0\%$  between 69 and 120 hours of cultivation and remained consistently above 92% up until 136 hours. It then plummeted down to  $1.1\% \pm 1.04\%$  during the next 24 hours, simultaneously reaching its maximum  $N_t$ , and rising again to  $22.6\% \pm 5.18\%$  at the end of the cultivation. The NC on the other hand, showed an initial viability of  $94.4\% \pm 2.42\%$ , which steadily decreased for the next 136 hours down to  $82.3\% \pm 1.66\%$ , followed by a more pronounced decrease during the next 48 hours and ending at  $48.1\% \pm 1.69\%$ .

Figure 38 shows the specific growth (A), apoptosis (B) and death (C) rates calculated differentially between the time-points of each sample. The graphs show the average of the triplicate cultures and the error bars depict the standard deviation.

The specific growth rate ( $\mu$ ) of both cultures followed a very similar progression during the first 96 hours. It was almost identical at the beginning with an average of  $0.043 \pm 0.0032$  1/h for both, reached its maximum (NC:  $\mu_{\max} = 0.048 \pm 0.0011$  1/h; E1:  $\mu_{\max} = 0.054 \pm 0.0010$  1/h) between 24 and 48 hours. During this time interval the  $\mu$  of the E1 culture was significantly ( $p < 0.005$ ) higher than its counterpart by  $12\% \pm 3.3\%$ . The progression of both cultures then followed a steady decrease until 96 hours. The  $\mu$  of the E1 culture then fell down to  $-0.083 \pm 0.0462$  1/h during the next 24 hours and reached  $-0.220 \pm 0.1137$  1/h at the end of its cultivation (both values are out of the range of the graph). The NC culture, on the other hand, followed a rather linear decrease after reaching its maximum up until 120 hours, at which point it fell down to  $0.009 \pm 0.0006$  1/h and decreased down to almost zero at the end of the cultivation.

The specific apoptotic rate ( $k_{ap}$ ) of the E1 culture was lower than its counterpart during the first 120 hours of cultivation. Nevertheless, the calculated values were significantly ( $p < 0.05$ ) lower only between 48 and 120 hours with an average difference of  $55\% \pm 30.5\%$ . Between 96 and 120 hours the  $k_{ap}$  of the E1 culture increased substantially to  $0.108 \pm 0.0065$  1/h during the next 24 hours and dropped down  $-0.342 \pm 0.0740$  1/h at the end of its cultivation (values lie outside of the range of the graph). The progression of the NC culture experienced alternate increase and decrease after 72 cultivation hours, ending at  $0.007 \pm 0.0020$  1/h.

## 4. RESULTS



**Figure 38** Specific growth ( $\mu$ ) (A), apoptosis ( $k_{ap}$ ) (B) and death ( $k_d$ ) (C) rates calculated differentially between the time-points of each sample. The graphs show the average of the triplicate cultures and the error bars depict the standard deviation.

During the first 24 hours of cultivation the specific death rate of the E1 ( $k_d = 0.08 \pm 0.017$  1/h) was significantly lower ( $p < 0.01$ ) than the NC culture ( $k_d = 0.14 \pm 0.013$  1/h) by  $44\% \pm 12.8\%$ . Both cultures then decreased in an almost linear fashion until 96 hours of cultivation with values that did not significantly differ from each other. The E1 culture then experienced a considerable increase reaching  $0.53 \pm 0.155$  1/h between 120 and 144 hours, followed by a substantial decrease down to  $-0.40 \pm 0.161$  1/h at the end of the cultivation. The NC on the other hand experienced during this same time interval an alternating slight increase followed by a stronger decrease and ending at  $0.02 \pm 0.003$  1/h, without coming into negative values.



## 4. RESULTS

Figure 39 shows the glucose concentration of the supernatant of each sample (A) and the glucose consumption rate calculated differentially between the time-points of each sample, plotted against the average glucose concentration between each time-point (B). The error bars display the standard deviation of the triplicate cultures.

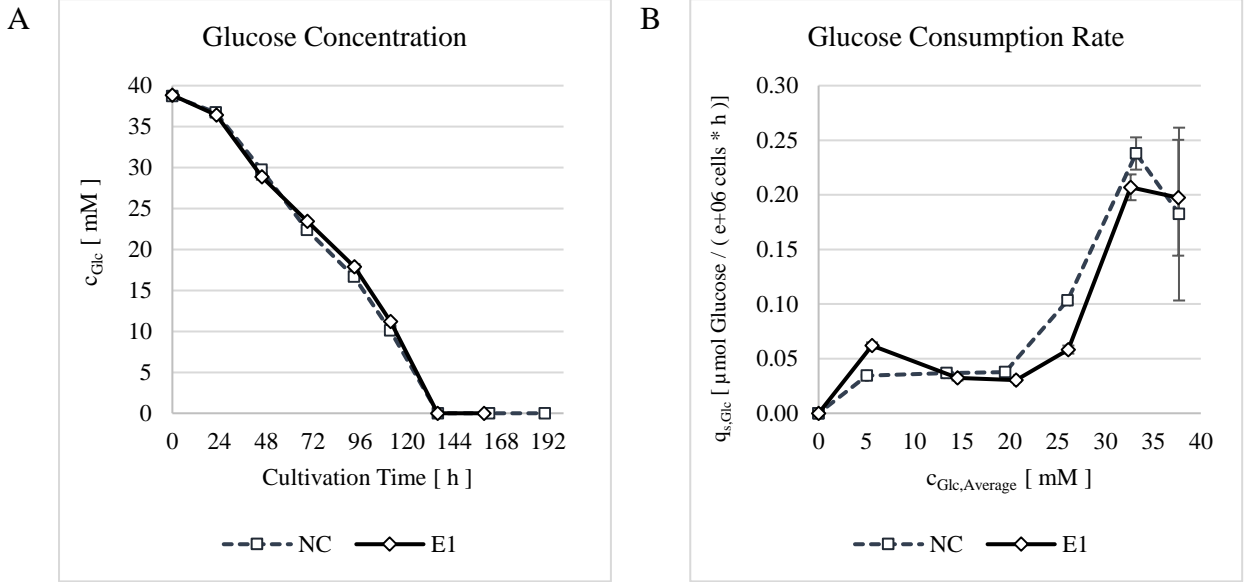


**Figure 39** Glucose concentration ( $c_{Glc}$ ) (A) and the glucose consumption rate ( $q_{s,Glc}$ ) calculated differentially between the time-points of each sample, plotted against the average glucose concentration between each time-point (B). The error bars display the standard deviation of the triplicate cultures.

The glucose concentration ( $c_{Glc}$ ) at the beginning of the cultivation was in average  $38.8 \pm 0.53$  mM for both cultures, and decreased steadily as the cultivation progressed until it was completely depleted at 144 hours. The graph depicting the glucose consumption rate ( $q_{s,Glc}$ ) describes an increased glucose consumption with increased  $c_{Glc}$  in the supernatant, which decreased in a parabolic fashion with decreasing  $c_{Glc}$ . The maximal  $q_{s,Glc}$  of the E1 and NC cultures were calculated at  $0.24 \pm 0.015$  and  $0.21 \pm 0.012$   $\mu\text{mol glucose per } 10^6 \text{ cells per hour}$  respectively for a glucose concentration of around 33 mM. The maximal  $q_{s,Glc}$  of the E1 culture was significantly ( $p < 0.05$ ) lower than its counterpart by  $13\% \pm 7.3\%$ . In the concentration range between 33 and 5 mM glucose the  $q_{s,Glc}$  of E1 was significantly ( $p < 0.05$ ) lower than NC an average of  $34\% \pm 17.3\%$ , with the greatest reduction resulting  $44\% \pm 3.9\%$  at a concentration of around 26 mM. The consumption rate of the NC culture remained constant at a value around  $0.04 \pm 0.004$   $\mu\text{mol glucose per } 10^6 \text{ cells per hour}$  at concentrations lower than 20 mM. At the same concentration range the E1 culture was significantly ( $p < 0.05$ ) lower and remained constant at a value of around  $0.03 \pm 0.03$   $\mu\text{mol glucose per } 10^6 \text{ cells per hour}$ . Nevertheless, it experienced a sudden increase to  $0.06 \pm 0.003$   $\mu\text{mol glucose per } 10^6 \text{ cells per hour}$  just before the

## 4. RESULTS

glucose was completely depleted. This sudden increase coincided with the substantial increase in specific apoptosis and death rates described above for the E1 culture and the complete depletion of glucose in the growth medium.

Figure 40 shows the glutamine concentration (A) measured in the supernatant of the samples and the glutamine consumption rate (B) calculated differentially between the time-points of each sample, plotted against the average glutamine concentration used to determine each rate. The values given in the graphs represent the average of each triplicate culture and the error bars display the standard deviation.

The glutamine concentration ( $c_{\text{Gln}}$ ) decreased steadily as the cultivation progressed, starting at  $3.5 \pm 0.06$  and  $3.7 \pm 0.01$  mM for the E1 and NC cultures respectively, until being completely depleted at 96 hours. The glutamine consumption rate ( $q_{\text{s,Gln}}$ ) of both cultures showed an almost identical linear increase with increasing  $c_{\text{Gln}}$  in the growth medium. The only difference between both cultures was determined at the beginning of the cultivation when the  $q_{\text{s,Gln}}$  of the E1 culture was  $16\% \pm 10.2\%$  lower ( $p < 0.1$ ) than its counterpart

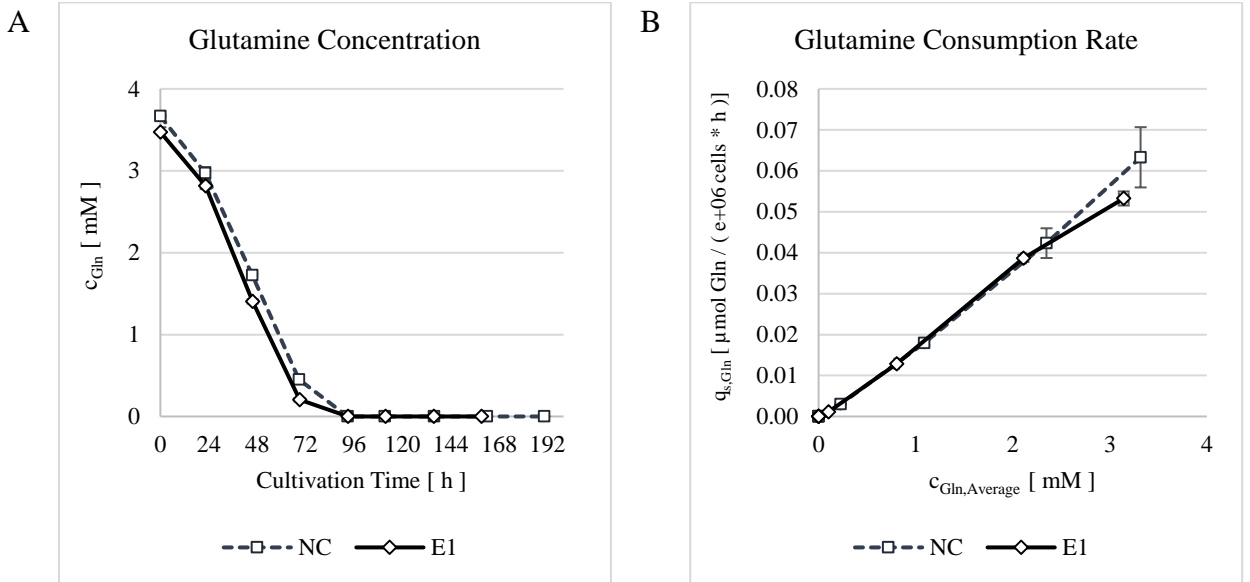


**Figure 40** Glutamine concentration ( $c_{\text{Gln}}$ ) (A) and the glutamine consumption rate ( $q_{\text{s,Gln}}$ ) calculated differentially between the time-points of each sample, plotted against the average glutamine concentration between each time-point (B). The error bars display the standard deviation of the triplicate cultures.

Figure 41 shows the lactate concentration ( $c_{\text{Lac}}$ ) profiles of the E1 and NC calculated as the average of each triplicate culture with the error bars displaying the standard deviation. The profiles can be divided into four different phases. The first 72 hours of cultivation were characterized by a net accumulation

## 4. RESULTS

---

of lactate from 0 to  $23.7 \pm 0.58$  and  $22.8 \pm 0.10$  mM for the NC and E1 cultures respectively. During this time interval the concentration profiles of both cultures was almost identical, except at 48 hours, when the  $c_{\text{Lac}}$  of the E1 culture was slightly higher than the NC. This phase coincided with the time interval in which the glutamine in the growth medium was almost completely depleted and the  $k_d$  of the cells was steadily decreasing.

The next phase was between 72 and 120 cultivation hours and was characterized by a slower lactate accumulation ending at  $26.5 \pm 0.42$  mM for the NC culture, and a net consumption of lactate ending at  $17.9 \pm 0.10$  mM for the E1 culture. During this phase the glutamine was completely depleted and towards the end of the phase, the glucose in the growth medium was completely consumed. The viability of the NC culture was already below 90% during this phase and an increase in apoptotic cells was experienced. The viability of the E1 culture, on the other hand, still remained above 92% and the percentage of apoptotic cells below 5%.

The next phase was between 120 and 144 hours, characterized by a second accumulation of lactate in the growth medium, which was more pronounced for the E1 culture, which ended at  $28.3 \pm 0.23$  mM. The NC culture increased to a  $c_{\text{Lac}}$  of  $32.4 \pm 0.86$  mM. During this phase there was no glucose or glutamine left in the growth medium and the E1 culture reached its maximum  $N_t$ , coupled with sudden hike in apoptotic cells and a substantial decrease in viability.

The fourth phase was between 144 and 168 hours for the E1 culture and between 144 and 192 hours for the NC culture, which was cultivated one day longer. The  $c_{\text{Lac}}$  of the E1 culture did not change during this phase, nevertheless the  $N_t$  decreased, possibly due to cell lysis, the viability increased slightly and there were no apoptotic cells anymore. On the other hand the  $c_{\text{Lac}}$  of the NC culture decreased, showing a net consumption of the metabolite. Furthermore the NC culture reached its maximum  $N_t$  during this phase, which was coupled with a steady decrease in viability and a net accumulation of apoptotic cells. The lactate production rates of both cultures was identical during the first three days of cultivation and becomes lower between 48 and 72 hours of cultivation at around 20 mM lactate in the supernatant. Is during this time interval that glutamine is halfway depleted.

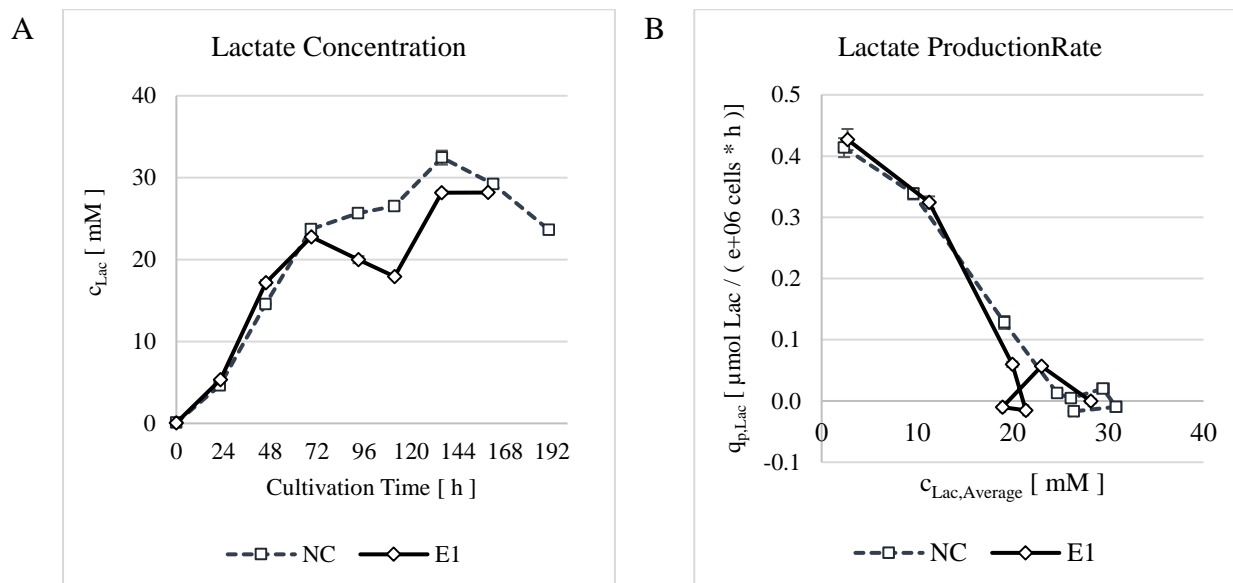


**Figure 41** Lactate concentration ( $c_{Lac}$ ) (A) and lactate production rate ( $q_{Lac}$ ) plotted against the average lactate concentration used to determine each rate (B) of the E1 and NC calculated as the average of each triplicate culture with the error bars displaying the standard deviation.

#### Testing of Fractions from Elution E2

Figure 42 shows the protein recovered in the TE3 experiment, performed to produce the fractions of elution E2 that were then tested on growing cells. The columns of the graph show the protein recovered in each fraction with the error bars displaying the standard deviation of the three measured samples. The amount of protein determined for fractions X1, X2, X3, X4 and X5 was  $0.7 \pm 0.04$ ,  $7.0 \pm 0.17$ ,  $1.0 \pm 0.03$ ,  $1.9 \pm 0.12$  and  $0.5 \pm 0.03$  mg respectively, which accounted to  $3.5\% \pm 0.99\%$ ,  $34.6\% \pm 9.51\%$ ,  $4.8\% \pm 1.33\%$ ,  $9.6\% \pm 2.71\%$  and  $2.3\% \pm 0.64\%$  of the protein loaded. A total of  $11.1 \pm 0.21$  mg protein was recovered from the membrane, representing a total recovery yield of  $54.9\% \pm 15.1\%$ . Fraction X4 from elution E2 was supplemented to exponentially growing cells following the procedure described in the *Materials and Methods* section from this chapter (see *Testing of Fractions from Elution E2*).

## 4. RESULTS

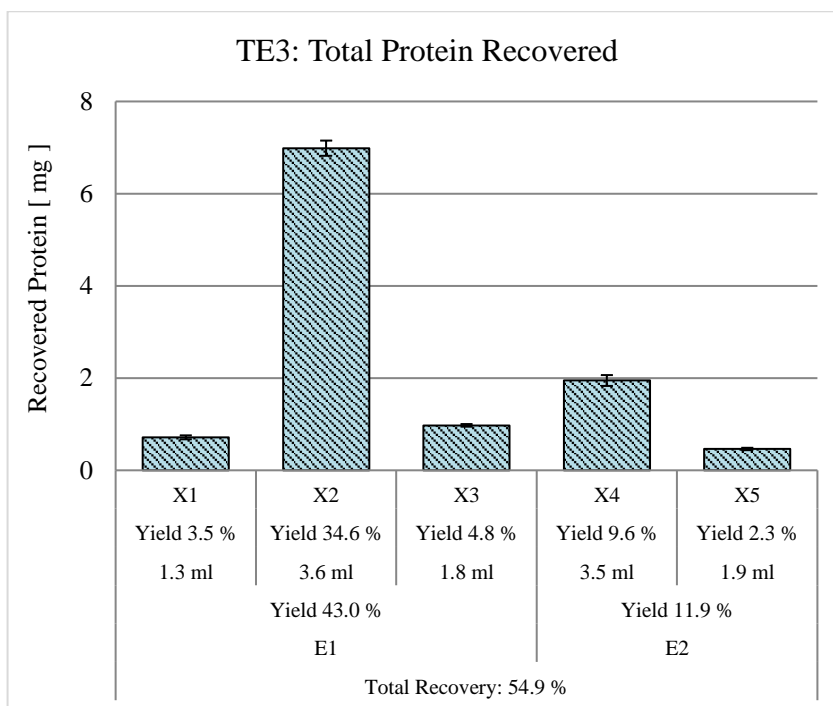


**Figure 42** Protein recovered in each fraction of the TE3 experiment. The error bars display the standard deviation from the three measures samples.

Figure 43 shows the specific growth (A) and death (B) rates calculated for the culture supplemented with the elution E2 fraction (E2) and the negative control (NC). The values given in the graphs show the average calculated for each triplicate culture and the error bars display the standard deviation.

Both cultures were inoculated at an average total cell density ( $N_t$ ) of  $1.16 \pm 0.064 \times 10^6$  cells/ml with a viability of  $93.5\% \pm 0.94\%$ . After 25 of cultivation the E2 and NC cultures reached an  $N_t$  of  $1.86 \pm 0.155$  and  $3.40 \pm 0.192 \times 10^6$  cells/ml respectively, with a viability of  $86.7\% \pm 1.49\%$  and  $93.0\% \pm 1.71\%$ . This resulted in a specific growth rate ( $\mu$ ) of  $0.019 \pm 0.0039$  1/h for the E2 culture, making it significantly ( $p < 0.001$ ) lower by  $59\% \pm 8.6\%$  than the NC culture, which was calculated at  $0.047 \pm 0.0024$  1/h. The resulting specific death rates ( $k_d$ ) of the E2 and NC cultures were  $0.005 \pm 0.0012$  and  $0.003 \pm 0.0011$  1/h respectively. Even though the  $k_d$  of the E2 culture was higher than the negative control, the significance value was low, yet still acceptable ( $p = 0.08$ ).

## 4. RESULTS

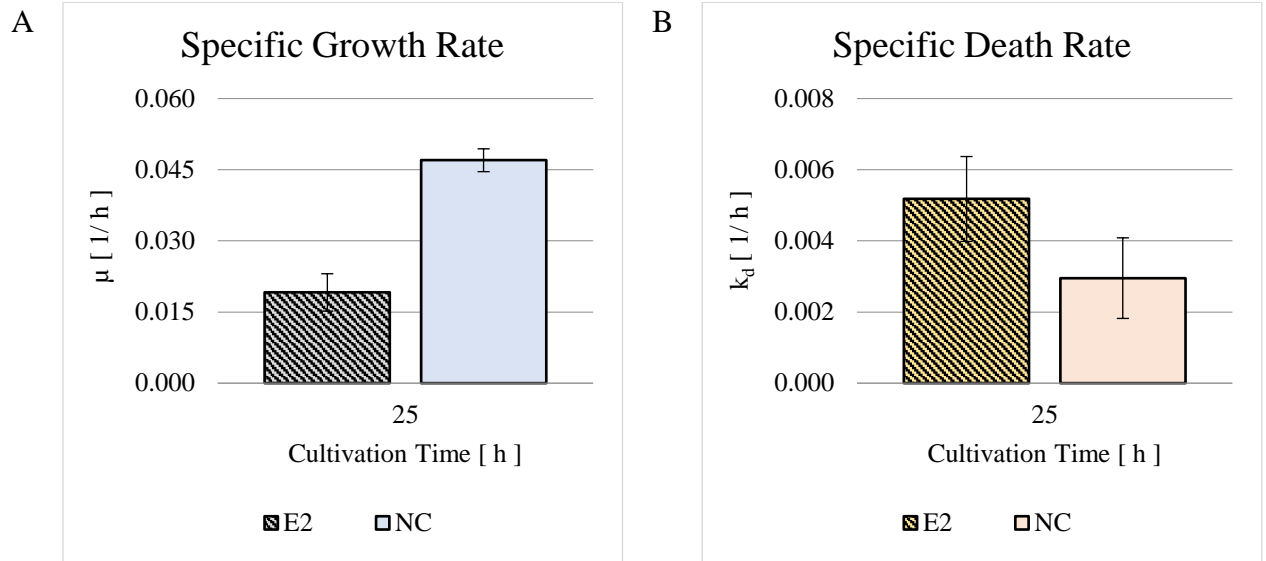


**Figure 43** Specific growth ( $\mu$ ) (A) and death ( $k_d$ ) (B) rates calculated for the culture supplemented with the elution E2 fraction (E2) and the negative control (NC). The values given in the graphs show the average calculated for each triplicate culture and the error bars display the standard deviation.

Figure 44 shows the viable cell density to glucose yield ( $Y_{x/s, Glc}$ ) (A) and the lactate to glucose yield ( $Y_{p/s}$ ) (B) calculated after the 25 hours of cultivation. The culture E2 produced  $0.07 \pm 0.016 \times 10^6$  cells and  $1.6 \pm 0.20 \mu\text{mol}$  lactate per  $\mu\text{mol}$  glucose, while the negative control produced  $0.30 \times 10^6$  cells and  $1.7 \pm 0.38 \mu\text{mol}$  lactate per  $\mu\text{mol}$  glucose. Supplementation of the elution E2 fraction to exponentially growing cells was associated with a  $77\% \pm 6.9\%$  decrease in  $Y_{x/s}$  compared to the negative control, while the lactate to glucose yield remained unchanged.

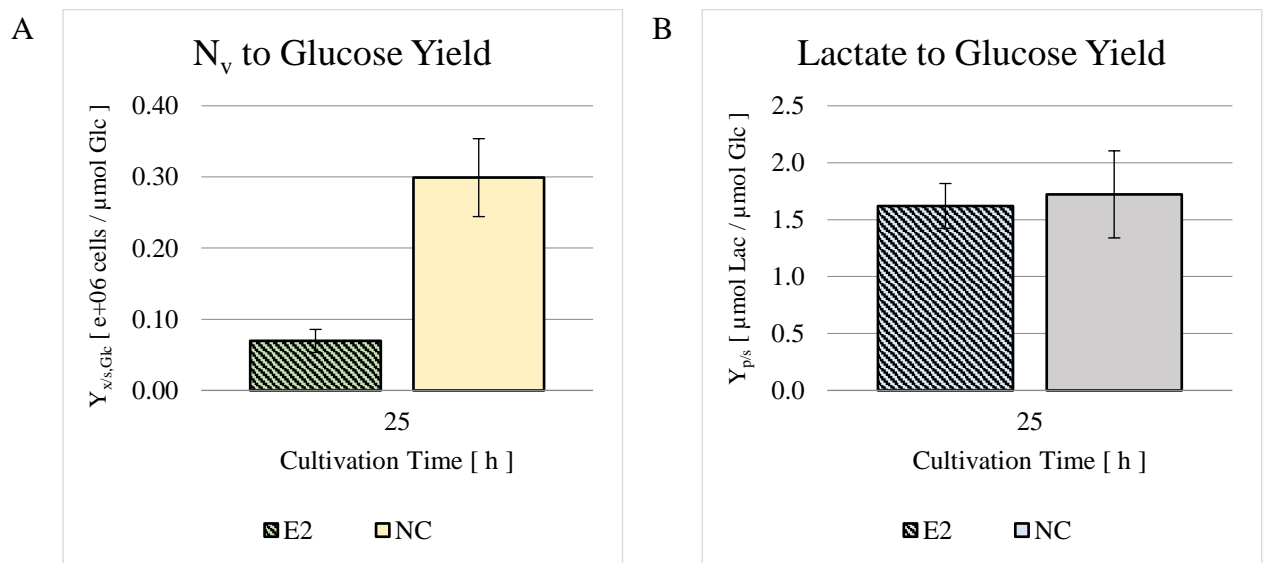


**Figure 44** Viable cell density ( $N_v$ ) to glucose yield ( $Y_{x/s, Glc}$ ) (A) and the lactate to glucose yield ( $Y_{p/s}$ ) (B) calculated after the 25 hours of cultivation. The values given in the graphs show the average calculated for each triplicate culture and the error bars display the standard deviation.

## 4. RESULTS

### Testing of Fractions from the optimized Elution E2

Figure 45 shows the total protein recovered from the first optimization experiments E2.EXP1. The columns correspond respectively from left to right to elution E1 and to the accumulated protein of fractions X0 – X5 from elution E2. The standard deviations were calculated from the measurements of the triplicate Bradford reaction. Additionally, the elution parameters, the recovery yield and the elution volumes are presented under each corresponding column. The amount of protein recovered in elutions E1 and E2 was  $15.0 \pm 1.48$  and  $3.5 \pm 0.41$  mg respectively, representing a recovery yield of  $21.1\% \pm 2.43\%$  and  $4.9\% \pm 0.65\%$ . Both elutions combined resulted in  $18.5 \pm 1.54$  mg protein, which represented a total recovery yield of  $26.0\% \pm 2.7\%$ .

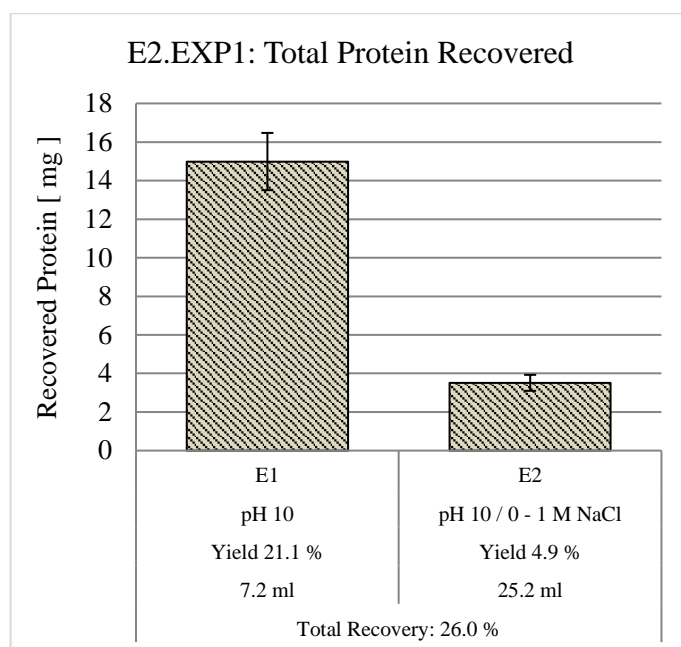


**Figure 45** Accumulated protein recovered in the fractions of elution E1 and E2 of the first optimization experiment E2.EXP1. The error bars display the standard deviation of the three samples measured.

Figure 46 shows the protein recovered in each fraction of the stepwise salt gradient of the elution E2 from the E2.EXP1 experiment. Each column corresponds from left to right to fractions X0 – X5 respectively. The standard deviations were calculated from the measurements of the triplicate Bradford reaction. The NaCl concentration of the pre-mixed buffer used for elution, the recovery yield and the elution volume of each fraction are presented below each corresponding column. Most of the protein was collected in the first two fractions X0 ( $0.9 \pm 0.28$  mg protein;  $1.3\% \pm 0.40\%$  yield) and X1 ( $1.3 \pm 0.21$  mg protein;  $1.8\% \pm 0.32\%$  yield), which were recovered with a total of 7.4 ml of the 0.2 M NaCl elution buffer. Their combined protein added to  $2.2 \pm 0.35$  mg, which represented  $3.1\% \pm 0.52\%$  of

## 4. RESULTS

the total protein loaded. Fractions X2 ( $0.8 \pm 0.22$  mg protein;  $1.1\% \pm 0.32\%$  yield), X3 ( $0.4 \pm 0.04$  mg protein;  $0.5\% \pm 0.07\%$  yield) and X4 ( $0.1 \pm 0.03$  mg protein;  $0.2\% \pm 0.04\%$  yield) showed steadily decreasing recovery yield with the increasing NaCl concentration of the elution buffer, reaching 0% at 1 M NaCl.

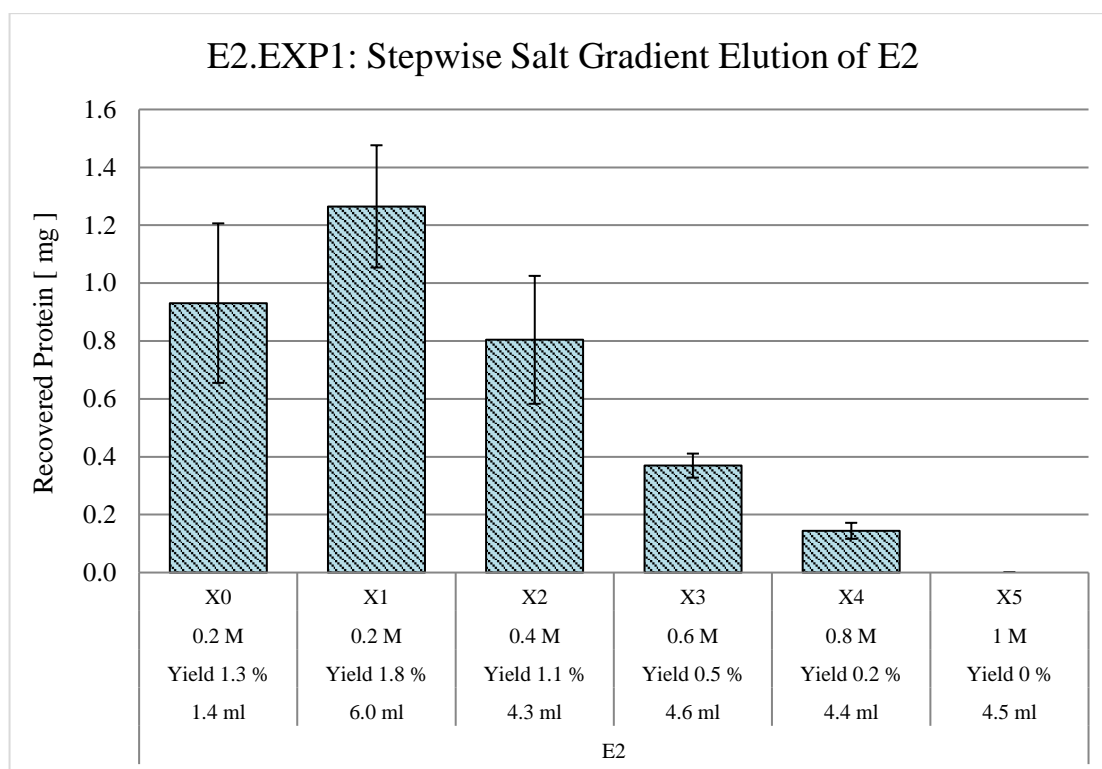


**Figure 46** Protein recovered in each fraction of the stepwise salt gradient of the elution E2 from the E2.EXP1 experiment. The error bars display the standard deviation of the three samples measured.

Figure 47 shows the accumulated total protein recovered in the elutions E1 and E2 of the second optimization experiment E2.EXP2. The columns correspond respectively from left to right to elution E1 and to the accumulated protein of fractions from elution E2. The standard deviations were calculated from the measurements of the triplicate Bradford reaction. The elution parameters, the recovery yield and the elution volumes are presented under each corresponding column. The amount of protein recovered in elution E1 and E2 was  $10.1 \pm 2.35$  and  $9.0 \pm 0.44$  mg respectively, representing a recovery yield of  $13.5\% \pm 3.87\%$  and  $12.0\% \pm 2.11\%$ . Both elutions combined added to a total protein of  $19.1 \pm 2.39$  mg protein, which represented a total recovery yield of  $25.4\% \pm 5.36\%$ .



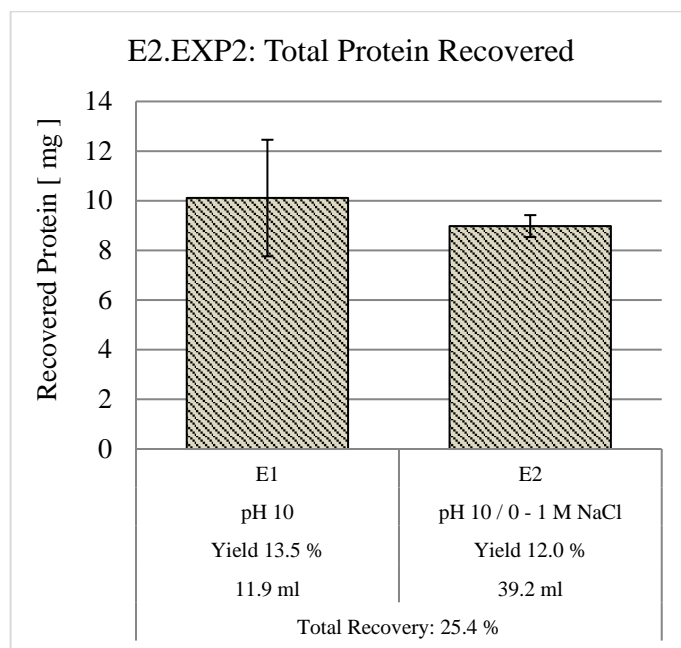
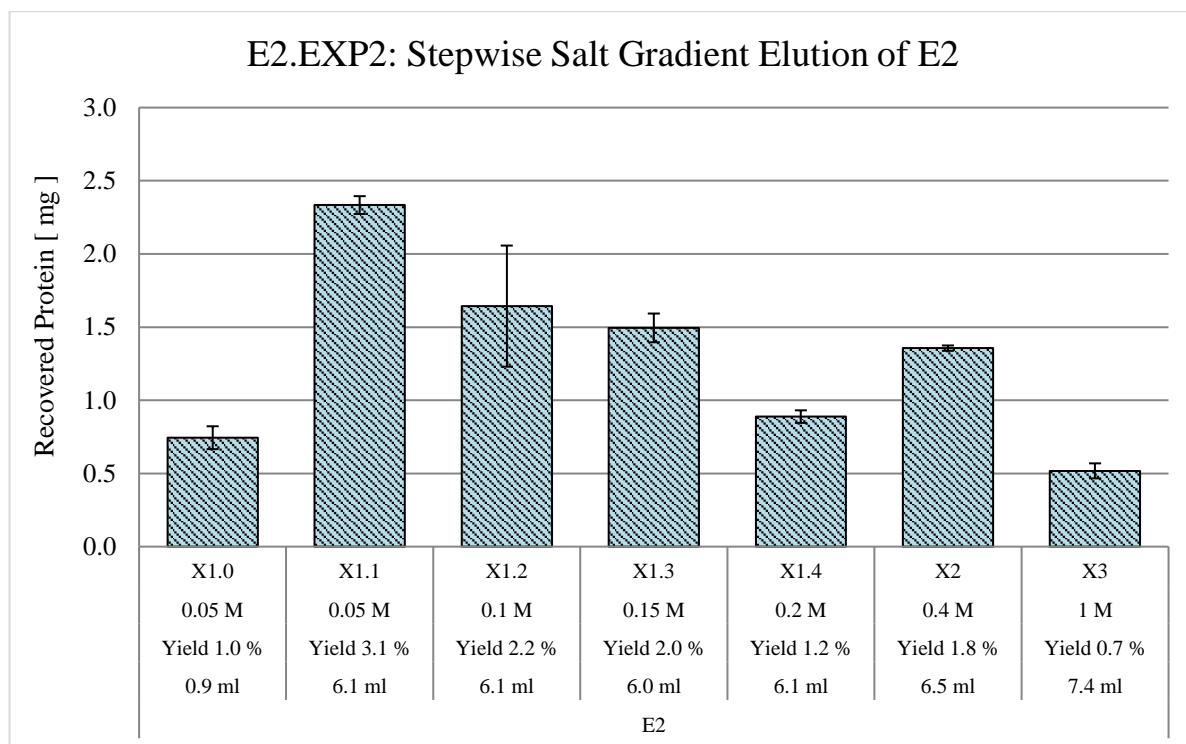


**Figure 47** Accumulated protein recovered in the fractions of elution E1 and E2 of the second optimization experiment E2.EXP2. The error bars display the standard deviation of the three samples measured.

Figure 48 shows the protein recovered in each fraction of the stepwise salt gradient of elution E2 from the E2.EXP2 experiment. The NaCl concentration of the pre-mixed buffer used for elution, the recovery yield and the elution volume of each fraction are presented below each corresponding column. The standard deviations were calculated from the measurements of the triplicate Bradford reaction.

The first five columns correspond from left to right to fractions X1.0 ( $0.7 \pm 0.08$  mg protein;  $1.0\% \pm 0.20\%$  yield), X1.1 ( $2.3 \pm 0.06$  mg protein;  $3.1\% \pm 0.53\%$  yield), X1.2 ( $1.6 \pm 0.41$  mg protein;  $2.2\% \pm 0.66\%$  yield), X1.3 ( $1.5 \pm 0.10$  mg protein;  $2.0\% \pm 0.36\%$  yield) and X1.4 ( $0.9 \pm 0.04$  mg protein;  $1.2\% \pm 0.21\%$  yield), which were recovered using the elution buffers with a NaCl concentration in the range between 0.05 – 0.2 M. The last two columns correspond to the X2 ( $1.4 \pm 0.02$  mg protein;  $1.8\% \pm 0.31\%$  yield) and X3 ( $0.5 \pm 0.05$  mg protein;  $0.7\% \pm 0.14\%$  yield) fractions, recovered with the pre-mixed buffers with a salt concentration of 0.4 and 1 M respectively.

## 4. RESULTS



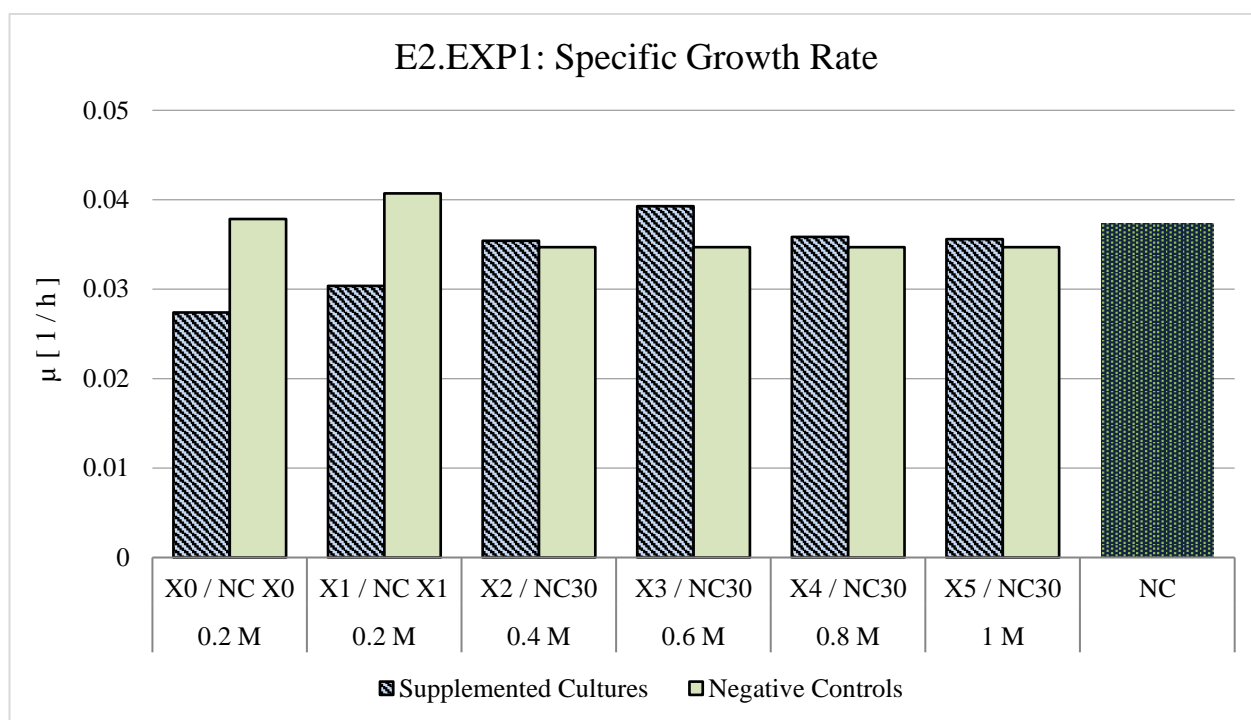
**Figure 48** Protein recovered in each fraction of the stepwise salt gradient of the elution E2 from the second optimization experiment E2.EXP2. The error bars display the standard deviation of the three samples measured.

Figure 49 shows the effect of the fractions X0 – X5 recovered in the E2.EXP1 experiment on the specific growth rate ( $\mu$ ) of exponentially growing cells after 17 hours of cultivation. Each pair of columns compares a culture supplemented with a fraction (left column) with its negative control (right column). Furthermore, the NaCl concentration of the pre-mixed buffer used for elution is presented under each corresponding pair. No error bars are available, since the screening was performed without replicate cultures.

The two fractions eluted with the 0.2 M NaCl elution buffer, X0 and X1, showed the previously determined effects associated with elution E2 when compared to their respective negative controls. The  $\mu$  of the culture supplemented with fraction X0 and its negative control (X0 NC) were calculated at 0.027 and 0.038 1/h respectively, representing a difference of 27.7%. The culture supplemented with fraction X1 and its negative control (X1 NC) showed a  $\mu$  of 0.030 and 0.041 1/h respectively, showing a 25.4% difference when compared to each other. The cultures supplemented with fractions X2, X3, X4 and X5 proliferated with a  $\mu$  of 0.039, 0.036, 0.036 and 0.037 1/h respectively. The negative control to which the latter cultures were compared (NC30) proliferated with a  $\mu$  of 0.035 1/h. Except for culture X3 that showed an increase of 13.1%, the  $\mu$  of the supplemented cultures X2 – X5 were very similar to NC30, with an average difference of 2.6%. The undisturbed culture proliferated with a  $\mu$  of 0.037

## 4. RESULTS

1/h, which was 1.4% lower than X0 NC, 8.3% lower than X1 NC and 7.5% higher than NC30. Since no replicate were cultivated, comparison between the cultures is not statistically relevant, but served as a point of reference for the second optimization of the salt concentration of the elution buffer.



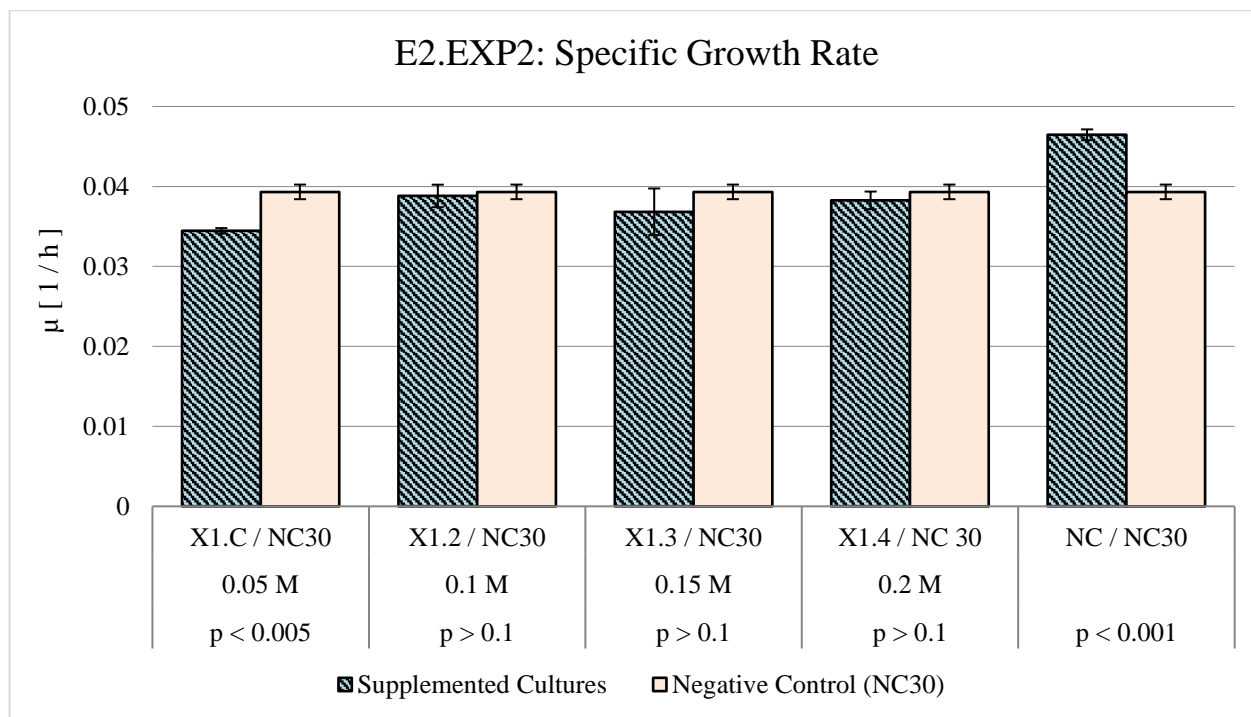
**Figure 49** Specific growth rate ( $\mu$ ) of the cultures supplemented with the fractions X0 X5 from the first optimization experiment E2.EXP1. No error bars are displayed, since the screening was performed without biological replicates.

Figure 50 shows effect of the fractions recovered in the E2.EXP2 experiment on the  $\mu$  of exponentially growing cells after 24 hours of cultivation. The first four pair of columns compare a culture supplemented with a fraction (left column) with the negative control NC30 (right column) and correspond respectively from left to right to fractions X1.C – X1.4. The last pair of columns compare the non-supplemented second negative control (NC, left column) with NC30 (right column). Furthermore, the NaCl concentration of the pre-mixed buffer used for elution is presented under each corresponding pair. The error bars represent the standard deviation calculated from the triplicate cultures.

The effect of decreased  $\mu$  associated with elution E2 and identified in fractions X0 and X1 from the first optimization experiment E2.EXP1, was identified in the culture supplemented with the combined fraction X1.C. Its  $\mu$  was calculated at  $0.034 \pm 0.0003$  1/h, which was significantly ( $p < 0.005$ ) lower by  $12\% \pm 2.2\%$  than the negative control NC30, which  $\mu$  was calculated at  $0.039 \pm 0.0009$  1/h. The cultures supplemented with the fractions X1.2 – X1.4 proliferated at  $0.039 \pm 0.0014$ ,  $0.037 \pm 0.0029$

## 4. RESULTS

and  $0.038 \pm 0.0011$  1/h respectively at did not show any significant differences when compared to NC30. The second negative control (NC) showed a  $\mu$  of  $0.046 \pm 0.0007$  1/h, and was significantly ( $p < 0.001$ ) higher than NC30 by  $18\% \pm 3.2\%$ . This indicates that the added NaCl and buffer had a possible negative effect on  $\mu$ .



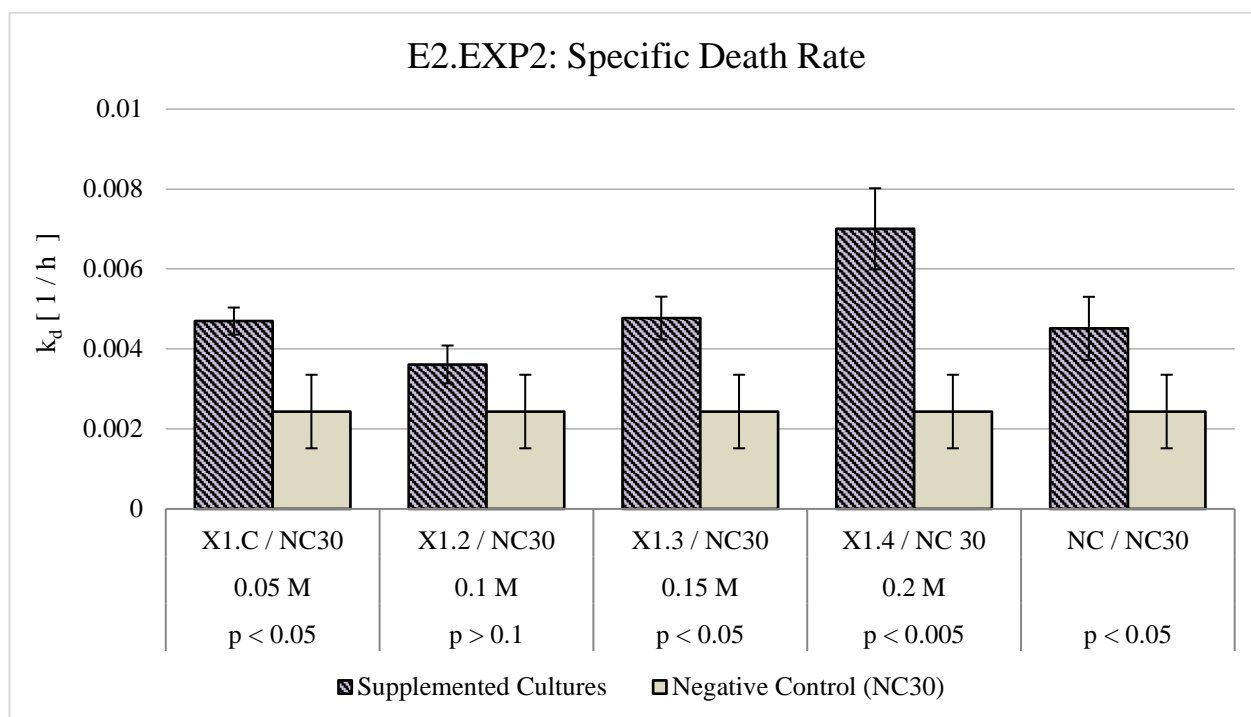
**Figure 50** Specific growth rate ( $\mu$ ) of the cultures supplemented with the fractions X1.C – X1.4 from the second optimization experiment E2.EXP2. The values were calculated as the average of the triplicate cultures and the error bars display the standard deviation.

Figure 51 shows the effect of the fractions generated in the E2.EXP2 experiment on the specific death rates ( $k_d$ ) of exponentially growing cells. The results are presented analogously to the specific growth rates. Each pair of columns compares the cultures supplemented with fractions X1.C – X1.4 and the second negative control (NC) with NC30. Furthermore, the NaCl concentration of the pre-mixed buffer used for elution is presented under each corresponding pair. The error bars represent the standard deviation calculated from the triplicate cultures.

The  $k_d$  of the cultures supplemented with fractions X1.C, X1.2, X1.3 and X1.4 were calculated at  $0.005 \pm 0.0003$ ,  $0.004 \pm 0.0005$ ,  $0.005 \pm 0.0005$  and  $0.007 \pm 0.0010$  1/h respectively. Except for the culture supplemented with fraction X1.2, the specific death rates of all supplemented cultures were significantly different from NC30, calculated at  $0.002 \pm 0.0009$  1/h. The cultures X1.C, X1.3 and X1.4 were higher than NC30 by  $93\% \pm 72.2\%$ ,  $96\% \pm 77.2\%$  and  $188\% \pm 23.5\%$  respectively. The  $k_d$  of the

## 4. RESULTS

second negative control (NC) was also significantly ( $p < 0.05$ ) higher than NC30 by  $85\% \pm 81.0\%$ , and was calculated at  $0.003 \pm 0.0009$  1/h.



**Figure 51** Specific death rate ( $k_d$ ) of the cultures supplemented with the fractions X1.C – X1.4 from the second optimization experiment E2.EXP2. The values were calculated as the average of the triplicate cultures and the error bars display the standard deviation.

These experiments showed that the proteins responsible for the effects associated with elution E2 can be recovered from the cation exchanger using an elution buffer with a concentration of 0.05 M NaCl. This resulted in the reduction of the amount of protein recovered, thus narrowing down the effects associated with elution E2 to  $4.1\% \pm 0.57\%$  (fractions X1.0 and X1.1 from the E2.EXP2 experiment) of the proteins found in conditioned medium. The low salt concentration at which the bioactive molecules were recovered has the additional advantage that a bigger volume of fraction can be supplemented to growing cells without negatively affecting the growth of the cells.

### 4.2.3 Concluding Remarks

This chapter presents the development and optimization of a cation exchanger membrane adsorption chromatography step for the capture and recovery of the components in conditioned medium harvested in the late exponential phase of growth. The optimization included testing two different binding pH values, two different elution strategies and two salt concentration profiles for the elution of bound components.

A total of six bind-and-elute experiments were performed using conditioned medium produced in six bioreactor batch cultivations. The first bind-and-elute experiment was executed at pH 3 and the proteins were recovered using a stepwise linear pH gradient. Elution was achieved at a pH values higher than 5.7 and the bound proteins were separated in five different fractions. Nevertheless, the recovery yield was very low, possibly due to protein precipitation resulting from adjusting the conditioned medium to the low binding pH. Furthermore, the recovered fractions had a very low concentration and contained citrate, which made testing in cell culture challenging.

The recovery yield of the purification step was improved by increasing the binding pH to 5 and citrate was removed from the elution buffer. Additionally, the concentration of the recovered protein was increased by performing a two-step elution and by minimizing the number of collected fractions. The first elution step E1 was achieved by increasing the pH of the mobile phase to 10. The second elution step E2 followed and was achieved by increasing the NaCl concentration of the mobile phase to 1M. Using this method, two fractions with high protein content were recovered from each elution step in two different experiments and were tested on exponentially growing cells.

The fraction from elution E1 showed a variety of effects when compared to a negative control, which included the improvement of cell survival and prevention of cellular death and apoptosis, a significant increase of the maximal specific growth rate and final total cell density, and a general decrease of the glucose uptake rate without altering the glutamine uptake rate. Additionally, the fraction from elution E1 was associated with the induction of fast and sudden cellular death after glucose and glutamine depletion. Testing of the fraction from the second elution E2 was associated with a significant reduction of the specific growth rate, a moderate increase in the specific death rate and a significant reduction in the biomass to glucose yield after 24 hours of cultivation.

Testing of E2 was limited by the high NaCl concentration of the elution buffer, which when supplemented to growing cells in large quantities, might have negative effects due to the increase in

#### 4. RESULTS

---

osmolarity. For this reason and in order to decrease the amount of protein recovered, the elution step E2 was optimized in two experiments. Two stepwise salt gradient profiles were tested to separate E2 into different fractions, which were then tested on exponentially growing cells. The conditioned medium components responsible for the effects previously established were recovered from the membrane adsorber at a NaCl concentration of 0.05 M.

### 4.3 Hydrophobic Interaction Chromatography and Evaluation of Fractions

#### 4.3.1 Screening for Optimal Conditions

Figure 52 shows the protein recovered in the fractions of the CE9 experiment (see Chapter 3.3.2, Table 18) used to generate the E2 fraction that was used for the development of the HIC MA step. The collected fractions X1, X2, X3 and X4 contained  $27.2 \pm 0.73$ ,  $1.6 \pm 0.05$ ,  $5.6 \pm 0.02$  and  $0.7 \pm 0.03$  mg protein respectively, corresponding to  $41.5\% \pm 4.25\%$ ,  $2.4\% \pm 0.24\%$ ,  $8.5\% \pm 0.84\%$  and  $1.0\% \pm 0.11\%$  of the total protein loaded into the cation exchanger respectively. A total of  $35.0 \pm 0.73$  mg protein was recovered, resulting in a total recovery yield of  $53.4\% \pm 5.39\%$ . The fraction X3 from elution E2 was used for the screening experiments.

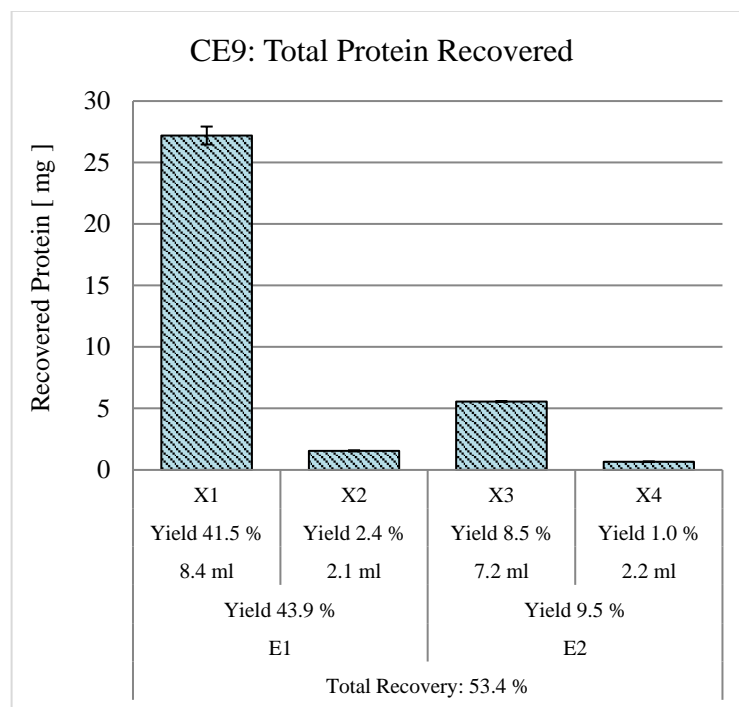


**Figure 52** Protein recovered in each fraction of the two-step elution CE9. Fraction X3 was used for the screening of optimal binding conditions for the Phenyl membrane. The error bars display the standard deviation of the three samples measured.

From the tested salts, only NaCl induced binding into the membrane adsorber as shown in Table 29. Adjustment of the load material by adding 2 and 3 M resulted in the recovery of  $7.4\% \pm 2.48$  and  $18.3\% \pm 3.89\%$  of the total protein loaded respectively. All the experiments, except for Exp 2.3, were loaded to 20% – 25% of the membrane binding capacity due to the scarce availability of the source material and the number of experiments. Because adding ammonium sulfate and sodium chloride



## 4. RESULTS

proved not to be effective, the corresponding 3 M experiments were not performed. The protein material was used in Exp 2.3 instead, allowing the membrane adsorber to be loaded at 75.4% of its dynamic binding capacity. Since only a fraction of the dynamic binding capacity of the membrane was utilized, it was not possible to determine from the results of the screening if the low recovery yield was a result of loss through precipitation, or because of either irreversible or insufficient binding into the membrane adsorber. It can be assumed that most of the protein was lost into the flow through because the recovery yield increased with increasing NaCl concentration and there was no significant formation of cloudiness besides a few small crystal-like white solid structures during adjustment.

**Table 29** Total protein loaded, percentage of membrane binding capacity used and total recovery yield for each experiment of the screening for optimal binding conditions

	Experiment	Protein Loaded	Percentage of Binding Capacity	Total Recovery Yield
		[ mg ]	[ % ]	[ % ]
Ammonium Sulfate	Exp 1.1	0.15	22.3%	0
	Exp 1.2	0.14	23.1%	0
Sodium Chloride	Exp 2.1	0.15	24.7%	0
	Exp 2.2	0.14	23.0%	7.4%
	Exp 2.3	0.45	75.4%	18.3%
Potassium Chloride	Exp 3.1	0.15	25.2%	0
	Exp 3.2	0.12	19.5%	0

Adding sodium chloride at a concentration of 3 M was chosen for the capture and recovery of the proteins of elution E2 into a Sartobind Phenyl membrane adsorber.

### 4.3.2 Testing of HIC Elution in cell Culture

#### Production of Elution E2 and Binding into the Phenyl Membrane

Figure 53 shows the protein recovered in the fractions of the cation exchanger CE10 experiment. Protein was recovered in fractions X2, X3 and X4, which contained  $8.1 \pm 1.84$ ,  $0.5 \pm 0.06$  and  $2.4 \pm 0.12$  mg protein respectively and corresponded to  $21.7\% \pm 5.03\%$ ,  $1.3\% \pm 0.18\%$  and  $6.3\% \pm 0.45\%$

## 4. RESULTS

of the total protein loaded. A total of  $10.9 \pm 1.84$  mg protein was recovered from the cation exchanger resulting a total recovery yield of  $29.3\% \pm 5.14\%$ . Half of the elution E2 fraction X4 was supplemented to growing cells to examine its effects, while the other half was captured into the HIC membrane adsorber.

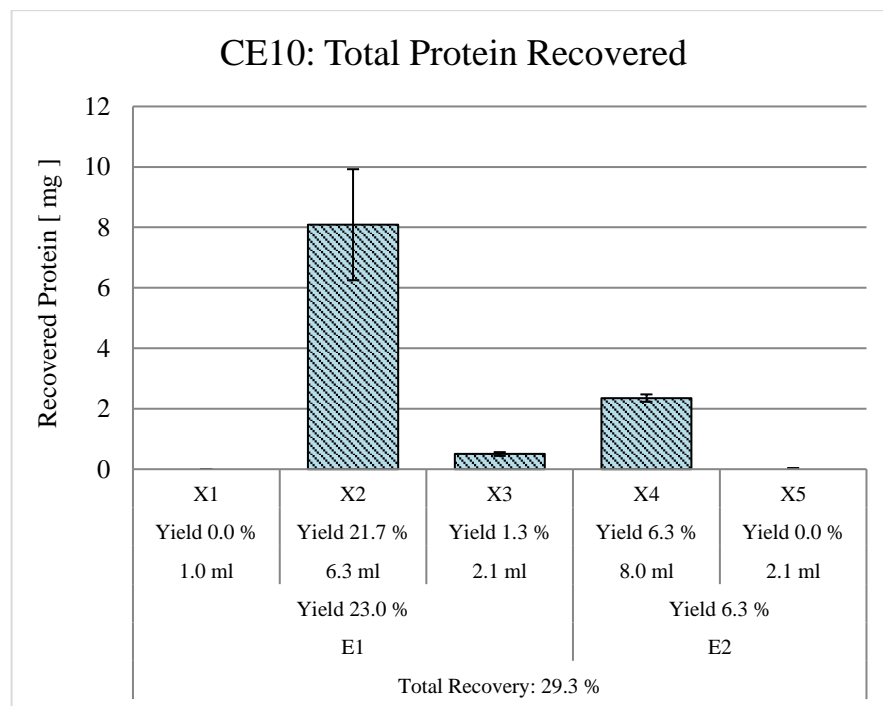


**Figure 53** Protein recovered in each fraction of the two-step elution CE10. Fraction X4 was used for binding into the Phenyl membrane under optimized conditions. The error bars display the standard deviation of the three samples measured.

Capture and recovery of the components of the elution E2 fraction X4 from the CE10 experiment into the Phenyl membrane adsorber was performed under the conditions chosen after the screening experiment. The protein solution was adjusted by adding 3 M NaCl and the membrane was loaded with  $0.9 \pm 0.05$  mg protein, which represented 142.0% of its dynamic binding capacity. (Table 30). A total of  $0.2 \pm 0.01$  mg protein was recovered in the collected fractions, representing a recovery yield of  $18.5\% \pm 2.00\%$ . The percentage of protein recovered was almost identical to the screening experiment at the same salt concentration, despite the considerable difference in protein loaded. This is a strong indication that at a NaCl concentration of 3 M the hydrophobic interaction of only 18% of the proteins in E2 is induced, resulting in binding into the membrane. The rest of the protein was either lost in the flow-through or through precipitation. This means that, without taking into consideration differences between batches and separations, 3.2 mg protein of E2 could be loaded into a single Sartobind Phenyl pico membrane capsule before the total membrane capacity of 0.6 mg would be reached. The bound components were recovered in fractions HE1, HE2 and HE3, which were then

## 4. RESULTS

pooled together (HE) resulting in an elution volume of 1.5 ml. This recovered elution HE contained only  $1.2\% \pm 0.15\%$  of the proteins found in the original conditioned medium used in experiment CE10.

**Table 30** Total protein loaded, percentage of dynamic membrane capacity used and total protein collected in the different fraction of the 3 M NaCl experiment. Fractions HE1, HE2 and HE3 were pooled together and tested on growing cells.

	Protein loaded	Percentage of Binding Capacity	Recovered Fractions			Total Recovery Yield
	[ mg ]	[ ml ]	PE	HE1 + HE2 + HE3	S1 + S2 + S3	[ % ]
3 M NaCl Experiment	0.9	142.0%	0	$0.2 \pm 0.01$	0	$18.5\% \pm 2.00\%$

### Examination of the Source Material

Figure 54 shows the specific growth rates ( $\mu$ ) calculated after 23 hours of cultivation for the experiment performed to examine the effect of the elution E2 fraction X4 (Table 19). The first pair of columns show the cultures inoculated at a low cell density. The corresponding column to the left shows the  $\mu$  of the culture to which the E2 fraction was given (LCD) while the one to the right corresponds to its negative control to which only BoC2 buffer was given (LCD NC30). The second, third and fourth pairs show the cultures inoculated at a medium cell density. The columns to the left correspond respectively to the cultures to which the E2 fraction X4 was given in conditioned medium (MCD CM) and in fresh medium (MCD FM), and the undisturbed culture (NC). The respective columns to the right all correspond to the medium cell density negative control to which only BoC2 buffer was given (NC30). The values were calculated as the average of the triplicate cultures and the error bars display the standard deviation.

Fraction X4 from elution E2 at a protein concentration of 0.009 mg/ml was associated with a reduction in the  $\mu$  of the cultures growing in conditioned medium during the first 23 hours of cultivation. The  $\mu$  of LCD and LCD NC30 was calculated at  $0.037 \pm 0.0019 \text{ h}^{-1}$  and  $0.041 \pm 0.0002 \text{ h}^{-1}$  respectively, resulting in a decrease of  $9\% \pm 4.6\%$  with a low significance of  $p < 0.1$  when compared with each other. The  $\mu$  of MCD CM and NC30 were calculated respectively at  $0.042 \pm 0.0030 \text{ h}^{-1}$  and  $0.047 \pm 0.0011 \text{ h}^{-1}$ , resulting in a reduction of  $11\% \pm 6.7\%$  with a low significance of  $p < 0.1$  when compared with each other.

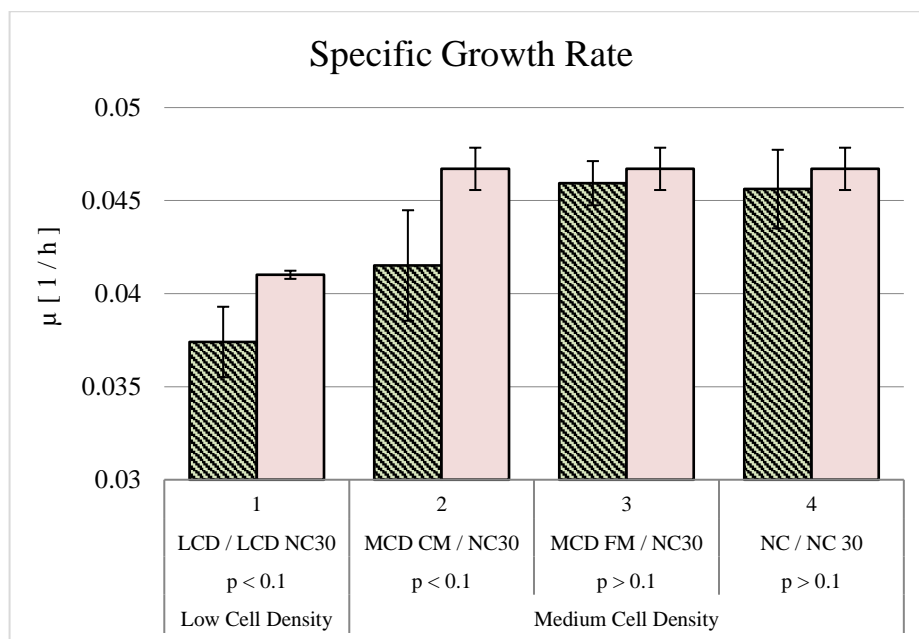


**Figure 54** Specific growth rates ( $\mu$ ) calculated after 23 hours of cultivation for the experiment performed to examine the effect of the elution E2 fraction X4. The values were calculated as the average of the triplicate cultures and the error bars display the standard deviation.

The specific growth rate of the cultures supplemented with the E2 fraction in conditioned medium experienced a similar reduction in  $\mu$ . Figure 55 compares the percentile decrease in  $\mu$  between LCD and LCD N30, and MCD CM and NC30 and shows no significant differences. This indicates that the  $N_t$  at the time of inoculation did not significantly influence the effect of the E2 fraction. On the other hand, supplementation in fresh medium (MCD FM) showed a weakened effect compared to conditioned medium: The  $\mu$  of MCD FM was calculated at  $0.046 \pm 0.0012 \text{ h}^{-1}$ , which was not significantly different from the corresponding negative control NC30 ( $p > 0.1$ ), but was  $10\% \pm 7.9\%$  higher than MCD CM with a low significance value of  $p = 0.12$ .

The undisturbed culture (NC) proliferated with a  $\mu$  of  $0.046 \pm 0.0021 \text{ h}^{-1}$ , showing that 3.1% of buffer BoC2 did not significantly affect the growth of the cells ( $p > 0.1$ ) during the first 23 hours of cultivation. Furthermore, there was a significant difference ( $p < 0.05$ ) of  $12\% \pm 2.2\%$  in  $\mu$  between both negative controls, LCD NC30 and NC30, which is consistent with the observations that inoculating at a low cell density results in the reduction of the specific growth rate within the first 24 hours of cultivation.

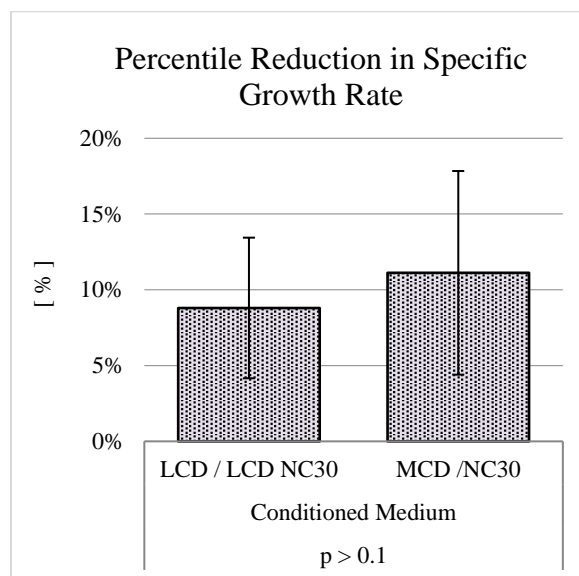


**Figure 55** Percentile decrease in  $\mu$  between LCD and LCD N30, and MCD CM and NC30.

Figure 56 shows the specific death rates ( $k_d$ ) of the different cultures calculated after 23 hours of cultivation, presented analogously to the specific growth rates. The left columns of the first, second, third and fourth pair of columns correspond respectively to the LCD, MCD CM, MCD FM and NC cultures. The left column of the first pair correspond to the LCD NC30 culture, while the left column of the second, third and fourth pairs correspond all to NC30. The LCD and LCD NC30 cultures had a  $k_d$  of  $0.002 \pm 0.0002 \text{ h}^{-1}$  and  $0.002 \pm 0.0007 \text{ h}^{-1}$  respectively. The medium cell density cultures MCD CM and MCD FM, and their negative control NC30 showed a specific death rate of  $0.002 \pm 0.0009 \text{ h}^{-1}$ ,  $0.004 \pm 0.0005 \text{ h}^{-1}$  and  $0.004 \pm 0.0007 \text{ h}^{-1}$  respectively.

There are no strong indications that the fraction from elution E2 had an effect on the  $k_d$  of CHO-K1. None of the supplemented cultures (LCD, MCD CM and MCD FM) showed any significant differences when compared to their corresponding negative controls (LCD NC 30 and NC30), despite the fact that there was a  $39\% \pm 24.7\%$  difference between MCD CM and NC30 with a low significance value ( $p = 1.2$ ). Additionally, supplementation with BoC2 buffer was associated with a significant ( $p > 0.05$ ) increase of  $66\% \pm 10.4\%$  in  $k_d$  when compared to the undisturbed culture (NC).

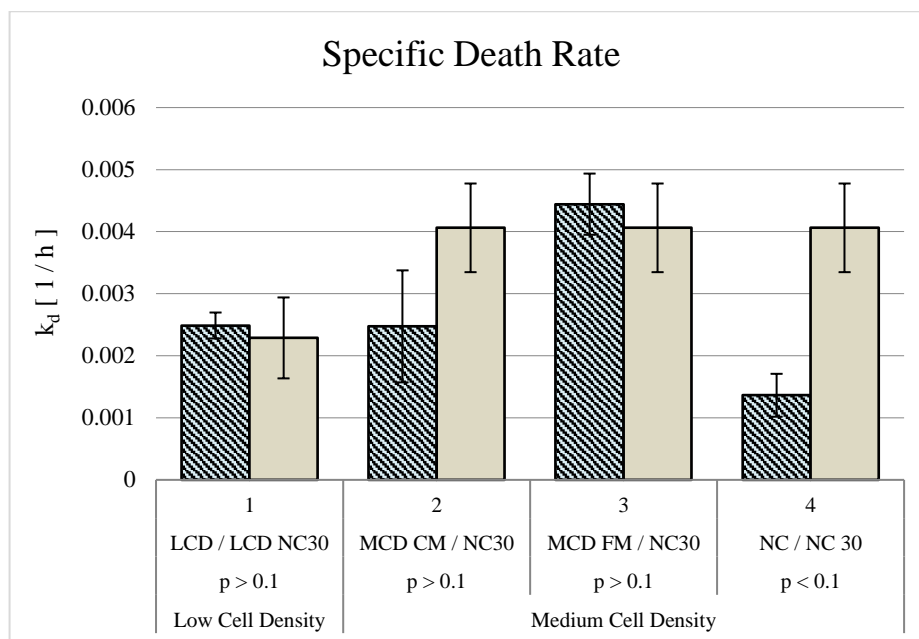


**Figure 56** Specific death rates ( $k_d$ ) calculated after 23 hours of cultivation for the experiment performed to examine the effect of the elution E2 fraction X4. The values were calculated as the average of the triplicate cultures and the error bars display the standard deviation.

The  $k_d$  of MCD FM was higher than MCD CM by a difference of  $44\% \pm 21\%$  with a low significance of  $p < 0.1$ . Furthermore, the  $k_d$  of NC30 was higher than LCD NC30 by a significant ( $p > 0.01$ ) difference of  $44\% \pm 18.9\%$ . These differences are indication that the presence of condition medium and the cell density were the factors significantly affecting the specific death rate of the cells rather than the supplementation of elution E2.2

The results presented are consistent with the previous examinations of elution E2 on growing cells and show that supplementation of the elution E2 fraction to exponentially growing cells is associated with a reduction of the specific growth rate during the first 23 hours of cultivation without significantly affecting the specific death rate. This effect seems to be magnified by the presence of conditioned medium and does not seem to be influenced by the cell density.

#### Testing of HIC Elution in Cell Culture

Figure 57 shows the specific growth rates ( $\mu$ ) calculated differentially after 21 and 46 cultivation hours for the experiment described in Table 22. Each time differential shows four different columns, the first and second one corresponding respectively to the cultures to which either the HIC elution HE (HE) or phosphate elution buffer HB without protein (Phos NC) were supplemented. The third and fourth columns correspond to the cultures inoculated at a low cell density in either conditioned (CM) or fresh

## 4. RESULTS

medium (FM) respectively without supplementation of protein or phosphate buffer. Comparison between the cultures is performed first between HE and its negative control Phos NC to determine the effects associated with the supplementation of the HIC elution HE. Then Phos NC is compared to the undisturbed culture inoculated in conditioned medium to determine the effects associated with the phosphate elution buffer. Finally comparison between both non-supplemented and undisturbed cultures is performed to assess the effect of conditioned and fresh medium.

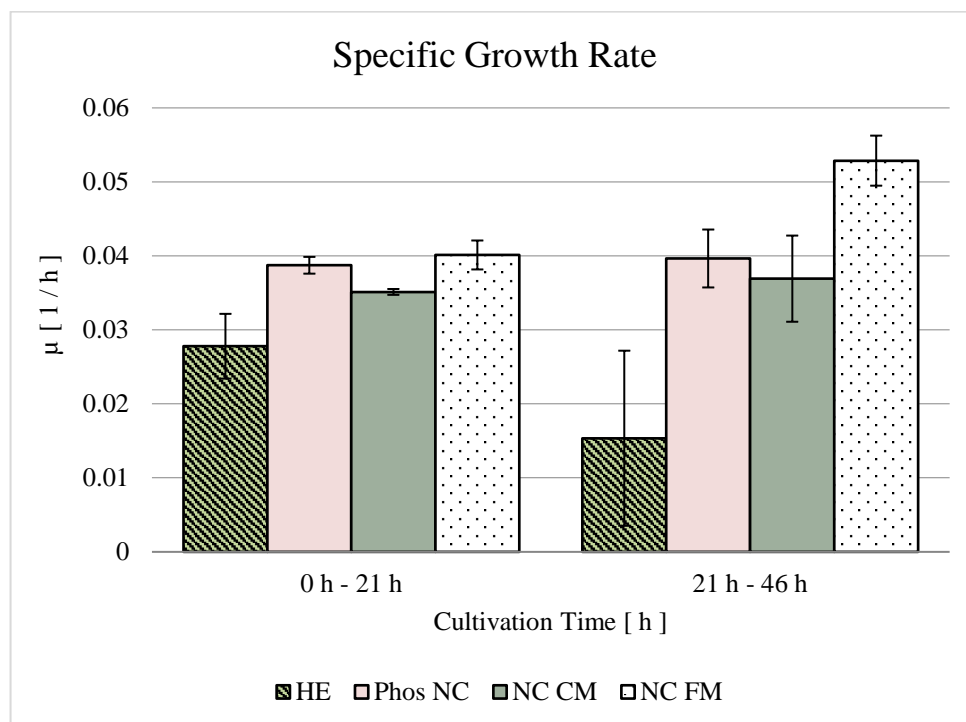


**Figure 57** Specific growth rate ( $\mu$ ) of the cultures supplemented with either the HIC elution (HE) or phosphate buffer (Phos NC) and cultivated in either conditioned (NC CM) or fresh (NC FM) medium. The values correspond to the average of the triplicate cultures and the error bars display the standard deviation.

Supplementation of exponentially growing cells with elution HE in conditioned medium to a final protein concentration of 0.007 mg/ml was associated with a reduction in  $\mu$  during the first 46 cultivation hours. These results were analogous to the effect of the source material indicating that the designed HIC purification step was successful in recovering the bioactive molecules responsible for the original effect.

The  $\mu$  of the supplemented culture (HE) and its negative control (Phos NC) were calculated at  $0.028 \pm 0.0036 \text{ h}^{-1}$  and  $0.039 \pm 0.0009 \text{ h}^{-1}$  respectively during the first 21 cultivation hours, resulting in a significant reduction ( $p < 0.05$ ) of  $28\% \pm 9.4\%$  when compared with each other. Between 21 and 46 cultivation hours the  $\mu$  were calculated at  $0.015 \pm 0.0097 \text{ h}^{-1}$  and  $0.040 \pm 0.0032 \text{ h}^{-1}$  for HE and Phos

## 4. RESULTS

---

NC respectively, resulting in a significant ( $p < 0.05$ ) difference of  $61\% \pm 24.6\%$  when compared with each other and an almost double increase in the size of the reduction.

Supplementation of the cultures with the phosphate buffer used for the HIC purification to a final concentration of 0.7 mM was associated with a small increase in  $\mu$  during the first 21 cultivation of cultivation, which then levels out within the next 24 hours. During the first 21 cultivation hours the  $\mu$  of the non-supplemented negative control cultures inoculated in conditioned (NC CM) and in fresh medium (FM) were calculated at  $0.035 \pm 0.0003 \text{ h}^{-1}$  and  $0.040 \pm 0.0016 \text{ h}^{-1}$  respectively, resulting in a significant ( $p < 0.05$ ) difference of  $12\% \pm 3.6\%$  when compared with each other and  $10\% \pm 2.8\%$  between NC CM and Phos NC. Between 21 and 46 cultivation hours NC CM and NC FM show a  $\mu$  calculated at  $0.037 \pm 0.0048 \text{ h}^{-1}$  and  $0.053 \pm 0.0028 \text{ h}^{-1}$  respectively. During this time interval the  $\mu$  of NC CM was a significantly lower ( $p < 0.05$ ) than the culture inoculated in fresh medium (NC FM) by  $30\% \pm 9.7\%$ , while there was no significant difference to the  $\mu$  of Phos NC.

Figure 58 compares the reduction in  $\mu$  of the low cell density cultures supplemented with either the source material (first column,  $9\% \pm 4.6\%$ ) or the HIC elution HE (second column,  $28\% \pm 9.4\%$ ) in conditioned medium calculated after 23 and 21 cultivation hours respectively. The magnitude of the effect associated with fraction X4 of elution E2 is significantly lower ( $p < 0.05$ ) by  $69\% \pm 19.4\%$  compared to elution HE. Considering that X4 and HE were supplemented to a final protein concentration of 0.009 and 0.007 mg/ml respectively, and that HE corresponds to only 18.8% (3 M NaCl recovery yield) of the proteins in the E2 fraction, the final protein concentration of the culture supplemented with the E2 fraction can be corrected to an effective concentration of 0.002 mg/ml. This is 76% lower than the protein concentration in the culture supplemented with HE and corresponds to the difference in percentile reduction of  $\mu$  between the E2 fraction and HE ( $69\% \pm 19.4\%$ ).



## 4. RESULTS

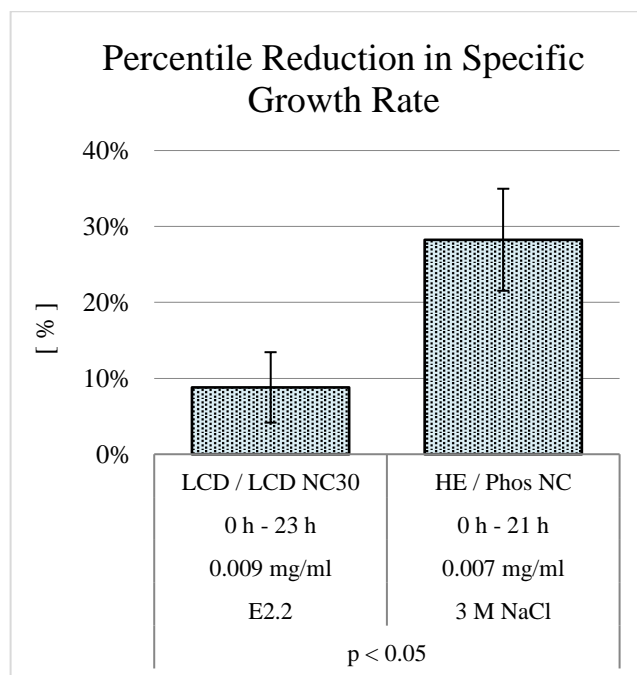


**Figure 58** Percentile reduction determined after supplementation of the fraction X4 from elution E2 (left column) and the HIC elution HE (right column).

Figure 59 shows the specific death rates ( $k_d$ ) calculated differentially after 21 and 46 hours of cultivation and are presented analogously to the specific growth rates. During the time interval, between 0 and 21 cultivation hours, the  $k_d$  of the cultures were calculated at  $0.000 \pm 0.0002 \text{ h}^{-1}$ ,  $0.002 \pm 0.0011 \text{ h}^{-1}$ ,  $0.002 \pm 0.0015 \text{ h}^{-1}$  and  $0.001 \pm 0.0008 \text{ h}^{-1}$  respectively for HE, Phos NC, NC CM and NC FM. Between 21 and 46 hours the  $k_d$  of the cultures were calculated at  $0.001 \pm 0.0007 \text{ h}^{-1}$ ,  $0.002 \pm 0.0002 \text{ h}^{-1}$ ,  $0.002 \pm 0.0011 \text{ h}^{-1}$  and  $0.005 \pm 0.0003 \text{ h}^{-1}$  respectively for HE, Phos NC, NC CM and NC FM.

The specific death rate of the culture supplemented with elution HE was significantly lower ( $p < 0.05$ ) than its negative control Phos NC during the first 21 cultivation hours. The difference between both cultures was  $93\% \pm 10.9\%$  and leveled out during the next 25 cultivation hours. The miniscule death rate calculated for HE during was the result of an increase in the viability from  $94.6\% \pm 0.73\%$  to  $96.7\% \pm 0.31\%$  ( $p < 0.1$ ). The  $k_d$  of Phos NC and NC CM did not significantly differ from each other and remained almost unchanged during the time course of the experiment, showing that supplementation with phosphate buffer did not have a significant effect on the  $k_d$  of the cells. On the other hand, inoculation in fresh medium was associated with a substantial increase in  $k_d$ , showing a significant ( $p < 0.05$ ) difference of  $51\% \pm 23.1\%$  compared to the culture inoculated in only conditioned medium (NC CM) between 21 and 46 cultivation hours.

## 4. RESULTS

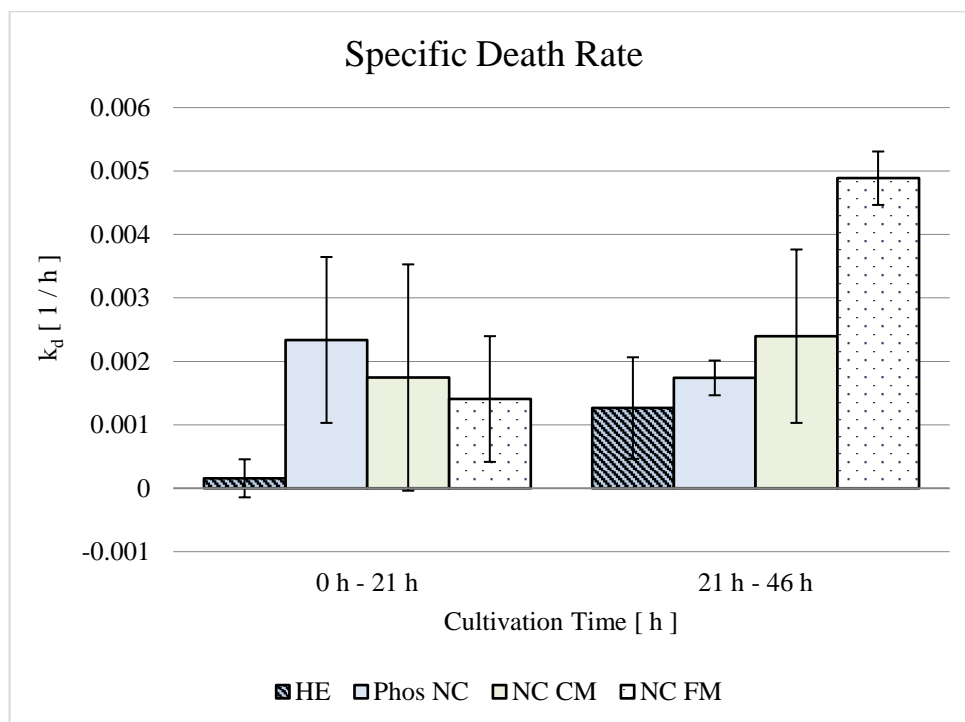


**Figure 59** Specific death rate ( $k_d$ ) of the cultures supplemented with either the HIC elution (HE) or phosphate buffer (Phos NC) and cultivated in either conditioned (NC CM) or fresh (NC FM) medium. The values correspond to the average of the triplicate cultures and the error bars display the standard deviation.

Figure 60 shows the yields ( $Y_{x/s, \text{Glc}}$ ) of viable cell density ( $N_v$ ) to glucose concentration ( $c_{\text{Glc}}$ ) calculated cumulative between 0 and 21 cultivation hours and between 0 and 46 hours. Each time interval shows four columns, corresponding respectively from left to right to the culture supplemented with elution HE (HE), its negative control supplemented with phosphate buffer (Phos NC), the negative control cultivated in conditioned medium (NC CM) and the negative control cultivated in only fresh medium (NC FM).

The  $Y_{x/s, \text{Glc}}$  determined during the first 21 cultivation hours for the HE, Phos NC and NC CM were calculated at  $0.23 \pm 0.049 \times 10^6$ ,  $0.27 \pm 0.060 \times 10^6$  and  $0.23 \pm 0.064 \times 10^6$  cells per  $\mu\text{mol}$  glucose respectively, showing no significant difference between each other. The yield of the negative control cultivated in fresh medium (NC FM) was calculated at  $0.14 \pm 0.027 \times 10^6$  cells per  $\mu\text{mol}$  glucose, which was  $65\% \pm 55.3\%$  lower than NC CM with a very low significance value of  $p = 0.14$ .

The cumulative  $Y_{x/s, \text{Glc}}$  determined between 0 and 46 cultivation hours for the cultures HE and Phos NC were calculated at  $0.14 \pm 0.060 \times 10^6$  and  $0.39 \pm 0.052 \times 10^6$  cells per  $\mu\text{mol}$  glucose respectively, resulting in a significant ( $p < 0.05$ ) difference of  $64\% \pm 16.0\%$  when compared with each other. The yield of NC CM was calculated at  $0.33 \pm 0.042 \times 10^6$  cells per  $\mu\text{mol}$  glucose and was not significantly

## 4. RESULTS

different from Phos NC. Finally, the yield of NC FM was calculated at  $0.19 \pm 0.014 \times 10^6$  cells per  $\mu\text{mol}$  glucose, which was significantly ( $p < 0.05$ ) lower than NC CM by  $68\% \pm 25.0\%$ .

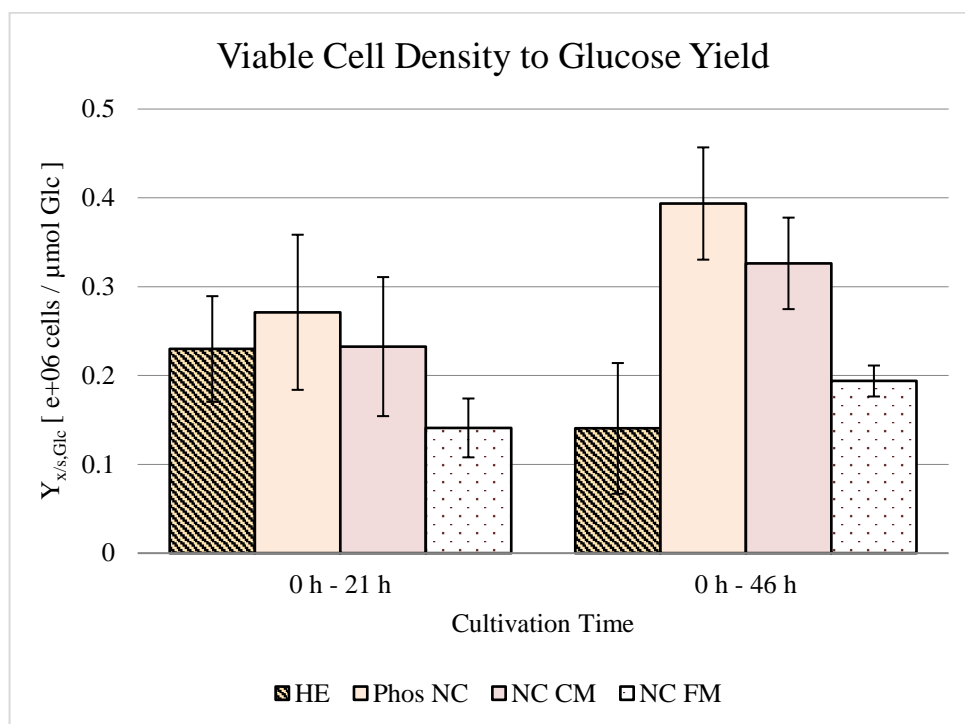


**Figure 60** Viable cell density ( $N_v$ ) to glucose yield ( $Y_{x/s, \text{Glc}}$ ) of the cultures supplemented with either the HIC elution (HE) or phosphate buffer (Phos NC) and cultivated in either conditioned (NC CM) or fresh (NC FM) medium. The values correspond to the average of the triplicate cultures and the error bars display the standard deviation.

The  $Y_{x/s, \text{Glc}}$  of the negative controls, Phos NC, NC CM and FM NC, calculated between 0 and 46 cultivation hours showed an increase in a similar magnitude when compared to the yields calculated between 0 and 21 cultivation hours. This contrasts with the yield calculated for the culture supplemented with elution HE, which showed a delayed net decrease as the cultivation progressed (Figure 61).

## 4. RESULTS

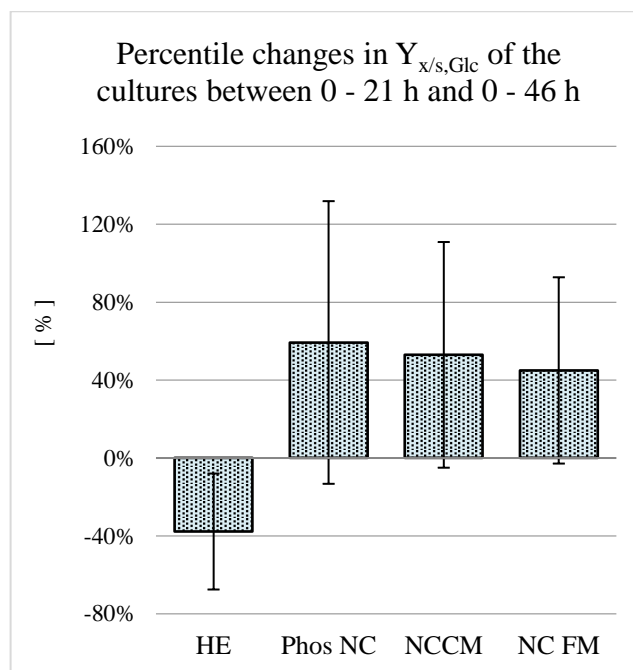


**Figure 61** Percentile change in  $Y_{x/s,Glc}$  of the cultures between 0 - 21 and 0 - 46 cultivation hours.

Figure 62 shows the yields ( $Y_{x/s,Gln}$ ) of viable cell density ( $N_v$ ) to glutamine concentration ( $c_{Gln}$ ) calculated cumulative between 0 and 21 cultivation hours and between 0 and 46 cultivation hours. Analogously to  $Y_{x/s,Glc}$ , each time interval shows four columns, corresponding respectively from left to right to the culture supplemented with elution HE (HE), its negative control supplemented with phosphate buffer (Phos NC), the negative control cultivated in conditioned medium (NC CM) and the negative control cultivated in only fresh medium (NC FM).

During the first 21 cultivation hours the  $Y_{x/s,Gln}$  of cultures HE and Phos NC, were calculated at  $1.1 \pm 0.15$  and  $1.6 \pm 0.06 \times 10^6$  cells per  $\mu\text{mol}$  glutamine respectively, resulting in a significant ( $p < 0.05$ ) difference of  $27\% \pm 10.1\%$  between each other. This difference increased to  $58\% \pm 19.2\%$  in the cumulative time interval between 0 and 46 cultivation hours, with yields that were calculated at  $0.9 \pm 0.38$  and  $2.0 \pm 0.18 \times 10^6$  cells per  $\mu\text{mol}$  glucose for HE and Phos NC respectively.

The glutamine yields of NC CM were calculated at  $1.6 \pm 0.06$  and  $2.0 \pm 0.18 \times 10^6$  cells per  $\mu\text{mol}$  glutamine respectively for the first and the second time intervals. They were not significantly different from Phos NC, showing that supplementation with phosphate buffer had no effect on the glutamine consumption of the cells.

The  $Y_{x/s,Gln}$  calculated for the NC FM were consistently lower than the yields of its counterpart cultivated in conditioned medium (NC CM). Between 0 and 21 hours, the yield of NC FM was

## 4. RESULTS

calculated at  $0.7 \pm 0.06 \times 10^6$  cells per  $\mu\text{mol}$  glutamine, resulting in a significant ( $p < 0.05$ ) of  $122\% \pm 33.5\%$  compared to NC CM. Between 0 and 46 hours, the yield was calculated at  $1.0 \pm 0.04 \times 10^6$  cells per  $\mu\text{mol}$  glutamine, resulting in a significant ( $p < 0.05$ ) difference of  $83\% \pm 28.6\%$ .

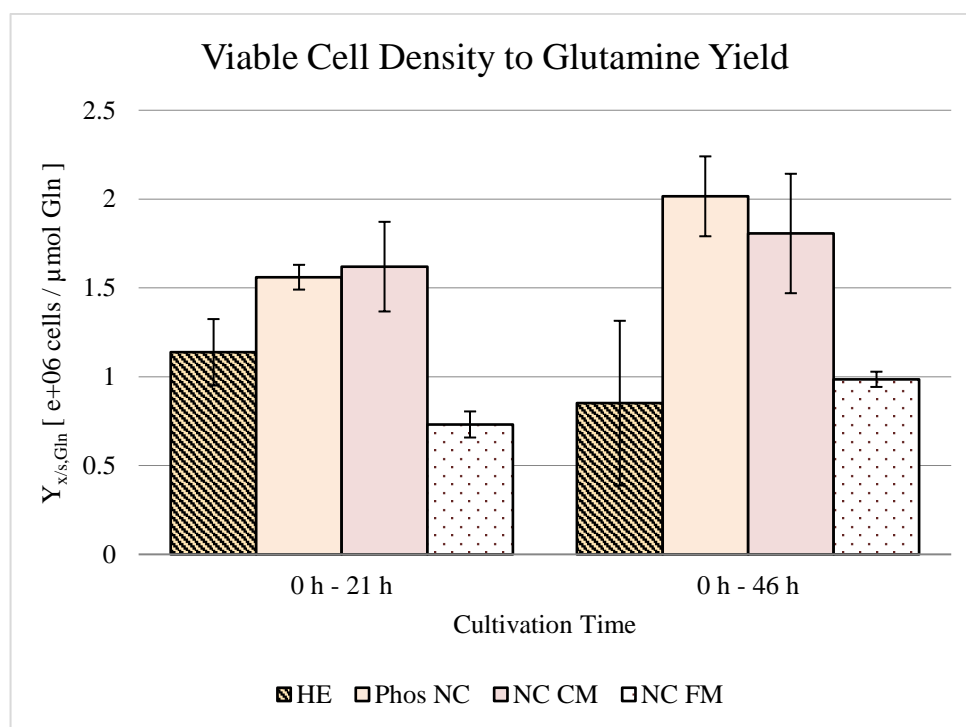


**Figure 62** Viable cell density ( $N_v$ ) to glutamine yield ( $Y_{x/s,\text{Gln}}$ ) of the cultures supplemented with either the HIC elution (HE) or phosphate buffer (Phos NC) and cultivated in either conditioned (NC CM) or fresh (NC FM) medium. The values correspond to the average of the triplicate cultures and the error bars display the standard deviation.

Similar to the glucose yields, however in lesser magnitude, the glutamine yields calculated for the negative controls showed an increase during the time interval between 0 and 46 cultivation hours compared to 0 and 21 cultivation hours. Furthermore, the yield of culture HE, which was consistently lower than its negative control Phos NC, showed a net decrease as the cultivation progressed (Figure 63).

## 4. RESULTS

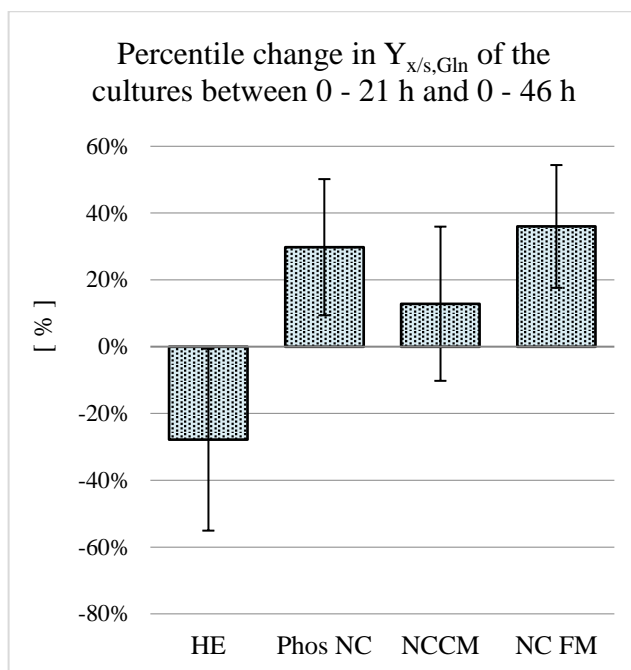


**Figure 63** Percentile change in  $Y_{x/s,Gln}$  of the cultures between 0 - 21 and 0 - 46 cultivation hours.

Figure 64 shows the yields of lactate produced to glucose consumed ( $Y_{p/s}$ ) calculated cumulative between 0 and 46 cultivation hours. They represent, respectively from left to right, the culture supplemented with elution HE (HE), its negative control supplemented with phosphate buffer (Phos NC), the negative control inoculated in conditioned medium (NC CM) and the negative control cultivated in fresh medium (NC FM).

The  $Y_{p/s}$  of the HE and Phos NC cultures were calculated at  $2.0 \pm 0.26$  and  $2.2 \pm 0.07$   $\mu\text{mol}$  lactate per  $\mu\text{mol}$  glucose and did not show a significant ( $p > 0.1$ ) difference compared to each other. The yield of the NC CM culture was calculated at  $2.1 \pm 0.06$   $\mu\text{mol}$  lactate per  $\mu\text{mol}$  glucose, and was lower than the Phos NC by a difference of  $7\% \pm 4.6\%$  with a low significant of  $p < 0.1$ , which indicates a minor effect of the phosphate buffer on the production of lactate. Finally, the yield of the NC FM culture did not show a significant difference to its counterpart NC CM, and was calculated at  $1.9 \pm 0.12$   $\mu\text{mol}$  lactate per  $\mu\text{mol}$  glucose.

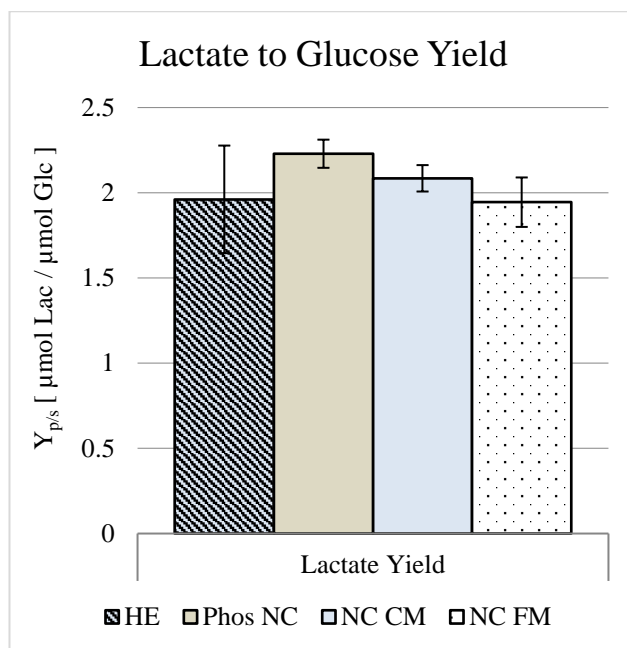


**Figure 64** Lactate to glucose yield ( $Y_{p/s}$ ) of the cultures supplemented with either the HIC elution (HE) or phosphate buffer (Phos NC) and cultivated in either conditioned (NC CM) or fresh (NC FM) medium. The values correspond to the average of the triplicate cultures and the error bars display the standard deviation.

These results show a correlation between the supplementation of elution HE to exponentially growing cells in conditioned medium harvested in the exponential phase of growth with a reduction in  $Y_{x/s, \text{Glc}}$  and  $Y_{x/s, \text{Gln}}$ , which translates to a higher consumption of the main substrates, glucose and glutamine, per cell. Interestingly, a similar increase in glucose and glutamine consumption was calculated for the culture inoculated in fresh medium (NC FM), which yields were consistently lower than its counterpart inoculated in conditioned medium (NC CM) throughout the cultivation. Nevertheless, this higher substrate consumption per cell can be attributed to the higher glucose and glutamine concentrations of the fresh medium. Supplementation of the cell culture with phosphate buffer used for the HIC purification process did not significantly affect the substrate consumption of the cells.

### 4.3.3 Concluding Remarks

This chapter presents the development of a hydrophobic interaction chromatography (HIC) membrane adsorption step for the orthogonal purification of the bioactive components of the elution E2 introduced in the previous chapter. The development consisted in the examination of ammonium sulfate, sodium chloride and potassium chloride at different concentrations to determine the optimal binding conditions.

Two bioreactor batch cultivations were performed for the generation of the conditioned medium used in the two two-step-elution experiments completed for the production of the two fractions from elution E2 that were used in the experiments. The fractions were recovered at 1 M NaCl. One fraction was used for screening the optimal binding conditions. Half of the other fraction was first tested on exponentially growing cells to verify its effect. Testing was performed in conditioned medium at a low and a medium cell density and in fresh medium at a medium cell density. The rest of the fraction was loaded into the HIC membrane under the optimal binding conditions and the bound components were recovered in a one-step elution using low conductivity phosphate buffer at pH 7.

From the three salts tested, only NaCl offered sufficient binding with a maximal recovery yield of 18% at 3 M NaCl. Testing of the E2 fraction confirmed the previously established decrease in specific growth rate without significant influence on the specific death rate. It was also shown that the presence of conditioned medium magnified the effect of the elution E2 and that it had a comparable magnitude in low and medium cell density in the presence of conditioned medium. The growth inhibitory effects associated with elution E2 were furtherly confirmed in the HIC elution. Moreover, there was a decrease in specific death rate during the first 24 hours that leveled out during the next 24 hours of cultivation. A 24 hour delayed reduction in the biomass to glucose and biomass to glutamine yields were also determined. The lactate to glucose yield on the other hand remained unchanged. Additionally, the increase in specific death rate in the absence of conditioned medium at around  $10^6$  cells/ml was observed again in these experiments.

The developed two-membrane process was successful in capturing, recovering and concentrating bioactive components responsible for a decrease in the specific growth rate and biomass to substrate yields from the conditioned medium of CHO-K1 cell culture. The process was able to narrow down the effect to only 1.2% of the total protein found in the original conditioned medium.



## 5 Discussion

### Capture and Fractionation of the Conditioned Medium Components

Binding of proteins into a cation exchanger requires the net charge of the proteins to be positively charged. This is achieved by diluting the loading material with cation exchanger compatible buffer and adjusting the pH value low enough to enable binding. Furthermore, the binding capacity is maximized by loading at low to moderate conductivities. Physicochemical characterization and 2-D gels of the proteins found in the supernatant of CHO-K1 have demonstrated a clear distribution towards the acidic species and low to mid molecular weights (<75 kDa) (Jin et al. 2010; Wimmer et al. 1994; Yuk et al. 2015). Despite the logical expectation that adjusting the conditioned medium to a lower pH would increase binding, thus increasing protein recovery after elution, yield of elution fraction E1 at pH 3 was lower compared to binding at pH 5. Mixing the conditioned medium with binding buffer A at pH 3 resulted in the formation of a significant amount of precipitates. This manifested in a major increase in turbidity and the quick fouling of the PES membranes used to filter the adjusted material prior to loading. Furthermore, proteins recovered after binding at pH 3, eluted at the higher pH steps, showing a tendency towards the more basic protein species. When this is compared with the 2-D-gel analysis performed by Jin et al. (2010) there is a strong indication that acidic protein species are lost through precipitation at pH 3. Recovery after binding at pH 5 was higher as less proteins were lost during the adjustment.

Separation of the secretome of CHO-K1 into different protein fractions was successfully achieved using the two-buffer system described in Ahamed et al. (2008). The system is composed of a low and a high pH buffer, both having the same composition: 20 mM citrate ( $pK_a$  1.13, 4.76, 6.3), 20 mM phosphate ( $pK_a$  7.2), 20 mM Bicine ( $pK_a$  8.26), and 20 mM CHES ( $pK_a$  9.5). Because of the evenly distributed  $pK_a$  values of the buffer species, increasing the volumetric ratio of the high to the low pH buffer resulted in the linear increase of the pH of the mixture. Elution using linear pH gradient, combined with a conventional salt gradient elution, offers a good method of separating the highly complex and diverse secretome of CHO-K1.

Because no FLPC system was used and in order to minimize operation complexity, a stepwise linear increase of the pH was used instead of a linear gradient. The highly linear correlation between the pH of the pre-mixed elution buffers to their corresponding amount of buffer B, showed that the buffer system of Ahamed et al. (2008) can be used to generate buffers with a predictable pH value. The

conductivity of the elution buffers also showed a highly linear relationship to increasing buffer B. This increase was a consequence of the higher conductivity of buffer B resulting from adding 1 M NaOH to titrate to pH 10. There was a slight decrease in linearity for both, pH and conductivity, in the collected fractions that contained the recovered proteins. This can be an indication of shifts caused by the proteins themselves. Furthermore, the pH and conductivity values were generally lower than the pre-mixed steps due to back-mixing of the elution buffer pushed through the membrane with the volume from the previous buffer still held in the membrane chamber.

Protein recovery was very low, possibly because most of the proteins was lost through precipitation at the low loading pH. Nevertheless, SDS-Page of the recovered fractions showed numerous protein bands spread along the whole size range. Most of these bands were distributed across several of the gel lanes, indicating that proteins of the same size eluted at different pH values. Protein bands found in only one lane were rather uncommon. Different isoforms, glycosylation patterns and posttranslational modifications might have an effect on the *pI* of proteins without changing their molecular weight, causing them to elute at different pH values. Fractions were given to growing cells (results not shown), but no effect could be identified. Testing of these fractions had two strong limitations, one being the low protein recovery, and the second one the presence of citrate in the eluted fractions, which may have a strong negative effect on the growth of CHO cells (Bai et al. 2011). Despite very low protein recovery, binding at pH 3 followed by the elution with a linear pH increase showed that the proteins in the conditioned medium of CHO-K1, which are present in very low concentrations, can be captured, recovered and fractionated.

In order to be able to obtain a measurable effect on growing cells, the recovery yield had to be improved and the protein concentration of the fractions had to be significantly increased. This first was accomplished by adjusting the conditioned medium to pH 5 instead of pH 3 before loading, thus reducing protein loss by precipitation. Protein concentration of the fractions was increased by performing a two-step isocratic elution instead of generating multiple fractions. Protein concentration could also be increased by loading more conditioned medium into the membrane using its full binding capacity, even though the effect of overloading on the recovery of the bioactive molecules has to be examined in detail. Brown et al. (2010) argued that overloading ion-exchanger membrane adsorbers could be used to remove HCP from monoclonal antibodies (mAbs) feedstocks in conditions in which both the product and impurities bind. Once the membrane is overloaded, better-binding impurities displace the bound product from the active sites, and elutes with a high purity into the flow through. A similar mechanism would be possible in the context of this work and should be taken into

consideration due to the highly complex nature of the secretome: bioactive proteins could be displaced by better binding HCP and lost into the flow through if the membrane adsorber is overloaded.

Citrate was removed from the elution buffers (BoC1 and BoC2) because of its strong effect on CHO-K1 cells and from the buffer used for the wash step (AoC) between loading and the first elution to avoid carry-over effect. Nonetheless, the rest of the buffer species was left (phosphate: pKa 7.2, Bicine: pKa 8.26, and CHES: pKa 9.5), still allowing the possibility of a fractionation using a pH gradient in the range of pH 6 - 10 in case a biological effect was identified in elution E1. Eventually, acetate (pKa 4.76) could also be used to substitute citrate, since it has a buffer capacity in the range of 3.6 - 5.6. The linearity of the pH gradient, and if and at which concentrations it would have an effect on CHO-K1 should be first assessed.

The two elutions E1 and E2 were recovered from the membrane at rather extreme pH and salt conditions (E1: pH 10; E2: pH 10 and 1M NaCl). In order to decrease protein degradation after elution, the recovered proteins were mixed straight away approx. 1:1 with fresh CHOMACS CD growth medium. This was done in order to stabilize the pH value and/or salt concentration to a more neutral region. The elutions were then frozen at -20° C and stored until they were used again. Due to the labor intensity and time required for the whole recovery and fractionation process, it was not possible to test the elutions immediately after they were recovered. Protein degradation during freezing and thawing and loss of biological effects was not examined in detail. Nevertheless, indications of negative effects were observed. Table 31 compiles the accumulated recovery yields of elutions E1 and E2, total recovery yield, the volume of the membrane and whether protein quantification was performed the same day of the separation and prior to freezing and storing for every cation exchanger experiment performed.

The experiments TE1, TE3 and CE9 all showed a higher protein recover, especially for elution E1. Each experiment was performed identically and the conditioned medium used was generated under exact same conditions. The only difference that can be accounted for, is that protein quantification through Bradford of TE2, E2.EXP1, E2.EXP2 and CE10 were performed one day after the capture and recovery and after the samples had been stored frozen overnight at -20° C. The protein concentrations of TE1, TE3 and CE9 were determined immediately after the proteins were recovered from the membrane. Furthermore, when the stored elutions were thawed at room temperature prior to testing on growing cells or to determine protein concentration, a white precipitate was consistently observed. This precipitate disappeared when the elutions were vortexed thoroughly. Without thorough examination and extensive proteomic analysis of the elutions and conditioned medium prior and

subsequent to freezing and thawing, it is impossible to know which proteins and to what extent they are destroyed or lost.

**Table 31** *Compilation of the accumulated recovery yields of elutions E1 and E2, total recovery yield, the volume of the membrane and whether protein quantification was performed prior to freezing and storing for every cation exchanger experiment performed.*

Experiment		TE1	TE2	TE3	E2.EXP1	E2.EXP2	CE9	CE10
E1 Yield	[ % ]	40.7	25.7	43.0	21.1	13.5	43.9	23.04
E2 Yield	[ % ]	6.0	14.9	11.9	4.9	12.0	9.5	6.3
Total Yield	[ % ]	46.7	40.7	54.9	26.0	25.4	53.4	29.3
Membrane volume	[ ml ]	0.08	2.8	2.1	2.1	2.8	2.1	2.1
Bradford performed same day?		yes	no	yes	no	no	yes	no

### First Elution E1

The effects of the conditioned medium components recovered from the cation exchanger in the first elution step E1 included an increase in the maximal specific growth rate and the increase of the survival capabilities of the cells by reducing apoptosis and increasing cell viability. Nonetheless, there was no effect on the initial lagging and the maximal specific growth rate was measured 24 hours after inoculation. An increase in cell survival and stimulation of proliferation are effects that have been widely documented in the literature for insulin-like growth factor – I (IGF-I). It has been documented that CHO-K1 cells are capable of producing a native form of this growth factor and that its expression is affected by medium composition and substrate and metabolite concentrations (Mohamed et al. 2011; Mohmad-Saberi et al. 2013). Because of the similarities of the effects presented in this work with those of IGF-I in the literature, and because CHOMACS CD growth medium did not contain supplemented IGF-I or any other growth factors or proteins, it seems likely that the process designed to capture the secretome of CHO-K1 was successful in recovering a native and bioactive form IGF-I produced by the cells during their cultivation. This represents a major advantage and opens the possibility of recycling this growth factor from the culture supernatant or even from the flow through of protein A purification steps, in the case of processes for the production of monoclonal antibodies (mAb's). Usually, a recombinant form of IGF-I is either supplemented into the growth medium, or it is

transfected into the cells, thus allowing autocrine growth (Sunstrom et al. 2000; Pak et al. 1996), both techniques associated with high costs and intense cloning and cell culture work. From a medium design perspective, the components recovered in the E1 elution step could potentially be used as an undefined supplement of serum-free growth medium that has similar effects to the supplementation of yeast and plant hydrolysates, with the advantage that the undefined components originated from the cells themselves and not from external sources.

This work showed that lactate metabolism can be influenced by proteins recovered from the secretome of CHO-K1. Mulukutla et al. (2010) describes different layers in which metabolic fluxes are regulated. The first one is the limitation resulting from the rates of the biochemical reactions themselves and their interconnection through intermediate metabolites, the second one is the allosteric regulation of enzymes, and the third one is the regulation of enzymes at transcriptional level and the global control of cell growth. Proteomic analysis of cells going through metabolic shift and glucose limitation has shown a strong decrease in the expression of  $\alpha$ -enolase, which is the enzyme responsible for the conversion of 2-phosphoglycerate to phosphoenolpyruvate (Pascoe et al. 2007; Wingens et al. 2015). Pascoe et al. (2007) associated this downregulation with the steady decrease in glucose uptake rate linked to glucose depletion during the time course of a cultivation. The results in this work indicate that, perhaps it is not only the glucose concentration the only parameter regulating the glycolytic pathway, but also the accumulation of a signaling factor in the conditioned medium. The lactate profiles indicate that the metabolic shift of the cultures supplemented with E1 probably happened between 48 and 72 hours of cultivation, and at 72 hours for the negative control. Because of the missing time points, it is difficult to determine if E1 triggered the metabolic shift earlier than the negative control. The more obvious effect, was that elution E1 stimulated lactate consumption after the metabolic shift. During the first 48 cultivation hours there was no difference in the lactate production rates, interestingly despite the lower glucose consumption rate of the E1 cultures. Moreover, the glutamine uptake rate of the cultures remained unaffected. It was between 48 and 72 hours that the net lactate production was significantly lowered, at which time glutamine was halfway depleted. It is necessary to determine if the lactate metabolism of the CHO-K1 cell line used in this work responds to glutamine supplementation in the same way as the cell line used by Zagari et al. (2013) in order to clarify if the initial lactate accumulation is a product of glutaminolysis and if the increased lactate consumption is a way for the cell to compensate for the shortage of pyruvate caused by the decrease of glucose uptake. Further indication for the accumulation of a possible signaling molecule that promotes lactate consumption is found in the experiments of Li et al. (2012) in which pyruvate

supplemented in the later stages of cultivation was not enough to stop lactate consumption while alanine still accumulated.

The influence of elution E1 on the glucose uptake and the lactate consumption and which enzymes and metabolic pathways are altered in order to increase lactate consumption are difficult to fathom without at least ammonium or alanine measurements. An increase of lactate consumption without changes in the alanine metabolism would be an indication of an activating effect of the components of E1 only in the enzyme lactate dehydrogenase (LDH). This would explain why in the experiments of Li et al. (2012) pyruvate feeding was not enough to stop lactate consumption. On the other hand, an increase in lactate consumption, coupled with a decrease in alanine concentration and an increase of ammonium would be an indication of an effect of E1 in the transfer of pyruvate into the TCA cycle. This would help understand better how the cells transition into a more balanced metabolism, in which the substrates are better utilized. The role of autocrine factors has not been studied yet. The fact that glutamine metabolism did not change, but rather the glucose consumption and lactate production (after glutamine was halfway depleted) were affected indicates that the components of E1 have a general effect on the glycolytic pathway, perhaps also regulating the transport of glucose into the cell.

### Second Elution E2

Supplementation of elution E2 caused a significant decrease in the specific growth rate, coupled with a decrease in the biomass to glucose yield. Despite less cells being produced, the supplemented culture was still metabolically active. Interestingly, the lactate to glucose yield remained almost unchanged for both cultures. Indications of growth inhibition in hybridoma cells caused by the accumulation of substances other than toxic waste metabolites, e.g. lactate or ammonium, has been reported in the literature (Zeng et al. 1998; Rønning et al. 1991; Lee et al. 1995). Considering that elution E2 was produced from conditioned medium harvested in the late exponential growth phase, and since CHOMACS does not contain any proteins or growth factors, it can be assumed that E2 contained an autoinhibitor produced by the cells during cultivation. More experiments that include cell cycle analysis and apoptosis measurements should be performed to determine the mechanism in which E2 affects the proliferation of the cells. It should also be examined if a culture can be rescued from the growth inhibited state and how long it would take. Strategies for the control of proliferation of producing cell lines has been used to increase the recombinant protein productivity. Some of these strategies include decreasing cell growth by lowering the cultivation temperature, supplementation of small molecules to arrest the cells in the G0/G1 phase or genetic engineering approaches (Du et al.

2015; Barron et al. 2011). The components of elution E2 could potentially be used as a novel strategy for the control of the proliferation of high cell density producing cultures.

The optimized salt elution for the cation exchanger step was able to confine the biological effects of E2 to only 4.1% of the total proteins in conditioned medium, while the HIC purification step was able to further narrow the effect down to 1.2%. Nevertheless, the HIC was tested and developed on the non-optimized cation exchanger salt elution, which confined to effect to 6% - 14% of the proteins in conditioned medium. A combination of the optimized cation exchanger salt elution and the HIC purification step could potentially narrow down the effects to only 0.74% of the total proteins. This would greatly facilitate the later identification of the bioactive components responsible for the growth inhibitory effects of E2.

### Conclusion

It is compelling that the components of E1 and E2 showed remarkably contrasting effects. This indicates the possible interplay of opposing signaling molecules during the time course of a cultivation. The general tendency of conditioned medium, regardless if it originated from the early or late exponential phase of growth, to increase viability and decrease the specific death rate mirrors the effects determined for E1. The specific growth rate reducing effects of conditioned medium from the late exponential phase of growth mirror the effects determined for E2. Identification of the bioactive components in the recovered fractions is crucial for the understanding of how these molecules interact with the cellular metabolism and mitogenic mechanisms. Furthermore it could potentially lead to a better understanding and control of the transition of cell cultures into different metabolic states and to the design of more efficient bioprocesses. Control of the metabolic state has been achieved through the employment of different feeding strategies, the use of alternative substrates like galactose or pyruvate and through the control of different cultivation parameters, but it has not been attempted through the supplementation of autocrine factor. Finally, these bioactive molecules produced by transformed mammalian cells could be valuable as potential therapeutic agents.

## 6 Summary and Outlook

This work examines the biological activity of conditioned medium and its influence in the growth and metabolic kinetics of CHO-K1 cell culture. It also presents a method developed for the capture, recovery and fractionation of the bioactive molecules responsible for some of the determined effects. The recovered components of conditioned medium were tested on exponentially growing cells and their influence on the growth, death and metabolism assessed.

Conditioned medium was generally associated with a 24 hours delayed reduction in the specific death rate and an increase in the viability of exponentially growing cells, regardless if it was harvested in the late or early exponential phase of growth. Conditioned medium from exponentially growing cells was associated with a moderate increase in the specific growth rate after 24 hours of cultivation. Conditioned medium from the late exponential phase was associated with a reduction in the specific growth rate of the cells after 24 hours of cultivation. Ultrafiltration of conditioned medium traced the growth decreasing effect down to the components smaller than 10 kDa. The effects of conditioned medium overlapped with a reduction in specific growth rate resulting from the inoculation at low cell densities (approx.  $3 \times 10^5$  cells/ml) in fresh medium or conditioned medium. The nature of this lagging period was also explored and the results showed the influence of a combination of the age of the inoculation culture and the inoculation cell density.

The recovery method was developed after several optimization steps and was based in the capture of the conditioned medium components into a cation exchanger membrane adsorber. The conditioned medium was produced in a bioreactor and the recovery yield was maximized at a binding pH of 5. The bound components were recovered from the membrane in a two-step elution. The first elution step E1 was performed by increasing the pH of the mobile phase to 10. The second elution step E2 was achieved by increasing the NaCl concentration of the mobile phase to 1 M. Several cation exchanger experiments were performed under the same exact conditions and the effects of the recovered components from each elution on exponentially growing cells were assessed.

The components recovered from the first elution step E1 were associated with a variety of effects which included an increase in the maximal specific growth rate, the increase of the survival capabilities of the cells by reducing apoptosis and increasing cell viability and sudden cellular death after the complete depletion of glucose and glutamine. Furthermore, the glucose consumption rate was generally decreased and lactate consumption was induced after glutamine was depleted. The glutamine



metabolism remained unchanged. The components from the second elution E2 were associated with a reduction in the specific growth rate of the cells and a decrease in the biomass to glucose yield, which describes a higher glucose consumption compared to a reduced production of biomass. The second elution step was optimized in two experiments. The goal was to reduce the amount of proteins that were recovered, which would facilitate the later identification of the bioactive components. The effects associated with E2 were detected at an elution concentration of 0.05 M NaCl and were traced down to 4.1% of the total proteins found in the original conditioned medium.

An orthogonal purification step for the bioactive components of the non-optimized second elution E2 was developed. The goal was to confine the biological effects of E2 to an even smaller portion of the components in conditions medium. A hydrophobic interaction chromatography (HIC) membrane adsorber was used for this step and the optimal binding conditions were assessed using different salts at different concentrations. Then a fraction containing the components of elution E2 was bound into the HIC membrane. The bound components were then recovered from the membrane using low conductivity phosphate buffer at pH 7. The decrease in specific growth rate and the biomass to glucose yield established before for E2 were successfully identified in the components recovered from the HIC membrane, narrowing down the biological effect to only 1.2% of the total proteins from the original conditioned medium. The developed HIC step in combination with the optimized salt concentration for E2 could potential narrow the biological effect down to only 0.74% of the total proteins in conditioned medium.

Identification or proteomic analysis of the bioactive molecules was not achieved in this work. Nonetheless, the effects described for E1 were very similar to the effects attributed to IGF-I, which is a growth factor usually supplemented to serum-free media to stimulate proliferation and is associated with high costs. The developed method could potentially be used for the capture and reutilization of IGF-I from the culture supernatant. Additionally, identification of the molecules responsible for the metabolic effects of E1, could potentially lead to the design of growth medium for a better utilization of glucose and a decreased accumulation of lactate. Finally the induction of sudden cellular death after substrate depletion should be further investigated to understand the mechanisms by which the cells either transition into a decline phase or induce apoptosis.

## 7 References

Ahamed, Tangir; Chilamkurthi, Sreekanth; Nfor, Beckley K.; Verhaert, Peter D E M; van Dedem, Gijs W K; van der Wielen, Luuk A M et al. (2008): Selection of pH-related parameters in ion-exchange chromatography using pH-gradient operations. In *Journal of chromatography. A* 1194 (1), pp. 22–29. DOI: 10.1016/j.chroma.2007.11.111.

Ahamed, Tangir; Nfor, Beckley K.; Verhaert, Peter D E M; van Dedem, Gijs W K; van der Wielen, Luuk A M; Eppink, Michel H M et al. (2007): pH-gradient ion-exchange chromatography: an analytical tool for design and optimization of protein separations. In *Journal of chromatography. A* 1164 (1-2), pp. 181–188. DOI: 10.1016/j.chroma.2007.07.010.

Allen, Martin J.; Boyce, James P.; Trentalange, Michael T.; Treiber, David L.; Rasmussen, Brian; Tillotson, Benjamin et al. (2008): Identification of novel small molecule enhancers of protein production by cultured mammalian cells. In *Biotechnology and bioengineering* 100 (6), pp. 1193–1204. DOI: 10.1002/bit.21839.

Baca, Martyna; Vos, Jelle de; Bruylants, Gilles; Bartik, Kristin; Liu, Xiaodong; Cook, Ken; Eeltink, Sebastiaan (2016): A comprehensive study to protein retention in hydrophobic interaction chromatography. In *Journal of Chromatography B* 1032, pp. 182–188.

Bai, Yunling; Wu, Changjian; Zhao, Jia; Liu, Yan-Hui; Ding, Wei; Ling, Wai Lam W. (2011): Role of iron and sodium citrate in animal protein-free CHO cell culture medium on cell growth and monoclonal antibody production. In *Biotechnology progress* 27 (1), pp. 209–219. DOI: 10.1002/btpr.513.

Bandaranayake, Ashok D.; Almo, Steven C. (2014): Recent advances in mammalian protein production. In *FEBS letters* 588 (2), pp. 253–260.

Barron, N.; Kumar, N.; Sanchez, N.; Doolan, P.; Clarke, C.; Meleady, P. et al. (2011): Engineering CHO cell growth and recombinant protein productivity by overexpression of miR-7. In *Journal of biotechnology* 151 (2), pp. 204–211.

Bates, Ronald C.; Kang, Xuezhen; Frey, Douglas D. (2000): High-performance chromatofocusing using linear and concave pH gradients formed with simple buffer mixtures: I. Effect of buffer composition on the gradient shape. In *Journal of Chromatography A* 890 (1), pp. 25–36.

Brown, Arick; Bill, Jerome; Tully, Timothy; Radhamohan, Asha; Dowd, Chris (2010): Overloading ion-exchange membranes as a purification step for monoclonal antibodies. In *Biotechnology and applied biochemistry* 56 (2), pp. 59–70. DOI: 10.1042/BA20090369.

- Büntemeyer, Heino; Wallerius, Claus; Lehmann, Jürgen (1992): Optimal medium use for continuous high density perfusion processes. In *Cytotechnology* 9 (1-3), pp. 59–67.
- Burgess, ANTONY W.; Camakaris, JAMES; Metcalf, DONALD (1977): Purification and properties of colony-stimulating factor from mouse lung-conditioned medium. In *Journal of Biological Chemistry* 252 (6), pp. 1998–2003.
- BURTEAU, CAROLINE C.; VERHOEYE, FRANÇOIS R.; MOLS, JOHANN F.; BALLEZ, JEAN-SÉBASTIEN; AGATHOS, SPIROS N.; SCHNEIDER, YVES-JACQUES (2003): FORTIFICATION OF A PROTEIN-FREE CELL CULTURE MEDIUM WITH PLANT PEPTONES IMPROVES CULTIVATION AND PRODUCTIVITY OF AN INTERFERON- $\gamma$ -PRODUCING CHO CELL LINE. In *In Vitro Cell Dev Biol Anim* 39 (7), p. 291. DOI: 10.1290/1543-706X(2003)039<0291:FOAPCC>2.0.CO;2.
- Chandler, David (2005): Interfaces and the driving force of hydrophobic assembly. In *Nature* 437 (7059), p. 640.
- Chaudhuri, Susmita; Maurya, Priyanka; Kaur, Manpreet; Tiwari, Ashutosh; Borth, Nicole (2015): Investigation of CHO Secretome: Potential Way to Improve Recombinant Protein Production from Bioprocess. In *J Bioprocess Biotech* 5 (240), p. 2.
- Chen, Lei; Xu, Yingbin; Zhao, Jingling; Zhang, Zhaoqiang; Yang, Ronghua; Xie, Julin et al. (2014): Conditioned medium from hypoxic bone marrow-derived mesenchymal stem cells enhances wound healing in mice. In *PloS one* 9 (4), pp. e96161.
- Chevallet, Mireille; Diemer, Helene; van Dorssealer, Alain; Villiers, Christian; Rabilloud, Thierry (2007): Toward a better analysis of secreted proteins: the example of the myeloid cells secretome. In *Proteomics* 7 (11), pp. 1757–1770. DOI: 10.1002/pmic.200601024.
- Clincke, Marie-Françoise; Mölleryd, Carin; Zhang, Ye; Lindskog, Eva; Walsh, Kieron; Chotteau, Véronique (2013): Very high density of CHO cells in perfusion by ATF or TFF in WAVE bioreactor™. Part I. Effect of the cell density on the process. In *Biotechnology progress* 29 (3), pp. 754–767.
- Dodge, Timothy C.; Ji, Guang-Yong; Hu, Wei-Shou (1987): Loss of viability in hybridoma cell culture—a kinetic study. In *Enzyme and microbial technology* 9 (10), pp. 607–611.
- Du, Zhimei; Treiber, David; McCarter, John D.; Fomina-Yadlin, Dina; Saleem, Ramsey A.; McCoy, Rebecca E. et al. (2015): Use of a small molecule cell cycle inhibitor to control cell growth and improve specific productivity and product quality of recombinant proteins in CHO cell cultures. In *Biotechnology and bioengineering* 112 (1), pp. 141–155.

- Dutton, R. L.; Scharer, J. M.; Moo-Young, M. (1999): Hybridoma growth and productivity: effects of conditioned medium and of inoculum size. In *Cytotechnology* 29 (1), pp. 1–10. DOI: 10.1023/A:1008060802286.
- Fekete, Szabolcs; Beck, Alain; Veuthey, Jean-Luc; Guillarme, Davy (2015): Ion-exchange chromatography for the characterization of biopharmaceuticals. In *Journal of pharmaceutical and biomedical analysis* 113, pp. 43–55.
- Franek, F.; Hohenwarter, O.; Katinger, H. (2000): Plant protein hydrolysates: preparation of defined peptide fractions promoting growth and production in animal cells cultures. In *Biotechnology progress* 16 (5), pp. 688–692. DOI: 10.1021/bp0001011.
- Franěk, František; Katinger, Hermann (2002): Specific effects of synthetic oligopeptides on cultured animal cells. In *Biotechnology progress* 18 (1), pp. 155–158.
- Ghosh, Raja (2002): Protein separation using membrane chromatography: opportunities and challenges. In *Journal of Chromatography A* 952 (1–2), pp. 13–27. DOI: 10.1016/S0021-9673(02)00057-2.
- Gronemeyer, Petra; Ditz, Reinhard; Strube, Jochen (2014): Trends in upstream and downstream process development for antibody manufacturing. In *Bioengineering* 1 (4), pp. 188–212.
- Gupta, Sanjeev Kumar; Srivastava, Santosh K.; Sharma, Ankit; Nalage, Vaibhav H. H.; Salvi, Darshita; Kushwaha, Hiralal et al. (2017): Metabolic engineering of CHO cells for the development of a robust protein production platform. In *PloS one* 12 (8), pp. e0181455.
- Heidemann, R.; Zhang, C.; Qi, H.; Larrick Rule, J.; Rozales, C.; Park, S. et al. (2000): The use of peptones as medium additives for the production of a recombinant therapeutic protein in high density perfusion cultures of mammalian cells. In *Cytotechnology* 32 (2), pp. 157–167. DOI: 10.1023/A:1008196521213.
- Jin, Mi; Szapiel, Nicolas; Zhang, Jennifer; Hickey, John; Ghose, Sanchayita (2010): Profiling of host cell proteins by two-dimensional difference gel electrophoresis (2D-DIGE): Implications for downstream process development. In *Biotechnology and bioengineering* 105 (2), pp. 306–316. DOI: 10.1002/bit.22532.
- Johnson, Thomas V.; DeKorver, Nicholas W.; Levasseur, Victoria A.; Osborne, Andrew; Tassoni, Alessia; Lorber, Barbara et al. (2014): Identification of retinal ganglion cell neuroprotection conferred by platelet-derived growth factor through analysis of the mesenchymal stem cell secretome. In *Brain : a journal of neurology* 137 (Pt 2), pp. 503–519. DOI: 10.1093/brain/awt292.

- Kang, Xuezen; Frey, Douglas D. (2004): Chromatofocusing of peptides and proteins using linear pH gradients formed on strong ion-exchange adsorbents. In *Biotechnology and bioengineering* 87 (3), pp. 376–387.
- Knudsen, Heather L.; Fahrner, Robert L.; Xu, Yuan; Norling, Lenore A.; Blank, Gregory S. (2001): Membrane ion-exchange chromatography for process-scale antibody purification. In *Journal of Chromatography A* 907 (1–2), pp. 145–154. DOI: 10.1016/S0021-9673(00)01041-4.
- Kopaciewicz, W.; Regnier, F. E. (1983): Mobile phase selection for the high-performance ion-exchange chromatography of proteins. In *Analytical Biochemistry* 133 (1), pp. 251–259.
- Kramarczyk, Jack F.; Kelley, Brian D.; Coffman, Jonathan L. (2008): High-throughput screening of chromatographic separations: II. Hydrophobic interaction. In *Biotechnology and bioengineering* 100 (4), pp. 707–720.
- Kröner, Frieder; Hubbuch, Jürgen (2013): Systematic generation of buffer systems for pH gradient ion exchange chromatography and their application. In *Journal of Chromatography A* 1285, pp. 78–87.
- Kuczewski, Michael; Fraud, Nathalie; Faber, Rene; Zarbis-Papastoitsis, Gregory (2010): Development of a polishing step using a hydrophobic interaction membrane adsorber with a PER.C6-derived recombinant antibody. In *Biotechnology and bioengineering* 105 (2), pp. 296–305. DOI: 10.1002/bit.22538.
- Lauffenburger, D.; Cozens, C. (1989): Regulation of mammalian cell growth by autocrine growth factors: analysis of consequences for inoculum cell density effects. In *Biotechnology and bioengineering* 33 (11), pp. 1365–1378. DOI: 10.1002/bit.260331102.
- Lee, Yuan-Kun; Yap, Peng-Kang; Teoh, Ai-Peng (1995): Correlation between steady-state cell concentration and cell death of hybridoma cultures in chemostat. In *Biotechnology and bioengineering* 45 (1), pp. 18–26. DOI: 10.1002/bit.260450104.
- Lee, Micky Fu Xiang; Chan, Eng Seng; Tey, Beng Ti (2014): Negative chromatography: Progress, applications and future perspectives. In *Process Biochemistry* 49 (6), pp. 1005–1011.
- Leeb, Elena; Holder, Aline; Letzel, Thomas; Cheison, Seronei Chelulei; Kulozik, Ulrich; Hinrichs, Jörg (2014): Fractionation of dairy based functional peptides using ion-exchange membrane adsorption chromatography and cross-flow electro membrane filtration. In *International Dairy Journal* 38 (2), pp. 116–123. DOI: 10.1016/j.idairyj.2013.12.006.

- Li, Jincai; Wong, Chun Loong; Vijayasankaran, Natarajan; Hudson, Terry; Amanullah, Ashraf (2012): Feeding lactate for CHO cell culture processes: impact on culture metabolism and performance. In *Biotechnology and bioengineering* 109 (5), pp. 1173–1186. DOI: 10.1002/bit.24389.
- Lim, U. Ming; Yap, Miranda Gek Sim; Lim, Yoon Pin; Goh, Lin-Tang; Ng, Say Kong (2013): Identification of autocrine growth factors secreted by CHO cells for applications in single-cell cloning media. In *Journal of proteome research* 12 (7), pp. 3496–3510. DOI: 10.1021/pr400352n.
- Liu, Cheng; Morrow, K. John (2016): *Biosimilars of Monoclonal Antibodies: A Practical Guide to Manufacturing, Preclinical, and Clinical Development*: John Wiley & Sons.
- Liu, Hui F.; Ma, Junfen; Winter, Charles; Bayer, Robert (2010): Recovery and purification process development for monoclonal antibody production. In : *MAbs*, vol. 2. Taylor & Francis, pp. 480–499.
- Ljunggren, Jan; Häggström, Lena (1995): Specific growth rate as a parameter for tracing growth-limiting substances in animal cell cultures. In *Journal of biotechnology* 42 (2), pp. 163–175.
- Luo, Jun; Vijayasankaran, Natarajan; Autsen, Jennifer; Santuray, Rodell; Hudson, Terry; Amanullah, Ashraf; Li, Feng (2012): Comparative metabolite analysis to understand lactate metabolism shift in Chinese hamster ovary cell culture process. In *Biotechnology and bioengineering* 109 (1), pp. 146–156. DOI: 10.1002/bit.23291.
- Mamounas, M.; Gervin, D.; Englesberg, E. (1989): The insulin receptor as a transmitter of a mitogenic signal in Chinese hamster ovary CHO-K1 cells. In *Proceedings of the National Academy of Sciences of the United States of America* 86 (23), pp. 9294–9298.
- Mhatre, R.; Nashabeh, W.; Schmalzing, D.; Yao, X.; Fuchs, M.; Whitney, D.; Regnier, F. (1995): Purification of antibody Fab fragments by cation-exchange chromatography and pH gradient elution. In *Journal of Chromatography A* 707 (2), pp. 225–231. DOI: 10.1016/0021-9673(95)00319-I.
- Mohamed, Vasila Packeer; Hashim, Yumi Zuhanis Has-Yun; Amid, Azura; Mel, Maizirwan; Kamarulzaman, Abdul Razak; Wahab, M. A.A.; Saberi, Salfarina Ezrina Mohmad (2011): Chinese hamster ovary (CHO-K1) cells expressed native insulin-like growth factor-1 (IGF-1) gene towards efficient mammalian cell culture host system. In *African Journal of Biotechnology* 10 (81), pp. 18716–18721.
- Mohmad-Saberi, Salfarina Ezrina; Hashim, Yumi Zuhanis Has-Yun; Mel, Maizirwan; Amid, Azura; Ahmad-Raus, Raha; Packeer-Mohamed, Vasila (2013): Metabolomics profiling of extracellular metabolites in CHO-K1 cells cultured in different types of growth media. In *Cytotechnology* 65 (4), pp. 577–586. DOI: 10.1007/s10616-012-9508-4.

## 7. REFERENCES

---

- Moreadith, R. W.; and Lehninger, A. L. (1984): The pathways of glutamate and glutamine oxidation by tumor cell mitochondria. Role of mitochondrial NAD (P)<sup>+</sup>-dependent malic enzyme. In *Journal of Biological Chemistry* 259 (10), pp. 6215–6221.
- Mosser, Mathilde; Chevalot, Isabelle; Olmos, Eric; Blanchard, Fabrice; Kapel, Romain; Oriol, Eric et al. (2013): Combination of yeast hydrolysates to improve CHO cell growth and IgG production. In *Cytotechnology* 65 (4), pp. 629–641.
- Mulukutla, Bhanu Chandra; Khan, Salmaan; Lange, Alex; Hu, Wei-Shou (2010): Glucose metabolism in mammalian cell culture: new insights for tweaking vintage pathways. In *Trends in biotechnology* 28 (9), pp. 476–484. DOI: 10.1016/j.tibtech.2010.06.005.
- Ng, Paul K.; He, Jie; Snyder, Mark A. (2009): Separation of protein mixtures using pH-gradient cation-exchange chromatography. In *Journal of chromatography. A* 1216 (9), pp. 1372–1376. DOI: 10.1016/j.chroma.2008.12.100.
- Ozturk, Sadettin; Hu, Wei-Shou (2005): Cell culture technology for pharmaceutical and cell-based therapies: CRC Press.
- Pak, S. C.; Hunt, S. M.; Bridges, M. W.; Sleight, M. J.; Gray, P. P. (1996): Super-CHO-A cell line capable of autocrine growth under fully defined protein-free conditions. In *Cytotechnology* 22 (1-3), pp. 139–146. DOI: 10.1007/BF00353933.
- Park, Byung-Soon; Kim, Won-Serk; Choi, Joon-Seok; Kim, Hyung-Ki; Won, Jong-Hyun; Ohkubo, Fumio; Fukuoka, Hirotaro (2010): Hair growth stimulated by conditioned medium of adipose-derived stem cells is enhanced by hypoxia: evidence of increased growth factor secretion. In *Biomedical Research* 31 (1), pp. 27–34.
- Pascoe, Deborah E.; Arnott, David; Papoutsakis, Eleftherios T.; Miller, William M.; Andersen, Dana C. (2007): Proteome analysis of antibody-producing CHO cell lines with different metabolic profiles. In *Biotechnology and bioengineering* 98 (2), pp. 391–410.
- Qian, Yueming; Lewis, Amanda M.; Sidnam, Sarah M.; Bergeron, Alison; Abu-Absi, Nicholas R.; Vaidyanathan, Nisha et al. (2017): LongR3 enhances Fc-fusion protein N-linked glycosylation while improving protein productivity in an industrial CHO cell line. In *Process Biochemistry* 53, pp. 201–209.
- Queiroz, J. A.; Tomaz, C. T.; Cabral, J. M.S. (2001): Hydrophobic interaction chromatography of proteins. In *Journal of biotechnology* 87 (2), pp. 143–159.

- Rea, Jennifer C.; Moreno, G. Tony; Lou, Yun; Farnan, Dell (2011): Validation of a pH gradient-based ion-exchange chromatography method for high-resolution monoclonal antibody charge variant separations. In *Journal of pharmaceutical and biomedical analysis* 54 (2), pp. 317–323.
- Recio, Isidra; Visser, Servaas (1999): Two ion-exchange chromatographic methods for the isolation of antibacterial peptides from lactoferrin: In situ enzymatic hydrolysis on an ion-exchange membrane. In *Journal of Chromatography A* 831 (2), pp. 191–201. DOI: 10.1016/S0021-9673(98)00950-9.
- Riordan, William; Heilmann, Steve; Brorson, Kurt; Seshadri, Kannan; He, Yi; Etzel, Mark (2009): Design of salt-tolerant membrane adsorbers for viral clearance. In *Biotechnology and bioengineering* 103 (5), pp. 920–929. DOI: 10.1002/bit.22314.
- Rønning, Øystein W.; Schartum, Mona; Winsnes, Andreas; Lindberg, Gro (1991): Growth limitation in hybridoma cell cultures: The role of inhibitory or toxic metabolites. In *Cytotechnology* 7 (1), pp. 15–24.
- Sell, C.; Baserga, R.; Rubin, R. (1995): Insulin-like growth factor I (IGF-I) and the IGF-I receptor prevent etoposide-induced apoptosis. In *Cancer research* 55 (2), pp. 303–306.
- Senczuk, Anna M.; Klinke, Ralph; Arakawa, Tsutomu; Vedantham, Ganesh; Yigzaw, Yinges (2009): Hydrophobic interaction chromatography in dual salt system increases protein binding capacity. In *Biotechnology and bioengineering* 103 (5), pp. 930–935.
- Shukla, Abhinav A.; Etzel, Mark R.; Gadam, Shishir (2006): Process scale bioseparations for the biopharmaceutical industry: CRC Press.
- Shukla, Abhinav A.; Yigzaw, Yinges (2007): 6 Modes of Preparative Chromatography. In *Process Scale Bioseparations for the Biopharmaceutical Industry*, p. 179.
- Singh, Satish Kumar (2011): Impact of product-related factors on immunogenicity of biotherapeutics. In *Journal of pharmaceutical sciences* 100 (2), pp. 354–387. DOI: 10.1002/jps.22276.
- Spearman, Maureen; Lodewyks, Carly; Richmond, Meika; Butler, Michael (2014): The bioactivity and fractionation of peptide hydrolysates in cultures of CHO cells. In *Biotechnology progress* 30 (3), pp. 584–593.
- Spens, Erika; Häggström, Lena (2005): Defined Protein-Free NS0 Myeloma Cell Cultures: Stimulation of Proliferation by Conditioned Medium Factors. In *Biotechnology progress* 21 (1), pp. 87–95.
- Sugino, Ilene K.; Sun, Qian; Springer, Carola; Cheewatrakoolpong, Noounanong; Liu, Tong; Li, Hong; Zarbin, Marco A. (2016): Two Bioactive Molecular Weight Fractions of a Conditioned Medium



- Enhance RPE Cell Survival on Age-Related Macular Degeneration and Aged Bruch's Membrane. In *Translational vision science & technology* 5 (1), p. 8. DOI: 10.1167/tvst.5.1.8.
- Sunstrom, N. A.; Gay, R. D.; Wong, D. C.; Kitchen, N. A.; DeBoer, L.; Gray, P. P. (2000): Insulin-like growth factor-I and transferrin mediate growth and survival of Chinese hamster ovary cells. In *Biotechnology progress* 16 (5), pp. 698–702. DOI: 10.1021/bp000102t.
- Tait, A. S.; Hogwood, C. E. M.; Smales, C. M.; Bracewell, D. G. (2012): Host cell protein dynamics in the supernatant of a mAb producing CHO cell line. In *Biotechnology and bioengineering* 109 (4), pp. 971–982. DOI: 10.1002/bit.24383.
- Talebi, Mohammad; Nordborg, Anna; Gaspar, Andras; Lacher, Nathan A.; Wang, Qian; He, Xiaoping Z. et al. (2013): Charge heterogeneity profiling of monoclonal antibodies using low ionic strength ion-exchange chromatography and well-controlled pH gradients on monolithic columns. In *Journal of Chromatography A* 1317, pp. 148–154.
- Templeton, Neil; Dean, Jason; Reddy, Pranhitha; Young, Jamey D. (2013): Peak antibody production is associated with increased oxidative metabolism in an industrially relevant fed-batch CHO cell culture. In *Biotechnology and bioengineering* 110 (7).
- Valente, Kristin N.; Lenhoff, Abraham M.; Lee, Kelvin H. (2014): Expression of difficult-to-remove host cell protein impurities during extended Chinese hamster ovary cell culture and their impact on continuous bioprocessing. In *Biotechnology and bioengineering*. DOI: 10.1002/bit.25515.
- Wahrheit, Judith; Niklas, Jens; Heinzle, Elmar (2014): Metabolic control at the cytosol-mitochondria interface in different growth phases of CHO cells. In *Metabolic engineering* 23, pp. 9–21.
- WARBURG, O. (1956): On the origin of cancer cells. In *Science (New York, N.Y.)* 123 (3191), pp. 309–314.
- Weaver, Justin; Husson, Scott M.; Murphy, Louise; Wickramasinghe, S. Ranil (2013a): Anion exchange membrane adsorbers for flow-through polishing steps: Part I. Clearance of minute virus of mice. In *Biotechnology and bioengineering* 110 (2), pp. 491–499. DOI: 10.1002/bit.24720.
- Weaver, Justin; Husson, Scott M.; Murphy, Louise; Wickramasinghe, S. Ranil (2013b): Anion exchange membrane adsorbers for flow-through polishing steps: Part II. Virus, host cell protein, DNA clearance, and antibody recovery. In *Biotechnology and bioengineering* 110 (2), pp. 500–510. DOI: 10.1002/bit.24724.

- Wells, Valerie; Mallucci, Livio (1991): Identification of an autocrine negative growth factor: mouse  $\beta$ -galactoside-binding protein is a cytostatic factor and cell growth regulator. In *Cell* 64 (1), pp. 91–97.
- Wells, Valerie; Mallucci, Livio (1992): Molecular expression of the negative growth factor murine  $\beta$ -galactoside binding protein (mGBP). In *Biochimica et Biophysica Acta (BBA)-Protein Structure and Molecular Enzymology* 1121 (3), pp. 239–244.
- Wilkens, Camila A.; Altamirano, Claudia; Gerdtzen, Ziomara P. (2011): Comparative metabolic analysis of lactate for CHO cells in glucose and galactose. In *Biotechnol. Bioprocess Eng.* 16 (4), pp. 714–724.
- Wimmer, Katharina; Harant, Hanna; Reiter, Manfred; Blöchl, Gerald; Gaida, Theo; Katinger, Hermann (1994): Two-dimensional gel electrophoresis for controlling and comparing culture supernatants of mammalian cell culture productions systems. In *Cytotechnology* 16 (3), pp. 137–146. DOI: 10.1007/BF00749900.
- Wingens, Marc; Gätgens, Jochem; Schmidt, Anica; Albaum, Stefan P.; Büntemeyer, Heino; Noll, Thomas; Hoffrogge, Raimund (2015): 2D-DIGE screening of high-productive CHO cells under glucose limitation--basic changes in the proteome equipment and hints for epigenetic effects. In *Journal of biotechnology* 201, pp. 86–97. DOI: 10.1016/j.jbiotec.2015.01.005.
- Woolley, John F.; Al-Rubeai, Mohamed (2009): The isolation and identification of a secreted biomarker associated with cell stress in serum-free CHO cell culture. In *Biotechnology and bioengineering* 104 (3), pp. 590–600. DOI: 10.1002/bit.22408.
- Wurm, Florian M. (2004): Production of recombinant protein therapeutics in cultivated mammalian cells. In *Nature biotechnology* 22 (11), pp. 1393–1398. DOI: 10.1038/nbt1026.
- Wurm, Florian M.; Hacker, David (2011): First CHO genome. In *Nature biotechnology* 29 (8), p. 718.
- Yamada, Tsuyoshi; Yamamoto, Koichi; Ishihara, Takashi; Ohta, Shigeru (2017): Purification of monoclonal antibodies entirely in flow-through mode. In *Journal of Chromatography B* 1061, pp. 110–116.
- Young, Jamey D. (2013): Metabolic flux rewiring in mammalian cell cultures. In *Current opinion in biotechnology* 24 (6), pp. 1108–1115.
- Yuk, Inn H.; Nishihara, Julie; Walker, Donald, JR; Huang, Eric; Gunawan, Feny; Subramanian, Jayashree et al. (2015): More similar than different: Host cell protein production using three null CHO cell lines. In *Biotechnology and bioengineering* 112 (10), pp. 2068–2083. DOI: 10.1002/bit.25615.

- Zagari, Francesca; Jordan, Martin; Stettler, Matthieu; Broly, Hervé; Wurm, Florian M. (2013): Lactate metabolism shift in CHO cell culture: the role of mitochondrial oxidative activity. In *New biotechnology* 30 (2), pp. 238–245. DOI: 10.1016/j.nbt.2012.05.021.
- Zeng, An-Ping; Deckwer, Wolf-Dieter; Hu, Wei-Shou (1998): Determinants and rate laws of growth and death of hybridoma cells in continuous culture. In *Biotechnology and bioengineering* 57 (6), pp. 642–654.
- Zhang, Huifeng; Wang, Haibin; Liu, Mei; Zhang, Tao; Zhang, Ji; Wang, Xiangjing; Xiang, Wensheng (2013a): Rational development of a serum-free medium and fed-batch process for a GS-CHO cell line expressing recombinant antibody. In *Cytotechnology* 65 (3), pp. 363–378. DOI: 10.1007/s10616-012-9488-4.
- Zhang, Jinyou; Robinson, David; Salmon, Peter (2006): A novel function for selenium in biological system: selenite as a highly effective iron carrier for Chinese hamster ovary cell growth and monoclonal antibody production. In *Biotechnology and bioengineering* 95 (6), pp. 1188–1197. DOI: 10.1002/bit.21081.
- Zhang, Liangyi; Patapoff, Thomas; Farnan, Dell; Zhang, Boyan (2013b): Improving pH gradient cation-exchange chromatography of monoclonal antibodies by controlling ionic strength. In *Journal of chromatography. A* 1272, pp. 56–64. DOI: 10.1016/j.chroma.2012.11.060.
- Zhu, Jianwei (2012): Mammalian cell protein expression for biopharmaceutical production. In *Biotechnology advances* 30 (5), pp. 1158–1170. DOI: 10.1016/j.biotechadv.2011.08.022.
- Zsebo, Krisztina M.; Wypych, Jette; McNiece, Ian K.; Lu, Hsieng S.; Smith, Kent A.; Karkare, Subash B. et al. (1990): Identification, purification, and biological characterization of hematopoietic stem cell factor from buffalo rat liver-conditioned medium. In *Cell* 63 (1), pp. 195–201. DOI: 10.1016/0092-8674(90)90300-4.

### 8 Lebenslauf

<b>Name</b>	Castillo Salvador
<b>Vorname</b>	Alan Eduardo
<b>Staatsangehörigkeit</b>	deutsch
<b>Geburtsdatum</b>	15.01.1987
<b>Geburtsort</b>	Ciudad de Mexico, Mexiko
<b>08.1994 - 06.2000</b>	Grundschule in Mexiko City
<b>09.2000 - 05.2006</b>	Gymnasium in Mexiko City Colegio Aleman Alexander von Humboldt
<b>10.2006 - 02.2014</b>	Studium an dem Karlsruher Institut für Technologie Abschluss: Diplom
<b>03.2014 - 05.2017</b>	Wissenschaftlicher Mitarbeiter an dem Institut für Bioverfahrenstechnik und Biosysteme (IBB) der Technischen Universität Hamburg Harburg
<b>06.2017 - 03.2019</b>	Fertigstellung der Doktorarbeit
<b>03.2019 - heute</b>	Kaufmännischer Angestellter bei KSP Rechtsanwälte